Quantitative regulation of inducible genes: comparing models of 'on/off' against continuously variable switches



Caroline Schneider

Keble College, University of Oxford

A thesis submitted for the degree of

Doctor of Philosophy

Trinity Term 2015

45 046 words

Quantitative regulation of inducible genes: comparing models of 'on/off' against continuously variable switches

Caroline Schneider

Keble College, University of Oxford

A thesis submitted for the degree of Doctor of Philosophy

Trinity Term 2015

Abstract

In order to respond rapidly and appropriately to their environment, cells activate internal signalling pathways, such as the mitogen-activated protein kinase (MAPK) pathways, which elicit appropriate responses through quantitative modulation of gene expression. Conceptually, gene expression may be regulated by a bistable switch or a continuously variable switch. The bistable switch considers the gene in either a stable 'on' state, where transcription happens at a constant rate intrinsic to the system, or a stable 'off' state, where transcription is not permitted. By contrast, the continuously variable switch considers gene transcription as a dynamic process, where the rate of transcription initiation varies with the intensity of the signal perceived. The work in this thesis focuses on the interface between the well-understood MAPK pathways and immediate-early (IE) genes and shows that a continuously variable switch would be more appropriate to convey quantitative regulation. Immunoblotting analyses of MAPK pathways after treatment of synchronised C3H 10T½ cells with the specific PP1 and PP2A protein phosphatase inhibitor, okadaic acid, revealed the presence of turnover of phosphorylation of transcription factor (TF) in the stress-activated MAPK pathways, suggesting dynamic regulation of these MAPK pathways. Analyses of the induction of IE genes c-*fos* and c-*jun* after perturbations of the turnover of phosphorylation by phosphatase or kinase inhibitors suggest that rather than static phosphorylation state dynamic turnover of phosphorylation may regulate IE gene induction. Finally, a simplified computational model of the interface is presented, which confirms that dynamic regulation linking rate of initiation to the turnover of phosphorylation of TFs would better convey quantitative responses.

Acknowledgments

Firstly, I am deeply grateful to Louis and Marta for giving me the opportunity to work in their groups and for their continuous help and support throughout my DPhil project. I would also like to thank Nick and Cath for sharing with me their extensive knowledge and for making the lab a pleasant place to work. I am extremely grateful to Nick for his valuable advice and stimulating discussions over lunch, his continued feedback and help during the writing of this thesis was invaluable.

My thanks also goes to Milan for his work and enthusiasm about the modelling part of the project. This part would not have been possible without his knowledge and the valuable inputs from Alessandro and David.

The work was part of the doctoral training centre and supported by the Engineering and Physical Sciences Research Council.

I thank my friends from the DTC, the Biochemistry department and College for making this experience unforgettable and enjoyable. Specifically, I would like to thank Kira, Nick, Andrea and Diana for fun coffee breaks, Jonny for coming and reminding me of our time as Part II, and Joanna, Ellie and El, also known as the 'Breakfast club' for keeping me sane during the writing of this thesis.

Finally, I would like to thank my parents, Claire and Thierry, my family Marion, Anna, Guillaume and Héloïse and Adrian for their unconditional support.

List of Publications

Ceska M, **Schneider C**, Abate A, Safranek D, Mahadevan LC, Kwiatkowska MZ Stochastic modelling of the interface between regulatory enzymes and transcriptional initiation at inducible genes, in preparation.

List of Abbreviations

ac	acetyl
An	anisomycin
AP-1	activating protein 1
BMK	big mitogen-activated protein kinase
CBP	CREB-binding protein
CD	common docking
cDNA	complementary DNA
ChIP	chromatin immunoprecipitation
CRE	3'-5'-cyclic AMP response element
CREB	CRE-binding protein
CTD	C-terminal domain
DUSP	dual-specificity phosphatase
DRB	5,6-dichlorobenzimidazole 1-β-D-ribofuranoside
EGF	epidermal growth factor
ERK	extracellular signal-regulated kinase
FISH	fluorescence *in situ* hybridization
GAPDH	glyceraldehyde 3-phosphate dehydrogenase
GF	growth factor
GFP	green fluorescent protein
gsc	*goosecoid*
H3K4me3	histone H3, lysine-4 trimethylated
H3K9ac	histone H3, lysine-9 acetylated
H3S10ph	histone H3, serine-10 phosphorylated

HAT	histone acetyltransferase
HDAC	histone deacetylase
HMGN1	high mobility group nucleosome binding domain 1
IE gene	immediate-early gene
JNK	Jun N-terminal kinase
KIM	kinase interaction motif
kDa	kilodalton
MAPK	mitogen-activated protein kinase
MAPKK	MAPK kinase
MAPKKK	MAPKK kinase
me	methyl
MKP	MAP kinase phosphatase
mRNA	messenger RNA
MSK	mitogen- and stress-activated protein kinase
NET-seq	native elongating transcript sequencing
OA	okadaic acid
PAGE	polyacrylamide gel electrophoresis
PDGF	platelet-derived growth factor
ph	phosphryl
PKA	protein kinase A
Pol II	RNA polymerase II
PP1	protein phosphatase 1
PP1c	PP1 catalytic subunit
PP2A	protein phosphatase 2A
PP2Ac	PP2A catalytic subunit

PPM	protein phosphatase Mg^{2+}/Mn^{2+} dependent
PPP	phosphoprotein phosphatase
PRISM	probabilistic model checker PRISM
pTEFb	positive transcription elongation factor
PTM	post-transcriptional modification
PTP	protein tyrosine phosphatase
qRT-PCR	quantitative reverse-transcription PCR
RNA-seq	RNA sequencing
RSRF	related-to-serum-response-factor
sAn	sub-inhibitory ansiomycin
SAPK	stress-activated protein kinase
SIE	c-*sis* inducible element
SRE	serum response element
SRF	serum response factor
TCF	ternary complex factor
TF	transcription factor
TPA	12-O-tetradecanoylphorbol-13-acetate
TSA	trichostatin A
UV	ultraviolet

Table of Contents

Abstract ..... **i**
Acknowledgments ..... **ii**
List of Publications ..... **iii**
List of Abbreviations ..... **iv**
Table of Contents ..... **vii**
List of Figures ..... **xiv**
List of Tables ..... **xvi**

Chapter 1: Introduction **1**

1.1 The different biological switching mechanisms **1**

1.1.1 All-or-nothing responses 1

1.1.2 Continuously variable switches 6

1.1.2.1 Definition of morphogen 6
1.1.2.2 The French flag model 8
1.1.2.3 Activin elicits different cell fate decisions in the Xenopus embryo 8
1.1.2.4 Notion of threshold and gradual response 10

1.2 Immediate-early genes: specific transcription due to their direct link to signalling pathways **12**

1.2.1 The characteristics of immediate-early gene expression 13

1.2.1.1 IE gene induction is transient and rapid 13
1.2.1.2 IE gene induction is quantitative and specific 14

1.2.2 The *jun* and *fos* families 15

1.2.2.1 The *jun* family 15
1.2.2.2 The *fos* family 16

1.2.3 The role of transcription factors in IE gene induction 16

1.2.3.1 c-*fos* promoter region 17
1.2.3.2 c-*jun* promoter region 20
1.2.3.3 Transcriptional regulation with multiple levels of control 21

1.2.4 The role of histone modifications in IE gene regulation 23

1.2.4.1 Histone tails and post-translational modifications 23
1.2.4.2 Histone acetylation 27
1.2.4.3 Histone phosphorylation 28
1.2.4.4 Histone phosphoacetylation 30

1.3 MAPK signalling pathways **31**

1.3.1 MAPK pathways transduce signals to nucleus through a three-tiered organisation 31

1.3.1.1 The mitogen activated protein kinase (MAPK) 33
1.3.1.2 The MAPK kinase (MAPKK) 35
1.3.1.3 The MAPKK kinase (MAPKKK) 36

1.3.1.4 Scaffold proteins 36
1.3.2 MAPK pathways are activated in parallel by various stimuli 37
1.3.2.1 Different stimuli activate MAPK pathways 37
1.3.2.2 MAPK substrates 38
1.4 Protein phosphatases 40
1.4.1 The tyrosine-specific phosphatases 42
1.4.2 The serine/threonine phosphatases 43
1.4.2.1 Sub-groups of serine/threonine phosphatases 43
1.4.2.2 Protein phosphatase 1 (PP1) 44
1.4.2.3 Protein phosphatase 2A (PP2A) 45
1.4.3 The dual-specificity phosphatases 46
1.5 Quantitative regulation of inducible genes 49
1.5.1 The view of MAPK pathways in regulation 49
1.5.1.1 Ultrasensitivity within the MAPK pathways 51
1.5.1.2 Ultrasensitivity and positive feedback loops in MAPK pathways generate all-or-nothing response 52
1.5.2 Coupling MAPK pathway and IE gene transcription 54
1.6 Summary 57

Chapter 2: Materials and Methods 58
2.1 Materials 58
2.1.1 Antibodies 58
2.1.2 Stimuli and inhibitors 58
2.2 Tissue Culture 58
2.3 Protein Extraction 61
2.3.1 Extraction of transcription factors 61
2.3.2 Acid extraction of histones 62
2.4 Polyacrylamide gel electrophoresis (PAGE) 62
2.4.1 Sodium dodecylsulphate (SDS) PAGE 62
2.4.2 ERK PAGE 63
2.5 Western blotting 64
2.5.1 Protein transfer 64
2.5.1.1 SDS transfer buffer 64
2.5.1.2 Towbin transfer buffer 64
2.5.2 Ponceau staining 64

2.5.3 Immunoblotting 65
2.5.4 Quantification of Western blots 65
2.6 RNA extraction 67
2.7 Northern blotting 68
2.7.1 Electrophoresis 68
2.7.2 RNA transfer and probing 68
2.7.3 Quantification of Northern blots 69
2.8 Real-time PCR 70
2.8.1 Preparation of genomic DNA for standards 70
2.8.2 cDNA synthesis 70
2.8.3 Analysis of real-time PCR data 71
2.9 Probabilistic model checker PRISM 73

Chapter 3: Okadaic acid reveals the existence of a phosphorylation turnover in quiescent cells 76

3.1 Introduction 76
3.1.1 Phosphatase and kinase inhibitors: tools to study turnover of phosphorylation 76
3.1.1.1 Specificity of inhibitors 76
3.1.1.2 Turnover of phosphorylation and phosphatase inhibition 80
3.1.2 Monitoring the turnover of phosphorylation 81
3.1.2.1 Advantage of cell culture 81
3.1.2.2 Quantification of turnover of phosphorylation 83
3.1.3 Summary 84
3.2 Results 85
3.2.1 Okadaic acid induces IE gene transcription 85
3.2.1.1 IE gene induction 85
3.2.1.2 Histone H3 phosphorylation 88
3.2.2 Effect of OA on MAPK pathways 91
3.2.2.1 OA does not activate ERK1/2 91
3.2.2.2 OA activates p38 phosphorylation 93
3.2.2.3 OA does not affect EGF-induced stimulation of ERK1/2 94
3.2.2.4 OA stimulates histone phosphorylation through the p38 pathway 95
3.2.2.5 OA activates the different downstream targets of p38 99

3.2.3 The JNK MAPK pathway is activated at the TF level after OA treatment ... 103

3.2.3.1 MEK4 and JNK are not phosphorylated after OA treatment ... 105
3.2.3.2 OA treatment generates accumulation of phosphorylated TFs of the JNK pathway ... 105

3.3 Discussion ... 111

3.3.1 Multiple level of action of OA in the p38 pathway ... 111

3.3.2 Turnover of phosphorylation in the JNK MAPK pathway ... 114

3.3.3 Is ERK dynamically regulated? ... 115

Chapter 4: Detailed analysis of c-fos and c-jun induction profiles ... 118

4.1 Introduction ... 118

4.1.1 Monitoring gene expression ... 118

4.1.1.1 Quantification of mRNA levels in synchronised cell population ... 118
4.1.1.2 Quantification of mRNA ... 120
4.1.1.3 Northern blotting and quantitative reverse-transcription PCR ... 121

4.1.2 Transcription and translation inhibition ... 123

4.1.2.1 Evaluating the degradation of mRNA ... 123
4.1.2.2 Phenomenon of superinduction and translational inhibition ... 124

4.1.3 Summary ... 127

4.2 Results ... 127

4.2.1 Quantitative profiles of c-*fos* and c-*jun* after sAn activation ... 127

4.2.1.1 c-*fos* and c-*jun* have characteristic expression profiles ... 128
4.2.1.2 Alternative polyadenylated forms of c-*jun* ... 133

4.2.2 Effect of mRNA degradation on c-*fos* and c-*jun* profiles ... 135

4.2.2.1 Inhibition of transcription reveals a constant rate of degradation ... 135
4.2.2.2 mRNA degradation does not affect the shape of the first phase of sAn-induced profiles ... 136

4.2.3 Disruption of the turnover of phosphorylation ... 140

4.2.3.1 Effect of phosphatase inhibitor ... 140
4.2.3.2 Effect of kinase inhibitors ... 143

4.3 Discussion ... 146

4.3.1 Protein phosphatases play an important role in IE gene regulation ... 146

4.3.1.1 OA induces c-fos and c-jun similarly ... 146

4.3.1.2 Link between turnover of phosphorylation and IE gene induction? 147

4.3.2 Pre-treatment with kinase inhibitors reveals the complexity of IE gene regulation 149

4.3.2.1 c-fos and c-jun induction cannot be attributed to a single pathway 149
4.3.2.2 The need for interactions between pathways 150
4.3.2.3 Different expression of c-fos and c-jun reflects different TF binding sites in their promoters 150

4.3.3 The specific IE gene profiles could be regulated at the initiation of transcription 152

Chapter 5: Investigation of a simplified computational model of the interface between MAPK pathways and IE genes 154

5.1 Introduction 154

5.1.1 Using computational models to gain insights into biological system . 154

5.1.1.1 Computational modelling and model checking 154
5.1.1.2 Different modelling approaches 156

5.1.2 PRISM, a tool for analysing stochastic systems 157

5.1.2.1 The need of a stochastic model 157
5.1.2.2 Modelling the interface 158
5.1.2.3 The probabilistic model checker PRISM 160

5.1.3 Summary 160

5.2 Description of the model 161

5.2.1 The signalling module 162

5.2.1.1 Experimental activation profiles 165
5.2.1.2 Modelled activation profiles 169

5.2.2 The initiation module and regulation functions 169

5.2.3 The mRNA module 175

5.2.4 Obtaining the initiation and induction curves 176

5.3 Results 176

5.3.1 Comparison of the two regulation functions 176

5.3.1.1 Difference in the information conveyed through regulation function 176
5.3.1.2 The initiation profiles are similar to the rate of initiation of transcription 179

5.3.2 The two types of switch induce different mRNA profiles 180
5.3.2.1 The capacity of the binary switch to convey dynamically varying quantitative information is limited 180
5.3.2.2 The continuously variable switch hypothesis induces quantitative mRNA profiles 184
5.3.3 The production and degradation rates control different phases of the mRNA profile 186

5.4 Discussion 193

5.4.1 Characteristics of continuously variable switch and binary switch 193
5.4.1.1 The continuously variable switch better conveys quantitative signal information 193
5.4.1.2 The continuously variable switch behaves like a binary switch under specific conditions 195
5.4.1.3 Frequency of transcription initiation is controlled by spatial constraint or dynamic turnover of phosphorylation 195

5.4.2 Biological interpretation of the parameters 196
5.4.2.1 The threshold as a specific activated kinase concentration 197
5.4.2.2 The exponent as kinase activity 198
5.4.2.3 The role of mRNA production and degradation rates 199
5.4.2.4 Additional regulatory steps 200

Chapter 6: Discussion 203

6.1 Dynamic regulation of MAPK pathways? 203

6.1.1 Bistability of the MAPK pathways 203
6.1.2 The signalling pathways can behave as binary or continuously variable switch depending on the conditions 206
6.1.3 Implications in diseases 208
6.1.3.1 The p38 and JNK pathways in disease 209
6.1.3.2 Phosphatases as potential drug targets 210

6.2 A role for turnover of phosphorylation of TFs in quantitative IE gene regulation? 212

6.2.1 Gene expression 212
6.2.2 Phosphorylation/dephosphorylation cycles allow resetting of transcription components 216
6.2.3 Example of dynamic regulation of IE gene expression: dynamic acetylation 217

6.3 Future work 218

6.3.1 Gene knockdown and knockout of proteins involved in the MAPK pathways 219
6.3.2 Single cell experiments 221
6.3.3 A simplified biological model 221
6.3.4 Further development for the computational model 222
6.4 Conclusion 224

References 225

List of Figures

Figure 1.1: The French flag model 9

Figure 1.2: Activin, a morphogen during *Xenopus* development 11

Figure 1.3: c-*fos* and c-*jun* promoter regions 18

Figure 1.4: Histone post-translational modifications (PTMs) 24

Figure 1.5: Histone modifications across active c-*fos* and c-*jun* genes 25

Figure 1.6: Mammalian MAPK pathways 32

Figure 1.7: Definition of ultrasensitive enzyme 50

Figure 1.8: Hypothetical switch hypotheses for IE gene regulation 56

Figure 2.1: Western blot quantification by ImageJ 66

Figure 2.2: Example of PRISM representation 75

Figure 3.1: Use of phosphatase and kinase inhibitors to study the reversible phosphorylation in signalling pathways 79

Figure 3.2: OA induces c-*fos* and c-*jun* expression 87

Figure 3.3: OA activates histone H3 phosphorylation and phosphoacetylation 90

Figure 3.4: OA activates p38 phosphorylation but not ERK1/2 phosphorylation 92

Figure 3.5: OA does not prolong EGF activation of ERK1/2 96

Figure 3.6: OA activation of histone H3 is inhibited by SB 203580, SP 600125 and H89 98

Figure 3.7: MSK1 is activated by OA and pre-treatment with SB 203580 does not inhibit this activation 100

Figure 3.8: CREB is activated by OA and is not inhibited after pre-treatment with SB 203580, H89 or SP 600125 102

Figure 3.9: HMGN1 is activated by OA and is inhibited after pre-treatment with SB 203580, H89 or SP 600125 104

Figure 3.10: MEK4 and JNK are not activated by OA 106

Figure 3.11: JNK transcription factors ATF-2 and c-Jun are phosphorylated after OA treatment 108

Figure 3.12: ATF-2 and c-Jun phosphorylation after OA treatment is inhibited by pre-treatment with SP 600125 but not SB 203580 110

Figure 3.13: The potential effects of OA on the p38 pathway revealed in this study 113

Figure 3.14: The potential effects of OA on the JNK pathway revealed in this study 116

Figure 4.1: Activation profiles of c-*fos* and c-*jun* after sAn stimulation obtained by qRT-PCR 129

Figure 4.2: Activation profiles of c-*fos* and c-*jun* after sAn stimulation obtained by Northern blotting 131

Figure 4.3: Induction of the alternative polyadenylated forms on c-*jun* expression profile 134

Figure 4.4: Constant rate of degradation for c-*fos* and c-*jun* 137

Figure 4.5: Effect of superinduction on c-*jun* and c-*fos* characteristic profiles 139

Figure 4.6: Activation profiles of c-*fos* and c-*jun* after OA stimulation 141

Figure 4.7: Pre-treatments with kinase inhibitors reveal difference in c-*fos* and c-*jun* induction 144

Figure 5.1: Abstraction of gene expression 159

Figure 5.2: Schematic representation of the simplified model of the interface between the MAPK pathways and IE gene 163

Figure 5.3: Experimental activation profiles for the JNK and p38 pathways 166

Figure 5.4: Approximation of p38 and JNK activation profiles 170

Figure 5.5: Schematic explanation of the parameters threshold and exponent 174

Figure 5.6: Threshold and exponent effects on the regulation and induction profiles 178

Figure 5.7: Threshold effect on mRNA profile for the binary switch 182

Figure 5.8: Threshold effect on mRNA profile for the continuously variable switch 185

Figure 5.9: Production and degradation rate effects on mRNA profiles for the binary switch 188

Figure 5.10: Production and degradation rate effects on mRNA profiles for the continuously variable switch 191

Figure 6.1: Gene transcription in 8 steps 214

List of Tables

Table 1.1: Simplistic classification and characteristics of the protein phosphatases 41

Table 2.1: Antibody used in Western blotting 59

Table 2.2: Compounds used 60

Table 2.3: Real-time PCR primer sequences and working concentrations 72

Table 5.1: Reaction networks used for computational model 164

Table 5.2: Parameters used to obtain approximation of p38 and JNK activation profiles estimated with COPASI 171

Table 5.3: Maximal and the time of the maximum 189

Table 5.4: Maximal and the time of the maximum 192

Chapter 1: Introduction

1.1 The different biological switching mechanisms

Cells exist in a changing environment and respond to external stimuli rapidly, quantitatively and specifically (Cano et al. 1995; Cohen 1997; Chang and Karin 2001). Understanding how cells can regulate gene expression to produce a quantitative response calibrated to the strength of stimulus remains a challenge (Hazzalin and Mahadevan 2002). This requires regulation of the rate of expression of inducible genes. Most gene induction profiles can be explained by a binary switch, where the gene is considered to be either in an 'off' (no transcription is possible) or an 'on' (transcription happens) stable conformation (Eisenberg and Levanon 2003). However, a more dynamic, continuously variable switch, which sees the rate of initiation of transcription varying with the signal, would better explain graded responses and inducible gene profiles (Hazzalin and Mahadevan 2002). These two types of switches for gene regulation are discussed further in this section.

1.1.1 All-or-nothing responses

The majority of active genes in any given cell are housekeeping and tissue-specific genes. Housekeeping genes have been described as 'always expressed' in most tissues to maintain cellular functions such as gene transcription, protein translation and metabolism (Watson et al. 1965; Adams et al. 1995; Butte et al. 2001). Tissue-specific genes are active only in some types of differentiated cell and serve specific purposes in these particular cells (Warrington et al. 2000; Hsiao et

al. 2001). Thus, housekeeping and tissue-specific genes are constitutively active in all cells and specialised cells respectively.

The development and advances of experimental techniques to measure gene expression have allowed these genes to be identified. Large-scale studies using microarray data (Warrington et al. 2000; Hsiao et al. 2001; Eisenberg and Levanon 2003) or expressed sequence tag (EST) data (Adams et al. 1995) have identified a large number of housekeeping genes and tissue-specific genes. In these studies, level of expression of multiple genes was analysed and compared. The sets of genes considered were composed of genes from different tissues and developmental stages. Genes showing expression in all the cell types studied were identified as housekeeping genes, while the tissue-specific genes were the genes expressed in only a specific subset of cells. The lists of housekeeping genes, depending on the study, range from hundreds to thousands of genes (Warrington et al. 2000; Hsiao et al. 2001; Eisenberg and Levanon 2003; Zhu et al. 2008), with 50 % coverage between studies (Eisenberg and Levanon 2013). These differences can be explained by the limited number of genes and tissue samples considered. Indeed, most of the experiments compared 7,000 genes from fewer than 20 tissue samples.

Technical development in terms of gene quantification not only allowed the identification of these genes, it also raised some divergences concerning the definition of housekeeping genes. Indeed, they are considered to be constitutively expressed in all cells, but should they also be considered to observe a constant level of expression across all tissues? Quantitative gene expression experiments

showed that many genes considered to be housekeeping genes do not present a constant level of expression in all cell types but have specific level for each cell type (Thellin et al. 1999; Lee et al. 2002; Eisenberg and Levanon 2013). This is the case for the housekeeping genes glyceraldehyde-3-phosphate dehydrogenase (*gapdh*) and β-actin (Barber et al. 2005). *gapdh* expression was analysed in 72 human tissues by quantitative reverse-transcription PCR (qRT-PCR). Heart and brain tissues presented high level of *gapdh* expression while pancreatic tissue had low level. The maximum difference found was a 15-fold variation (Barber et al. 2005). Barber et al. (2005) suggested that these differences were due to the role of *gapdh* in the glycolytic pathway. *gapdh* catalyses the reversible oxidative phosphorylation of glyceraldehyde-3-phosphate, which is important for both glycolysis and gluconeogenesis. Its expression would therefore be higher in energy demanding tissues. *gapdh* expression is also induced after treatment with insulin, in insulin-sensitive tissues (Alexander et al. 1988). This illustrates that even the typical housekeeping gene *gapdh* exhibits deviations to the original definition, as its expression changes in response to metabolic variations. This points out the limitations of the housekeeping gene definition towards the complexity behind gene regulation.

For the purpose of this study we will consider that a housekeeping gene is a gene transcribed in all cell types, but that its expression and rate of induction are particular to a cell type and to the culture conditions. Indeed, even though differences of level of expression for some housekeeping genes have been observed, in various studies, from one tissue type to another, their expression is constant in a given cell type (Thellin et al. 1999; Butte et al. 2001; Lee et al. 2002;

Barber et al. 2005; Eisenberg and Levanon 2013). These genes can thus be thought of being transcribed at a reasonably constant rate when in a stable 'on' conformation. In this constitutively active state, it is conceivable that the system supports an intrinsic set rate of transcription for these genes. Thus, for housekeeping and tissue specific genes, gene regulation can be thought of as a binary switch: the gene is either 'off' and not transcribed or 'on' and transcribed at a relatively constant rate.

The induction of a specific gene involves discrete biochemical reactions and low number of molecules (McAdams and Arkin 1999), as there is only one pair of any gene per cell. Thus, a small variation does not average away but can be significant. Single cell experiments have highlighted cell-to-cell variations in background gene expression among cells within a homogeneous population (Kepler and Elston 2001; Blake et al. 2003; Raser and O'Shea 2005; Raj and van Oudenaarden 2008; Raj and van Oudenaarden 2009). These variations are referred to as noise and gene expression is considered to be a stochastic and noisy process. Different sources of noise have been identified: intrinsic fluctuations are due to the randomness inherent to transcription and translation, while extrinsic noise corresponds to the fluctuations in other cellular components (Elowitz et al. 2002; Ozbudak et al. 2002; Swain et al. 2002; Raser and O'Shea 2004). In eukaryotes, transcriptional burst, which consists of the gene transitioning between states of transcriptional activity and inactivity, and chromatin remodelling have been suggested as important sources of intrinsic noise (Becskei et al. 2005; Chubb et al. 2006; Raj et al. 2006; Warren et al. 2006; Raj and van Oudenaarden 2008). Noise in gene transcription confers genetic variability as shown in single cell analysis using fluorescently labelled probes for hybridization (Levsky et al. 2002), or using

reporter genes (Takasuka et al. 1998; Sigal et al. 2006), or single-cell PCR (Warren et al. 2006; Hayashi et al. 2008; Diercks et al. 2009). Analysis of gene regulation at the population level conceals this variability as a result of averaging across the population (Shalek et al. 2013) and can be misleading. As well as masking molecular heterogeneity, population studies generate assumptions on the behaviour of the individual by extrapolation of the data of the population level to the single cell level. Thus if two cells within a population express distinct genes at the single cell level, it could be miss-interpreted as co-expression at the population level (Bengtsson et al. 2005; Stahlberg and Bengtsson 2010).

As a consequence, an 'on/off' gene expression profile at single cell level can appear as a graded one at population level, due to the variability in individual cell responses and noise in gene expression. However, in order to investigate the link between signalling pathway and gene regulation in the same model and because synchronisation and the presence of negative feedbacks in the system (see Section 1.4.3) reduce the importance of noise (Becskei and Serrano 2000; Raser and O'Shea 2005; Austin et al. 2006; Dublanche et al. 2006), we have used synchronised cell culture and population level data in this thesis (further detailed in Section 4.1.1). Nevertheless, additional investigations at single cell level would be needed to complete the study presented in this thesis (see Section 6.3.2). It is important to emphasis that for the use of our model to closely analyse events at the interface between signalling and gene initiation, it is essential that the model pertains to events in a single cell, rather than in a population.

1.1.2 Continuously variable switches

In specific contexts, such as morphogenesis in developing embryos, cells respond to external stimuli by eliciting a graded response, which depends on the signal perceived (Gurdon and Bourillot 2001). This concept is further detailed in this section through the example of graded response observed in *Xenopus* embryos.

1.1.2.1 Definition of morphogen

A morphogen is a signalling molecule, which by forming a gradient of concentration determines the arrangement and fate of responding cells, referred to as pattern formation (Wolpert 1969). With pattern formation comes the concept of positional information for a cell. Indeed, pattern formation is concerned with the spatial arrangement of the cells. In a developing system, the position of a cell may be defined with respect to one or more points in the system, which constitutes positional information (Wolpert 1969). Cells defined with respect to the same points form a field. The cells are considered identical in the field, and are organised into patterns under the morphogen action. Each cell reacts differently depending on its position in the field, i.e. depending on the concentration of morphogen that it perceives (Wolpert 1969).

However, the positional information is an abstract concept and assumes a morphogen gradient in its steady state. But gradient formation is a dynamic process; a gradient needs time to achieve its steady state (Gurdon and Bourillot 2001; Kutejova et al. 2009; Wartlick et al. 2009). Thus, cells can be exposed to varying concentrations of morphogen: cells nearest to the source of morphogen

could perceive increasing concentration of morphogen. The temporal dynamics of the cellular response to a morphogen gradient has been suggested to be a consequence of multiple factors such as temporal alterations to the morphogen gradient itself, the dynamics of the signal transduction and transcription (Kutejova et al. 2009). It is, however, still unclear how cells interpret a dynamic gradient. They could respond to the gradient only once it reached its steady state or after a specific time, or they could continuously adapt their responses and gene expression with time (Gurdon and Bourillot 2001). The latter seems more likely as it has been shown that different morphogen target genes are expressed successively. This is the case for Dpp signalling in Drosophila wing, where *sal* and *omb* are induced successively (Lecuit and Cohen 1998). To better understand the interpretation of a morphogen gradient, quantitative monitoring of the transduction of the response to the morphogen gradient in single cell and in real time or at specific time would be needed rather than measurements with a static gradient.

Several conditions have to be respected in order to identify a signalling molecule as a morphogen (reviewed in Gurdon and Bourillot 2001). First of all, a concentration gradient of this signalling molecule, starting from a source, needs to exist over a population of close and distant cells. Secondly, the response from the cells to the signalling molecule has to be direct, and not require protein synthesis. Thirdly, different quantitative responses depending on the concentration of the signalling molecule need to be observed in the field of cells. Finally, over- or under-expression of morphogen should affect gene expression in the direction of high-concentration response or low-concentration response, respectively.

1.1.2.2 The French flag model

The French flag model was first proposed by Lewis Wolpert in 1967 and abstracts the definition of a morphogen. In this model, cells are considered arranged in a field and have the option of choosing between three states of differentiations depending on the concentration of morphogen they perceive (Wolpert 1969). The French flag problem appears to require the presence of a mechanism specifying polarity, such as a morphogen forming a concentration gradient in a field of identical cells, and a mechanism for regulating the differential response of the cells, such as thresholds (Wolpert 1969). In the example in Figure 1.1, assuming that cells at the origin secrete a morphogen that diffuses across the field, generating a concentration gradient of morphogen, two thresholds are required. The concentrations above threshold 1 elicit the blue response, the concentrations below threshold 1 and above threshold 2 elicit the white response, and the concentrations below threshold 2 or absence of morphogen detection elicit the red response (Figure 1.1). The cells in the field must have a receptor-based mechanism in order to allow a specific and concentration-dependent re-programming of gene transcription. Understanding how gene transcription is quantitatively re-programmed to elicit a response calibrated to the signal perceived remains a challenge.

1.1.2.3 Activin elicits different cell fate decisions in the Xenopus embryo

An example of morphogenesis is seen during *Xenopus* development. It has been shown that *Xenopus* blastula cells are exposed to a concentration gradient of activin during development and that gene expression is re-programmed in an

Figure 1.1: The French flag model

Abstraction of the notion of morphogen using the French flag model. A row of cells is represented at the bottom part. Assuming that the cells at the origin diffuse a morphogen to the right, a gradient of morphogen concentration is created represented on the graph (top). The cells have the choice between three cell fate decisions, represented by the colours blue, white and red, depending on the concentration of morphogen perceived. Concentrations above threshold 1 produce a 'blue' response, concentrations above threshold 2 and below threshold 1 exhibit a 'white' response, and concentrations below threshold 2 or absence of morphogen detection lead to a 'red' response.

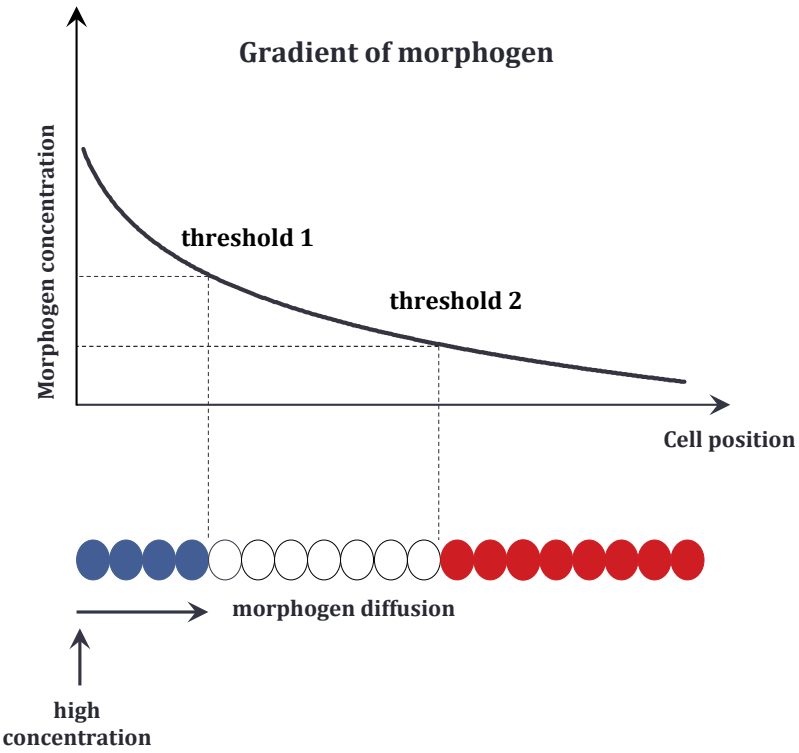
Gradient of morphogen
Morphogen concentration
threshold 1
threshold 2
Cell position
morphogen diffusion
high
concentration

activin concentration dependent way (Green and Smith 1990; Green et al. 1992). By exposing dissociated *Xenopus* blastula cells to different concentrations of activin, Green and Smith showed that this factor is instructive and specifies different types of cells; activin can thus be defined as a morphogen. The different types of cells were characterised through the analysis of expression of a spectrum of mesoderm-specific genes. At low or zero doses of activin, cells expressed epidermal keratin, specific to epidermis cells; at slightly higher doses, posterolateral mesoderm specific genes were expressed (*XIHbox6*, *Xbox3* and *Xbra*); at high doses of activin aggregate formed muscle, as muscle-specific actins were detected; at even higher doses an expression of *Xbra* was detected as well as the expression of *goosecoid* (*gsc*) indicating the formation of the Notochord; and finally at very high doses of activin expression of *gsc* alone was detected, expressed in the dorsal lip or 'organiser' (Green et al. 1992, Figure 1.2 A).

Similar observations have been reported in normal tissue rather than dissociated cells confirming activin in its role of morphogen in *Xenopus* embryo (Gurdon et al. 1994). By constructing various animal cap conjugates, which consists of isolating the animal cap to identify the signals inducing it to form the mesoderm (Slack 1991; Gurdon et al. 1994), three levels of responses have been observed: nearest to the signal source, the gene *gsc* is expressed, in the middle distance the gene *Xbra* is expressed and no specific expression is observed further away (Figure 1.2 B).

1.1.2.4 Notion of threshold and gradual response

From this concept, where cells have different responses to signalling molecule concentrations, comes the notion of threshold. Indeed, a specific concentration of

Figure 1.2: Activin, a morphogen during *Xenopus* development

Identification of activin as a morphogen during *Xenopus* development by experiments with (A.) dispersed cells and (B.) animal cap conjugates.

A. The different fates observed after exposing dispersed cells to a specific concentration of activin are specified in the table (Green and Smith 1990).
B. Closer to the source of activin *gsc* expression is observed, while *Xbra* expression is detected further away from the source (Gurdon et al. 1994).

A.

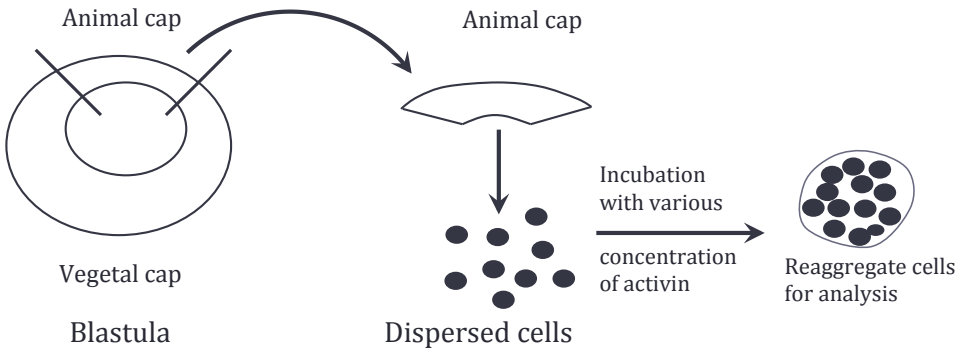

low → high [activin]

epidermal keratin	*XIHbox6, Xbox3, Xbra*	muscle-specific actin	*Xbra, gsc*	*gsc*
epidermis cells	posterolateral mesoderm	muscle	Notochord	'organiser'

B.

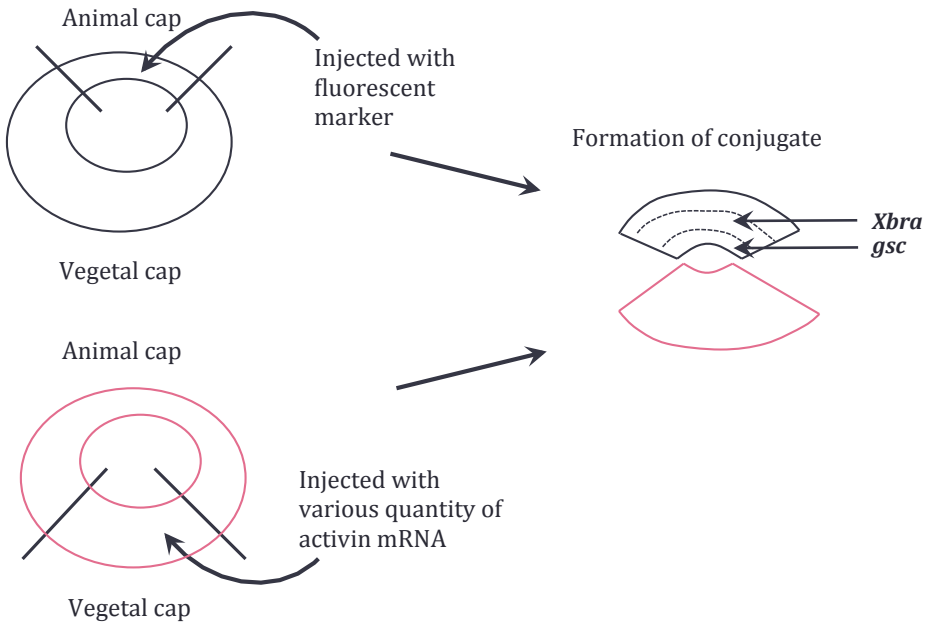

factor, constituting the threshold, is needed to specify how cells, depending on the concentration of factor perceived in respect to this threshold, should react. A cell could be considered to have two options: respond or not. In this view, a binary switch would fit perfectly, the threshold acting as a trigger to switch the response 'on' or 'off' the response. However, as seen in the example described above and in other morphogen examples such as Decapentaplegic (Dpp) in *Drosophila* (Zecca et al. 1995), a morphogen can elicit at least three different cell fates, showing that a more complex response than an 'on/off' switch is necessary. A more gradual and quantitative response calibrated to the concentration of morphogen would better explain the specific gene expression observed depending on the signal perceived. Gene expression would then no longer be switched to the 'on' state in a stable manner. It would be a more dynamic process directly coupled to the strength and duration of the signal.

1.2 Immediate-early genes: specific transcription due to their direct link to signalling pathways

Immediate-early (IE) genes are an example of inducible genes, defined as being directly linked to biochemical pathways (Cohen 1997; Kyriakis and Avruch 2001). These specific genes are induced through various signalling pathways to elicit the appropriate cell decision after stimulation (Cohen 1997; Chang and Karin 2001; Kyriakis and Avruch 2001). The promoter regions of IE genes contain multiple transcription factor (TF) binding sites (reviewed in Treisman 1996; Kyriakis and Avruch 2001). Therefore, these genes can be induced by various signalling pathways and constitute a means for convergence of signals (Treisman 1996;

Davies et al. 2000). They produce signal-calibrated responses and are thus a good biological model to study the quantitative regulation of gene expression.

1.2.1 The characteristics of immediate-early gene expression

1.2.1.1 IE gene induction is transient and rapid

Immediate early genes (Lau and Nathans 1987; Almendral et al. 1988), or 12-O-tetradecanoylphorbol-13-acetate (TPA)-inducible sequences (Angel et al. 1987; Lim et al. 1987), have been identified by differential screening of complementary DNA (cDNA) library prepared from RNA of resting cells exposed to serum or growth factors (Foster et al. 1982; Cochran et al. 1983; Linzer and Nathans 1983; Hirschhorn et al. 1984; Forsdyke 1985; Zhou et al. 1995). IE genes are the first genes to be transcribed after stimulation (Lau and Nathans 1987; Almendral et al. 1988; Bravo 1990; Thomson et al. 1999). Many of them, including c-*fos* and c-*jun*, encode transcription factors, which control the expression of other genes and thus elicit the secondary response to stimulation (Halazonetis et al. 1988; Hai and Curran 1991; Ryseck and Bravo 1991). IE genes are transcribed even in the presence of protein synthesis inhibitors such as cycloheximide and anisomycin (Lau and Nathans 1985; Greenberg et al. 1986), showing that they do not require synthesis of new proteins. This illustrates their direct link to signalling pathways; all the elements required for their induction are already present in quiescent cells.

Due to their direct link to internal signalling pathways, IE gene induction is rapid. c-*fos* transcription, for example, starts within 5 min after stimulation with growth factors and it is at its highest point after 10 min (Greenberg and Ziff 1984; Kruijer

et al. 1984; Muller et al. 1984). Similar results are observed for c-*jun*, its transcription increases after 15 min and peaks at 60 min (Lamph et al. 1988; Quantin and Breathnach 1988; Ryseck et al. 1988).

Besides being rapid, c-*fos* and c-*jun* induction is transient. After 15 min of stimulation with growth factors, c-*fos* transcription starts to decrease and returns to its initial level within 30 min (Greenberg and Ziff 1984; Kruijer et al. 1984; Muller et al. 1984). Similar results are observed for c-*jun*, which goes back to pre-stimulation level after 2 h (Lamph et al. 1988; Quantin and Breathnach 1988; Ryseck et al. 1988). Compared to other genes which are transcribed for hours or more, the IE genes observed a limited, rapid induction. The direct link between IE genes and signalling pathways, as well as the negative regulation they exercise on the mitogen activated protein kinase (MAPK) pathways (Keyse and Emslie 1992; Sun et al. 1993; Zheng and Guan 1993) confer them a rapid and transient induction; they can be turned 'on' and 'off' within minutes. The transient expression of IE gene transcripts is also explained by their extreme instability (Edwards and Mahadevan 1992).

1.2.1.2 IE gene induction is quantitative and specific

IE genes have been shown to be induced by different external stimuli such as growth factors and stress (Herschman 1991; McMahon and Monroe 1992; Hibi et al. 1993; Kyriakis et al. 1994; Rouse et al. 1994; Cano et al. 1995; Gupta et al. 1995; Livingstone et al. 1995; Marshall 1995; van Dam et al. 1995). These various stimuli produce different and highly reproducible profiles of gene induction, with a single gene displaying different and specific profiles for each stimulus and a

stimulus inducing a specific pattern of IE gene induction, affecting each gene differently (Cooper 1994; Cano et al. 1995; Cano and Mahadevan 1995; Seger and Krebs 1995; Hazzalin et al. 1997; Hazzalin and Mahadevan 2002). As these experiments have been carried out at the population level, rather than indicating a synchronous response of every cell, the profiles observed here could be the result of the summation of slightly distinct responses of individual cells that collectively make up these profiles (see Section 1.1.1).

In addition to being specific to the stimulus and gene, the induction profiles of IE genes are quantitative. Indeed, IE gene induction is dependent on the strength and latency of the incoming stimulus. Different concentrations of the same stimulus produce a different induction profile (Almendral et al. 1988; Cano et al. 1995; Hazzalin et al. 1997; Hazzalin et al. 1998). Understanding how this specific and quantitative response is produced is made harder by the presence of multiple TF binding sites at the promoter regions of IE genes, allowing for the possibility of cumulative activation (see Section 1.2.3; Treisman 1996; Kyriakis and Avruch 2001).

1.2.2 The *jun* and *fos* families

1.2.2.1 The jun *family*

The *jun* family is composed of three members in mammals: c-*jun*, *jun*B and *jun*D (reviewed in Herdegen and Leah 1998). *jun* was first described as the oncogene of the avian sarcoma virus 17 (Maki et al. 1987). c-*jun*, isolated from human cells (Bohmann et al. 1987), is an intronless gene localized on the chromosome 1

(Hattori et al. 1988). It has 50% identity with *jun*B and *jun*D (Hirai et al. 1989; Nomura et al. 1990). The three members of the *jun* family are transiently induced following stimulation (Kovary and Bravo 1991; Hill and Treisman 1995). They have different basal levels of expression, with *jun*D having a high basal level due to the presence of an octamer motif in its promoter (Herdegen and Leah 1998).

1.2.2.2 The fos *family*

The *fos* family counts four members: c-*fos*, *fos*B and the two *fos* related antigen *fra*1 and *fra*2, presenting less similarity to c-*fos* than *fos*B (Herdegen and Leah 1998). *fos* was first described as the oncogene of the Finkel-Biskis-Jinkins murine osteogenic sarcoma virus (Curran and Teich 1982) before its cellular homologue was described (Curran et al. 1983) and characterised as a nuclear protein (Curran et al. 1984). The different members of the *fos* family exhibit various induction profiles (Bartel et al. 1989; Gruda et al. 1994). While c-*fos*, *fos*B and *fra*2 are relatively transiently induced, *fra*1 has a prolonged expression and stays at its maximum after 8 hours of stimulation.

1.2.3 The role of transcription factors in IE gene induction

The promoter regions of IE genes contain different regulatory elements. These regulatory elements are specific DNA sequences recognised by TFs. By binding to the promoter region of the genes, the TFs regulate their expression (reviewed in Sng et al. 2004).

TFs regulate gene transcription in different ways. For example, they can directly recruit the transcriptional machinery (reviewed in Fuda et al. 2009), or they can recruit chromatin-remodelling proteins (Kuo and Allis 1998; Sterner and Berger 2000), which by modifying the structure of the chromatin allows access of other factors to DNA or by modifying histones form binding platforms recognised by regulatory proteins. This is the case for the TF cAMP response element binding protein (CREB), which recruits CREB-binding protein (CBP), which was found to possess acetyltransferase activity (Bannister and Kouzarides 1996; Kuo et al. 1996; Ogryzko et al. 1996). p300/CBP mediates the dynamic acetylation of histone H3 tri-methylated on lysine 4 (H3K4me3) which appears to be important for IE gene expression (Crump et al. 2011, see Section 1.2.4).

1.2.3.1 c-fos *promoter region*

The promoter of the proto-oncogene c-*fos* contains multiple regulatory elements including a c-*sis* inducible element (SIE) (Wagner et al. 1990), a serum response element (SRE) (Hayes et al. 1987; Shaw et al. 1989; Treisman 1992), an activating protein 1 (AP-1)-like site, an AP-1/ 3'-5'-cyclic AMP response element (CRE) site (Fisch et al. 1987; Fisch et al. 1989) and a CRE (Sheng et al. 1988; Figure 1.3).

The SIE at -346 bp upstream of c-*fos* transcription initiation site has been found to be specifically inducible by conditioned medium containing platelet-derived growth factor (PDGF)-like growth factor activity (Hayes et al. 1987; Wagner et al. 1990). The transcription factors Signal Transducer and Activator of Transcription (STAT) and TFII-I, activated by serine phosphorylation, bind to this regulatory element (Yang et al. 2003). While the SIE is not necessary for the epidermal growth

Figure 1.3: c-*fos* and c-*jun* promoter regions

Schematic representation of the transcription factors binding sites at c-*fos* and c-*jun* promoter regions. This representation is not on scale.

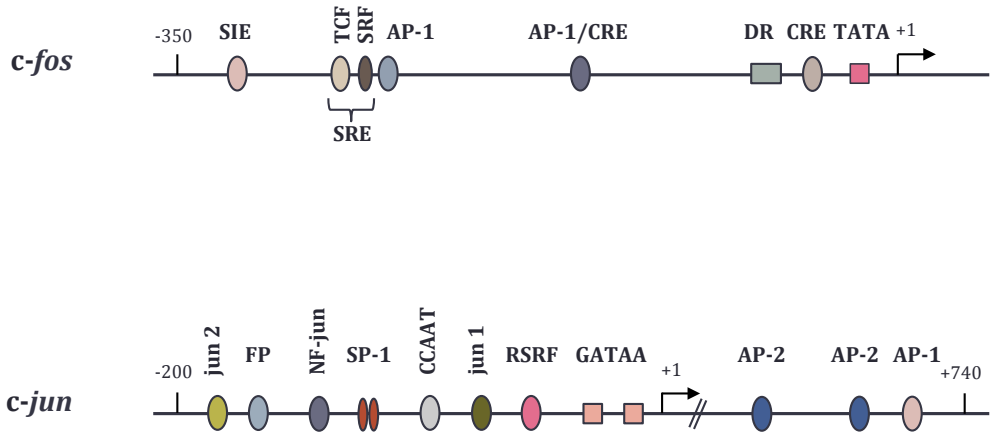
c-fos
-350
SIE
TCF
SRF
AP-1
SRE
AP-1/CRE
DR
CRE
TATA
+1
c-jun
-200
jun 2
FP
NF-jun
SP-1
CCAAT
jun 1
RSRF
GATAA
+1
AP-2
AP-2
AP-1
+740

factor (EGF) and TPA induction of c-*fos* (Leaman et al. 1996), it maximizes this induction (Yang et al. 2003). Moreover, the activation of the protein STAT3 alone induces c-*fos* transcription through the SIE site (Yang et al. 2003).

The SRE of c-*fos* promoter comprises a region of dyad symmetry, recognised by a dimer of serum response factor (SRF), and an E26 transformation-specific (Ets) domain-binding motif, recognised by a member of the ternary complex factor (TCF) family, such as Elk1 (Treisman 1987; Shaw et al. 1989). Results from genomic footprinting experiments suggest that the SRE site is constitutively occupied (Herrera et al. 1989; Treisman 1992). The formation and activation of the ternary complex at the SRE are required for serum, TPA and EGF induction of c-*fos* transcription (Treisman 1985; Gilman et al. 1986; Treisman 1986; Greenberg et al. 1987), its kinetics of phosphorylation and dephosphorylation parallels the activation and repression of c-*fos* (Rivera et al. 1993). The TCF has been shown to be activated by the extracellular signal-regulated kinase (ERK), p38 and Jun N-terminal kinase (JNK) pathways and thus to link c-*fos* induction with MAPK pathways (Marais et al. 1993; Zinck et al. 1993; Gille et al. 1995; Whitmarsh et al. 1995; Hazzalin et al. 1996; Price et al. 1996; Tan et al. 1996; Whitmarsh et al. 1997).

The AP-1-like site located adjacent to the SRF/TCF site has been shown to have a positive effect on c-*fos* induction after EGF and TPA stimulation (Fisch et al. 1989) and cytokines and environmental stresses (Raingeaud et al. 1996). Some experiments showed an auto-downregulation of c-Fos protein on c-*fos* induction after serum stimulation (Sassone-Corsi et al. 1988). It is thought that c-Fos protein

interacts with the SRE ternary complex but there is no evidence of a role for AP-1 in this downregulation, as mutations of this site did not disturb the downregulation (Fisch et al. 1989).

The CRE of c-*fos*, which mediates responses to various stimuli, is bound by CREB (Montminy and Bilezikjian 1987). The activation of CREB is carried out by the protein kinase A (PKA; Chrivia et al. 1993) or by mitogen- and stress-activated protein kinase (MSK1/2; Deak et al. 1998), which phosphorylate CREB at Serine 133. This phosphorylation allows recruitment of the transcription cofactor and lysine acetyltransferase CBP, which interacts with basal transcription factor TFIIB (Chrivia et al. 1993; Arias et al. 1994; Kwok et al. 1994).

1.2.3.2 c-jun *promoter region*

The IE gene c-*jun* is regulated and induced in response to various stimuli through multiple specific sequences located at its promoter region (Angel et al. 1988; Han et al. 1992; Herr et al. 1994; Rozek and Pfeifer 1995). Among these specific sequences, there are two AP-1, NF-jun, SP-1, CCAAT and 'related-to-serum-response-factor' (RSRF) sites as well as two AP-2 and an AP-1 site located after the start site (Figure 1.3).

The IE gene c-*jun* promoter, unlike c-*fos* promoter, does not contain a SRE site, required for induction by serum and other inducing agents, but a RSRF (Han et al. 1992). This site, located at -59 bp upstream of c-*jun* start site, is also referred to as MEF2 site (Han and Prywes 1995). It has been shown to be sufficient to mediate

EGF, TPA and serum induction of c-*jun* (Han et al. 1992). Moreover the RSRF site is found to be crucial for EGF induction of c-*jun* (Han et al. 1992).

The two AP-1 or TPA-responsive element sites, jun1 and jun2 mediate TPA induction (Angel et al. 1987; Chiu et al. 1987; Lee et al. 1987). The transcription factor c-Jun binds to AP-1 site as a homodimer or heterodimer, jun1 binds Jun:Jun, Jun:Fos and Jun:ATF2 complexes while jun2 predominantly binds Jun:ATF2 dimers (see Section 1.2.3.3; Herdegen and Leah 1998). The AP-1 sites of c-*jun* promoter thus mediate a positive autoregulatory loop, the IE gene c-*jun* positively regulates its own transcription through the AP-1 sites (Angel et al. 1988). ChIP evidence (Bruna et al. 2003) and genomic footprinting analysis (Herr et al. 1994) suggests that jun1 and jun 2 are permanently occupied by c-Jun. As RSRF, the AP-1 sites have been shown to be sufficient to mediate EGF and serum induction, the level of induction being different for both regulatory elements (Han et al. 1992), as well as ultraviolet (UV) and stress responses (Derijard et al. 1994; Kyriakis et al. 1994; Gupta et al. 1995; Livingstone et al. 1995; Raingeaud et al. 1995; van Dam et al. 1995).

1.2.3.3 Transcriptional regulation with multiple levels of control

As seen by the examples of c-*fos* and c-*jun*, IE genes are controlled by multiple regulatory elements. These regulatory elements are bound by specific TFs to transactivate IE genes (see section 1.2.3.1 and 1.2.3.2). This regulation allows induction of IE genes under different conditions and multiple levels of control for their induction.

The presence of multiple regulatory elements around the promoter region can lead to various combinations and thus specific induction (Treisman 1996; Kyriakis and Avruch 2001). This is illustrated by the fact that both AP-1 and RSRF sites of c-*jun* promoter have been shown to be individually sufficient for EGF, serum and TPA induction (Han et al. 1992). However, the level of the induction observed differs when the sites are considered independently or in combination (Han et al. 1992). Similar results are observed for the SIE site of c-*fos*, which maximises the EGF and TPA induction (Yang et al. 2003).

Most of the TFs bind to DNA as homo- or heterodimers and some regulatory elements are selective towards these TF complexes, the transcription factor AP-1, which are homodimers or heterodimers comprised of TFs from the Jun, Fos and ATF families, organised into Jun-Jun, Jun-Fos, or Jun-ATF dimers, is an example of this level of control (Nakabeppu et al. 1988; Ryseck and Bravo 1991). The AP-1 complexes, as they contain a member of the Jun family, can bind to the regulatory element TRE (Karin et al. 1997), however the heterodimers containing ATF2 preferentially bind to the CRE (Karin et al. 1997). A difference in IE gene expression can lead to the formation of different TF complexes by changing the ration of complex components, and thus activates distinct biological responses as the different complexes present various DNA binding affinities (Hai and Curran 1991; Kovary and Bravo 1991; Ryseck and Bravo 1991; Kovary and Bravo 1992; Cook et al. 1999).

1.2.4 The role of histone modifications in IE gene regulation

In eukaryotic cells, DNA is compacted into chromatin (McGhee and Felsenfeld 1980). The elementary subunit of chromatin structure is the nucleosome. It consists of 146 base pairs of DNA wrapped around an octamer consisting of two each of the four core histones H2A, H2B, H3 and H4 (McGhee and Felsenfeld 1980). The linker histone, histone H1, interacts with the nucleosome to further compact chromatin (Robinson and Rhodes 2006).

1.2.4.1 Histone tails and post-translational modifications

The crystal structure of the nucleosome has revealed that the histone octamer can be divided into two H2A-H2B dimers facing two H3-H4 dimers (Richmond et al. 1984; Luger et al. 1997). The N-terminal regions, and in some cases C-terminal regions of the core histones, are not required for complex formation (McGhee and Felsenfeld 1980). The tails of all eight histones protrude from the core nucleosome and are thus accessible for post-translational modification (PTM, Figure 1.4). These histone PTMs, such as lysine and arginine methylation, lysine acetylation (see Section 1.2.4.2), and serine and threonine phosphorylation (see Section 1.2.4.3), display specific distributions (reviewed in Lee and Mahadevan 2009), for example upon induction tri-methylated H3K4 (H3K4me3), H3K36me3 and di-methylated H3K79 (H3K79me2) have a specific distribution across c-*fos* and c-*jun* (Edmunds et al. 2008). As can be observed after EGF stimulation (Figure 1.5 A; Edmunds et al. 2008), c-*fos* and c-*jun* genes present a similar profile of histone modifications; a profile of typical histone modifications associated with active genes is presented Figure 1.5 B.

Figure 1.4: Histone post-translational modifications (PTMs)

A. Schematic representation of the nucleosome, the histones tails protrude from the core nucleosome and are the targets of PTMs.
B. Representation of three PTMs. Acetylation (1) and methylation (2) target lysine residues, while phosphorylation (3) targets serine residues. KAT and HDAC stand for lysine acetyltransferase and histone deacetylase respectively. KMT and KDM stand for lysine methyltransferase and lysine demethylase respectively.

A.

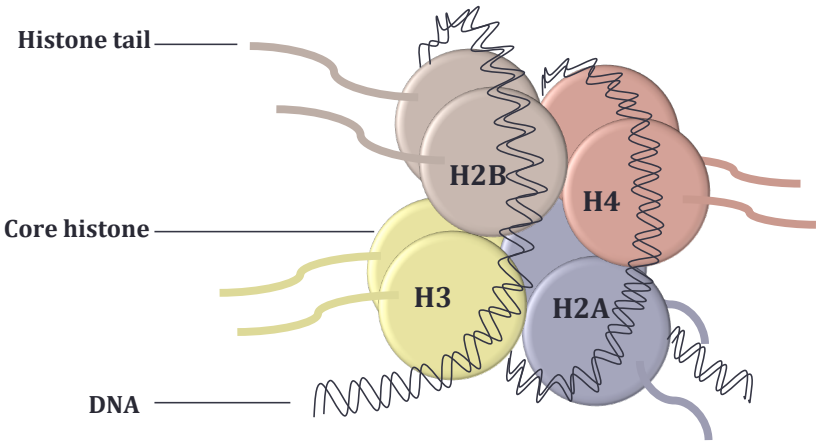
Histone tail
Core histone
DNA
H2B
H4
H3
H2A

B.

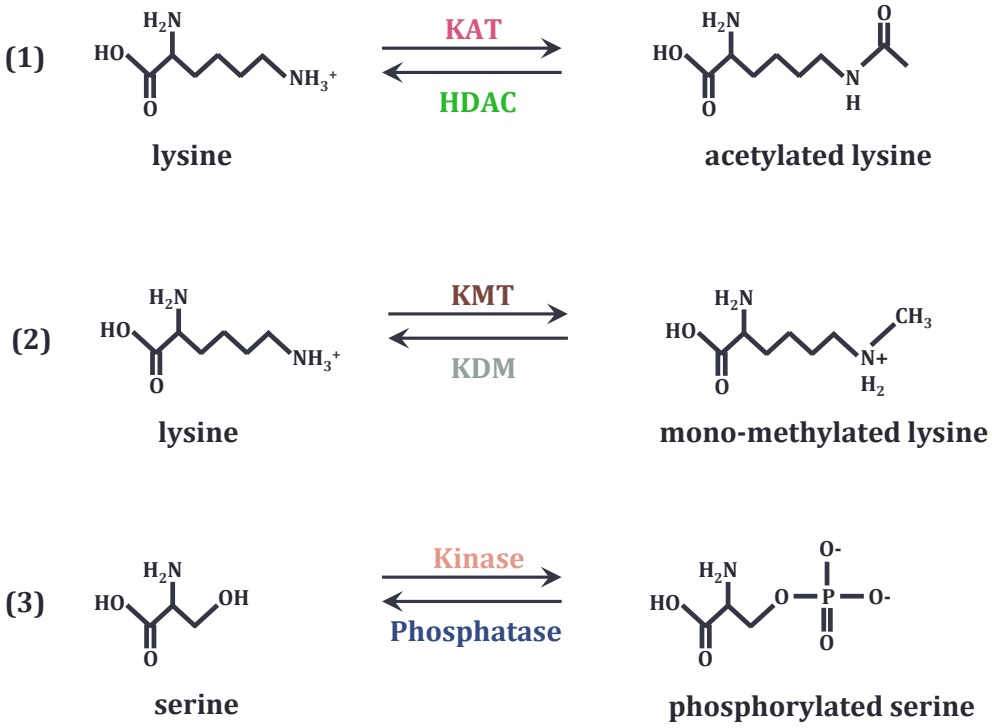
(1)
KAT
HDAC
lysine
acetylated lysine
(2)
KMT
KDM
lysine
mono-methylated lysine
(3)
Kinase
Phosphatase
serine
phosphorylated serine

Figure 1.5: Histone modifications across active c-*fos* and c-*jun* genes

Distribution of histone modifications associated with active c-*fos* and c-*jun*. Histone H3 (H3) is methylated (me), di-methylated (me2), tri-methylated (me3) or acetylated (ac) on indicated lysine (K) residues, and phosphorylated (ph) on serine (S) residue.

A. Distribution of acetylated and methylated histone H3 across c-fos and c-jun after EGF stimulation. Quiescent C3H 10T½ cells were untreated (black line, control) or stimulated with EGF (50 ng/ml) for 15 (red line), 30 (green line), 60 (light blue line) or 120 (dark blue line) minutes. Formaldehyde crosslinked mononucleosomes were prepared for ChIP. Aliquots of chromatin were immunoprecipitated with H3K9ac (i), H3K4me3 (ii), H3K36me3 (iii) or H3K79me2 (iv) specific antibodies. Recovered DNA sequences were quantified by real-time PCR. Figure taken from (Edmunds et al. 2008).

A.

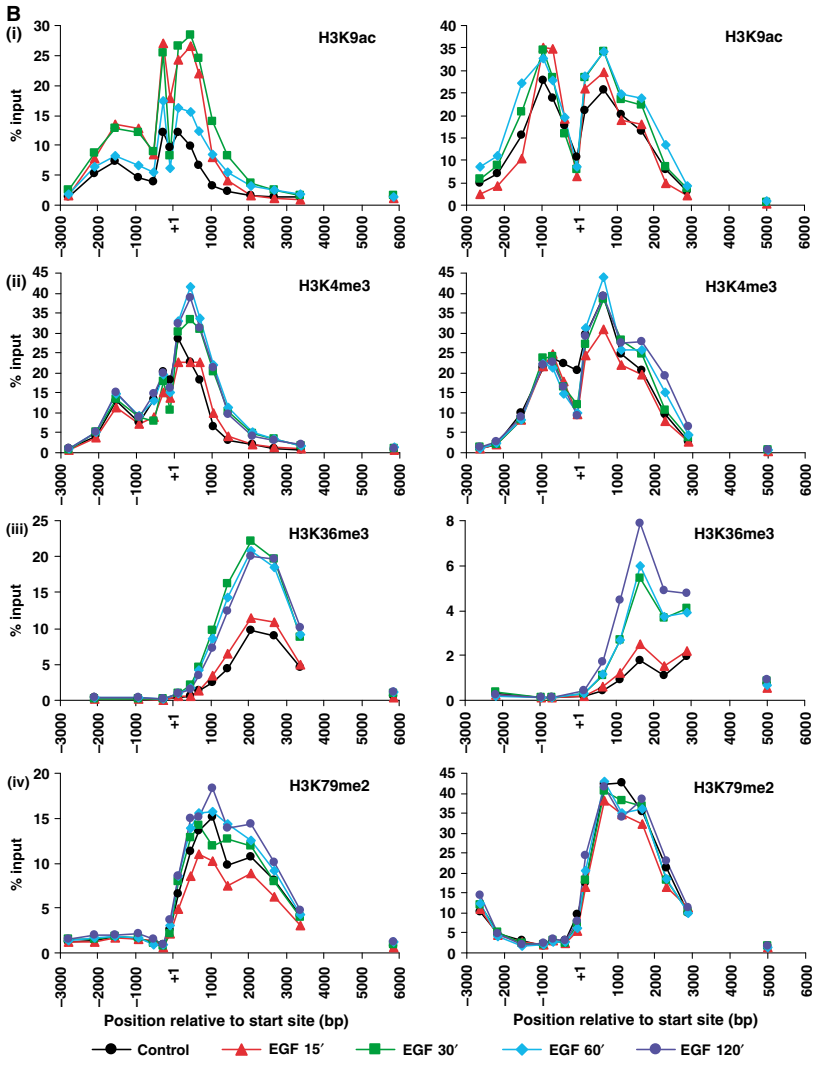
B
(i)
H3K9ac
(ii)
H3K4me3
(iii)
H3K36me3
(iv)
H3K79me2
% input
Position relative to start site (bp)
Control
EGF 15′
EGF 30′
EGF 60′
EGF 120′

Figure 1.5: Histone modifications across active c-*fos* and c-*jun* genes

Distribution of histone modifications associated with active c-*fos* and c-*jun*. Histone H3 (H3) is methylated (me), di-methylated (me2), tri-methylated (me3) or acetylated (ac) on indicated lysine (K) residues, and phosphorylated (ph) on serine (S) residue.

B. Schematic representation of the distribution of typical histone modifications associated with active c-*fos* and c-*jun*. Adapted from (Thomson et al. 2001; Edmunds et al. 2008; Lee and Mahadevan 2009).

B.

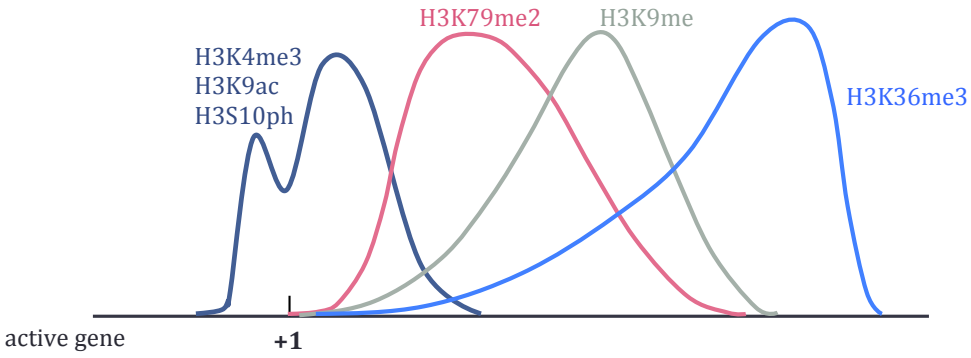
H3K79me2
H3K9me
H3K4me3
H3K9ac
H3S10ph
H3K36me3
active gene
+1

Histone PTMs are associated with various biological phenomena such as transcription, DNA compaction and DNA synthesis (reviewed in Campos and Reinberg 2009). The variety of biological outputs associated with the same or similar histone PTMs raised the question: how can the same histone modification control two different biological phenomena? Histone H3 serine 10 phosphorylation is associated with IE gene induction (Thomson et al. 1999) as well as mitotic chromosome condensation (Hendzel et al. 1997; Wei et al. 1999). This suggests that a single histone motif does not function alone, and a combination of modifications may recruit specific binding proteins fundamental for biological functions (Taverna et al. 2007). This observation led to a histone code hypothesis (Strahl and Allis 2000; Turner 2000). This hypothesis considers that histone PTMs act in combination to specify a downstream function. It links histone modifications to a specific biological output. However, a signalling network model of chromatin hypothesis has also been proposed (Schreiber and Bernstein 2002). In this model, the combination of multiple histone modifications is believed to confer bistability, robustness and adaptability to the system.

1.2.4.2 Histone acetylation

Histone lysine residues can be acetylated (Allfrey et al. 1964); this is a dynamic process (Forsberg et al. 2000; Hazzalin and Mahadevan 2005) controlled by histone acetyltransferases (HATs), which add the acetyl group, and histone deacetylases (HDACs), which remove the acetyl group. H3K4me3 is subject to dynamic acetylation at all lysine residues, excluding lysine 4 (Hazzalin and Mahadevan 2005). This characteristic is evolutionarily conserved and has been shown to be mediated by p300/CBP (Crump et al. 2011). Moreover, dynamic

acetylation seems to be essential for RNA polymerase II association and IE gene induction, linking histone acetylation to gene regulation (Crump et al. 2011).

The loss of the lysine positive charge by the addition of an acetyl group reduces the affinity of histone tails for DNA, resulting in changes in DNA compaction and accesibility (Eberharter and Becker 2002). Acetylated lysine residues have also been shown to form platforms allowing the recruitment of various effectors involved in gene regulation via bromodomains (Dhalluin et al. 1999; Zeng and Zhou 2002), making histone acetylation an important modification in gene induction. Acetylation has been associated with transcription of both housekeeping and inducible genes (Allegra et al. 1987; Chen and Allfrey 1987; Sterner et al. 1987; Boffa et al. 1990; Hebbes et al. 1994) and the protein involved in acetylation have been shown to interact with the transcriptional machinery (Abraham et al. 1993; Kee et al. 1996; Dallas et al. 1997; Nakajima et al. 1997a; Nakajima et al. 1997b; Neish et al. 1998); some HATs were even first described as TFs (Chrivia et al. 1993; Kwok et al. 1994; Brownell et al. 1996).

1.2.4.3 Histone phosphorylation

Phosphorylation of histone H3 on serine 10 (H3S10ph) was first associated with mitotic phosphorylation on condensed chromosome, phosphorylated by the kinase Aurora B (Clayton and Mahadevan 2003). A second mode of H3S10ph has been described: a minute fraction of histone H3 associated with IE genes is transiently phosphorylated on serine 10 concomitantly with gene induction (Mahadevan et al. 1991). The nucleosomal response, which consists of the phosphorylation of histone H3 at serine 10, and of the high mobility group nucleosome binding

domain 1 (HMGN1) on serine 6, is coupled with IE gene induction (Mahadevan et al. 1991; Barratt et al. 1994; Thomson et al. 1999). This response involves the ERK and p38 MAPK pathways. The downstream kinases of ERK and p38, MSK1/2, have been shown to phosphorylate histone H3 and HMGN1 *in vitro* (Thomson et al. 1999) and *in vivo* (Soloaga et al. 2003).

Members of the phospho-serine adaptor 14-3-3 family have been identified by affinity chromatography of nuclear extracts as phosphorylated histone H3 binding proteins (Macdonald et al. 2005; Walter et al. 2008; Winter et al. 2008). Chromatin immunoprecipitation (ChIP) experiments showed that 14-3-3ζ is recruited to c-*fos* and c-*jun* upon gene activation (Macdonald et al. 2005). The 14-3-3 proteins form homo- or heterodimers proteins presenting two sites of phosphorylation binding thus, 14-3-3 may interact with phosphorylated histone H3 and recruit another phosphorylated protein required for gene induction (Macdonald et al. 2005).

Histone H3 serine 28 constitutes another phosphorylation site. Like histone H3 serine 10, it is associated with mitotic phosphorylation under the action of Aurora B kinase (Goto et al. 1999; Goto et al. 2002) and MAPK pathway-mediated phosphorylation, via MSK1/2 (Soloaga et al. 2003). Although serine 10 and serine 28 phosphorylated histone H3 present similar profiles and share characteristics, they are targeted to different pools of histone H3, and may thus carry different functions (Dyson et al. 2005).

1.2.4.4 Histone phosphoacetylation

Even though acetylation and phosphorylation of histone are regulated independently (Thomson et al. 2001), studies using antibodies that recognise both or a single modification showed that the same histone tails can be simultaneously phosphorylated and acetylated (Cheung et al. 2000; Clayton et al. 2000). ChIP assays revealed that upon gene activation, nucleosomes at IE gene promoters, typified by c-*fos* and c-*jun*, were phosphoacetylated, phosphorylation and acetylation being independently targeted to the same nucleosomes (Clayton et al. 2000). Moreover, phosphorylation of histone H3 by MAPK pathways has been shown to be targeted to a minute fraction of total histone sensitive to hyperacetylation when treated with histone deacetylase inhibitor, such as trichostatin A (TSA; Barratt et al. 1994).

Other crosstalk between histone phosphorylation and acetylation has been reported. Indeed, 14-3-3 binding affinity to phosphorylated serine 10 histone H3 increases if the histone H3 is also acetylated on lysine 4 or 16 (Macdonald et al. 2005; Walter et al. 2008; Winter et al. 2008). Moreover, histone H3 serine 10 phosphorylation has been shown to enhance recruitment of the HAT GCN5, which acetylates histone H3 on lysine 14 (Cheung et al. 2000; Agalioti et al. 2002). Once again, crosstalk between PTMs is revealed to be important for biological mechanisms, pointing towards the theory of the existence of a histone code.

1.3 MAPK signalling pathways

In order to respond rapidly and specifically to various external stimuli, cells activate internal pathways regulating gene transcription. The mitogen activated protein kinase (MAPK) cascades, conserved through evolution (Lange-Carter et al. 1993), are one example of such internal pathways, involved in regulation of multiple processes such as cell proliferation, cell differentiation and apoptosis (Chang and Karin 2001; Kyriakis and Avruch 2001). They are controlled by reversible phosphorylation and respond to different signals, including growth factors and stress, by inducing IE gene transcription (Edwards and Mahadevan 1992; Hibi et al. 1993; Freshney et al. 1994; Kyriakis et al. 1994; Rouse et al. 1994; Cano et al. 1995; Gupta et al. 1995; Marshall 1995; Hazzalin et al. 1996; Figure 1.6).

1.3.1 MAPK pathways transduce signals to nucleus through a three-tiered organisation

MAPK signalling is activated by multiple phosphorylation events and the three-tiered organisation of the core signalling module is common to all the pathways (Widmann et al. 1999). MAPKs are activated by MAPK kinases (MAPKKs), which are activated by MAPKK kinases (MAPKKKs; Marshall 1994). Multiple MAPK pathways are active in mammalian cells, the four best characterised ones being: the extracellular signal-regulated kinase (ERK) 1/2 pathway, the p38 pathway, the Jun N-terminal kinase (JNK) pathway and the big mitogen-activated protein kinase (BMK) 1, also referred to as ERK5, pathway (Chang and Karin 2001; Kyriakis and Avruch 2001; Johnson and Lapadat 2002; Figure 1.6).

Figure 1.6: Mammalian MAPK pathways

Schematic representation of the four main MPAKs and their substrates including transcription factors, downstream kinases and nucleosomal proteins. The four MAPKs are the extracellular-signal regulated protein kinase (ERK), the stress p38 kinases (p38), the c-Jun amino-terminal kinase (JNK) and big MAPK (BMK/ERK5)

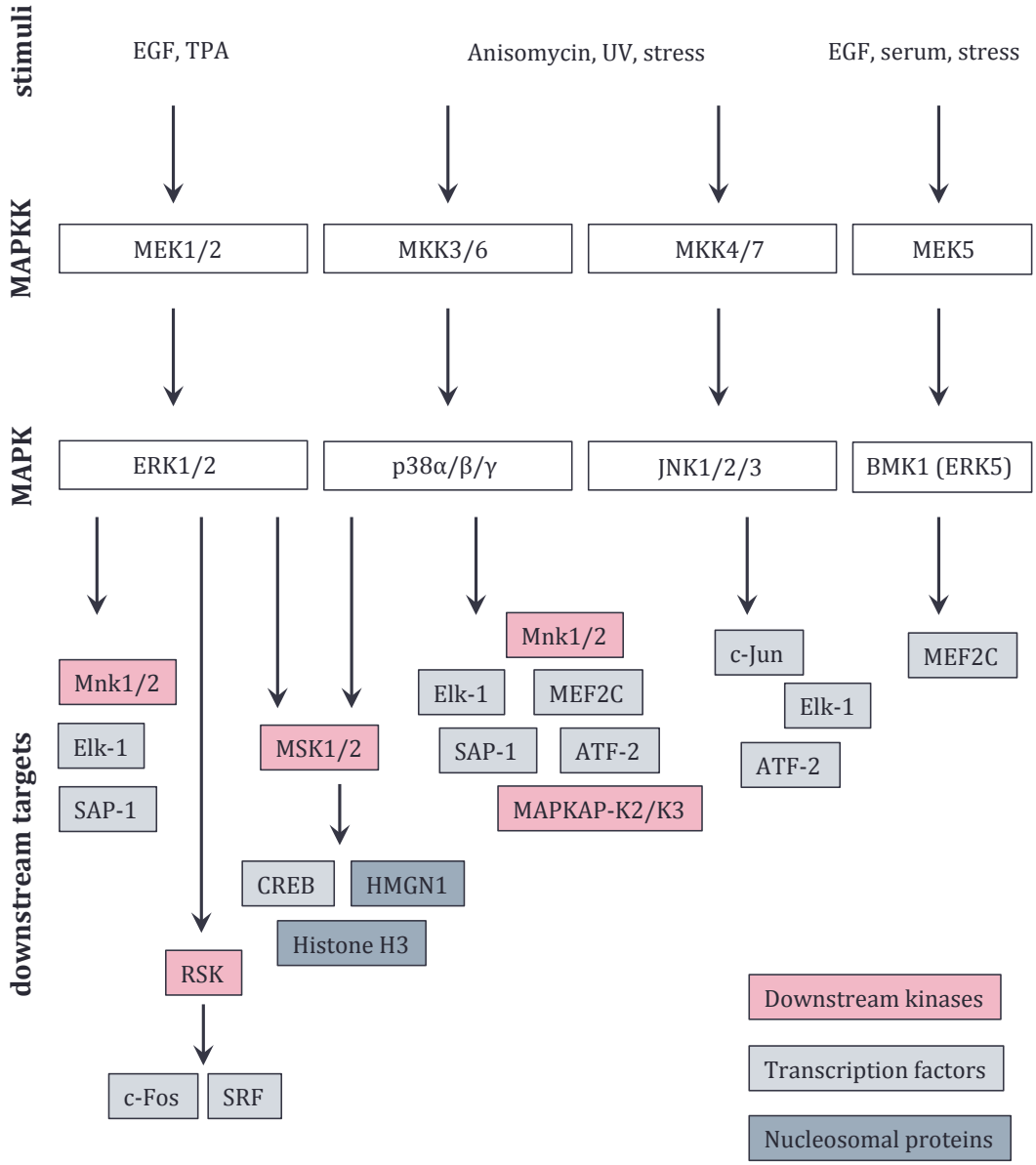
stimuli
EGF, TPA
Anisomycin, UV, stress
EGF, serum, stress
MAPKK
MEK1/2
MKK3/6
MKK4/7
MEK5
MAPK
ERK1/2
p38α/β/γ
JNK1/2/3
BMK1 (ERK5)
downstream targets
Mnk1/2
Elk-1
SAP-1
MSK1/2
CREB
HMGN1
Histone H3
RSK
c-Fos
SRF
Mnk1/2
Elk-1
MEF2C
SAP-1
ATF-2
MAPKAP-K2/K3
c-Jun
Elk-1
ATF-2
MEF2C
Downstream kinases
Transcription factors
Nucleosomal proteins

An alignment study of the catalytic domain of the MAPKs has shown alternating regions of high and low conservation. Eleven conserved subdomains have been identified (Hanks et al. 1988).

1.3.1.1 The mitogen activated protein kinase (MAPK)

The last components of the core signalling modules are MAPKs. They are proline-directed serine/threonine kinases, activating their downstream targets by phosphorylation of serine and threonine residues preceding a proline residue (Chang and Karin 2001). This phenomenon contributes to substrate specificity to MAPKs. However, it is not sufficient to explain the high degree of substrate specificity observed, which is directed by the presence of specific binding sites on the substrates (Kallunki et al. 1994; Yang et al. 1998; Tanoue et al. 2000). For example JNK binds to a specific region within the trans-activation domain of c-Jun, which enables c-Jun phosphorylation at serines 63 and 73 (Hibi et al. 1993; Derijard et al. 1994). However, v-Jun, which is the c-Jun viral homolog, lacks this domain. Its phosphorylation by JNK was thus found inefficient (Hibi et al. 1993; Derijard et al. 1994).

MAPKs are activated by dual-specificity kinases, which phosphorylate concomitantly threonine and tyrosine residues of a conserved motif Thr-X-Tyr, where 'X' is a different amino acid in each of the MAPK families (Anderson et al. 1990). The conserved motif is located in the kinase activation loop of the kinase domain subdomain VIII (Payne et al. 1991; Nishida and Gotoh 1993).

The kinases ERK1/2 were the first MAPKs to be identified. They were discovered in an effort to identify downstream targets phosphorylated on tyrosine residues after EGF treatment (Boulton and Cobb 1991). ERK1/2 are 85% identical in sequence, ERK2 being slightly shorter, and share many functions (Lloyd 2006). Their conserved motifs are Thr^{202}-Glu-Tyr^{204} and Thr^{185}-Glu-Tyr^{187} for ERK1 and ERK2 respectively.

The p38 subfamily is encoded by four different genes. The protein kinase p38 was first purified by anti-phosphotyrosine immunoaffinity chromatography (Glenney 1991). Independently, p38 was described in two studies as the reactivating kinase (RK) directly upstream of the MAPKAP kinase-2 that phosphorylates the small heat-shock protein hsp27 (Freshney et al. 1994; Rouse et al. 1994). It was then cloned using a specific nucleotide probe obtained from the peptide sequence to screen a murine liver cDNA library. It contains the conserved amino acid sequences of MAPK, and enzymatic activity requires the phosphorylation of the conserved motif Thr^{180}-Gly-Tyr^{182} (Han et al. 1994). Cloning studies also identified p38 as the mammalian homologue of yeast HOG1 (Han et al. 1994).

Research efforts focusing on c-Jun phosphorylation on serines 63 and 73 led to the discovery of the JNK kinases (Pulverer et al. 1991; Smeal et al. 1991; Hibi et al. 1993). These kinases were cloned simultaneously by two groups using, for one specific primers designed from the amino acid sequence of purified p54 JNK kinase (Kyriakis et al. 1994), and for the other, degenerate primers derived from conserved region of known MAPKs (Derijard et al. 1994). The conserved motif of JNK proteins is Thr^{183}-Pro-Tyr^{185}. The JNK subfamily is encoded by three genes and

due to various splicing, different isoforms can be identified: splicing in the catalytic region results in two types, while splicing in the COOH terminus gives two polypeptides of 54 kDa and 46 kDa (Hibi et al. 1993). The transcription factors c-Jun and ATF2, substrates of JNK proteins (Hibi et al. 1993; Gupta et al. 1995), contain JNK binding domains. The JNK isoforms present different binding affinities for these substrates (Kyriakis et al. 1994; Gupta et al. 1996).

The MAPKK MEK5, identified by degenerate PCR (English et al. 1995; Zhou et al. 1995), was used in a yeast-two hybrid screening to identify the protein kinase ERK5 (Zhou et al. 1995). ERK5 is also known as BMK1 as it is twice the size of the other MAPKs (Lee et al. 1995; Zhou et al. 1995). Its amino-terminal half contains the kinase domain and is similar to ERK1/2 with the conserved motif Thr-Glu-Tyr. The carboxyl-terminal half is specific to ERK5 and has been shown to enhance transcriptional activity of target molecules (reviewed in Nishimoto and Nishida 2006).

1.3.1.2 The MAPK kinase (MAPKK)

MAPK kinases (MAPKKs) are dual specificity kinases; they phosphorylate threonine and tyrosine residues (Gomez and Cohen 1991). They lie upstream of MAPKs in the MAPK signalling pathways and are themselves activated by phosphorylation of serine and threonine residues in a conserved region of activation loop of subdomain VIII of the kinase domain (Gomez and Cohen 1991).

While MAPKs have multiple substrates (see Section 1.3.2.2), MAPKKs are more substrate specific: ERK1/2 are activated by MAPKK1 and MAPKK2 (Alessi et al.

1994; Marshall 1994), JNK by MAPKK4 and MAPKK7 (Meier et al. 1996; Lawler et al. 1998), p38 by MAPKK3 and MAPKK6 (Derijard et al. 1995; Cuenda et al. 1996; Raingeaud et al. 1996; Cuenda et al. 1997), and ERK5 by MAPKK5 (English et al. 1995; Zhou et al. 1995; Chao et al. 1999).

1.3.1.3 The MAPKK kinase (MAPKKK)

As multiple different signals activate MAPK cascades, it is not surprising that various serine/threonine protein kinases act as MAPKKK. These include the Raf kinases for the ERK pathway (Marshall 1995), the MEK kinase (MEKK): MEKK1 (Lange-Carter et al. 1993), MEKK2 and MEKK3 (Blank et al. 1996; Ellinger-Ziegelbauer et al. 1997), MEKK4 (Gerwins et al. 1997) the mixed lineage kinases (MLKs; Dorow et al. 1993; Gallo et al. 1994; Holzman et al. 1994).

MAPKKK regulation is not fully understood but it requires different steps: recruitment to the membrane and phosphorylation by upstream kinases (Kyriakis and Avruch 2001). The best regulation understood is the Ras/Raf activation. The MAPKKK Raf is recruited to the membrane by Ras-GTP after external stimulation (Avruch et al. 1994; Marshall 1995). At the membrane, Raf phosphorylation is associated with activation (King et al. 1998).

1.3.1.4 Scaffold proteins

Due to the multiplicity and diversity of MAPK pathways, their selectivity is crucial in order to respond specifically and rapidly to external stimuli. This is in part achieved by scaffold proteins. The MEK-partner 1 (MP1) protein has been demonstrated to be an ERK pathway scaffolding protein (Schaeffer et al. 1998). It

not only promotes signalling from MEK1 to ERK1 by binding to both kinases, but it also favours their activation. The JNK interacting proteins 1 and 2 (JIP1 and JIP2 respectively) have a similar role for the JNK and p38 pathways (Dikic et al. 1996; Whitmarsh et al. 1998; Yasuda et al. 1999; Morrison and Davis 2003). They bind to select MAPK pathway components, thus placing kinases close to their downstream targets. This organisation of MAPK pathways not only confers specificity to MAPK pathways, it limits crosstalk within the different pathways.

1.3.2 MAPK pathways are activated in parallel by various stimuli

Multiple different stimuli activate MAPK pathways (Hibi et al. 1993; Cano et al. 1994; Han et al. 1994; Kyriakis et al. 1994). While some stimuli activate only one pathway, others can activate several pathways in parallel (Cano and Mahadevan 1995). Another level of complexity is added by the fact that the different MAPK pathways share downstream targets and, as seen in Section 1.2, IE gene promoters are regulated by various TFs. Therefore, IE genes can receive information from various pathways at the same time. This complexity within MAPK cascades raises questions of the impact of parallel activation and of the organisation of selectivity within the cascades (Cano and Mahadevan 1995; Figure 1.6).

1.3.2.1 Different stimuli activate MAPK pathways

Various stimuli from growth factors (Marshall 1995) to osmotic stresses and UV irradiation (Edwards and Mahadevan 1992; Hibi et al. 1993; Kyriakis et al. 1994; Cano et al. 1995; Gupta et al. 1995; Livingstone et al. 1995; van Dam et al. 1995) activate MAPK pathways. These activations are highly reproducible, quantitative,

characteristic to the length and strength of the stimulus and cell type specific (Cooper 1994; Seger and Krebs 1995; Hazzalin and Mahadevan 2002). ERK pathway is more strongly activated by growth factors and mitogens, while JNK and p38 pathways are stress-activated pathways, being activated by pharmacological agents, heat shock and UV irradiation. This specific and diverse activation allows cells to respond adequately to various types of stimuli.

The specific activation of MAPK pathways is cell type dependent, for example EGF has been shown to induce differentiation in PC12 neuronal cells, while it induces proliferation in fibroblasts (Marshall 1995). In C3H 10T½, mitogens such as insulin, epidermal growth factor (EGF) or PDGF are strong activators of the ERK pathway (Cano et al. 1994). EGF activates transiently all four pathways; however, it activates the ERK pathway more rapidly and strongly, it is fully activated after only 1 minute (Cano et al. 1995; Hazzalin et al. 1997). Similarly, TPA strongly activates ERK but weakly activates JNK and does not activate p38 pathway (Cano and Mahadevan 1995). Conversely, p38 and JNK pathways, but not the ERK pathway, are strongly activated by anisomycin at both inhibitory and sub-inhibitory concentrations (see Section 4.1.2.2; Cano et al. 1994; Hazzalin et al. 1996).

1.3.2.2 MAPK substrates

At the end of the MAPK cascade lie TFs, downstream protein kinases and other nuclear or cytoplasmic proteins (Edmunds and Mahadevan 2004). MAPK pathways control gene expression by phosphorylation of promoter-specific transcription factors (Karin and Hunter 1995; Treisman 1996; Kyriakis and Avruch 2001),

co-regulators (Yang et al. 2003) and by initiating chromatin modifications along inducible genes either directly, which is the case for the nucleosomal response (Thomson et al. 1999; see Section 1.2.4.3), or indirectly by promoting association with chromatin modifier enzymes, such as histone acetyltransferases (Mayr and Montminy 2001; Yang et al. 2003). Studies in yeasts showed that MAPKs can be functional components of transcription complexes and recruit factors independently of their kinase domain (Alepuz et al. 2003; De Nadal et al. 2004), suggesting a bifunctional role for MAPKs in gene regulation (reviewed in Edmunds and Mahadevan 2004).

The MAPK proteins show selectivity for their substrates as they are proline-directed kinases (Chang and Karin 2001) and by the presence of specific binding domains (Kallunki et al. 1994; Yang et al. 1998; Tanoue et al. 2000; see Section 1.3.1.1). However, the MAPK pathways activated in parallel share some downstream targets (Treisman 1996; Kyriakis and Avruch 2001). Thus, the mitogen- and stress-regulated kinases MSK1/2 are downstream of the ERK and the p38 pathways. MSK1/2 are responsible for the nucleosomal response (see Section 1.2.4.3; Soloaga et al. 2003). The nucleosomal response happens concomitantly with IE gene induction, and as it is downstream of ERK and p38 pathways, it occurs after mitogen and stress activation. As well as activating the nucleosomal response, MSKs are CREB kinases, phosphorylating the transcription factor CREB on serine 133 (Deak et al. 1998).

As described in Section 1.2.3.3, AP-1, which was first described for their role in the TPA response (Lee et al. 1987), are dimers composed of Jun, Fos and ATF subunits

(Angel and Karin 1991). AP-1 regulation through MAPK pathways happens at two levels. Firstly, there is a post-translational modification, which consists of a direct activation through JNK and p38 pathways, p38 phosphorylating ATF2 (Raingeaud et al. 1995) and JNK phosphorylating c-Jun (Derijard et al. 1994; Kyriakis et al. 1994) and ATF2 (Gupta et al. 1995; Livingstone et al. 1995; Raingeaud et al. 1995; van Dam et al. 1995). Secondly, there is regulation exercised through fresh induction of *fos* and *jun* family proteins by ERK, p38 and JNK pathways (Hill and Treisman 1995).

An overlapping set of IE genes is induced after various stimuli, leading to different cell fate decision. Multiple TFs are downstream of the same pathway, and as seen with the example of c-*fos* and c-*jun*, IE gene promoter regions contain multiple regulatory elements (see Section 1.2.3). Thus, a gene could receive contradictory information from various pathways, or TFs could work in coordination (combinatorial regulation). Understanding how the information is conveyed by the MAPK pathways and integrated is crucial to understand how an overlapping set of gene can produce different responses.

1.4 Protein phosphatases

The enzymes that oppose protein kinases are protein phosphatases (Cohen 1989); they catalyse the hydrolysis of phosphate from a phosphoprotein. In mammals/higher eukaryotes, there are two main families of protein phosphatases: the tyrosine-specific phosphatases and the serine/threonine-specific phosphatases, briefly described below (Table 1.1).

Table 1.1: Simplistic classification and characteristics of the protein phosphatases

The phosphatases discussed in this thesis are indicated in bold.

phosphatase families	groups	sub-groups	characteritics and examples		
Class I Cys-based tyrosine phosphatase (PTP)	Classical PTPs	receptor-type PTPs	PTPα, CD45, CD148, IA-2	signature motif Cys(X)5Arg	
		non-transmembrane PTPs	PTP1B, TCPTP, SHP1, LYP		
	Dual-specificity phosphatases (DUSPs)	**MKPs**	DUSP1-10, DUSP16	bind to MAPK through kinase interaction motif (KIM)	
		atypical DSPs	VHR, PIR, Laforin		
		Slingshots	SSH1, SSH2, SSH3		
		PRLs	PRL-1, PRL-2, PRL-3		
		CDC14s	CDC14A, KAP, PTP9O22		
		PTENs	PTEN, TPIP, tensin C1ten		
		Myotubularins	MTMA		
Class II Cys-based PTPs			CDC25A, CDC25B		
Class III Cys-based PTPs			LMPTP		
HAD family (Asp-based)			Eya, CTD, cronophin		
Mg^{2+}-dependent protein phosphatases (PPM)			PP2C		
phosphoprotein phosphatase (PPP)			**PP1**	catalytic subunit PP1c	
				regulatory subunit interacting with RVxF motif of PP1c	
			PP2A	core subunit	subunit A
					catalytic subunit PP2Ac
				subunit B	
FCP family			FCP		

1.4.1 The tyrosine-specific phosphatases

Tyrosine phosphatases can be divided into the classical protein tyrosine phosphatases (PTPs) and the dual-specificity phosphatases (DUSPs) described below (see Section 1.4.3; Zhang 1998). The PTPs can themselves be divided into two groups: the non-transmembrane PTPs composed of a catalytic domain and regulatory elements that control their function and location; and the receptor-type PTPs composed of a catalytic domain and a transmembrane domain that retains them within the plasma membrane (Zhang 1998). PTPs have been associated with the regulation of numerous cellular events (Walton and Dixon 1993), and in particular the immune response (Mustelin et al. 2005).

The catalytic domain of PTPs, an approximately 250 amino acid sequence, is the only highly conserved sequence (Zhang et al. 1994a) and contains the signature motif: $Cys(X)_5Arg$, where 'X' can be any amino acid (Zhang et al. 1994b). This motif allows dephosphorylation of tyrosine by a specific catalytic mechanism (Pannifer et al. 1998). The phosphate on the substrate is first transferred to the cysteine residue in the signature motif and then hydrolysed by water to release the phosphate anion (Guan and Dixon 1991; Pot and Dixon 1992; Zhou et al. 1994; Pannifer et al. 1998).

Associated with the PTP catalytic domain are amino- and carboxy-terminal extensions that have targeting motifs and protein-protein interaction domains (Walton and Dixon 1993; Li and Dixon 2000). These regulatory domains allow the formation of different protein complexes and direct PTPs to specific locations (Walton and Dixon 1993; Li and Dixon 2000). For example the protein tyrosine

phosphatase 1B (PTP1B) has a PTP catalytic domain at the N-terminus region and a hydrophobic regulatory region at the C-terminus region, which localizes PTP1B to the cytoplasmic surface of the endoplasmic reticulum (Cool et al. 1989; Cool et al. 1990; Zander et al. 1991; Cool et al. 1992; Frangioni et al. 1992).

1.4.2 The serine/threonine phosphatases

1.4.2.1 Sub-groups of serine/threonine phosphatases

The second main family of protein phosphatases is the serine/threonine phosphatases. They can be divided into two groups: the phosphoprotein phosphatase (PPP) and the Mg^{2+}-dependent protein phosphatases (PPM; Barford et al. 1998). For this study, okadaic acid, a protein phosphatase 1 (PP1) and protein phosphatase 2A (PP2A) inhibitor (Bialojan and Takai 1988; Cohen et al. 1990), has been used. These two PPPs are described below (see Section 1.4.2.2 and 1.4.2.3).

There are a lot more serine/threonine protein kinases than there are serine/threonine phosphatases and their catalytic domain is conserved (Barford 1996; Morrison et al. 2000; Cohen 2002). This raises the question of how protein phosphatases can specifically regulate phosphorylation turnover? This is achieved by the association of the protein phosphatase catalytic domains with a large variety of regulatory domains containing different binding sites, as described for PP1 and PP2A catalytic subunits (PP1c and PP2Ac) (Hubbard and Cohen 1993; Wera and Hemmings 1995; Faux and Scott 1996). Through their binding sites, the regulatory subunits control phosphatase activity by conferring substrate

specificity as well as targeting protein phosphatases to specific subcellular locations (Hubbard and Cohen 1993; Cohen 2002).

1.4.2.2 Protein phosphatase 1 (PP1)

In mammals, there are four isoforms of the PP1 catalytic subunit (PP1c): PP1α, PP1β, PP1γ1 and PP1γ2 (Cohen 1988; Dombradi et al. 1990; Sasaki et al. 1990). These isoforms can interact with many different regulatory subunits through a short sequence, Arg-Val-X-Phe, where 'X' is any amino acid, referred to as the RVxF motif and present on all the regulatory subunits interacting with PP1c (Egloff et al. 1997; Zhao and Lee 1997; Barford et al. 1998). Co-crystallisation experiments of PP1c and regulatory subunits showed that the RVxF motif binds to a hydrophobic channel of PP1c distinct form the catalytic site (Egloff et al. 1995; Egloff et al. 1997). This interaction allows other weaker interactions to happen, which can stabilise binding, regulate specificity and modulate activity (reviewed in Cohen 2002). The regulation of PP1 could thus be explained by a combinatorial effect of multiple binding sites. Moreover, the fact that most of the regulatory subunits bind through the same motif explains why PP1c mainly interacts with only one regulatory subunit at a time.

Three groups of regulatory subunits can be identified (Bollen 2001). They can either be activity-modulating proteins (including inhibitors, activators and chaperones), targeting proteins (binding PP1c and specific substrates) or substrates (Bollen 2001). Indeed, several A-kinase-anchoring proteins by binding to both PKA and PP1c keep them in close proximity (Schillace and Scott 1999). PP1 plays also an important role in the control of glycogen metabolism, several PP1c-

targeting subunits can target PP1 to glycogen. They include GM, GL, R5 and R6 (Doherty et al. 1996; Wu et al. 1996; Armstrong et al. 1997; Armstrong et al. 1998; Wu et al. 1998). Association of PP1c with GM in skeletal muscle enhances PP1 activity towards glycogen synthase and phosphorylase and targets it to the sarcoplasmic reticulum (Wu et al. 1996). Finally, the rehnoblastoma tumour suppressor protein, playing a role in cell cycle through its capacity to associate with and influence number of cellular protein, is also a PP1c substrate, and it is dephosphorylated during the cell cycle (Ludlow et al. 1990; Ludlow et al. 1993; Wu et al. 2009).

1.4.2.3 Protein phosphatase 2A (PP2A)

PP2A is a holoenzyme composed of three subunits: a scaffolding protein A subunit, holding a regulatory B subunit and a catalytic C subunit together (Mumby and Walter 1993; Mayer-Jaekel and Hemmings 1994; Kremmer et al. 1997). The 36 kDa catalytic C subunit and the 65 kDa A subunit compose the core enzyme, while the subunit B confers subcellular localization and substrate specificity to PP2A. Indeed, there are numerous B subunits (Healy et al. 1991; Mayer et al. 1991; Zolnierowicz et al. 1994; McCright and Virshup 1995; Csortos et al. 1996; McCright et al. 1996; Tanabe et al. 1996; Tehrani et al. 1996; Zolnierowicz et al. 1996; Strack et al. 1999) compared to 2 isoforms for both the A (Green et al. 1987; Stone et al. 1987; Arino et al. 1988) and C (Hemmings et al. 1990) subunits. Despite their lack of sequence similarity, the binding of the B subunits to the core enzyme is mutually exclusive (Mayer-Jaekel and Hemmings 1994; Janssens and Goris 2001).

PP2A activity is not only regulated by its B subunit, but also by post-translational modifications. It has been shown to be phosphorylated on tyrosine 307 of its catalytic subunit, resulting in enzyme inactivation (Chen et al. 1992). However, PP2A is able to re-activate itself rapidly, as phosphorylation of PP2Ac is enhanced in presence of okadaic acid (OA; Chen et al. 1992). The catalytic subunit is also subjected to methylation on leucine 309 (Li and Damuni 1994).

Multiple proteins have been identified as PP2A substrates, involving PP2A in many different biological processes such as cell cycle, cell transformation and signal transduction (reviewed in Janssens and Goris 2001). By its action on Cdc25 and Wee1, PP2A inhibits the pathway leading to Cdc2 dephosphorylation and prevents entry to mitosis (Kinoshita et al. 1993; Lee et al. 1994). Interactions between SV40 small tumour antigen and the core heterodimer of PP2A resulted in the inhibition of the dephosphorylation of MEK1 and ERK1 (Sontag et al. 1993) and CREB (Wheat et al. 1994), suggesting that PP2A is involved in their dephosphorylation. The scaffold protein casein kinase (CKII) binds to PP2A and MEK1 in quiescent cells, allowing PP2A to dephosphorylate MEK1. Finally, PP2A is present in the nucleus (Turowski et al. 1995) and has been involved in dephosphorylation of TFs, such as CREB, and histone H3 (Nowak et al. 2003).

1.4.3 The dual-specificity phosphatases

The dual-specificity phosphatases (DUSPs) are part of the PTPs and they contain the signature motif of PTPs (see section 1.4.1) in their catalytic domain, but can also dephosphorylate serine/threonine residues (Zhang 1998). The main example

of DUSP is the mitogen-activated protein kinase phosphatases (MKPs), dedicated to the specific regulation of MAPKs (Keyse 2000).

Mammalian cells count ten catalytically active MKPs, sharing a common structure (Dickinson and Keyse 2006; Owens and Keyse 2007). Their C-terminal catalytic domain possess similarities with the PTP VH-1 (Guan et al. 1991), while their N-terminal domain has a regulatory role, conferring subcellular localisation and substrate specificity (Camps et al. 2000; Theodosiou and Ashworth 2002). The substrate specificity seems to be achieved by a kinase interaction motif (KIM) present on the N-terminal domain of MKPs (Nichols et al. 2000; Tanoue et al. 2000; Tanoue et al. 2002). This motif contains positively charged arginine residues and hydrophobic amino acids (leucine, isoleucine or valine). The differences in number of positive charges and hydrophobic amino acid are thought to contribute to the substrate specificity of MKPs. The KIM domain interacts with a 'common docking' (CD) site composed of negatively charged aspartic acid residues and additional sequence on MAPKs (Tanoue et al. 2000; Tanoue et al. 2001; Chang et al. 2002; Tanoue et al. 2002).

As mentioned above, MKPs possess substrate specificity and specific subcellular localisation. Based on these characteristics, three subfamilies can be found (Camps et al. 2000; Theodosiou and Ashworth 2002). The first are the mitogen- and stress-inducible nuclear MKPs, containing DUSP1, DUSP2, DUSP4 and DUSP5. The second are the cytoplasmic ERK-specific MKPs, composed of DUSP6, DUSP7 and DUSP9. Finally, the third subfamily are JNK/p38-specific MKPs, containing DUSP8, DUSP10 and DUSP16, which can be either nuclear or cytoplasmic phosphatases. After

binding to the specific substrate, some MKPs undergo conformational changes, which activate their catalytic sites. This is the case for DUSP6, which becomes activated after binding to ERK2.

MKPs exercise a spatial and temporal control on MAPK. By dephosphorylating MAPK, they play a key role in controlling the magnitude and duration of kinase activity, and thus the signalling response and physiological output (Keyse 2000; Saxena and Mustelin 2000). MAPK can be recognised and bound by MKP, even in its dephosphorylated form. MKPs can thus behave as anchoring protein and control MAPK subcellular localisation. The localised dephosphorylated MAPK may participate in non-catalytic functions or accumulate in a region where they need to be rapidly activated and liberated (Caunt and Keyse 2013).

Another characteristic of some MKPs is that their expression is induced by mitogen and stress stimuli, so by the MAPK pathways. This forms an autoregulatory negative feedback loop in the MAPK pathway. This phenomenon is observed for CL 100 (DUSP1), later renamed MKP-1 (Sun et al. 1993), which is rapidly induced after growth factors and stress (Keyse and Emslie 1992; Noguchi et al. 1993). Moreover, as some MKPs can dephosphorylate multiple MAPKs, induction of their expression can lead to crosstalk within pathways. This may be the case for MKP-1, which can act on the three MAPKs ERK, p38 and JNK, but has a substrate preference for JNK (Slack et al. 2001; Caunt and Keyse 2013).

1.5 Quantitative regulation of inducible genes

1.5.1 The view of MAPK pathways in regulation

MAPK pathways have previously been used as a model to investigate the issue of whether it functions as a two-state switch or a continuously variable switch. In previous studies in *Xenopus* oocytes, where transcriptional regulation was not the focus, MAPK pathways have been thought to convert a graded response into a switch-like output. Indeed, in their model of the well-conserved structure of the MAPK pathways, Huang and Ferrell have predicted that the MAPK would exhibit an ultrasensitive response, which consists of transforming a graded response into a more switch-like one (Ferrell 1998, Figure 1.7), to stimulation (Huang and Ferrell 1996). Numerous models of the MAPK pathways have been developed using deterministic methods, such as ODEs, or stochastic methods (Huang and Ferrell 1996; Brightman and Fell 2000; Schoeberl et al. 2002; Somsen et al. 2002; Gong and Zhao 2003; Wiley et al. 2003; Chapman and Asthagiri 2004; Kofahl and Klipp 2004; Vayttaden et al. 2004; Kolch et al. 2005; Heath et al. 2007). These models mainly focused on the transduction of the signal within the signalling pathway and investigated potential feedbacks, in particular for the ERK pathway. Here we concentrate on the literature related to the study and model developed by Ferrell, as it has been previously implemented in the probabilistic model checker PRISM, and is used in our study (see Chapter 5).

Figure 1.7: Definition of ultrasensitive enzyme

An ultrasensitive enzyme differs from a Michaelis-Menten enzyme and exhibits a step-like response curve (Ferrell 1998)

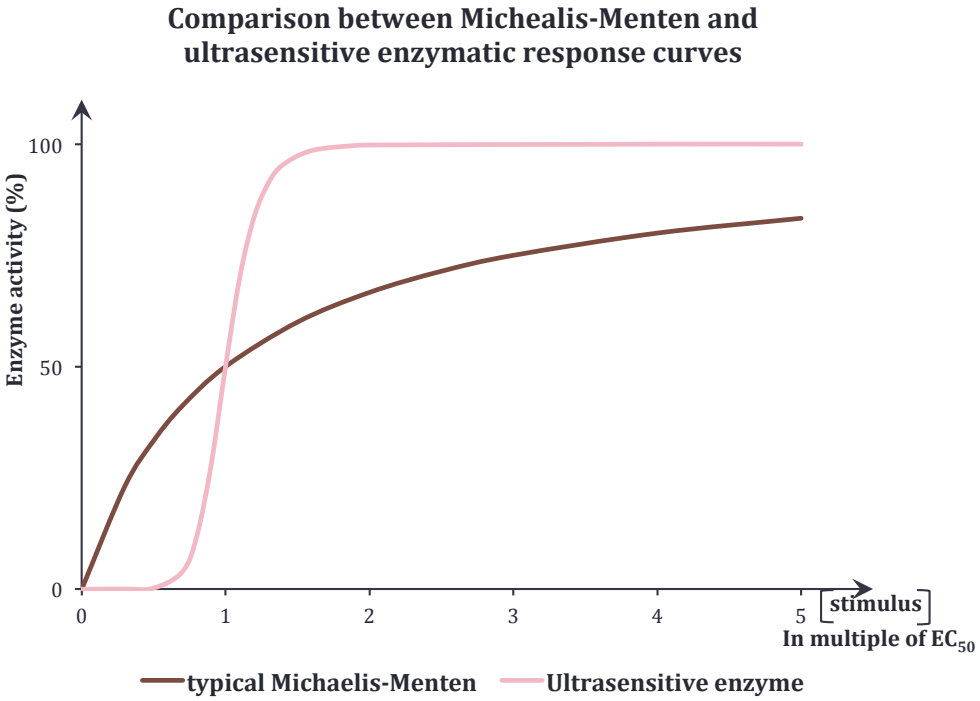

Michaelis-Menten	Ultrasensitive enzyme
$response = \frac{[stimulus]}{EC_{50} + [stimulus]}$	$response = \frac{[stimulus]^n}{EC_{50}^n + [stimulus]^n}$
EC_{50} is stimulus concentration at which the response is half maximal	EC_{50} is stimulus concentration at which the response is half maximal
[stimulus] designates the concentration of stimulus	[stimulus] designates the concentration of stimulus
	n is the Hill coefficient

1.5.1.1 Ultrasensitivity within the MAPK pathways

The predicted ultrasensitive response to stimulus of MAPK has multiple explanations. Indeed, ultrasensitivity can be generated by various phenomena: it can either be intrinsic to the three-tiered organisation of MAPK pathways, it can be generated by enzyme cooperativity, or by enzymes operating near saturation (Ferrell 1996).

The intrinsic ultrasensitivity conferred by the MAPK pathways has been revealed by the mathematical model of the pathway carried out by Huang and Ferrell (1996). They observed that both MAPKK and MAPK exhibit an ultrasensitive response to stimulus. Only the degree of ultrasensitivity, and not the behaviour, was observed to be dependent on the values of the model parameters. These results were aligned with experiments on *Xenopus* oocytes extract (Huang and Ferrell 1996) and *Xenopus* oocytes (Ferrell and Machleder 1998). After being exposed to progesterone, the oocyte undergoes maturation and activates the Mos/MEK1/ERK MAPK pathway (Masui and Clarke 1979; Sagata 1997). In this system, ERK exhibits an ultrasensitive response to progesterone (Huang and Ferrell 1996).

The activation of the MAPK requires the dual-phosphorylation of threonine and tyrosine residues (see Section 1.3.1). In their mathematical model, Huang and Ferrell considered the MAPK phosphorylation as being a two-step process. This characteristic contributes to the ultrasensitive response of MAPK by adding cooperativity. Indeed, the degree of ultrasensitivity of MAPK was considerably

lower when the phosphorylation was considered as a single-step process (Huang and Ferrell 1996); however, no evidence suggests a single-step mechanism.

Ultrasensitivity can also be generated when enzymes operate near saturation, which is referred to as 'zero-order ultrasensitivity' (Ferrell 1996). In the MAPK pathway this could be the case due to translocation. Indeed, once activated, MAPK translocate from the cytoplasm to the nucleus where protein phosphatases could be at saturation, resulting in a switch-like response (Ferrell 1998). However, there is no evidence for that and multiple protein phosphatases, with different subcellular localisation, can deactivate the same MAPK (see Section 1.4). Moreover, specific MAPK protein phosphatases (DUSPs) are induced after stimulus (see Section 1.4.3). Hence, it seems unlikely that protein phosphatases would operate at saturation.

1.5.1.2 Ultrasensitivity and positive feedback loops in MAPK pathways generate all-or-nothing response

Xenopus oocyte maturation is an all-or-nothing response (Masui and Clarke 1979; Sagata 1996). Indeed, the oocyte maturation is the process by which oocytes arrested at the first meiotic prophase resume meiosis until the second meiotic metaphase after exposure to progesterone. Once the oocyte undergoes maturation it cannot stop at an intermediate stage. Thus, the *Xenopus* oocytes convert a continuously variable stimulus, which is the concentration of progesterone, into an all-or-nothing response that is the oocyte maturation. Mos was found to accumulate throughout the process, its levels still increasing after 13 hours of stimulation with progesterone (Sagata et al. 1988; Watanabe et al. 1989), and to

undergo a selective degradation soon after the completion of meiosis (Watanabe et al. 1989; Nishizawa et al. 1993). The combination of the ultrasensitive response of the Mos/MEK1/ERK MAPK pathway and the existence of a positive feedback loop, which stabilises and promotes accumulation of Mos, contributes to this bistable response (Ferrell and Machleder 1998). The protein synthesis inhibitor cyclohexamide was used to inhibit the positive feedback loop and thus illustrate that both mechanisms are needed to observe an all-or-nothing response.

A similar bistable response has been observed for the JNK pathway in *Xenopus* oocyte maturation and stress response, JNK being activated after stimulation with progesterone and osmotic stress, such as sorbitol. This response is also the result of the combination of both mechanisms (Bagowski and Ferrell 2001; Bagowski et al. 2003).

One characteristic of such bistability is that it confers 'memory' to the system (Ferrell 1998). Indeed, it has the potential to stay 'on' long after the triggering stimulus thanks to the feedback loop. This is important for the *Xenopus* oocyte maturation, which cannot go back once maturation commences. Besides, both states need to be stable.

In this thesis, 'binary', 'bistable' and 'two-state', are used to describe a system, which can only be found in two different stable states, for example, stable 'on' and 'off' states. However, as described above, the term 'bistable' adds a notion of memory to the system. Thus, a bistable switch exhibits hysteresis, the system stays 'on' even if the stimulus is lowered back below the threshold, and there is a

discontinuity in the stimulus-response curve. In comparison, a binary or two-state switch exhibits a switch-like response that is an ultrasensitive stimulus-response curve (Ferrell 1998).

1.5.2 Coupling MAPK pathway and IE gene transcription

The studies describing MAPK pathways as exhibiting an all-or-nothing response do not have gene transcription as an end point. In the context of IE gene regulation, this bistable behaviour of MAPK pathways would limit the possibility for MAPK pathways to produce a quantitative response calibrated to the stimulus perceived.

Indeed, as described in Section 1.2, IE genes observe highly reproducible stimulus-specific responses. Thus, the signalling pathways must convey the information from the cell receptor to the nucleus to quantitatively induced IE genes. The precise interface at which quantitative control is transmitted to the gene therefore lies at the junction between intracellular signalling enzymes, which like all enzymes exist in high numbers and follow the laws of enzyme biochemistry, and the gene, of which there can only be two copies in any given cell. How can the information conveyed by signalling pathways be transmitted and overcome this discontinuity? How can IE genes be quantitatively regulated?

Assuming that the rates of transcriptional elongation are relatively constant, the key determinant for the quantitative regulation lies in the rate of transcriptional initiation (Hazzalin and Mahadevan 2002). Figure 1.8 shows two extreme hypotheses for MAPK pathway regulation of IE genes. The first one considers the MAPK pathways as ‘on/off’ switch, where transcription is only possible in the

stable 'on' conformation and happens at a constant transcriptional initiation rate, which is intrinsic to the system. This hypothesis requires the action of an external factor to be turned 'off'. Conversely, the second hypothesis sees MAPK pathway regulation as more dynamic. The rate of transcriptional initiation is directly linked to the signalling pathway and varies to reflect the signal perceived (Figure 1.8). This regulation seems more likely to produce the specific and quantitative IE genes profiles described in Section 1.2.

The direct link between the rate of transcriptional initiation and the MAPK pathways could be seen as the turnover of phosphorylation of TFs, which play a crucial role in IE gene induction and are downstream the MAPK pathways (see Section 1.2.3; Karin and Hunter 1995; Treisman 1996; Kyriakis and Avruch 2001). One cycle of phosphorylation and dephosphorylation of the TF could correspond to a single transcriptional initiation event (Hazzalin and Mahadevan 2002), phosphorylation of TF being a dynamic and transient process. Protein kinases and phosphatases would have the same importance in IE gene regulation and this regulation would only be possible if there is a dynamic phosphorylation turnover. The MAPK pathways would be seen as continuously variable switch and not as bistable switch.

Figure 1.8: Hypothetical switch hypotheses for IE gene regulation

A. Representation of the stable 'on/off' switch. After stimulation, TF is phosphorylated by MAPK and inducible gene transcription is turned 'on'. The gene supports a set rate of transcription intrinsic to the system. Gene transcription is turned 'off' by dephosphorylation of TF by phosphatases.
B. Representation of the dynamic switch. IE gene regulation is considered to be a more dynamic process: each initiation event is coupled with a single cycle of phosphorylation/dephosphorylation of TF. Thus the frequency of rate of initiation if directly coupled to the signal conveyed by internal signalling pathways.

A. Bistable switch

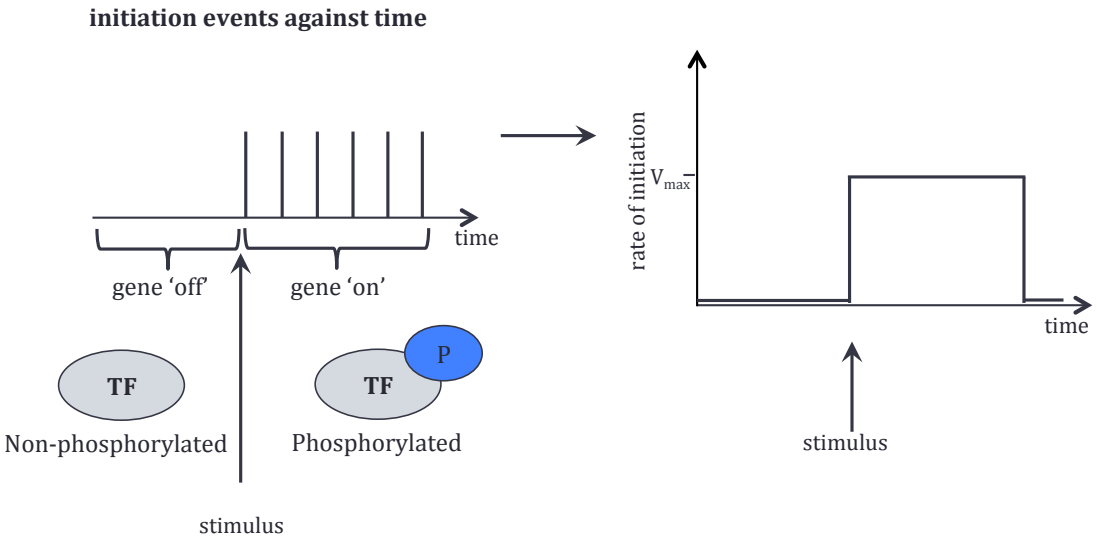

B. Continuously variable switch

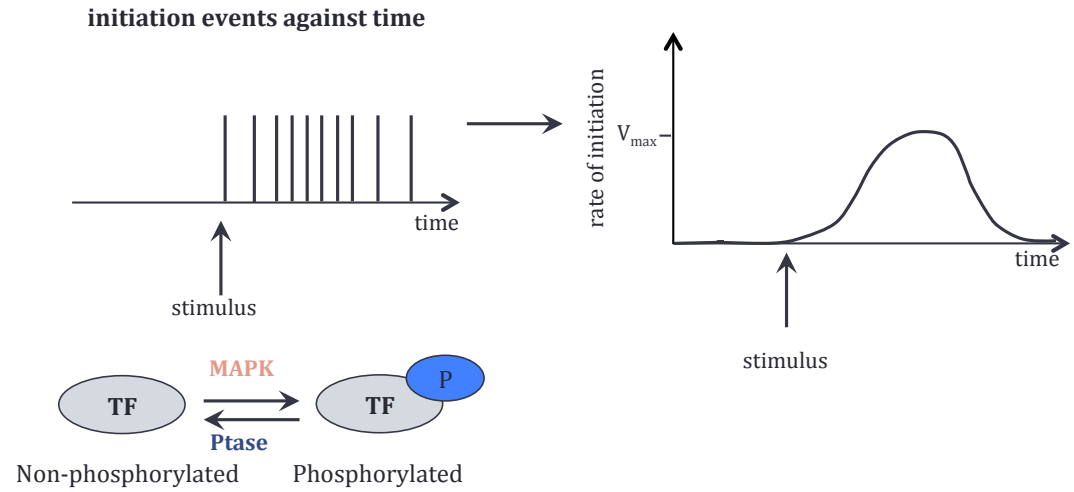

Dynamic turnover of phosphorylation:
Each initiation event is coupled with a single phosphorylation/dephosphorylation cycle

1.6 Summary

The work in this thesis aims to compare the bistable switch and the continuously variable switch hypotheses in MAPK pathway regulation of IE genes transcription (described in Hazzalin and Mahadevan 2002). In order to understand how cells can quantitatively regulate gene expression, we focused on the specific interface between MAPK pathways and IE genes. We investigated the importance of the turnover of phosphorylation in this quantitative regulation at both signalling and transcription levels. The use of the phosphatase inhibitor, okadaic acid (OA), revealed the presence of a phosphorylation turnover for the stress pathways, JNK and p38, in quiescent mouse fibroblast cells. We found that OA inhibits the protein phosphatases opposing MAPK, preventing dephosphorylation of TFs, by concomitant inhibition of MAPK and treatment with OA. We used the inducible c-*fos* and c-*jun* as models to ask how perturbations of the turnover of phosphorylation affects IE induction, and revealed a complex regulation where it seems that the turnover of phosphorylation rather than phosphorylation itself plays a crucial role. Finally, we compared mathematically the two hypotheses for the interface between signalling pathways and IE genes, using a simplified model of this specific interface informed by our analyses of MAPK pathways and inducible genes. We found that a more dynamic regulation at the interface seems to be better suited to convey quantitative information.

Chapter 2: Materials and Methods

2.1 Materials

The chemicals used in this work were obtained from VWR or Sigma, actinomycin D was purchased from Enzo Lifesciences, okadaic acid from Millipore and the cell culture reagents were acquired from Invitrogen.

2.1.1 Antibodies

The antibodies used in this study are listed in Table 2.1, as well as the concentrations at which they are used for Western blots. All the secondary antibodies used are donkey polyclonal antibodies purified by affinity, and are conjugated with horseradish peroxidase (HRP). The anti-rabbit- was obtained from GE Healthcare, the anti-sheep/goat-HRP from AbD serotec and the anti-mouse-HRP from GE Healthcare.

2.1.2 Stimuli and inhibitors

The different stimuli and inhibitors used in this study are shown in Table 2.2. The concentrations of each compound are also indicated (Table 2.2).

2.2 Tissue Culture

Mouse C3H 10T½ fibroblast cells were grown in Dulbecco's Modified Eagle's Medium (DMEM) with 10 % (v/v) foetal calf serum (FCS) in 6 % CO_2 at 37 °C, until

Table 2.1: Antibody used in Western blotting

antibody	source	species	Western blot conditions: antibody concentration primary	secondary	ECL method
MEK4ph (Thr261)	CST 9151	rabbit polyclonal PA	1:1000	1:2500	1
ERK1/2	Zymed 13-6200	mouse monoclonal	1:2500	1:5000	1
p38	Santa Cruz sc728	rabbit polyclonal AP	1:5000	1:5000	2
p38ph (Thr180/Tyr182)	CST 9211	rabbit polyclonal PA	1:1000	1:2500	2
JNK	CST 9252	rabbit polyclonal PA	1:1000	1:2500	2
JNKph (Thr183/Tyr185)	CST 4671	rabbit monoclonal	1:2000	1:2500	2
MSK1	lab antibody (a)	sheep polyclonal AP	1:2000	1:2500	2
HMGN1ph (Ser 6)	lab antibody (b)	sheep polyclonal AP	1:2000	1:5000	1
H3S10ph	lab antibody (b)	rabbit polyclonal AP	1:5000	1:5000	2
H3K9acS10ph	lab antibody (c)	sheep polyclonal AP	1:4000	1:4000	2
CREBph (Ser133)	Upstate 06-519	rabbit polyclonal PA	1:1000	1:5000	1
ATF-2	Santa Cruz sc187	rabbit polyclonal AP	1:1000	1:2500	2
c-Jun	Santa Cruz sc1694	rabbit polyclonal AP	1:500	1:2500	2

AP: affinity purified; PA: protein A purified; (a) (Dyson et al. 2005); (b) (Thomson et al. 1999); (c) (Clayton et al. 2000)
ECL method 1: Immobilon Western Chemiluminescent HRP Substrate (Millipore)
ECL method 2: Solution composed of 1.25 mM Luminol, 0.2 mM Coumaric acid, 100 mM Tris-HCl pH 8.5 and 2.7 mM H_2O_2

Table 2.2: Compounds used

compound	concentrations
sAn	25 ng/ml
Anisomycin	10 µg/ml
EGF	50 ng/ml
NaF	50 mM
TPA	100 nM
OA	1 µM, 500 nM or 100 nM
actinomycin	5 µg/ml
SB 203580	10 µM
SP 600125	10 µM
H89	10 µM
U0126	10 µM

90-95 % confluence. The stock cells were cultured in 75 cm^2 flasks and split 1:14 or 1:16 into 10 cm dishes for experiments with 10 ml of DMEM with 10 % (v/v) FCS. Once the cells are 90-95 % confluence, they were quiesced in 5 ml of DMEM with 0.5 % (v/v) FCS in 6 % CO_2 at 37 °C, for 16-18 hours for synchronisation.

2.3 Protein Extraction

2.3.1 Extraction of transcription factors

After stimulation, media was aspirated and cells were harvested and lysed with 200 µl of ice-cold high salt lysis buffer [20 mM HEPES (4-(2-hydroxyethyl)-1-piperazineethanesulfonic acid) pH 8.0, 5 mM EDTA (ethylenediaminetetraacetic acid), 10 mM EGTA (ethylene glycol tetraacetic acid), 5 mM NaF (sodium fluoride), 10 % glycerol, 1 mM DTT (dithiothreitol), 400 mM NaCl (sodium chloride), 0.4 % Triton X-100, 1x protease inhibitors, 1 mM sodium orthovanadate, 20 mM β-glycerophosphate, 1 µM microcystin, 10 mM sodium butyrate]. Samples were kept on ice for 20 minutes before centrifuged at 13,000 rpm for 10 minutes. The supernatant, containing the transcription factors, was transferred to fresh tube and adjusted to 1x Laemmli buffer [10 mM Tris-HCl pH 6.8, 10 % (v/v) glycerol, 2 % (w/v) SDS (sodium dodecyl sulphate), 1 % β-mercaptoethanol, 0.01 % (w/v) bromophenol blue] for analysis and incubated at 95 °C for 2-3 minutes. The pellet was used for histone extraction.

The protease inhibitors used in the high salt lysis buffer were: 2 µg/ml aprotinin, 5 µg/ml leupeptin, 50 µg/ml soybean trypsin inhibitor, 100 nM tosyl lysyl

chloromethyl ketone, 100 nM tosyl phenylalanyl chloromethyl ketone and 2 mM phenylmethylsulphonyl fluoride.

2.3.2 Acid extraction of histones

The pellets from high salt lysis of cells, containing nuclear proteins, were acid extracted for analysis of histone with 75 µl 0.4 M hydrochloric acid for 30 minutes on ice, and centrifuged at 13,000 rpm for 5 minutes at 4 °C. The supernatant was transferred and histone precipitated with 1 ml acetone overnight at -20 °C, then centrifuged at 13,000 rpm for 20 minutes at 4 °C. The pellet was washed twice with pre-chilled acetone at -20 °C then air-dried. They were re-suspended in 8 M urea, 10 mM Tris-HCl pH 7.5 and adjusted to 1x Laemmli buffer (see Section 2.3.1) for analysis.

2.4 Polyacrylamide gel electrophoresis (PAGE)

2.4.1 Sodium dodecylsulphate (SDS) PAGE

For histone and c-Jun analyses 15 % mini SDS PAGE gels were used, and for ATF-2 and CREB analyses 10 % big SDS PAGE gels were used. These gels were run following standard protocols (Laemmli 1970) and prepared with Protogel solutions (National Diagnostics). The 15 % SDS PAGE gel resolving part is composed of 375 mM Tris-HCl pH 8.8, 0.1 % (w/v) SDS, 15 % (w/v) acrylamide and 0.4 % (w/v) bisacrylamide, and its stacking part is composed of 125 mM Tris-HCl pH 6.8, 0.1 % SDS, 5 % (w/v) acrylamide and 0.13 % (w/v) bisacrylamide. The 10 % SDS PAGE gel resolving part differs from the 15 % SDS PAGE one only from the percentage of acrylamide, which is 10 % (w/v). The gels were polymerised by

addition of 0.1 % (v/v) tetramethylethylenediamine (TEMED) and 0.1 % (w/v) ammonium persulfate (APS) for the resolving parts, and 0.3 % (v/v) TEMED and 0.05 % (w/v) APS for the stacking parts.

Histone or high salt lysate fractions were loaded, electrophoresed at 150 V (mini gels) or 200 V (big gels) in Laemmli running buffer [25 mM Tris, 192 mM glycine, 0.1 % (w/v) SDS] and transferred to polyvinylidene difluoride (PVDF) membrane for immunoblotting by SDS transfer buffer (see Section 2.5.1.1) for histone and c-Jun and by Towbin transfer buffer (see Section 2.5.1.2) for ATF-2 and CREB.

2.4.2 ERK PAGE

For ERK, p38, JNK, MSK1 and HMGN1 15 % ERK PAGE gels were used. These gels were run in a similar way as SDS PAGE gels (see Section 2.4.1). The resolving part of the gel is composed of 375 mM Tris-HCl ph 8.8, 15 % (w/v) acrylamide and 0;086 (w/v) bisacrylamide, while the stacking part is composed of 250 mM Tris-HCl pH 6.8, 5 % (w/v) acrylamide and 0.13 % (w/v) bisacrylamide. The resolving part was polymerised by addition of 0.1 % (v/v) TEMED and 0.1 % (w/v) APS and the stacking part by addition of 0.1 % (v/v) TEMED and 0.05 % APS.

High salt lysate fractions were loaded, electrophoresed at 150 V in Laemmli buffer (see Section 2.4.1) and transferred to PVDF membrane for immunoblotting by Towbin transfer buffer (see Section 2.4.2).

2.5 Western blotting

2.5.1 Protein transfer

After electrophoresis, proteins were transferred to PVDF membranes. Two transfer buffers were used depending on the proteins (see Section 2.4).

2.5.1.1 SDS transfer buffer

Once separated by electrophoresis, the proteins were transferred to PVDF membrane (Immobilion-P Millipore) using 0.5 % Laemmli running buffer [12.5 mM Tris, 96 mM glycine, 0.05 % (w/v) SDS] containing 10 % (v/v) methanol. The PVDF membrane was pre-wetted in methanol and once assembled the transfer was carried out at 200 mA for high salt lysate fractions or at 60 mA for histone overnight.

2.5.1.2 Towbin transfer buffer

Proteins could also be transferred to PVDF membrane using Towbin transfer buffer [25 mM Tris, 192 mM glycine, 20 % (v/v) methanol]. The transfer was carried out at 200 mA overnight or for 6 hours for the membranes probed against JNK.

2.5.2 Ponceau staining

After transfer, the membranes were stained using Ponceau S solution [0.4 % (w/v) Ponceau S, 5 % (v/v) acetic acid] for 5 minutes and destained with methanol. The membranes were air-dried and scanned and used as loading control.

2.5.3 Immunoblotting

Dried membranes were probed with primary antibody in a blocking solution of 5 % (w/v) skimmed milk powder, phosphate-buffered saline (PBS) [137 mM NaCl, 8 mM Na_2HPO_4, 1.5 mM KH_2PO_4, 2.7 mM KCl] and 0.1 % (v/v) Tween 20 for 1 hour at room temperature. The membranes were then washed three times in PBS containing 0.1 % (v/v) Tween 20 for 10 minutes before being probed with secondary antibody in blocking solution for 1 hour and washed again three times in PBS containing 0.1 % (v/v) Tween 20. For the anti-phospho-JNK antibody a TBS [20 mM Tris-HCl pH 8.0, 150 mM NaCl] solution containing 0.1 % (v/v) Tween 20 was used instead of PBS.

The detection of bound antibodies was done by enhanced chemiluminescence (ECL) using either the Immobilon Western Chemiluminescent HRP Substrate (Millipore; Table 2.1, method 1) or a solution composed of 1.25 mM Luminol, 0.2 mM Coumaric acid, 100 mM Tris-HCl pH 8.5 and 2.7 mM H_2O_2 (Table 2.1, method 2). After incubation for 1 minute, the membranes were exposed to X-ray (Kodak) film to visualise the signal.

2.5.4 Quantification of Western blots

While the Western blots presented in Chapter 3 were analysed qualitatively, the ones presented in Chapter 5 were quantified. After scanning the blots, the intensity of the signal was obtained using ImageJ 1.46r (National Institutes of Health, USA, http://imagej.nih.gov/ij). Each lane, corresponding to a single sample, is selected and the profile plot obtained (Figure 2.1 A). The profile represents the relative

Figure 2.1: Western blot quantification by ImageJ

A. Quiescent C3H 10T½ cells were stimulated with sAn (25 ng/ml; lanes 2-9) for the indicated times. Cell extracts were separated on ERK gels and probed with anti-phospho-p38 antibodies. (Lane 1: control, untreated). To quantify the blot obtained, once open in ImageJ 1.46r, a lane is selected on the blot as indicated by the yellow rectangle lane 2 (i) and the profile plot corresponding at this lane is obtained (ii).
B. Background correction is applied and the area, which represents the intensity of the band for the lane selected, is obtained.

All these steps are repeated for each lanes of the blot.

A.

i.

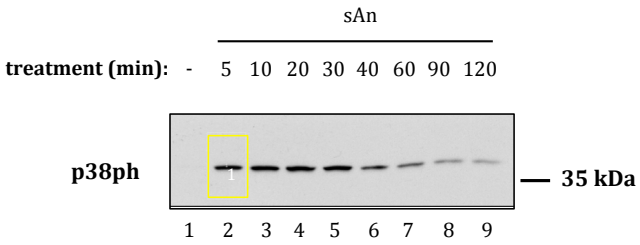

ii.

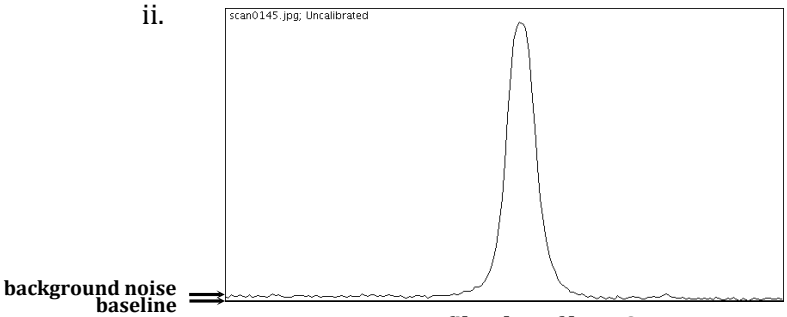

Profile plot of lane 2

B.

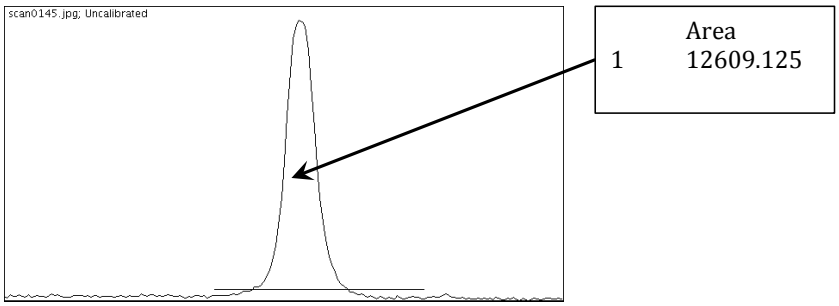

density of the contents of the lane (the peak corresponding to the dark signal). Due to background noise, the peak does not start at the base line and must be closed off manually for background corrections (Figure 2.1 B). The area under the peak corresponds to the intensity of the signal.

For Western blot quantification, the proportionality of the signal perceived with the antibody to the protein concentration, referred to as the linear range of the antibody, was verified by means of a standard curve based on a dilution profile of the protein, associated with each blot quantified (see Section 5.2.1.1). Data are normalised against the total amount of protein in the same sample, by the use of an anti-protein-specific antibody or Ponceau S staining, for loading control. Data are presented as relative activation (see Section 5.2.1.1).

2.6 RNA extraction

Total RNA was extracted following the acid guanidinium thiocyanate-phenol-chloroform extraction (Chomczynski and Sacchi 1987). After stimulation, media was aspirated and cells were harvested and lysed with 600 µl of solution D [4 M guanidinium thiocyanate, 25 mM sodium citrate pH 7, 0.5 % (w/v) sarcosyl, 0.1 M β-mercaptoethanol]. 2 M sodium acetate pH 4 (67 µl), water-saturated phenol (600 µl) and chloroform-isoamyl alcohol mixture (49:1; 240 µl) were added with thorough mixing after the addition of each reagent, before a 10 minute incubation on ice. Samples were then centrifuged at 13,000 rpm for 10 minutes at 4 °C. The aqueous phase, containing RNA, was transferred to a fresh tube, mixed with isopropanol (850 µl) and incubated overnight at -20 °C to precipitate RNA, which was then collected by centrifugation at 13,000 rpm for 10 minutes. The pellet was

resuspended in 300 µl solution D, followed by precipitation with addition of 200 µl isopropanol and incubation at -20 °C for at least 1 hour. RNA was pelleted as before, by centrifugation at 13,000 rpm for 10 minutes, and washed in 70 % (v/v) ethanol then absolute ethanol. The pellet was air-dried and resuspended in 50 µl sterile dimethyl pyrocarbonate (DMPC)-treated water. The concentration of RNA was determined by spectrophotometry for each sample.

2.7 Northern blotting

2.7.1 Electrophoresis

To 7.3 µl aliquots containing 5 µg RNA, 10 µl formamide, 0.7 µl formaldehyde and 2 µl 5x formaldehyde running buffer [0.1 M 3-(N-morpholino)propanesulphonic acid (MOPS) pH 7.0, 40 mM sodium acetate, 5 mM EDTA pH 8.0] were added. The aliquots were then incubated at 65 °C for 15 minutes and cooled on ice. 2 µl formaldehyde loading buffer [50 % (v/v) glycerol, 1 mM EDTA pH 8.0, 0.25 % (w/v) bromophenol blue, 0.25 % xylene cyanol FF] and 1 µl ethidium bromide (1 mg/ml) were added to the samples before they were loaded and resolved on formaldehyde-agarose gels [1 % (w/v) agarose, 1.23 % (v/v) formaldehyde in 1x formaldehyde running buffer]. Gels were run for 2 h 20 at 65 V in 1x formaldehyde running buffer and RNA visualised by UV transillumination.

2.7.2 RNA transfer and probing

RNA was transferred onto nylon membrane (Hybond-N^+, GE Healthcare) by capillary transfer for 4 hours in 0.05 M NaOH. After transfer, the membranes were washed in 2x SSC [0.3 M NaCl, 30 mM sodium citrate pH 7.0] and air-dried.

Before probing, membranes were wet in 2x SSC and pre-hybridised in Church buffer [0.5 M sodium phosphate pH 7.2, 1 % (w/v) BSA, 1 mM EDTA pH 8.0, 7 % (w/v) SDS] at 65 °C for 1 hour. The c-*fos*, c-*jun* and *gapdh* probes used have been previously described (Hazzalin et al. 1997).

[α-^{32}P]-dCTP-labelled probes were obtained using the Random Primed DNA Labelling Kit (Roche) and unincorporated [α-^{32}P]-dCTP was removed using SigmaSpin Post-Reaction Clean-Up columns (Sigma). The probes were denatured at 95 °C for 5 minutes before addition to the Church buffer. Hybridisation was done overnight at 65 °C. Membranes were washed twice in 2x SSC, 0.1 % SDS for 10 minutes and twice in 0.2x SSC, 0.1 % SDS for 10 minutes, and wrapped in Saran-Wrap.

Membranes were successively probed for c-*fos*, c-*jun* and *gapdh* and stripped by incubation in a boiling 0.1 % SDS solution between each probing.

2.7.3 Quantification of Northern blots

All the Northern blots presented in Chapter 4 were analysed quantitatively. Blots were visualised by phosphorimager FUJIFILM FLA-7000 for quantification. As for Western blots, Northern blots were quantified using ImageJ 1.46r (see section 2.5.4) with background corrections. c-*fos* and c-*jun* results are normalised against *gapdh* results for loading control and presented as relative RNA levels.

2.8 Real-time PCR

2.8.1 Preparation of genomic DNA for standards

C3H 10T½ cells were washed and harvested in PBS, pelleted by centrifugation at 2,500 rpm for 4 minutes and resuspended in lysis buffer [10 mM Tris-HCl pH 8.0, 400 mM NaCl, 2 mM EDTA pH 8.0]. A solution of 0.5 % SDS is added before treatment with proteinase K (250 µg/ml) overnight at 37 °C. Protein are precipitated by increasing the concentration of NaCl to 1.5 M and pelleted by centrifugation at 3,000 rpm for 15 minutes. DNA is precipitated by addition of 2 volumes of absolute ethanol, isolated and redissolved in 1x TE [10 mM Tris-HCl pH 8.0, 10 mM EDTA pH 8.0]. Sonication is performed for 15 minutes at room temperature using Sonics Vibracell VC130 sonicator with 3 mm probe. The fragment sizes are checked by agarose-TAE gel electrophoresis to ensure that 100-300 bp fragments are obtained. Serial two-fold dilutions are made in TE buffer.

2.8.2 cDNA synthesis

After RNA extraction (see Section 2.6), contaminating DNA was removed from 5 µg aliquots of RNA by DNase digestion using the TURBO DNA-free kit (Ambion).

RNA was then reverse transcribed using M-MLV reverse transcriptase (Life Technologies), following the manufacturer's instructions. 100 ng RNA in 25 µl final volume was incubated with reverse transcriptase at 37 °C for 30 minutes, followed by 5 minutes at 95 °C to inactivate the enzyme.

2.8.3 Analysis of real-time PCR data

Real-time PCR was performed using the ABI Prism 7000 sequence detection system (Applied Biosystems). All primers were designed with Primer Express 2.0 software (Applied Biosystems). c-*fos* and c-*jun* amplicons were detected by the 5' nuclease (Taqman) assay using 5'-FAM 3'-TAMRA-labelled probes and qPCR Mastermix Plus (Eurogentec; Table 2.3). The *gapdh* amplicon was detected by the SYBR Green assay using SYBR Green PCR Master Mix (Applied Biosystems; Table 2.3).

Each PCR plate included standard curves, which were obtained from the gDNA serial dilution samples, to ensure sample dilutions were in linear range, and control samples to ensure the absence of contamination. The controls included a no-template control (NTC) to confirm absence of contamination, a positive (RT^+) and negative control (RT^-), which consisted of the same sample (stimulation with sAn for 30 minutes) reverse transcribed in presence or absence of reverse transcriptase respectively, to confirm the absence of contaminating genomic DNA. The data obtained for c-*fos* and c-*jun* were normalised against that obtained for *gapdh* for loading control, and are presented as relative RNA levels.

Table 2.3: Real-time PCR primer sequences and working concentrations

	primer sequence				final concentration (nM)	
primer name	**forward**	**reverse**	**5' FAM 3' TAMRA probe**	**amplicon (bp)**	**forward**	**reverse**
***c-fos* +2078**	GGATTTGACTGGAGGTCTGCC	TGGGCTCAGGGTCGTTGA	CTGAGGAGGCCTTCACCCTGCCC	86	900	900
***c-jun* +1119**	TGCTCAAGCTGGCGTCG	GTGTAGTGGTGATGTGCCCATT	CTGGAGCGCCTGATCATCCAGTCC	72	300	300
***c-jun* +1651**	CCCCTATCGACATGGAGTCTCA	CACTTGGAGGCGGCAATG	TCCTCATGCGCTTCCTCTCTGCCTT	79	900	300
***gapdh* RT-PCR**	CTCGTCCCGTAGACAAAATGG	TGGTGACCAGGCGCCCAAT	-	69	500	500

all 5' FAM 3' TAMRA probes were used at 200 nM

2.9 Probabilistic model checker PRISM

The analysis of the simplified model of the interface between MAPK pathways and IE gene is carried out using the probabilistic model checker PRISM (Kwiatkowska et al. 2011). A detailed description of the model is given in Section 5.2.

PRISM accepts probabilistic models of biochemical reaction systems written in the reactive modules notation and can perform a variety of analyses, such as computing the probability or the expectation of a certain event occurring. The computed quantities can be plotted in a graph against different model parameters to analyse trends and make predictions that can be compared to experimental data.

In PRISM, a system is described as parallel composition of several modules, with each module controlling a number of variables. The behaviour of each module, that is, the state changes that occur, is specified by a number of guarded commands of the form: *[act] guard → rate : update*; where *act* is an action label, *guard* is a predicate over the variables, *rate* is a real-valued expression and *update* describes the new state of the variables. The command is enabled if the system satisfies the predicate *guard* and the transition that updates the module's variables according to *update* can occur with the rate *rate*. The action label *act* allows synchronisation between commands across modules. For example, in the module 'bell-shape generator' K_PP is a phosphorylated kinase and A, B are virtual substances, initially present at 100 and 1 molecules, respectively. The reaction network is shown in Figure 2.2. The production of phosphorylated kinase happens under the conditions 'A>0 & K_PP<100 & K_PP>0' and at the rate 'kProd*A*K_PP' (mass-action kinetics).

The values of the variables are then updated '(A'=A-1) & (K_PP'=K_PP+1)' (Figure 2.2), that is, A is decremented by one and K_PP is incremented by 1.

The model can be augmented with transition rewards, which are cumulated each time the transition is taken (Figure 2.2). This is what is used to obtain the expected number of initiation events and mRNA molecules in Chapter 5.

Figure 2.2: Example of PRISM representation

A. Description of the system of reaction used to represent the bell shape activation of MAPK (i) and its PRISM encoding (ii). A and B are virtual substances initially present at 100 and 1 molecules respectively. K-PP represents the phosphorylated MAPK and is initially set to 1 molecule. The production and degradation of phosphorylated kinase occur at the rate kProd and kDegr respectively.
B. Example of a reward structure in PRISM, which allows to analyse the frequency of transcription initiation by adding 1 to the rewards every time the step 'initiation' (not shown) of the model happens.

A.

i.

$$A + K_PP \xrightarrow{kProd} 2\ K_PP$$

$$B + K_PP \xrightarrow{kDegr} 2B$$

ii.

```
module bell-shape generator

   //     initial values
   K_PP  : [0..100] init 1;
   A     : [0..100] init 100;
   B     : [0..100] init 1;


   // population thresholds have been estimated using COPASI (ODE model) in
order to fit the activation profile
   [] A>0 & K_PP<100 & K_PP>0-> kProd*A*K_PP : (A'=A-1) & (K_PP'=K_PP+1);
   [] K_PP>0 & B>0 & B<100 -> kDegr*K_PP*B : (K_PP'=K_PP-1) & (B'=B+1);


endmodule
```

B.

```
// the reward allowing us to analyse the frequency of transcription initiation

rewards "fire"

        [initiation] true :1;

endrewards
```

Chapter 3: Okadaic acid reveals the existence of a phosphorylation turnover in quiescent cells

3.1 Introduction

The tumour promoter Okadaic acid (OA) was identified as a specific inhibitor of phosphatases PP1 and PP2A (Bialojan and Takai 1988; Cohen et al. 1990). In previous experiments, OA was also shown to be an inducer of IE gene expression (Herschman et al. 1989; Mahadevan et al. 1991). OA induces IE genes with different kinetics than are observed after TPA induction. After TPA stimulation IE gene expression peaks around 60 minutes and returns to baseline values by 3 hours, whereas IE gene expression only peaks after 3 hours and declines to basal levels 5 to 8 hours after OA stimulation (Herschman et al. 1989). IE gene induction by OA has further been associated with the nucleosomal response by ^{32}P-phospho-labelling experiments (Mahadevan et al. 1991). In this study, we have used OA to reveal and investigate the turnover of phosphorylation in p38 and JNK MAPK pathways, which are also known as stress-activated protein kinases (SAPKs), in quiescent mouse fibroblast cells.

3.1.1 Phosphatase and kinase inhibitors: tools to study turnover of phosphorylation

3.1.1.1 Specificity of inhibitors

Inhibitors are powerful tools to help understand and study signalling events. In particular, they can be used rapidly and simply in cells grown in culture to identify the physiological role of specific proteins, by inhibiting endogenous enzymes.

Inhibitors have been used to discuss the roles of specific enzymes involved in signalling pathways by inhibiting their effect, as well as the order of signalling events by examining downstream events, which are also affected. For processes controlled by reversible phosphorylation, both kinase and phosphatase inhibitors have been extensively used (Cohen et al. 1990; Cohen 1997).

The toxin OA (Figure 3.1 A) isolated from the marine sponge *Halichodria okadaii*, once identified as a specific protein phosphatase PP1 and PP2A inhibitor, has helped improved the knowledge of phosphatase activities (reviewed in Cohen et al. 1990). Enzymatic assays have been carried out to identify the half-maximal inhibitory concentration (IC_{50}) of OA against serine/threonine protein phosphatases type 1, 2A, 2B and 2C (Bialojan and Takai 1988; Cohen et al. 1989). PP2A is completely inhibited *in vitro* by 1 nM okadaic acid, PP1 has an IC_{50} of 10-15 nM okadaic acid, PP2B is less sensitive to OA and requires concentrations of okadaic acid higher than 1 µM to be inhibited, and PP2C is not affected at concentration lower than 10 µM. These differences enable to better identify the substrate specificities of these protein phosphatases *in vitro* (Cohen et al. 1989).

However, the specificity and the efficiency of an inhibitor vary when used *in vivo*. While at 1 nM, OA presents a strong specificity for PP2A *in vitro*, when studying its effect *in vivo*, higher concentrations (1 µM) are required and the intracellular concentrations of OA are unknown, as some cells might be impermeable to this compound (Cohen et al. 1990). It is thus not possible to distinguish the effect of PP2A and PP1 *in vivo* using OA, but OA is specific to these two protein phosphatases (Cohen et al. 1989; Cohen et al. 1990). Due to their lack of specificity

the phosphatase inhibitors sodium fluoride (NaF) and sodium orthovanadate cannot be used to investigate the roles of specific protein phosphatases.

In similar ways, kinase inhibitors have been used to investigate MAPK signalling pathways. Thus, specific ERK and p38 pathway inhibitors have been used to compare their respective effect on the nucleosomal response (Thomson et al. 1999). Further, investigations using the specific p38 inhibitor SB 203580 have been carried out to understand the role of the p38 pathway in anisomycin- and stress-induced IE gene expression (Hazzalin et al. 1997). These studies reveal the importance of the p38 pathway in IE gene induction as well as the existence of crosstalk between MAPK pathways. The inhibition of p38 enhances the induction of *fos* and *jun* genes after stimulation with EGF and TPA, strong activators of the ERK pathway. This complexity of MAPK pathways and IE gene induction was first discovered with the use of kinase inhibitors.

The specificities of many kinase inhibitors have been the focus of several studies *in vitro* (Davies et al. 2000; Bain et al. 2003; Bain et al. 2007). These studies emphasise the importance of verifying the specificities of kinase inhibitors, not only against members of a gene family, but also against other unrelated kinases. Indeed, SB 203580, a p38α and p38β inhibitor, has been found to inhibit Raf and LCK *in vitro* but not the closely related p38γ and p38δ (Davies et al. 2000). These studies revealed also that many compounds previously considered as specific are in fact non-specific inhibitors, for example Rottlerin, which was considered as a

Figure 3.1: Use of phosphatase and kinase inhibitors to study the reversible phosphorylation in signalling pathways

A. Structure of phosphatase and kinase inhibitors used in this chapter (i) phosphatase inhibitor okadaic acid, (ii) p38 inhibitor (SB 203580), (iii) JNK inhibitor (SP 600125), (iv) MEK 1 inhibitor (U0126), (v) MSK1/2 inhibitor (H89)
B. Schematic representation of the multiple steps of reversible phosphorylation in the MAPK pathway. '**P**' indicates one or more phosphorylation events.

A.

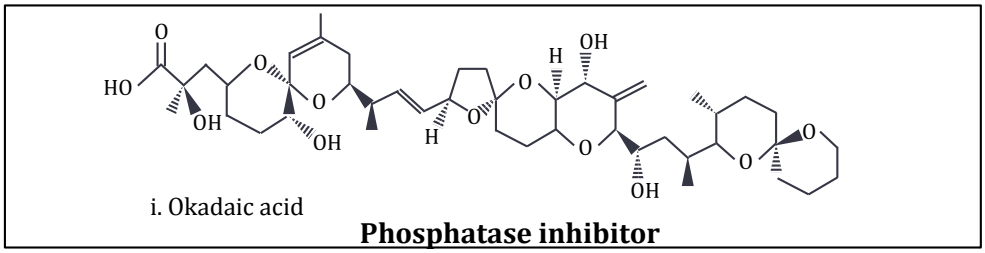

i. Okadaic acid

Phosphatase inhibitor

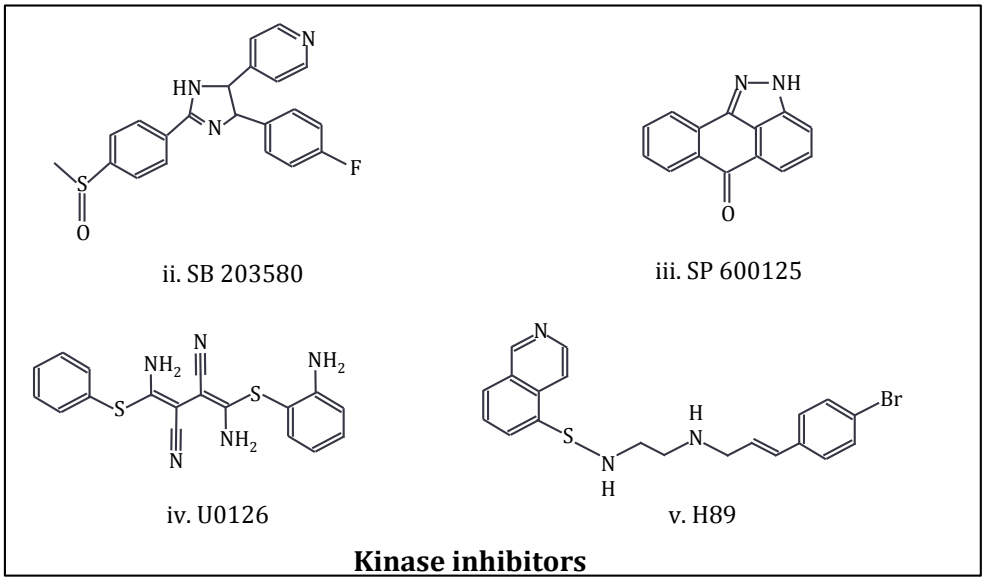

ii. SB 203580

iii. SP 600125

iv. U0126

v. H89

Kinase inhibitors

B.

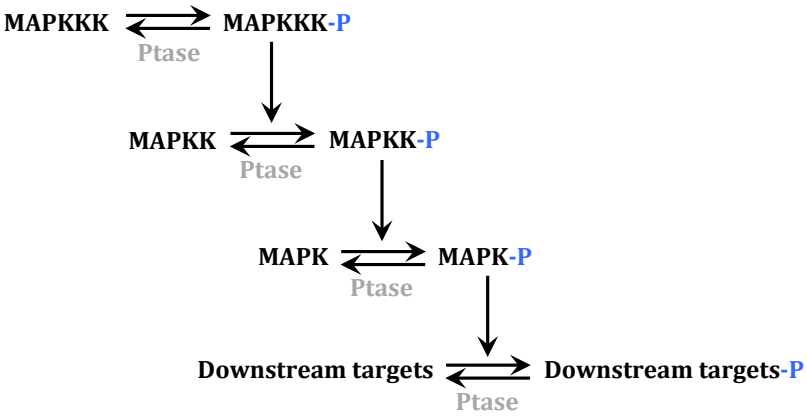

protein kinase C (PKC) inhibitor and then revealed to be non-specific (Davies et al. 2000). They can no longer be used to identify physiological substrates but can help to exclude the involvement of particular protein kinases in cellular process (Bain et al. 2003).

Different kinase inhibitors have been used in this study. The pyridinyl imidazole SB 203580 (Figure 3.1 Aii) is a specific inhibitor of p38α and p38β (Lee et al. 1994; Cohen 1997; Davies et al. 2000). It does not affect the other MAPKs, namely ERK and JNK, in mouse fibroblast C3H 10T½ cells (Hazzalin et al. 1997). SP 600125 (Figure 3.1 Aiii) was developed as a JNK isoform inhibitor but *in vitro* assays revealed the non-specificity of this compound (Bain et al. 2003; Bain et al. 2007). SP 600125 strongly inhibits, among other proteins, casein kinase 1 delta (CK1δ), phosphorylase kinase (PhK) and Aurora B (Bain et al. 2003; Bain et al. 2007). However, there is no specific inhibitor for JNK reported so far, SP 600125 allows preliminary investigations but the results require cautious interpretation. The compound U0126 (Figure 3.1 Aiv), by inhibiting MKK1, is an inhibitor of the ERK pathway. Finally the compound H89 (Figure 3.1 Av), previously described as a PKA inhibitor, was found to also inhibit MSK1 (Davies et al. 2000).

3.1.1.2 Turnover of phosphorylation and phosphatase inhibition

MAPK pathways are regulated by reversible phosphorylation. In our study, phosphorylation and dephosphorylation are associated with activation and deactivation respectively (see section 1.3, Figure 3.1 B). Inhibition of phosphatases prevents deactivation by preventing removal of the phosphate. Used together with a 'direct' activator of MAPK pathways, such as anisomycin or EGF, a phosphatase

inhibitor is expected to increase and/or prolong the activation by inhibiting kinase deactivation. However, used on its own, a phosphatase inhibitor would only activate MAPK pathways and induce IE gene expression if there is, in quiescent cells, a turnover of phosphorylation, i.e. a dynamic regulation of MAPK pathways.

In order to investigate the turnover of phosphorylation, a relatively specific phosphatase inhibitor needs to be used. In this study, the non-competitive inhibitor OA, inhibiting PP1 and PP2A protein phosphatases, was used, as it has already been shown to induce IE genes on its own (Herschman et al. 1989; Mahadevan et al. 1991). The positive control was obtained after stimulation with EGF, TPA, NaF or sub-inibitory anisomycin. Anisomycin is a protein synthesis inhibitor and a signalling agonist (Mahadevan and Edwards 1991; see Section 4.1.2.2). In this chapter, we used this compound at concentration lower than those require for protein synthesis inhibition and is referred to as sub-inhibitory anisomycin (sAn).

3.1.2 Monitoring the turnover of phosphorylation

3.1.2.1 Advantage of cell culture

To study quantitative gene regulation and the interface between MAPK pathways and IE gene expression, one of the best models is cultured cells (Hazzalin and Mahadevan 2002). A homogenous cell population can be synchronised so cells respond to external stimuli virtually instantaneously and simultaneously. One of the main advantages with this model is that it allows studying, within the same system, both gene expression and signalling events; quantitative differences in

signalling intensity, occupancy at the gene, mRNA accumulation and half-lives can be determined in this system.

However, one main challenge of this model is to make sure that cells are properly synchronised and respond simultaneously. Conditions of synchronisation vary between cell systems. C3H 10T½ mouse fibroblasts can be synchronised by quiescence (Barratt et al. 1994; Cano et al. 1994; Hazzalin et al. 1997). In medium with reduced amount of serum-supplement (0.5 % FCS), C3H 10T½ cells are synchronised in the G_0 phase, where no expression of c-*fos* and c-*jun* is observed. IE genes mediate the transition from G_0-arrested cells to proliferating cells after growth factor (GF) stimulation (Ryseck et al. 1988). The ability to synchronise cultured cells make this system the best to study IE gene induction. Due to the absence of *fos* and *jun* induction in G_0, a small change in IE gene induction after GFs stimulation can be observed. Previous work in the lab using quiesced C3H 10T½ mouse fibroblasts, have shown that the whole cell population responds in less than 1 minute to the external stimulus EGF (Cano et al. 1995). Indeed, phosphorylation of the kinase ERK induces a shift on the gel, which can be detected by ERK antibody (see Section 3.1.2.2). After EGF stimulation, all ERK kinase molecules are seen to be phosphorylated as they have all shifted within a minute (Cano et al. 1995). Therefore, we have chosen to investigate the quantitative regulation of IE genes using C3H 10T½ cultured cells, which can be synchronised and easily quiesced.

3.1.2.2 Quantification of turnover of phosphorylation

In cultured cell models, quantitatively monitoring signalling events is a challenge. Western blots give a 'snapshot', which shows the state of a population of cells at a fixed time, it is thus difficult to obtain information on a dynamic event (reviewed in Clayton et al. 2006). As with investigation of dynamic acetylation of histone H3, where HDAC inhibitors were used to characterise the turnover of acetylation, use of the phosphatase inhibitor OA is described in this chapter to study the turnover of phosphorylation (Hazzalin and Mahadevan 2005).

Western blots can give useful qualitative information on differences in levels between samples, but rigorous control experiments are needed in order to obtain quantitative information. In this chapter, Western blot results are used qualitatively and Ponceau S staining of the membranes is used as loading control. Using Western blots, we compare the activity of various signalling proteins to identify the ones that are affected by OA. Many antibodies and anti-phospho antibodies targeting the phosphorylated form of the protein are used in this study. They include antibodies against kinases, TFs, histone H3 and the nuclear protein HMGN1. The conditions at which each antibody worked best were optimised. Moreover, OA is used in combination with kinase inhibitors to identify the steps at which OA acts.

Further in this thesis (see Chapter 5), Western blots are used quantitatively to obtain activation curves of different kinases and TFs. For quantitative analysis, it is necessary to ensure that the antibody used is in its linear range of action (so that a doubling of epitope results in a doubling of antibody binding), by performing a

standard curve on every blot carried out. Moreover, the results obtained have to be normalised against a loading control.

Both phospho-specific, recognising the phosphorylated form of proteins, and anti-protein-specific, recognising both non-phosphorylated and phosphorylated forms of proteins, antibodies are used in this study. The use of an anti-protein-specific antibody rather than a phospho-specific one gives more information on the proportion of activation of the protein, when the modification of this protein induced a difference in migration, so a shift can be observed on the gel. Indeed, it is possible to assess the percentage of phosphorylated proteins by comparing the intensity of the shifted band (corresponding to the phosphorylated band) and the basal (non-phosphorylated) band. The combination of phospho-specific and mobility shifts of anti-protein-specific antibodies is valuable for the investigation of a turnover of phosphorylation.

However, the sensitivity of western blots, due to the sensitivity of the antibody and the detection method, is a limiting factor. If no signal is detected, for a modified protein, it could either mean that the protein does not exist in the modified form in these cells or that the levels of modified proteins are to low to be detected by western blotting. In this chapter, the latter explanation is used to interpret our results and reveal turnover of phosphorylation in quiescent cells.

3.1.3 Summary

The main aim of experiments described in this chapter is to characterise the effect of OA at various kinases of MAPK signalling pathways, this phosphatase inhibitor

having been shown to induce IE gene expression and activate the nucleosomal response. Using OA to investigate the role of phosphatases in the MAPK pathways regulation consists of a new use of this inhibitor. OA revealed the presence of a turnover of phosphorylation in quiescent cells, which suggests a more dynamic regulation of the MAPK pathways. We have assessed, by Western blotting, that the main effect of OA is on the stress-induced MAPKs, the p38 and the JNK pathways.

3.2 Results

3.2.1 Okadaic acid induces IE gene transcription

3.2.1.1 IE gene induction

The phosphatase inhibitor OA has been shown to induce IE gene expression, while used on its own in Swiss 3T3 and C3H 10T½ cells (Herschman et al. 1989; Mahadevan et al. 1991). This characteristic makes it a good compound to investigate the possibility of a dynamic turnover of phosphorylation within MAPK pathways, in quiescent cells. We first investigated the effect of a time-course of OA on induction of the IE genes c-*fos* and c-*jun* by Northern blotting using *gapdh* as loading control. Cells were treated with OA 1 μM for different times, as this concentration activates the strongest signalling response (see Section 3.2.1.2). A time-point was taken every ten minutes between 10 and 120 minutes (Figure 3.2, lanes 4-15).

The induction of c-*fos* after OA stimulation is detected after a 20 minute treatment (Figure 3.2, lane 5), mRNA levels increase until 60 minutes and then remain relatively stable until at least 120 minutes (Figure 3.2, lanes 6-15). In our

experiments, after 45 minutes of OA 1 μM treatment, morphological changes of cells could be observed, and after 120 minutes of treatment cells started to detach (data not shown). Hence the maximum treatment time that could be done was 120 minutes. However, experiments treating density-arrested 3T3 and C3H 10T½ cells with OA at 100 ng/ml (0.1nM), show that IE gene expression levels, after OA treatment, are back to basal levels by 5 to 8 hours (Herschman et al. 1989). In comparison to induction of c-*fos* gene by other compounds, such as EGF and sAn (reviewed in Hazzalin and Mahadevan 2002), the OA induction is more sustained. However, a similar intensity can be observed for the positive control, sAn (Figure 3.2, lanes 2 and 3), and OA induction (Figure 3.2, lanes 4-15). Furthermore, EGF and sAn induction of c-*fos* gene are comparable in intensity (Hazzalin et al. 1996). Thus, OA seems to induce c-*fos* as strongly as sAn or EGF.

Induction of c-*jun* by OA has some similarities with c-*fos* induction. It is also detectable after 20 minutes of treatment and mRNA is still visible after 120 minutes (Figure 3.2, lanes 5 and 15). However, mRNA levels appear to slowly decrease after 80 minutes, especially for the upper band (Figure 3.2, lanes 11-15). The two bands detected for c-*jun* result from alternative polyadenylation of c-*jun* gene, which possesses three polyadenylation sites (Ryseck et al. 1988). Moreover, by qualitatively comparing the intensity of the different signals, c-*jun* induction by OA appears to be weaker than the one observed after sAn activation, as the intensity observed after OA induction (Figure 3.2, lanes 4-15) is not as strong as the one observed after sAn stimulation (Figure 3.2, lanes 2 and 3).

Figure 3.2: OA induces c-*fos* and c-*jun* expression

Quiescent C3H 10T½ mouse cells were stimulated with sAn (25 ng/ml; lanes 2 and 3), or treated with OA (1 μM; lanes 4-15) for the indicated times. Lane 1 is the negative control (untreated cells). Total RNA was extracted following the acid thiocyanate-phenol-chloroform extraction (see Section 2.6) and probed by Northern blotting for expression of c-*fos* (top), c-*jun* (middle) and *gapdh* (bottom). This is one experiment representative of three repeats. The quantification of these blots is presented in Figure 4.6.

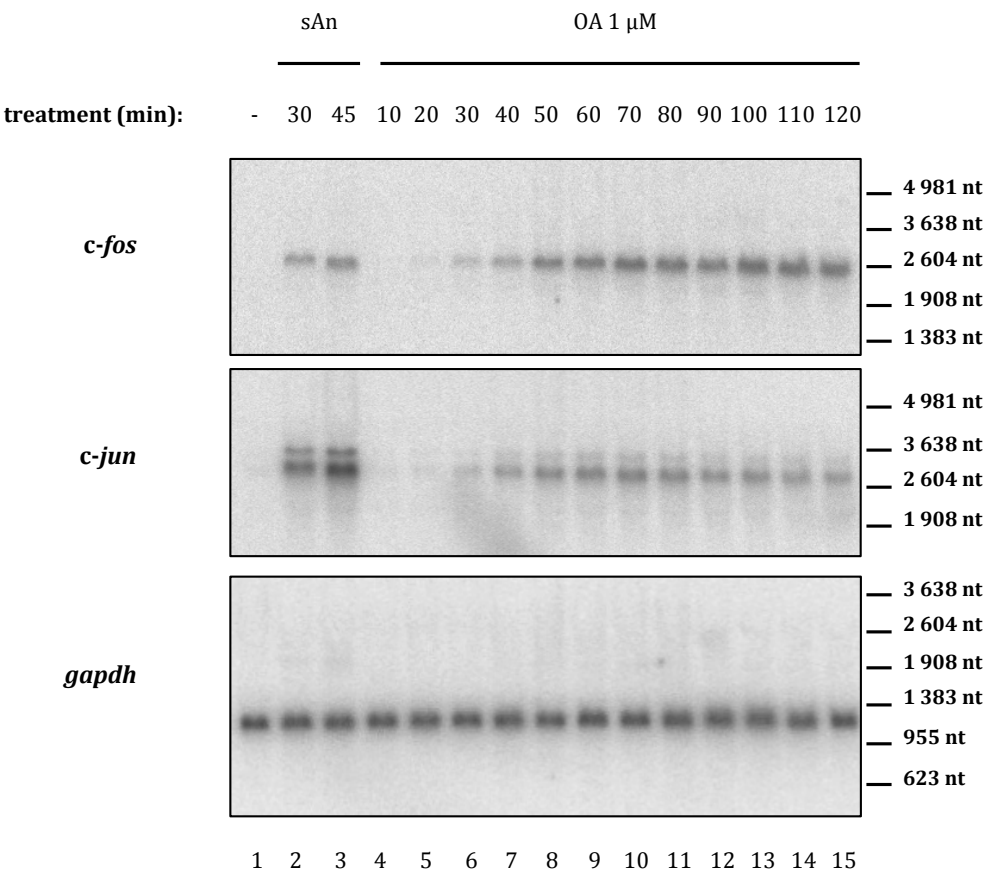
sAn
OA 1 µM
treatment (min):
- 30 45 10 20 30 40 50 60 70 80 90 100 110 120
c-fos
4 981 nt
3 638 nt
2 604 nt
1 908 nt
1 383 nt
c-jun
4 981 nt
3 638 nt
2 604 nt
1 908 nt
gapdh
3 638 nt
2 604 nt
1 908 nt
1 383 nt
955 nt
623 nt
1 2 3 4 5 6 7 8 9 10 11 12 13 14 15

The capacity of OA to induce c-*fos* and c-*jun* transcription suggests the involvement of the phosphatases PP1 and PP2A in the negative regulation of these genes. OA may inhibit the dephosphorylation of protein(s) involved in IE gene induction. In order to investigate this, we asked whether the induction of c-*fos* and c-*jun* by OA happens through the MAPK pathways.

3.2.1.2 Histone H3 phosphorylation

IE gene induction through MAPK pathways has been associated with the nucleosomal response, which consists of the phosphorylation of histone H3 on serine 10 and of HMGN1 on serine 6 (Thomson et al. 1999). Moreover, histone H3 phosphoacetylation has been found to be associated with c-*fos* and c-*jun* promoter regions upon induction (Clayton et al. 2000). Thus, to answer the question whether the IE gene induction by OA happens through the MAPK pathways, we carried out Western blotting experiments using specific antibodies against phospho-histone H3, which recognises histone H3 phosphorylated on serine 10 (H3S10ph), and against phosphoacetyl-histone H3, which detects histone H3 acetylated on lysine 9 and phosphorylated on serine 10 (H3K9acS10ph). The anti-phospho-H3 antibody used is not occluded by acetylation at adjacent lysine 9 (Dyson et al. 2005), while the anti-phosphoacetyl-H3 antibody can recognise phosphoacetylated histone H3 tails but not the histone H3 tails carrying a single modification (H3K9ac or H3S10ph; Clayton et al. 2000). Previous ^{32}P-phosphate labelling experiments have shown that OA, as well as inducing IE genes, activates the nucleosomal response (Mahadevan et al. 1991).

As shown in Figure 3.3, OA activates histone H3 phosphorylation and phosphoacetylation. Indeed, an increase in intensity after OA stimulation (Figure 3.3, lanes 3-8) compared to the control (Figure 3.3, lane 1) can be observed for both H3S10ph and H3K9acS10ph. Besides, as seen for IE gene induction, OA activation of signalling pathways has different kinetics than sAn stimulation. OA-activated histone phosphoacetylation is probably targeted to IE genes.

In order to identify the best conditions to study the potential OA effect on the MAPK pathways, different concentrations of OA were used. The results for OA 500 nM (Figure 3.3, lanes 6, 7 and 8) and 1 µM (Figure 3.3, lanes 3, 4 and 5) are shown in Figure 3.3. Both histone H3 phosphorylation and phosphoacetylation after treatment with OA 500 nM are barely activated after 30 minutes (Figure 3.3, lane 6) and a comparable if not stronger increase in signal intensity than after sAn 30 minutes stimulation, is observed after 60 and 90 minutes (Figure 3.3, lanes 2, 7 and 8). After treatment with OA 1 µM, histone H3 phosphorylation increases slightly after 30 minutes while histone H3 phosphoacetylation is barely activated (Figure 3.3, lane 3). This difference between histone phosphorylation and phosphoacetylation was not observed consistently (data not shown) and is not observed after a 60 or a 90 minutes OA treatment, for which a strong activation for both phosphorylation and phosphoacetylation is observed (Figure 3.3, lanes 4 and 5). From the study carried on histone H3 phosphorylation and phosphoacetylation, OA 500 nM or OA 1 µM after 60 minutes seem to both be adequate conditions to study OA effect.

Figure 3.3: OA activates histone H3 phosphorylation and phosphoacetylation

Quiescent C3H 10T½ cells were stimulated for 30 minutes with sAn (25 ng/ml, lane 2), or treated with OA at 1 μM (lanes 3, 4 and 5) or at 500 nM (lanes 6, 7 and 8) for the indicated times. Lane 1 is the negative control (untreated cells). Histones were acid extracted (see Section 2.3.2), resolved on SDS-PAGE gels (see Section 2.4.1) and probed using antibodies against H3S10ph (top) or H3K9acS10ph (middle). Ponceau staining (bottom) is used as loading control. This is one experiment representative of four repeats.

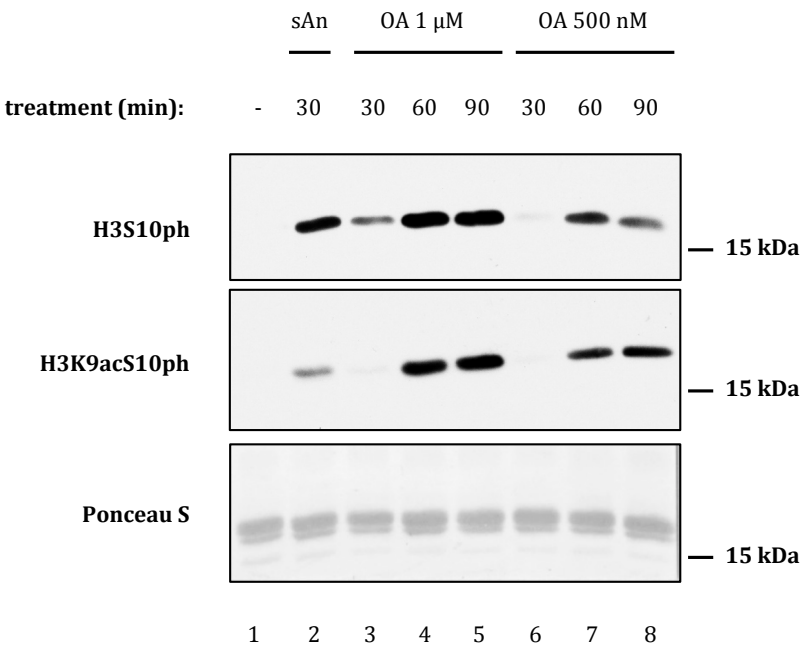
sAn
OA 1 µM
OA 500 nM
treatment (min):
- 30 30 60 90 30 60 90
H3S10ph
15 kDa
H3K9acS10ph
15 kDa
Ponceau S
15 kDa
1 2 3 4 5 6 7 8

3.2.2 Effect of OA on MAPK pathways

Histone H3 phosphorylation is mediated by MSKs, which lies immediately downstream of the ERK and p38 pathways (Thomson et al. 1999). After showing that OA activates histone H3 phosphoacetylation, we asked whether OA activates the MAPK pathways or not, and whether its activation is specific to one MAPK pathway or to multiple pathways. Therefore, we looked at the activation of the kinases ERK1/2 and p38 by Western blotting to identify the MAPK pathway activated by OA.

3.2.2.1 OA does not activate ERK1/2

We used an anti-protein-specific antibody for ERK1/2 (Figure 3.4), the activation of ERK1/2 can be observed by the presence of a shift on the gel. The anti-ERK antibody allows the detection of both the phosphorylated forms (slow migrating bands; Figure 3.4, lanes 3 and 4, top panel) and the non-phosphorylated forms (fast migrating bands; Figure 3.4, lanes 1, 2 and 5-13, top panel) of ERK1/2, and thus allows identifying the proportion of phosphorylated proteins (see Section 3.1.2.2).

After NaF activation, used as positive control, a complete activation of ERK1/2 can be observed (Figure 3.4, lanes 3 and 4). After 30 and 60 minutes of NaF stimulation, ERK1/2 signals have completely shifted indicating a full activation of these kinases (Figure 3.4, lanes 3 and 4). However, after OA treatment, no activation of ERK1/2 is observed independent of the concentration of OA used

Figure 3.4: OA activates p38 phosphorylation but not ERK1/2 phosphorylation

Quiescent C3H 10T½ cells were stimulated for 30 minutes with sAn (25 ng/ml; lane 2), or for 30 or 60 minutes with NaF (50 mM; lanes 3 and 4), or treated with OA 1 μM (lanes 5, 6 and 7), or OA 500 nM (lanes 8, 9 and 10), or OA 100 nM (lanes 11, 12 and 13) for the indicated times. Lane 1 is the negative control (untreated cells). Cells were lysed with high-salt lysis buffer (see Section 2.3.1) and cell extracts were separated on ERK gels (see Section 2.4.2) and probed with anti-ERK1/2 (top) or anti-phospho-p38 (middle) antibodies. Ponceau staining (bottom) is used as loading control. This is one experiment representative of four repeats.

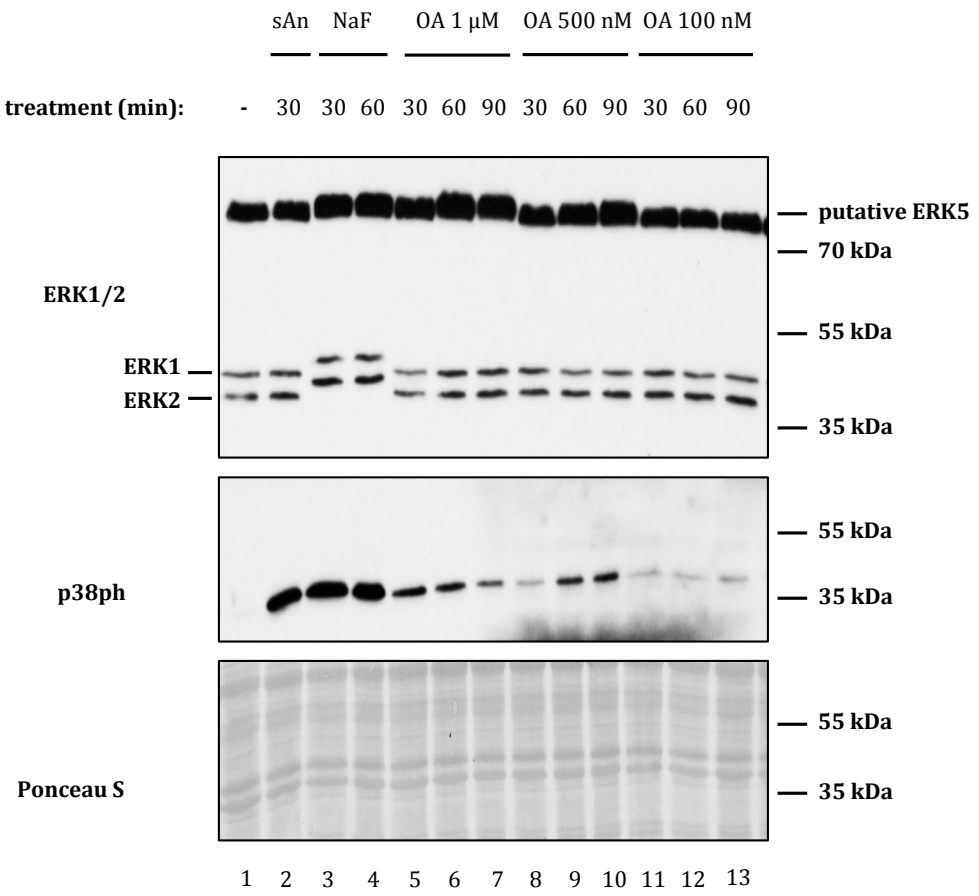
sAn
NaF
OA 1 µM
OA 500 nM
OA 100 nM
treatment (min):
- 30 30 60 30 60 90 30 60 90 30 60 90
ERK1/2
ERK1
ERK2
putative ERK5
70 kDa
55 kDa
35 kDa
p38ph
55 kDa
35 kDa
Ponceau S
55 kDa
35 kDa
1 2 3 4 5 6 7 8 9 10 11 12 13

(Figure 3.4, lanes 5-13). Therefore, OA does not seem to have an effect on the ERK pathway.

3.2.2.2 OA activates p38 phosphorylation

To investigate the effect of OA on the p38 pathway, an anti-phospho-p38-specific antibody was used. The anti-phospho-p38 antibody detects p38 only when activated by phosphorylation at threonine 180 and tyrosine 182. By using this antibody, we showed that OA activates p38 phosphorylation as a signal can be observed after OA stimulation. This activation depends on OA concentration. Indeed for OA at 1 μM, p38 activation is observed after 30 minutes and decreases after 90 minutes (Figure 3.4, lanes 5 and 7). While for OA at 500 nM, only a small increase in p38 activation is observed after 30 minutes and keeps on increasing up to 90 minutes (Figure 3.4, lanes 8-10). Finally OA at 100 nM activates really weakly p38 phosphorylation (Figure 3.4, lanes 11-13). It is to be noted here that the weak activation observed after OA 100 nM treatment, as well as the decrease of p38 activation after 90 minutes treatment with OA 1 μM were not observed every time the experiment was repeated (data not shown). The latter may be linked to the toxicity of OA, particularly at longer time points, which could disturb the cells. It is thus difficult to draw any conclusion for this time-point, but it does not affect the conclusion that OA activates p38 at earlier time points, as these results are reproducible.

PP1 and PP2A must dephosphorylate p38 or negatively regulate a signalling event upstream of p38 in order to explain the p38 phosphorylation observed after OA treatment. The main protein phosphatases of p38 are the DUSPs, which can

dephosphorylate both threonine and tyrosine residues (see Section 1.4.3), while PP1 and PP2A are serine/threonine phosphatases (see Section 1.4.2). However only a single dephosphorylation of one residue would prevent kinase activity. PP1 and PP2A could deactivate p38 by dephosphorylation of its threonine residue or they could dephosphorylate upstream kinases of p38 such as the MAPKK, which are phosphorylated on serine and threonine residues (see Section 1.3.1.2).

The presence of DUSPs dephosphorylating p38 can explain the weak activation observed for p38 after OA treatment (Figure 3.4), dephosphorylation of p38 being either not or only partially inhibited. Indeed, even though OA activates p38 phosphorylation, this activation appears to be weaker than the activation generated by sAn or NaF stimulations, as can be evaluated by the intensities of the bands (Figure 3.4, lanes 2-10). This difference in activation of p38 phosphorylation between sAn and OA stimulations is not observed at the level of histone H3 phosphorylation (Figure 3.3).

Although these results do not allow to conclude on the specific action of OA, so on the role of PP1 and PP2A in the p38 pathway, it reveals the presence of a basal turnover of phosphorylation in this pathway and suggests that the histone phosphorylation after OA treatment results from the p38 pathway.

3.2.2.3 OA does not affect EGF-induced stimulation of ERK1/2

To further preclude the involvement of ERK1/2 in OA-induced response, we investigated the effect of OA treatment on EGF-induced activation of ERK1/2 by treating C3H 10T½ cells with EGF and OA simultaneously (Figure 3.5). Three

different concentrations of OA are used (1 µM, 500 nM and 100 nM). ERK1/2 is fully activated after a 10 minute treatment of EGF, as seen by the complete shift observed (Figure 3.5, lane 2). This activation is transient and after a 30 minute stimulation with EGF, the level of activated ERK1/2 decreases, which is indicated by the detection of both non-phosphorylated ERK1/2 (fast migrating bands) and phosphorylated ERK1/2 (slow migrating bands) on the gel (Figure 3.5, lane 3) and ERK1/2 is back to unstimulated levels after a 60 minute treatment (data not shown). A similar time course is observed after simultaneous stimulation of cells by OA and EGF (Figure 3.5, lanes 10, 11, 12, 13, 14 and 15). OA does not affect the kinetics of EGF activation of ERK1/2, which suggests that PP1 and PP2A are not involved in deactivation of ERK1/2 or their upstream kinases.

3.2.2.4 OA stimulates histone phosphorylation through the p38 pathway

The results obtained for ERK1/2 and p38 suggest that OA stimulates histone phosphorylation through the p38 pathway. This is also supported by the use of specific inhibitors for the different MAPK pathways looking at their effect on histone phosphorylation (Figure 3.6). The use of OA in combination with kinase inhibitors can further help our understanding of its effect in MAPK regulation and activation, as the nucleosomal response is downstream of the ERK and the p38 pathways. The use of specific ERK and p38 inhibitors in combination with OA would permit conclusion on which of these pathways OA prevents deactivation of and thus locate more precisely the point of turnover of phosphorylation.

The compound sAn is used as a positive control for the p38 and JNK pathways (Figure 3.6, lanes 2-5), while TPA is the positive control for the ERK pathway

Figure 3.5: OA does not prolong EGF activation of ERK1/2

Quiescent C3H 10T½ cells were stimulated for 10 or 30 minutes with EGF (50 ng/ml; lanes 2 and 3) or OA 1 μM (lanes 4 and 5) or OA 500 nM (lanes 6 and 7) or OA 100 nM (lanes 8 and 9), or treated simultaneously for 10 or 30 minutes with EGF (50 ng/ml) and OA 1 μM (lanes 10 and 11), or EGF (50 ng/ml) and OA 500 nM (lanes 12 and 13), or EGF (50 ng/ml) and OA 100 nM (lanes 14 and 15). Lane 1 is the negative control (untreated cells). Cells were lysed with high-salt lysis buffer (see Section 2.3.1) and cell extracts were separated on ERK gels (see Section 2.4.2) and probed with anti-ERK1/2 (top) antibody. Ponceau staining (bottom) is used as loading control. This is one experiment representative of two repeats.

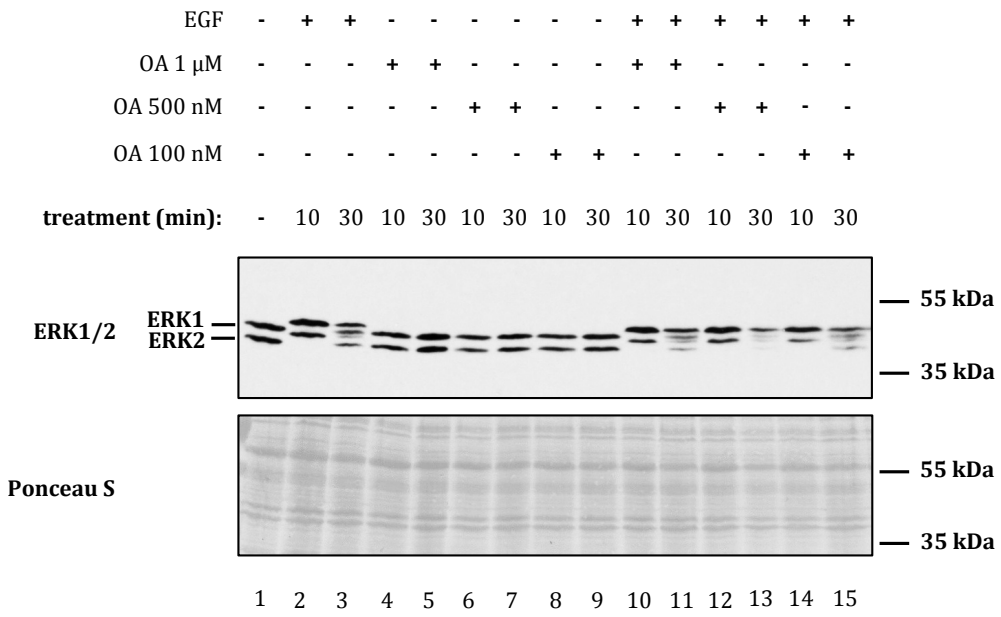
EGF - + + - - - - - - + + + + + +
OA 1 µM - - - + + - - - - + + - - - -
OA 500 nM - - - - - + + - - - - + + - -
OA 100 nM - - - - - - - + + - - - - + +
treatment (min): - 10 30 10 30 10 30 10 30 10 30 10 30 10 30
ERK1/2
ERK1
ERK2
55 kDa
35 kDa
Ponceau S
55 kDa
35 kDa
1 2 3 4 5 6 7 8 9 10 11 12 13 14 15

(Figure 3.6, lanes 6 and 7). Pre-treatment with SB 203580, H89 or SP 600125 inhibits OA activation of histone H3 phosphorylation (Figure 3.6, lanes 9-11). Conversely, pre-treatment with U0126, inhibiting the ERK pathway, does not have any effect on OA activation of histone H3 phosphorylation and phosphoacetylation (Figure 3.6, lane 12), confirming that histone H3 phosphorylation observed after OA stimulation is through the p38 pathway.

Comparing the effect of kinase inhibitor pre-treatments on sAn and OA stimulation, we can observe some differences. Only a partial inhibition of histone H3 phosphorylation and phosphoacetylation is observed after pre-treatment with SB 203580 for OA treatment (Figure 3.6, lane 9) compared to the complete inhibition observed for the sAn-induced histone H3 phosphorylation (Figure 3.6, lane 3), suggesting that inhibition of p38 only partially affects the OA-activation of phosphorylation of histone H3, downstream target of p38. Thus, OA may inhibit a downstream step(s) of p38 or another pathway, kinase leading to histone H3 phosphorylation to allow this phosphorylation. Besides, the strong inhibition of OA-induced phosphorylation observed after pre-treatment with SP 600125, differs from the partial inhibition observed for sAn-induced activation (Figure 3.6, lanes 5 and 11), which also suggests the presence of another pathway or kinase. SP 600125 is a non-specific inhibitor and has been shown to inhibit, among many other kinases, Aurora B, which is the kinase responsible for the mitotic phosphorylation of histone H3 (Clayton and Mahadevan 2003). But if histone H3 phosphorylation after OA treatment was due to inhibition of dephosphorylation of Aurora B or upstream signalling events leading to activation of Aurora B, no inhibition would be expected after H89 pre-treatment, while OA-induced histone

Figure 3.6: OA activation of histone H3 is inhibited by SB 203580, SP 600125 and H89

Quiescent C3H 10T½ were pre-treated for 30 minutes (indicated by '+') with the p38 inhibitor SB 203580 ('SB', 10 μM; lanes 3, 9 and 13), the MSK inhibitor H89 (10 μM; lanes 4, 10 and 14), the JNK inhibitor SP 600125 ('SP', 10 μM; lanes 5, 11 and 15) or the MEK1 inhibitor U0126 ('U', 10 μM; lanes 7, 12 and 16), followed by treatment for 30 minutes with sAn (25 ng/ml; lanes 2, 3, 4 and 5), for 30 minutes with TPA (100 nM; lanes 6 and 7), for 60 minutes with OA (1 μM; lanes 8, 9, 10, 11 and 12) or untreated ('-'; lanes 13, 14, 15 and 16). Lane 1 is the negative control (untreated cells). Histones were acid extracted (see Section 2.3.2), resolved on SDS-PAGE gels (see Section 2.4.1) and probed using antibodies against H3S10ph (top) or H3K9acS10ph (middle). Ponceau staining (bottom) is used as loading control. This is one experiment representative of three repeats.

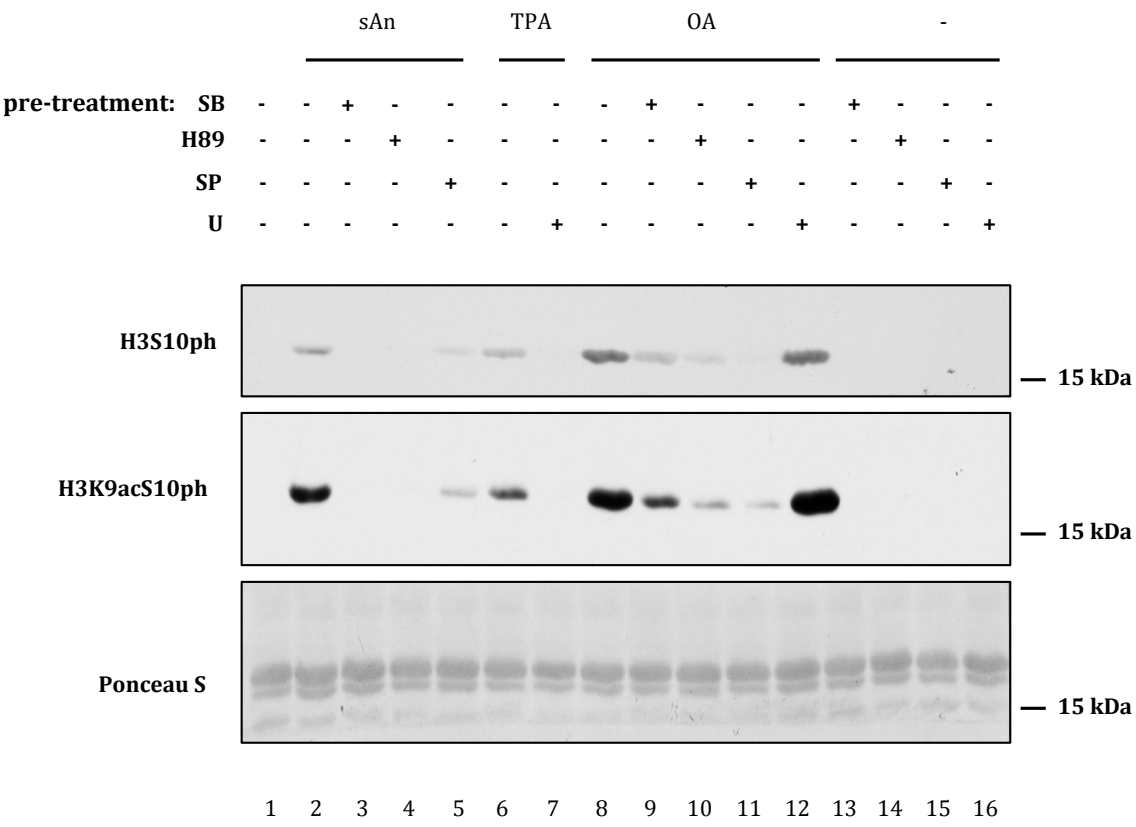
sAn
TPA
OA
-
pre-treatment:
SB - - + - - - - - + - - - + - - -
H89 - - - + - - - - - + - - - + - -
SP - - - - + - - - - - + - - - + -
U - - - - - - + - - - - + - - - +
H3S10ph
H3K9acS10ph
Ponceau S
15 kDa
15 kDa
15 kDa
1 2 3 4 5 6 7 8 9 10 11 12 13 14 15 16

H3 phosphorylation is in fact fully inhibited by H89 (Figure 3.6, lane 10). This indicates that OA activates histone H3 phosphorylation through MSK1/2.

3.2.2.5 OA activates the different downstream targets of p38

We further investigated the effect of OA on the p38 pathway by looking at the downstream targets of p38. The phosphorylated form of MSK1, direct downstream kinase of p38, is detected by a shift on the gel and by the use of an anti-MSK1 antibody. We showed that this direct downstream kinase of p38 is activated by OA, and were able to determine the proportion of MSK1 phosphorylated (Section 3.1.2.2). Similarly to histone H3, a small proportion of MSK1 is phosphorylated after 30 minutes of OA treatment, as indicated by the shift observed (Figure 3.7 A, lanes 3 and 6). After 60 minutes of treatment with OA at 1 µM, a complete shift is observed, indicating full activation of MSK1 (Figure 3.7 A, lane 4). The complete activation only appears after 90 minutes of treatment with OA 500 nM (Figure 3.7 A, lane 8). As seen previously for p38 activation (Section 3.2.2.2) the kinetics of activation depends on the concentration of OA used.

To corroborate the results obtained for histone H3, for pre-treatment experiments with the different kinase inhibitors, the effects of these inhibitors on MSK1 were investigated. In the same way as for histone phosphorylation, pre-treatment with SB 203580 only partially inhibits OA activation of MSK1 while it fully inhibits sAn activation (Figure 3.7 B, lanes 3 and 8). In addition, MSK1 phosphorylation after OA treatment is inhibited by pre-treatment with SP 600125, which is not the case after sAn stimulation (Figure 3.7 B, lanes 4 and 9). As expected, the combination of SB 203580 and SP 600125 had the same effect as SB 203580 alone for sAn

Figure 3.7: MSK1 is activated by OA and pre-treatment with SB 203580 does not inhibit this activation

A. Quiescent C3H 10T½ cells were stimulated for 30 minutes by sAn (25 ng/ml; lane 2), or treated with OA 1 μM (lanes 3, 4 and 5) or with OA 500 nM (lanes 6, 7 and 8) for indicated times. Lane 1 is the negative control (untreated cells). Cells were lysed with high-salt lysis buffer (see Section 2.3.1) and cell extracts were separated on ERK gels (see Section 2.4.2) and probed using an antibody against MSK1 (top). Ponceau staining (bottom) is used as loading control. This is one experiment representative of two repeats.
B. Quiescent C3H 10T½ were pre-treated for 30 minutes (indicated by '+') with the p38 inhibitor SB 203580 ('SB', 10 μM; lanes 3, 6, 8, 11, 12 and 15), the MSK inhibitor H89 (10 μM; lanes 5, 10 and 14), the JNK inhibitor SP 600125 ('SP', 10 μM; lanes 4, 6, 9, 11, 13 and 15), followed by stimulation for 30 minutes with sAn (25 ng/ml; lanes 2, 3, 4, 5 and 6), or treatment for 60 minutes with OA (1 μM; lanes 7, 8, 9, 10 and 11), or untreated ('-'; lanes 12, 13, 14 and 15). Lane 1 is the negative control (untreated cells). Cells were lysed with high-salt lysis buffer (see Section 2.3.1) and cell extracts were separated on ERK gels (see Section 2.4.2) and probed using an antibody against MSK1 (top). Ponceau staining (bottom) is used as loading control. This is one experiment representative of three repeats.

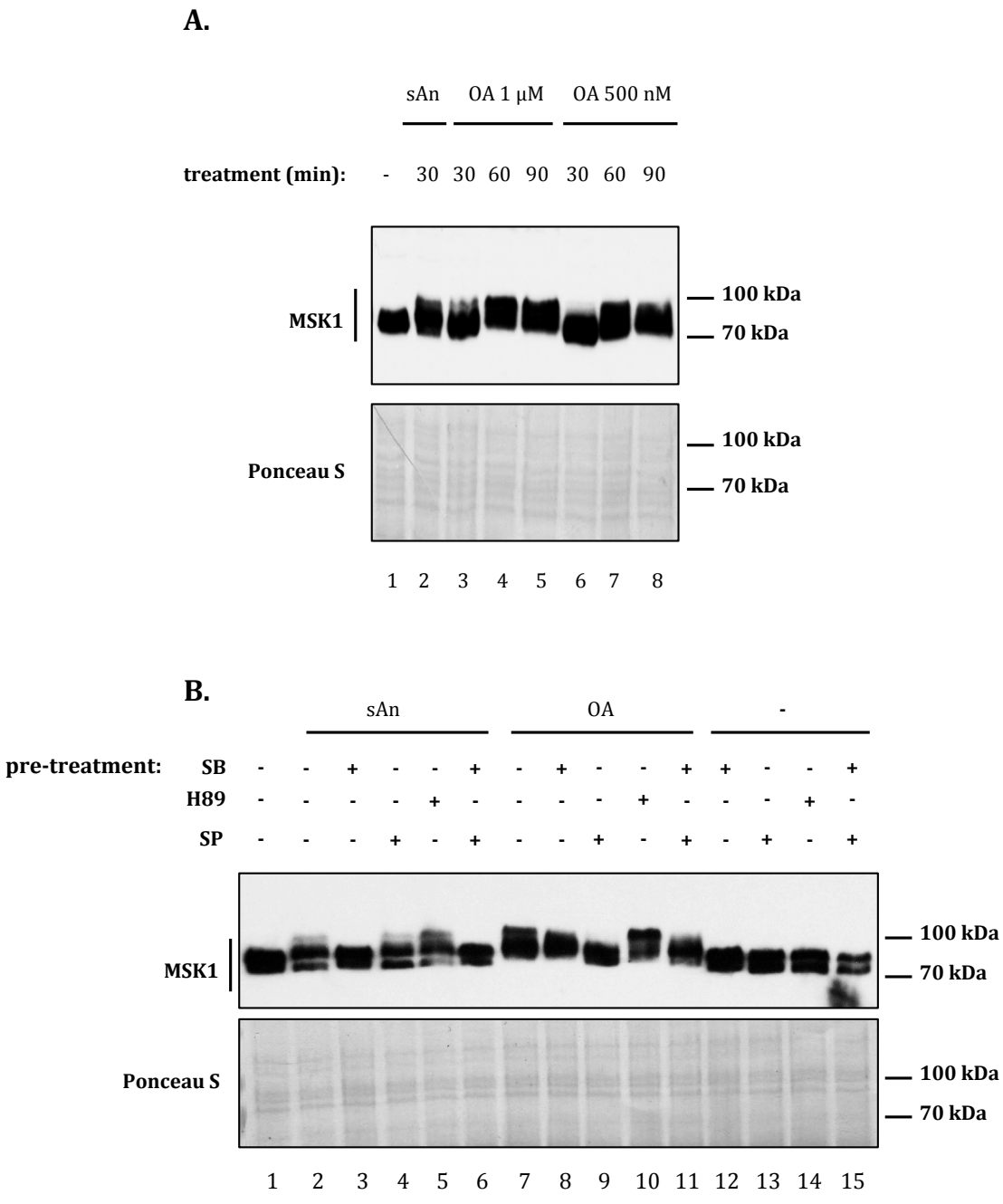
A.
sAn
OA 1 µM
OA 500 nM
treatment (min):
- 30 30 60 90 30 60 90
MSK1
100 kDa
70 kDa
Ponceau S
100 kDa
70 kDa
1 2 3 4 5 6 7 8
B.
sAn
OA
-
pre-treatment:
SB
H89
SP
MSK1
100 kDa
70 kDa
Ponceau S
100 kDa
70 kDa
1 2 3 4 5 6 7 8 9 10 11 12 13 14 15

stimulation (Figure 3.7 B, lanes 6 and 3) and the same effect as SP 600125 for OA treatment (Figure 3.7 B, lanes 11 and 9). Finally, pre-treatment with H89 had no effect on MSK1 activation after OA or sAn treatment, as H89 inhibits MSK1 action but not its activation (Figure 3.7 B, lanes 5 and 10; Davies et al. 2000).

As well as histone H3, MSK1 also phosphorylates the nucleosomal protein HMGN1 (Soloaga et al. 2003) and the transcription factor CREB (Deak et al. 1998; Figure 1.6). We investigated the effect of OA treatment on these two proteins to compare them with histone H3 (Figure 3.8 and Figure 3.9).

An anti-phospho-CREB antibody was used, detecting CREB phosphorylated at serine 133. This activation follows similar patterns as histone H3 phosphorylation for OA stimulation on its own but not after pre-treatment with kinase inhibitors. Indeed, CREB phosphorylation is observed only weakly after 30 minutes of treatment with OA at 1 µM and is not observed after 30 minutes of treatment with OA 500 nM (Figure 3.8 A, lane 3 and 7). In addition, both concentrations strongly activate CREB phosphorylation after 60 minutes (Figure 3.8 A, lanes 4, 6 and 8) and phosphorylation further increases after 90 minutes (Figure 3.8 A, lanes 5 and 9). However, pre-treatment with either SB 203580, SP 600125 or H89 does not inhibit CREB phosphorylation after OA treatment (Figure 3.8 B, lanes 7-11). In comparison sAn activation of CREB is inhibited by pre-treatment with SB 203580 and H89 (Figure 3.8 B, lanes 3 and 5). This suggests that, unlike after sAn stimulation, CREB activation after OA-treatment is not mediated solely through MSK1/2.

Figure 3.6: CREB is activated by OA and is not inhibited after pre-treatment with SB 203580, H89 or SP 600125

A. Quiescent C3H 10T½ cells were stimulated for 30 minutes by sAn (25 ng/ml; lane 2), or treated with OA 1 μM (lanes 3, 4, 5 and 6) or with OA 500 nM (lanes 7, 8 and 9) for indicated times. Two batches of OA were used and their effect after 60 minutes was compared (1 μM; lanes 4 and 6). Lane 1 is the negative control (untreated cells). Cells were lysed with high-salt lysis buffer (see Section 2.3.1) and cell extracts were separated on big SDS gels (see Section 2.4.1) and probed using an antibody against phospho-CREB (top). Ponceau staining (bottom) is used as loading control. This is one experiment representative of two repeats.
B. Quiescent C3H 10T½ were pre-treated for 30 minutes (indicated by '+') with the p38 inhibitor SB 203580 ('SB', 10 μM; lanes 3, 6, 8, 11, 12 and 15), the MSK inhibitor H89 (10 μM; lanes 5, 10 and 14), the JNK inhibitor SP 600125 ('SP', 10 μM; lanes 4, 6, 9, 11, 13 and 15), followed by stimulation for 30 minutes with sAn (25 ng/ml; lanes 2, 3, 4, 5 and 6), or treatment for 60 minutes with OA (1 μM; lanes 7, 8, 9, 10 and 11), or untreated ('-'; lanes 12, 13, 14 and 15). Lane 1 is the negative control (untreated cells). Cells were lysed with high-salt lysis buffer (see Section 2.3.1) and cell extracts were separated on big SDS gels (see Section 2.4.1) and probed using an antibody against phospho-CREB (top). Ponceau staining (bottom) is used as loading control. This is one experiment representative of three repeats.

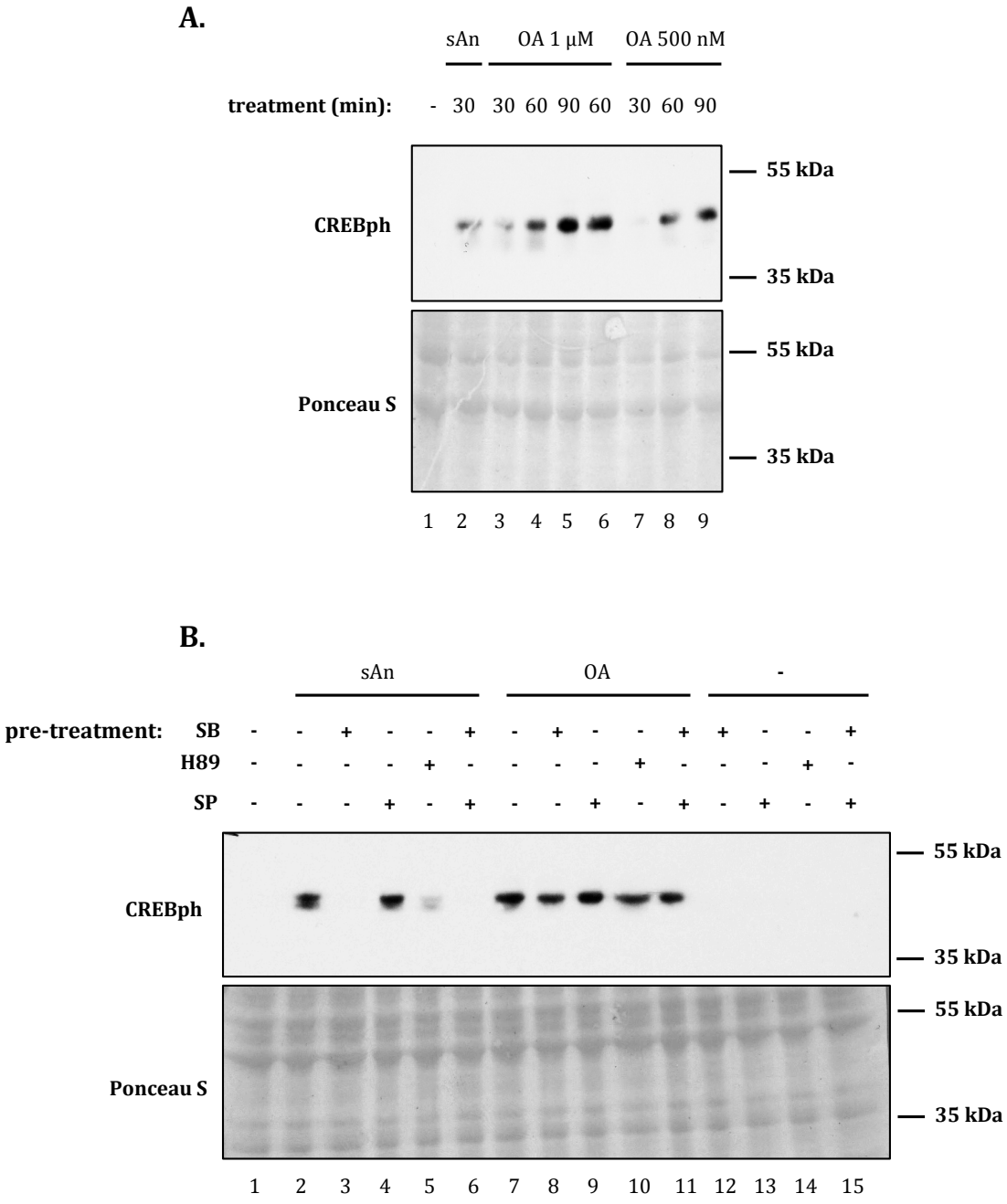
A.
sAn
OA 1 µM
OA 500 nM
treatment (min):
- 30 30 60 90 60 30 60 90
CREBph
55 kDa
35 kDa
Ponceau S
55 kDa
35 kDa
1 2 3 4 5 6 7 8 9
B.
sAn
OA
-
pre-treatment:
SB
H89
SP
CREBph
55 kDa
35 kDa
Ponceau S
55 kDa
35 kDa
1 2 3 4 5 6 7 8 9 10 11 12 13 14 15

The other nucleosomal protein activated by MSK1, HMGN1, is also phosphorylated under OA treatment. An anti-phospho-HMGN1 antibody was used (Figure 3.9). In contrast with histone H3 and CREB phosphorylation, which are strongly activated after 60 minutes, HMGN1 is only strongly and reproducibly activated after 90 minutes of OA treatment at 1 μM and 500 nM (Figure 3.9 A, lanes 5 and 8). No activation of HMGN1 is observed after 30 minutes treatment with OA and a weaker activation is observed after 60 minutes than after 90 minutes of treatment (Figure 3.9 A, lanes 3, 4, 5, 6, 7 and 8).

HMGN1 behaves more like histone H3 in its sensitivity to kinase inhibitors, and can be explained by MSK1 activation after the various pre-treatment. Indeed, HMGN1 phosphorylation after OA treatment is only partially inhibited by pre-treatment with SB 203580 but complete inhibition is observed after pre-treatment with SP 600125 (Figure 3.9 B, lanes 7 and 8), which would be expected as SP 600125 inhibits OA-dependent MSK1 activation. Pre-treatment with SP 600125 also partially inhibits HMGN1 activation by sAn (Figure 3.9 B, lanes 4). This indicates that OA-induced activation of HMGN1 is through MSK1/2.

3.2.3 The JNK MAPK pathway is activated at the TF level after OA treatment

After showing that OA activates the stress pathway p38, we wondered if it had any action on the other stress-activated MAPK pathway, the JNK pathway. We performed Western blots for proteins of the JNK pathway, appearing at various steps within the pathway.

Figure 3.7: HMGN1 is activated by OA and is inhibited after pre-treatment with SB 203580, H89 or SP 600125

A. Quiescent C3H 10T½ cells were stimulated for 30 minutes by sAn (25 ng/ml; lane 2), or treated with OA 1 μM (lanes 3, 4 and 5) or with OA 500 nM (lanes 6, 7 and 8) for indicated times. Lane 1 is the negative control (untreated cells). Cells were lysed with high-salt lysis buffer (see Section 2.3.1) and cell extracts were separated on ERK gels (see Section 2.4.2) and probed using an antibody against phospho-HMGN1 (top). Ponceau staining (bottom) is used as loading control. This is one experiment representative of two repeats.
B. Quiescent C3H 10T½ were pre-treated for 30 minutes (indicated by '+') with the p38 inhibitor SB 203580 ('SB', 10 μM; lanes 3, 5, 7, 9, 10 and 12), the JNK inhibitor SP 600125 ('SP', 10 μM; lanes 4, 5, 8, 9, 11 and 12), followed by stimulation for 30 minutes with sAn (25 ng/ml; lanes 2, 3, 4 and 5), or treatment for 60 minutes with OA (1 μM; lanes 6, 7, 8 and 9), or untreated ('-'; lanes 10, 11 and 12). Lane 1 is the negative control (untreated cells). Cells were lysed with high-salt lysis buffer (see Section 2.3.1) and cell extracts were separated on ERK gels (see Section 2.4.2) and probed using an antibody against phospho-HMGN1 (top). Ponceau staining (bottom) is used as loading control. This is one experiment representative of two repeats.

A.

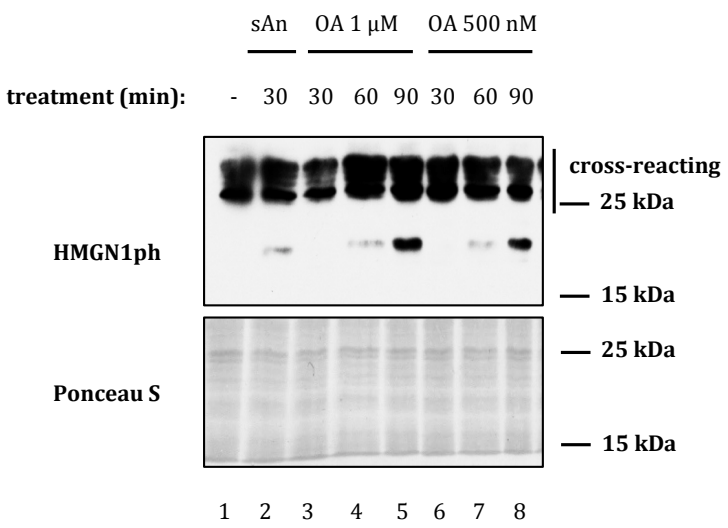
sAn
OA 1 µM
OA 500 nM
treatment (min):
- 30 30 60 90 30 60 90
cross-reacting
25 kDa
HMGN1ph
15 kDa
25 kDa
Ponceau S
15 kDa
1 2 3 4 5 6 7 8

B.

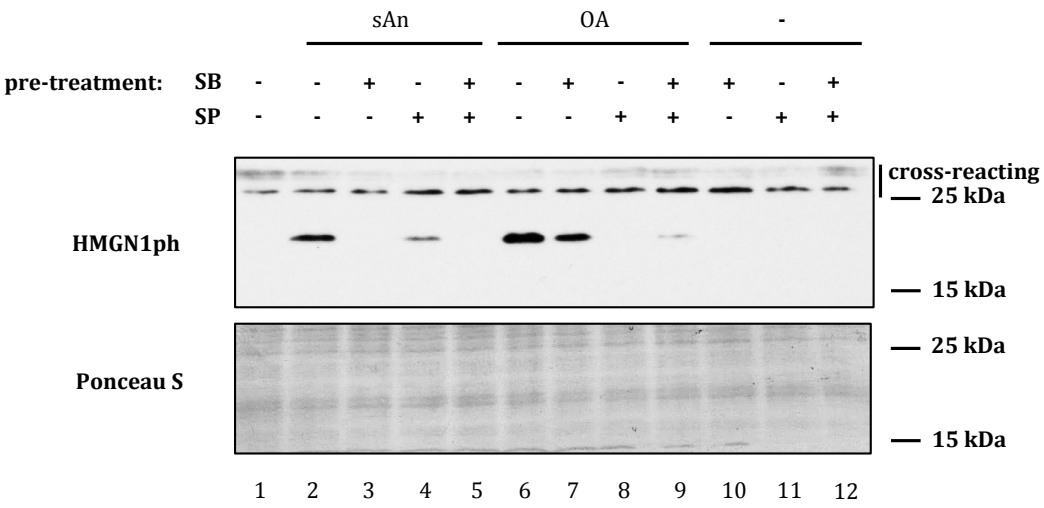
sAn
OA
-
pre-treatment:
SB - - + - + - + - + + - +
SP - - - + + - - + + - + +
cross-reacting
25 kDa
HMGN1ph
15 kDa
25 kDa
Ponceau S
15 kDa
1 2 3 4 5 6 7 8 9 10 11 12

3.2.3.1 MEK4 and JNK are not phosphorylated after OA treatment

The effect of OA on the JNK pathway was first analysed by investigating MEK4, which is an upstream kinase of JNK, using specific anti-phospho-MEK4. This antibody recognises the activated form of MEK4 phosphorylated on threonine 261. No activation of this kinase is observed after treatment with OA 1 μM for 30, 60 or 90 minutes (Figure 3.10, top panel, lanes 3-5) or OA 500 nM for 30, 60 or 90 minutes (Figure 3.10, top panel, lanes 6-8). This indicates that OA does not inhibit phosphorylation of the upstream kinase of JNK.

We further investigated the effect of OA on JNK pathway by using an anti-phospho-JNK antibody recognising JNK phosphorylated on threonine 183 and tyrosine 185. As for MEK4, no activation of JNK is observed after treatment with OA 1 μM for 30, 60 or 90 minutes (Figure 3.10, middle panel, lanes 3-5) or OA 500 nM for 30, 60 or 90 minutes (Figure 3.10, middle panel, lanes 6-8). This suggests either that OA does not inhibit phosphorylation of JNK and/or its upstream targets or that unlike the p38 pathway, the JNK pathway does not present a turnover of phosphorylation in quiescent cells. sAn was used as a positive control for these experiments, after a 30 minute treatment with sAn, both MEK4 and JNK were phosphorylated (Figure 3.10, lane 2).

3.2.3.2 OA treatment generates accumulation of phosphorylated TFs of the JNK pathway

As every step of MAPK pathways is controlled by reversible phosphorylation, OA could affect the signalling events downstream of JNK. Therefore, we investigated

Figure 3.8: MEK4 and JNK are not activated by OA

Quiescent C3H 10T½ cells were stimulated for 30 minutes with sAn (25 ng/ml; lane 2) or treated for the indicated times with OA 1 μM (lanes 3, 4 and 5) or with OA 500 nM (lanes 6, 7 and 8). Lane 1 is the negative control (untreated cells). Cells were lysed with high-salt lysis buffer (see Section 2.3.1) and cell extracts were separated on ERK gels (see Section 2.4.2) and probed against phospho-MEK4 (top) or phospho-JNK (middle). Ponceau staining (bottom) is used as loading control. This is one experiment representative of three repeats.

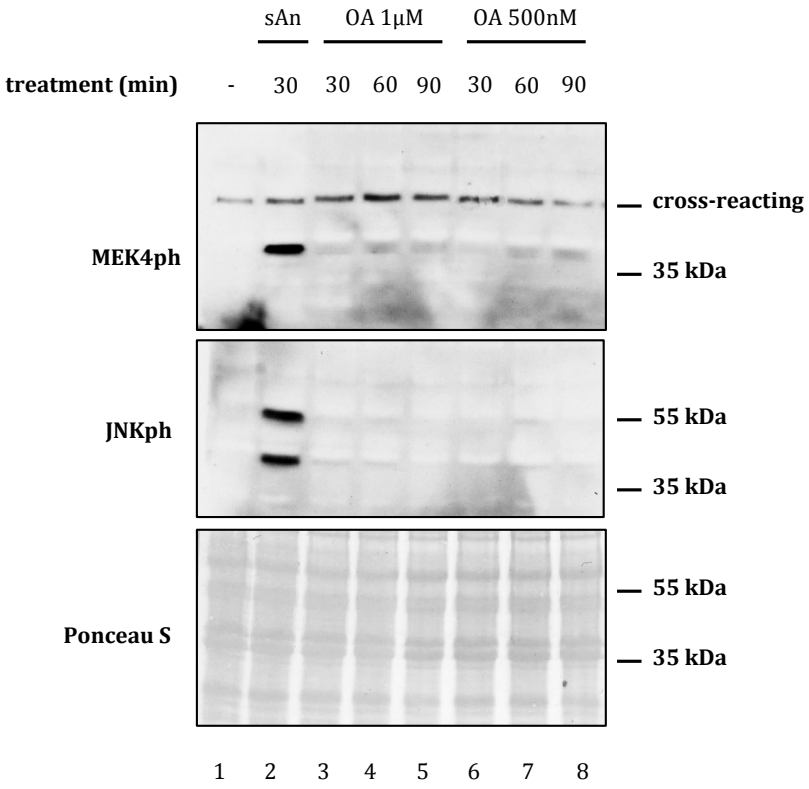
sAn
OA 1μM
OA 500nM
treatment (min)
-
30
30
60
90
30
60
90
MEK4ph
cross-reacting
35 kDa
JNKph
55 kDa
35 kDa
Ponceau S
55 kDa
35 kDa
1
2
3
4
5
6
7
8

OA effect on the JNK pathway by looking at the TFs c-Jun and ATF-2. We used an anti-c-Jun and an anti-ATF-2 antibodies, which allow the detection of the unphosphorylated forms of the proteins (fast migrated bands; Figure 3.11, lane 1) and phosphorylated forms (slow migrating bands; Figure 3.11, lane 2). The TF c-Jun is phosphorylated by JNK under external stimuli on serine residues, Ser63 and Ser73 (Pulverer et al. 1991), while ATF-2 is activated by phosphorylation of two closely spaced threonine residues within its N-terminal activation domain: Thr69 and Thr71 (Gupta et al. 1995; Livingstone et al. 1995). Surprisingly, even without detectable phosphorylation of JNK (Figure 3.10), both ATF-2 and c-Jun produce a complete activation after treatment with OA at 1 µM and 500 nM for 60 minutes (Figure 3.11, lanes 4 and 6) and are still activated after 90 minutes (Figure 3.11, lanes 5 and 7). This suggests that OA inhibits the dephosphorylation of these TFs, and that PP1 and/or PP2A act opposite of the JNK kinase.

The two phosphorylation sites of ATF-2 produce band shifts observed after OA (Figure 3.11, lanes 4-7) and sAn stimulations (Figure 3.11, lane 2). An additional, slower migrating band is observed for ATF-2 after OA treatment for 60 and 90 minutes (Figure 3.11, lanes 4-7), suggesting additional modification(s). Other ATF-2 phosphorylation sites have been reported, including serine residues in the N- and C-terminal domains such as Ser90, which was found not to be critical for the transcriptional activity of ATF-2 in comparison to Thr69 and Thr71 (Livingstone et al. 1995; reviewed in Bhoumik et al. 2007). These other phosphorylation sites could explain this additional band observed. OA could inhibit the negative regulation of a signalling pathway, which would lead to the

Figure 3.9: JNK transcription factors ATF-2 and c-Jun are phosphorylated after OA treatment

Quiescent C3H 10T½ cells were stimulated for 30 minutes by sAn (25 ng/ml; lane 2) or treated for the indicated times with OA 1 μM (lanes 3, 4 and 5) or with OA 500 nM (lanes 6 and 7). Lane 1 is the negative control (untreated cells). Cells were lysed with high-salt lysis buffer (see Section 2.3.1) and cell extracts were separated on big SDS-PAGE gel (see Section 2.4.1) for ATF-2 and SDS-PAGE (see Section 2.4.1) for c-Jun and probed against ATF-2 (top) or c-Jun (middle). Ponceau staining (bottom) is used as loading control. This is one experiment representative of three repeats. For clarity, irrelevant samples on the c-Jun blot were removed and the junction is represented by the vertical line on the blot.

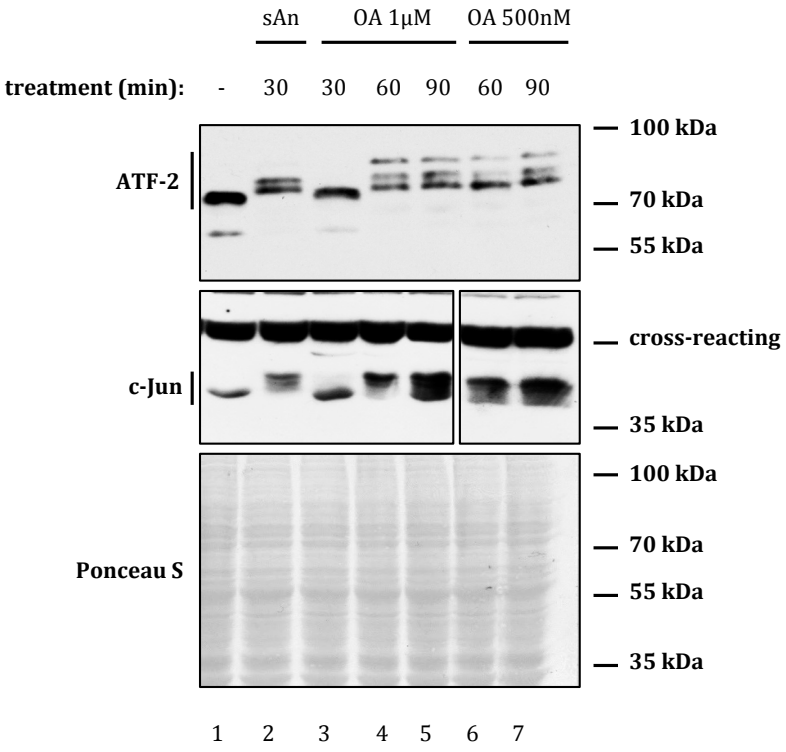
sAn
OA 1µM
OA 500nM
treatment (min):
-
30
30
60
90
60
90
ATF-2
c-Jun
Ponceau S
100 kDa
70 kDa
55 kDa
cross-reacting
35 kDa
100 kDa
70 kDa
55 kDa
35 kDa
1
2
3
4
5
6
7

phosphorylation of ATF-2 on additional residues. These additional modifications, as not functionally relevant, would not affect ATF-2 activation.

Pre-treatment with the JNK inhibitor SP 600125 inhibits the phosphorylation of ATF-2 and c-Jun after both sAn and OA treatment (Figure 3.12, lanes 4 and 7). These complete inhibitions by SP 600126 are in agreement with the fact that OA-induced activation of c-Jun and ATF-2 is via JNK. However pre-treatment with SB 203580, as expected, does not inhibit ATF-2 and c-Jun activation by OA and sAn (Figure 3.12, lanes 3 and 6). It even seems to enhance their activation. Indeed, the third band of ATF-2 is more intense in the presence of SB 203580 than after OA treatment on its own (Figure 3.12, lanes 5 and 6). A more intense signal is observed as well for the band corresponding to phosphorylated c-Jun (slower migrating band) after SB 203580 pre-treatment followed by OA treatment (Figure 3.12, lane 6). However, as c-*jun* expression is induced, care needs to be taken to conclude on this increase. The increase in intensity observed after SB 203580 pre-treatment suggests the existence of crosstalk between p38 and JNK pathways. This may indicate an inhibition of JNK by p38 in untreated cells. As no enhancement is observed after sAn treatment (Figure 3.12, lane 3), the inhibition of JNK by p38 must be weak to only be revealed by inhibition of the negative regulation. Indeed, sAn is a 'direct' and strong activator of JNK pathway (Figure 3.10, lane 2), while OA does not activate JNK phosphorylation (Figure 3.10, lanes 3-8), which could allow to detect a small variation. This type of crosstalk between JNK and p38 kinases was also described in response to UV light in COS-1 cells (Seo et al. 2002).

Figure 3.10: ATF-2 and c-Jun phosphorylation after OA treatment is inhibited by pre-treatment with SP 600125 but not SB 203580

Quiescent C3H 10T½ cells were pre-treated with the p38 inhibitor SB 203580 ('SB', 10 µM; lanes 3, 6 and 8) or the JNK inhibitor SP 600125 ('SP', 10 µM; lanes 4, 7 and 9) before being stimulated with sAn (25 ng/ml; lanes 2, 3 and 4), or OA (1 µM; lanes 5, 6 and 7), or unstimulated ('-'; lanes 8 and 9). Lane 1 is the negative control (untreated cells). Cells were lysed with high-salt lysis buffer (see Section 2.3.1) and cell extracts were separated on big SDS-PAGE gel (see Section 2.4.1) for ATF-2 and SDS-PAGE (see Section 2.4.1) for c-Jun and probed against ATF-2 (top) or c-Jun (middle). Ponceau staining (bottom) is used as loading control. This is one experiment representative of three repeats.

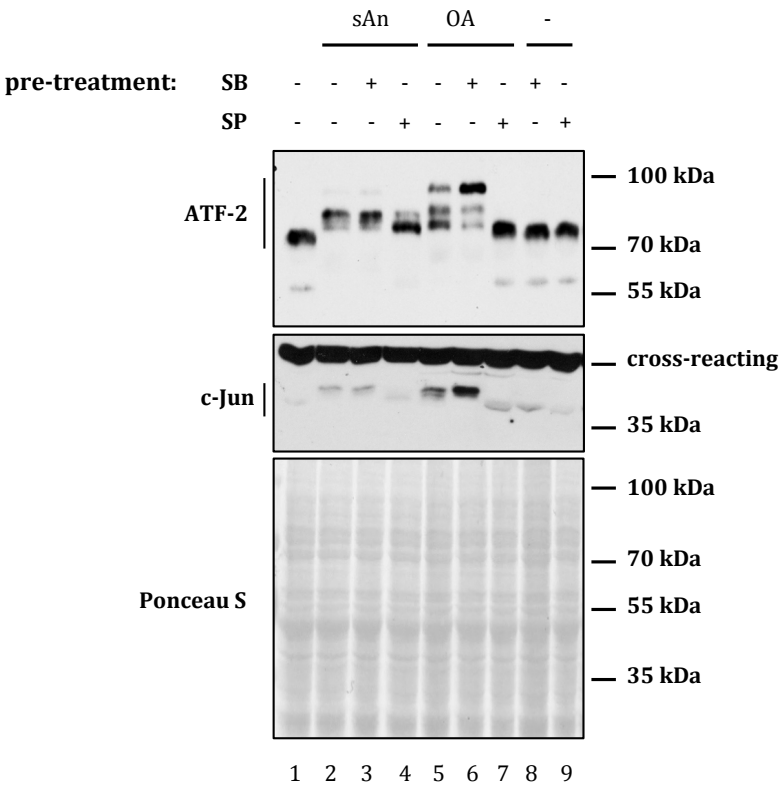
sAn
OA
-
pre-treatment:
SB - - + - - + - + -
SP - - - + - - + - +
ATF-2
100 kDa
70 kDa
55 kDa
c-Jun
cross-reacting
35 kDa
Ponceau S
100 kDa
70 kDa
55 kDa
35 kDa
1 2 3 4 5 6 7 8 9

Furthermore, on the ATF-2 blot on Figure 3.12, a faint third band can be observed after sAn stimulation and SB 203580 treatment followed by sAn stimulation (Figure 3.12, lanes 2 and 3), so the third slower migrating band observed after OA treatment is physiological. As JNK was found to phosphorylate ATF-2 on threonine and serine residues *in vitro* (Gupta et al. 1995) and this additional band is observed really weakly after sAn stimulation (Figure 3.13), JNK could be the kinase phosphorylating these additional sites.

3.3 Discussion

The IE genes c-*fos* and c-*jun* showed a prolonged induction after OA treatment (Figure 3.2). Our results suggest that this induction is explained by the inhibition of negative regulation of the MAPK signalling pathways by OA. The main issues raised by the data are the effects of OA on the different MAPK pathways, which revealed the presence of a turnover of phosphorylation in quiescent cells for the p38 and the JNK pathway but not for the ERK pathway. The potential effects of OA on p38 and JNK pathways are discussed below and regrouped on Figure 3.13 and Figure 3.14 respectively.

3.3.1 Multiple level of action of OA in the p38 pathway

The work in this chapter suggests that OA acts at multiple steps in the p38 pathway (Figure 3.13). In order to explain the p38 activation observed after OA treatment, OA must act either upstream of p38 by inhibiting the dephosphorylation of upstream kinase(s) of p38, or/and inhibit p38 dephosphorylation. But, the weak activation observed for p38 (Figure 3.4) after OA

treatment contrasts with the strong activation of histone H3 phosphorylation (Figure 3.3), CREB (Figure 3.8), HMGN1 (Figure 3.9) and the complete activation of MSK1 (Figure 3.7). This indicates that OA may also act downstream of p38. Pre-treatment experiments with kinase inhibitors are consistent with an action of OA at multiple steps in the pathway. Indeed, the fact that histone phosphorylation is only partially inhibited by SB 203580 pre-treatment but completely inhibited by H89 pre-treatment (Figure 3.6), indicates that OA must act on MSK1/2 negative regulation.

However, SB 203580 inhibits p38 activity (Davies et al. 2000), so even if PP1 and PP2A were acting on MSK1/2, we would expect complete inhibition after SB 203580 pre-treatment. As it is not what we observed (Figure 3.7), OA must prevent the dephosphorylation of another kinase or a pathway activating MSK1/2 (Figure 3.13). The potential existence of an additional pathway activating MSK1 after OA treatment is also suggested by the inhibition of OA-induced MSK1 activation after pre-treatment with SP 600125 (Figure 3.7).

The full inhibition of MSK1 activation after OA stimulation by pre-treatment with SP 600125 inhibitor could also be explained by preventing MSK1 autocatalysis. But because SP 600125 does not affect MSK1 phosphorylation activated by sAn stimulation (Figure 3.7), this inhibitor does not seem to directly act on MSK1. Thus, OA probably inhibits the negative regulation of another pathway leading to MSK1 phosphorylation, which is inhibited by SP 600125 and not activated by sAn (Figure 3.13). This excludes any explanation involving crosstalk between the JNK and the p38 MAPK pathways, as JNK is activated by sAn (Figure 3.10). PKA has been shown

Figure 3.11: The potential effects of OA on the p38 pathway revealed in this study

This schematic representation of the p38 pathway summarises the effect of OA on this pathway revealed in this chapter. These effects are represented by the dotted lines. '**P**' indicates one or more phosphorylation events.

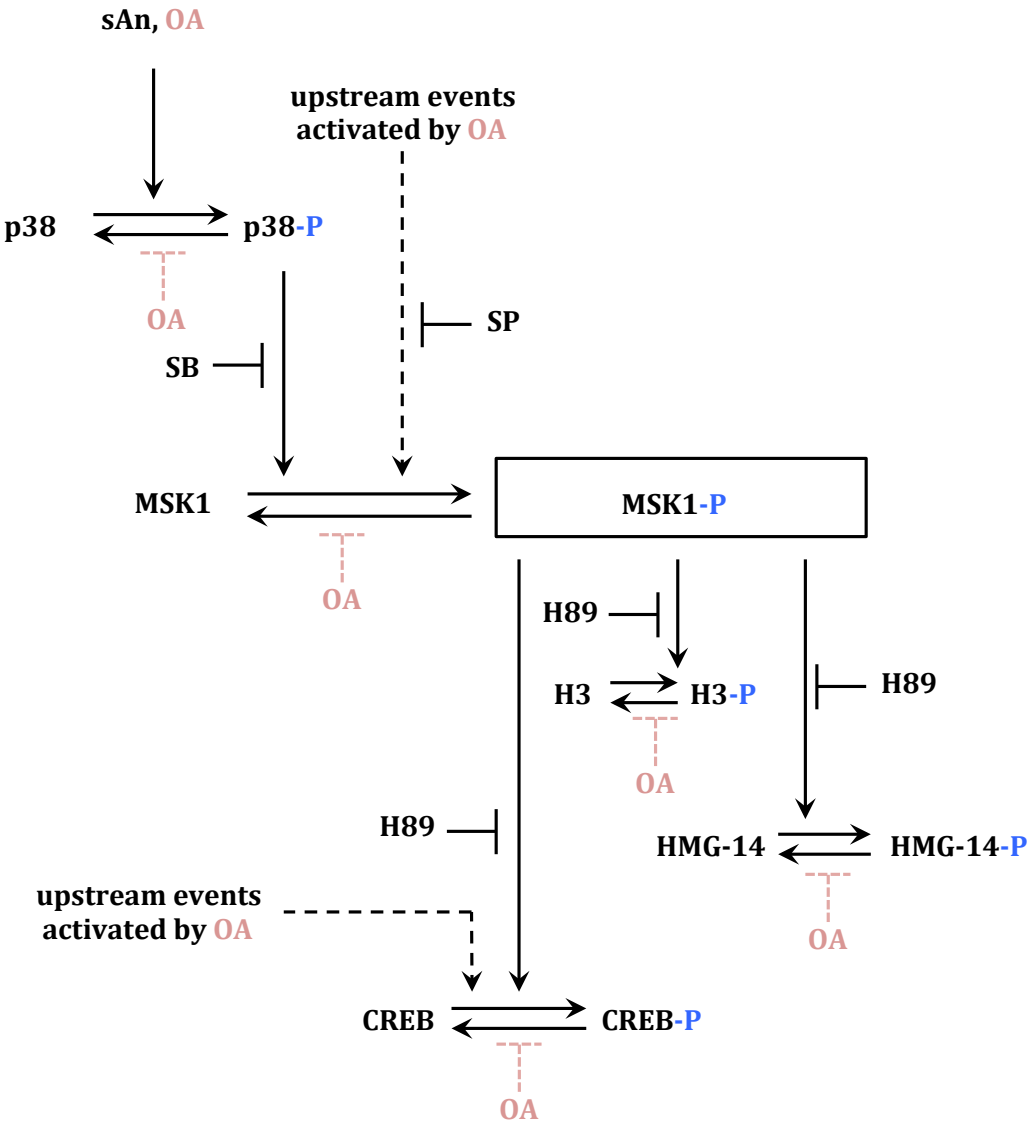
sAn, OA
upstream events activated by OA
p38
p38-P
OA
SB
SP
MSK1
MSK1-P
OA
H89
H3
H3-P
OA
H89
H89
HMG-14
HMG-14-P
OA
upstream events activated by OA
CREB
CREB-P
OA

to interact with different MAPK-activated protein kinases such as RSK1 and MK5 (Kostenko et al. 2011). However, this kinase is not inhibited by SP 600125 (Bain et al. 2003) but, is inhibited by H89 (Davies et al. 2000). As MSK1 activation after OA treatment is inhibited by pre-treatment with SP 600125 but not by pre-treatment with H89 (Figure 3.7), PKA cannot be the potential alternative kinase responsible for MSK1 activation after OA treatment.

Unlike histone H3 and HMGN1, pre-treatments with SP 600125 or H89 did not inhibit OA-induced CREB activation, which was unexpected as all three proteins are downstream of MSK1 and as OA-induced MSK1 activation is inhibited by SP 600125 and its action by H89 (Figure 3.7; Davies et al. 2000). In order to explain this characteristic, CREB needs to be activated by another signalling pathway, activated by OA (Figure 3.13). PKA has been shown to phosphorylate the TF CREB (Chrivia et al. 1993), but once again as this kinase is inhibited by H89, an inhibition or at least a partial inhibition of CREB phosphorylation after OA treatment by this inhibitor would be expected if PKA were responsible for CREB activation (Davies et al. 2000). CREB phosphorylation after OA treatment is not inhibited by SB 203580, H89 nor SP 600125 (Figure 3.8). Thus, the alternative kinase or pathway responsible for its activation would need to be insensitive to all these inhibitors.

3.3.2 Turnover of phosphorylation in the JNK MAPK pathway

As no activation of either kinase MEK4 or JNK was observed after OA treatment (Figure 3.10), it seems that PP1 and PP2A do not take part in the negative regulation of the signalling steps upstream of JNK or there is no dynamic turnover

of phosphorylation in this pathway. However, the TFs c-Jun and ATF-2 downstream of JNK do become phosphorylated after OA treatment (Figure 3.11), suggesting that OA acts downstream of JNK, and revealing the presence of a phosphorylation turnover in quiescent cells within the JNK MAPK pathway, so a dynamic regulation of this pathway (Figure 3.14).

Pre-treatment with SP 600125 completely inhibits c-Jun and ATF-2 activation after OA treatment (Figure 3.12). This result is in agreement with the involvement of PP1 and PP2A for dephosphorylation of these TFs, they seem to be the phosphatases acting to oppose JNK. However, JNK needs to undergo a turnover of phosphorylation in quiescent cells for phosphorylated JNK (at non-detectable levels; see Section 3.1.2.2) to be present.

3.3.3 Is ERK dynamically regulated?

Unlike the p38 and JNK pathways, for which turnover of phosphorylation has been revealed by OA, we showed that ERK1/2 is not activated after OA treatment (Figure 3.4). Two explanations are possible. This could suggest that PP1 and PP2A do not dephosphorylate ERK1/2 and/or are not responsible for the dephosphorylation of an upstream kinase of ERK1/2. But it could also be explained by the lack of turnover of phosphorylation in this pathway in quiescent cells. Indeed, in the absence of basal turnover of phosphorylation, the inhibition of protein phosphatases would not be sufficient to activate the ERK pathway.

Stimulating C3H 10T½ cells simultaneously with EGF and OA shows a similar response to EGF stimulation on its own. OA does not affect the rate of

Figure 3.12: The potential effects of OA on the JNK pathway revealed in this study

This schematic representation of the JNK pathway summarises the effect of OA on this pathway revealed in this chapter. These effects are represented by the dotted lines. **'P'** indicates one or more phosphorylation events.

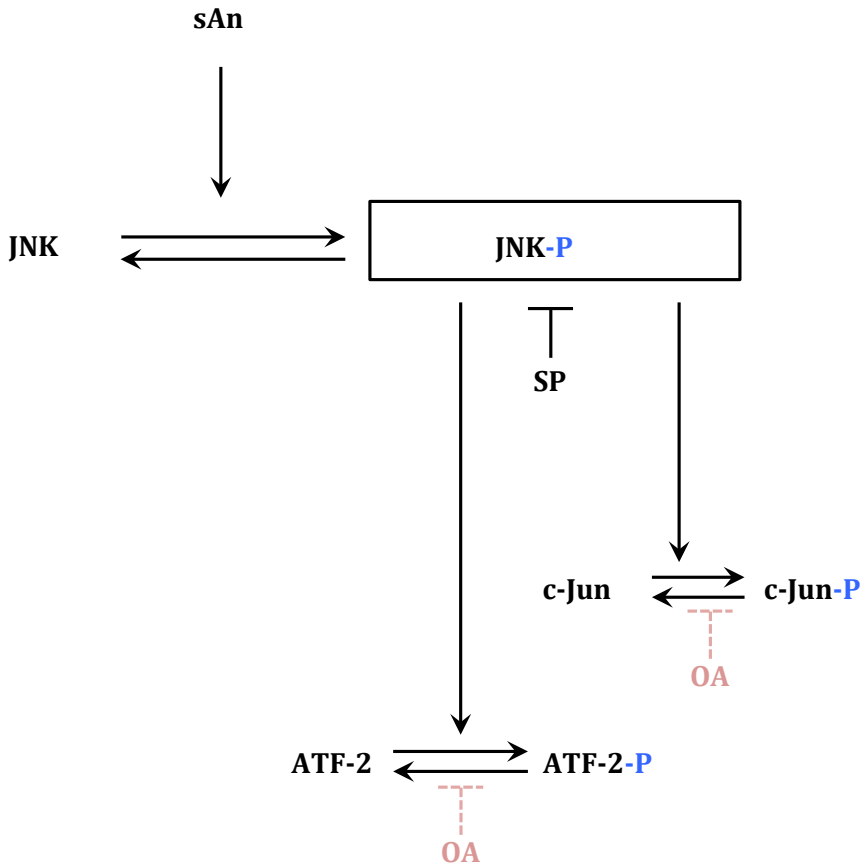
sAn
JNK
JNK-P
SP
c-Jun
c-Jun-P
OA
ATF-2
ATF-2-P
OA

dephosphorylation of ERK1/2 (Figure 3.5). If PP1 and PP2A were involved in ERK1/2 negative regulation, we would expect a prolongation of the EGF activation. The similarity of the activation of ERK1/2 by EGF on its own or in combination with OA indicates that PP1 and PP2A are not involved in ERK1/2 dephosphorylation. Moreover, the fact that U0126 pre-treatment does not even partially inhibit histone H3 phosphorylation (Figure 3.6) agrees with these results, an action of PP1 and PP2A in opposition to ERK1/2 pathway seems unlikely. However, it does not allow to conclude on the existence of a turnover of phosphorylation in this pathway.

Chapter 4: Detailed analysis of c-fos and c-jun induction profiles

4.1 Introduction

4.1.1 Monitoring gene expression

In the previous chapter, we characterised and revealed dynamic turnover of phosphorylation in the MAPK pathways. In an effort to understand how IE genes expression may be quantitatively regulated by these pathways, we then investigated the effect of perturbations of this turnover on gene expression.

4.1.1.1 Quantification of mRNA levels in synchronised cell population

In order to easily compare and relate the variation in gene expression to the results obtained previously for the signalling pathways, and so try to understand the link between the two, we wanted to use the same system, that is, synchronised cells in culture. However, while it is possible to obtain quantitative information on kinase activation using synchronised cells (see Section 3.1.2.1), quantification of RNA levels in this system presents some difficulties. The shift detected by the use of an anti-protein-specific antibody can provide qualitative information on phosphorylated and non-phosphorylated forms of a protein (see Section 3.1.2.2), and the intensity of the signal of an anti-phospho-specific antibody can be quantified (see Section 3.1.2.2). These techniques have been used to show that in response to EGF stimulation, every single cell within a synchronised population has reacted to maximal levels within 1 minute (Cano et al. 1995). This indicates

that in a synchronised cell population, the signalling response happens simultaneously and virtually instantaneously, which is a crucial point for interpretation of quantitative information. But, these observations cannot be done at the level of transcription and the transcriptional response might not be instantaneous and synchronised in every cell.

A way to overcome these complications linked to RNA quantification would be to quantify gene expression using a reporter gene. The gene of interest is fused to a reporter gene, which can be easily detected, such as luciferase or GFP (green fluorescent protein). Thus, monitoring the expression of the reporter gene gives access to the expression of the gene of interest. However, as the detection of gene expression, for this method, is at the protein level, it involves translation, which can induce additional differences in the expression levels by additional regulation. Moreover, there is an additional time delay associated with protein synthesis.

Another way would be to use single-cell analysis of gene expression, which would avoid the average levels of RNAs in a cell population. FISH (fluorescence *in situ* hybridisation) uses fluorescent probes to detect mRNA (Langer-Safer et al. 1982). However, the quantification is difficult due to fluorescence noise (Femino et al. 1998). The MS2 system, in which GFP is fused to the RNA-binding protein MS2, also allows localisation and quantification of mRNA, but again background noise makes quantification challenging, specifically for low or single copy RNA molecules (Bertrand et al. 1998; Chubb et al. 2006).

4.1.1.2 Quantification of mRNA

Assuming that the transcriptional response is almost instantaneous like the signalling response, synchronised cells in culture can be used. Northern blotting and qRT-PCR are commonly used to evaluate mRNA levels. These methods monitor the average levels of mRNA in the bulk population, rather than directly measuring transcription. With either method, any differences observed in mRNA levels could be due to posttranscriptional mechanisms involved in mRNA stability and thus not reflect gene transcription. This effect was observed for all-or-none responses at the single cell level, which gave graded responses while considering a population of cells (Bagowski and Ferrell 2001). As the link between IE gene and signalling pathway is more likely to be at the initiation step of transcription (see Section 1.5; Hazzalin and Mahadevan 2002), monitoring mRNA levels may not reflect the immediate effect of MAPK pathway regulation on initiation.

Unlike these two methods, the nuclear run-on assay allows a direct measure of the level of transcription of a particular gene. Briefly, cells are chilled and lysed resulting in polymerase pausing, before incubating the nuclei in the presence of ^{32}P-labelled UTP, which can be incorporated into transcripts that were being synthesised. Nascent ^{32}P-labelled RNAs are isolated and hybridised to a membrane containing the gene(s) of interest. The amount of radioactivity detected is proportional to the nascent transcripts and thus to the frequency of initiation. The differences observed by nuclear run-on assay cannot be due to posttranscriptional mechanisms. However, it requires a large amount of radioactivity and is only accurate for highly active genes due to the presence of a high background (Greenberg and Ziff 1984; Murphy 1993; Smale 2009). Native elongating transcript

sequencing (NET-seq) is another method to capture nascent RNA transcripts by revealing the density of RNA polymerase across the genome (Churchman and Weissman 2012). Similarly to RNA-seq, which quantifies RNA transcripts, this method is a high resolution method and covers a broad range of transcripts, while we are focusing on c-*fos* and c-*jun*.

For this study, due to the extreme instability of IE gene transcripts with short half-lives (see Section 1.2.1.1; Edwards and Mahadevan 1992), we considered that the measurement of average mRNA levels would give an acceptable approximation of gene transcription. Besides, assuming that the rates of transcriptional elongation and mRNA degradation are relatively constant, the gene expression observed represent an approximation of initiation of transcription. Therefore, we used Northern blotting and qRT-PCR to quantify c-*fos* and c-*jun* gene expression.

4.1.1.3 Northern blotting and quantitative reverse-transcription PCR

Both methods were used as unlike qRT-PCR, Northern blotting requires a size separation of RNA prior to hybridisation. Thus, it allows one to detect and distinguish the different transcripts derived from the same gene, as is the case for c-*jun,* with the two transcripts detected corresponding to alternative polyadenylation sites (Ryseck et al. 1988). This specificity of Northern blots enables a comparison of expression of the different transcripts of one gene more easily than by other methods.

For quantification, these methods require applying a normalisation against a reference gene. Here *gapdh* is used, as it has a constant level of expression under

the conditions being tested (see Section 1.1.1; Edwards and Mahadevan 1992; Hazzalin et al. 1996; Thomson et al. 1999). Using *gapdh* to normalise the results for both Northern blotting and qRT-PCR allows a closer comparison of the data obtained by the two methods.

For qRT-PCR, mRNA is reverse transcribed to cDNA, which can then be quantified using fluorescent reporter molecules to measure the amplification of the targeted sequence during each cycle of the PCR reaction. The number of cycles of amplification required to generate enough fluorescence to reach the threshold level of detection is proportional to the number of copies of mRNA originally present (Bustin et al. 2005). In our experiments, cDNA synthesis prior to PCR is carried out using random primers. Even though the use of random primers can be less sensitive in comparison to specific primers, it allows multiple RNA templates to be reverse transcribed in the same reaction. Thus the expression of multiple genes, and in particular the reference gene can be monitored from the same cDNA sample (Bustin et al. 2005).

Northern blots do not provide an absolute quantification of gene expression, but they can be used to compare the relative expression in samples under different experimental conditions (reviewed in Reue 1998). Here we are interested in the variations of mRNA levels over time, rather than the specific values. Thus, having access to the relative expression gives sufficient information for our study. To obtain quantitative results with Northern blotting, we use a phosphorimager. The intensity of the band detected corresponds to the relative abundance of mRNA present. Indeed, the intensity is coupled with the amount of radiolabeled (^{32}P)

probe hybridised to the mRNA sequence of interest. Phosphorimaging is more sensitive and has a greater dynamic range than X-ray film, which makes it a better choice for quantification of Northern blots.

4.1.2 Transcription and translation inhibition

Further characteristics of c-*fos* and c-*jun* induction profiles have been identified and investigated by the inhibition of translation or transcription.

4.1.2.1 Evaluating the degradation of mRNA

Inhibition of transcription has previously been used to evaluate the stability of IE gene transcripts and determine the rates of their mRNA degradation. Transcription was inhibited by the transcription inhibitor DRB (5,6-dichlorobenzimidazole 1-β-D-ribofuranoside; Edwards and Mahadevan 1992). This compound has been shown to block elongation at or close to the site of initiation of transcription by inhibiting the positive transcription elongation factor (pTEFb), and thus inhibiting phosphorylation of the paused RNA polymerase II (Zandomeni et al. 1982; Zhu et al. 1997). After treatment with DRB, the half-lives of c-*fos* and c-*jun* transcripts were derived by Northern blotting analysis, which highlighted the high instability of IE gene RNA transcripts (Edwards and Mahadevan 1992; see Section 4.1.2.2).

Here we use actinomycin D, which rapidly inhibits RNA synthesis by interfering with elongation. This compound binds to DNA, and thus immobilises DNA transcription complex (Sobell 1985). It is composed of two cyclic peptides lined together by a phenoxazine derivative. The phenoxazone ring intercalates between

dinucleotide GX, where 'X' is either A, T, C or G. The pentapeptide chains can form hydrogen bonds with guanine residues on the opposite chains in the case of GC sequences (Sobell 1985).

4.1.2.2 Phenomenon of superinduction and translational inhibition

IE gene induction can be increased and prolonged by the use of protein synthesis inhibitors in combination with stimulating agent. This phenomenon is referred to as superinduction (Cochran et al. 1983; Lau and Nathans 1987). While the induction of c-*fos* by the growth factor EGF on its own is transient and returns to basal levels within 1 h, it is prolonged and enhanced for over 1 h by stimulating cells with EGF in combination with a protein synthesis inhibitor. A similar effect is seen in the signalling cascades, and the nucleosomal response is prolonged under these conditions (Edwards and Mahadevan 1992).

The phenomenon of superinduction was initially attributed to the disappearance of labile repressor following protein synthesis inhibition (Pontecorvi et al. 1988). It was thought that the c-*fos* was kept turned 'off' by labile repressors interacting with serum response factor (SRE-SRF) complexes to repress c-*fos* transcription. However, it has been shown that not all protein synthesis inhibitors used on their own induce c-*fos* transcription (Edwards and Mahadevan 1992), which would be expected for the labile repressor hypothesis. Indeed, only anisomycin and cycloheximide were proved to strongly induce IE gene transcription on their own, while puromycin and emetine failed to do so (Edwards and Mahadevan 1992). The increased transcription of IE genes is thus explained by the delay in IE gene transcriptional shut-off. The protein synthesis inhibitors prevent negative

regulation by blocking stimulus-induced synthesis of repressor proteins, such as the dual protein phosphatase MKP-1, which is activated after stress and growth factor (Sun et al. 1993; Li et al. 2001).

A second mechanism allows protein synthesis inhibition to stabilise IE gene mRNA transcripts due to the coupling of mRNA degradation with its translation (Edwards and Mahadevan 1992). Indeed, the use of translational inhibitors, such as anisomycin and cycloheximide, which inhibit translation by binding to the 60S ribosomal subunit, and thus result in polysome stabilisation (Barbacid and Vazquez 1975), could trap mRNAs on polysomes decreasing their accessibility to nucleases (Cochran et al. 1983). This would also explain the weak superinduction observed with puromycin, which inhibits transcription by disassembling polysomes (Edwards and Mahadevan 1992). For example, the half-life of c-*fos* is prolonged from 9 min, after EGF stimulation, to several hours, after stimulation with EGF in combination with protein synthesis inhibitor (Rahmsdorf et al. 1987; Edwards and Mahadevan 1992).

As well as inhibiting translation, some protein synthesis inhibitors, such as anisomycin, were found to act as signalling agonist. Indeed, anisomycin has been shown to activate IE gene transcription at a concentration lower than that necessary for protein synthesis inhibition (Mahadevan and Edwards 1991; Edwards and Mahadevan 1992; Hazzalin et al. 1996), decoupling signalling and gene induction from translational arrest. Anisomycin used at sub-inhibitory concentrations (sAn) activation of IE genes is comparable to the activation observed after growth factor activation. This similarity proves that the

accentuated and prolonged effect observed with anisomycin is a consequence of translational arrest. By inhibiting protein synthesis, anisomycin induces a delay in transcriptional shut-off and stabilises mRNA transcripts.

sAn was further found as an agonist for stress responses, inducing IE genes through the stress signalling pathways (Hazzalin et al. 1998). The agonist-like action of sAn has been revealed by desensitisation experiments. After having been activated by a compound, signalling pathways do not respond for a short period of time to the same stimulus (reviewed in Collins and Rozengurt 1984), this is referred to as homologous desensitisation. The absence of IE gene induction, after sAn stimulation in desensitised cells, is explained by the inability of sAn to activate the signalling pathways. The phenomenon of homologous desensitisation is a specific characteristic of an agonist (Collins and Rozengurt 1984). While no heterologous desensitisation is observed in sAn desensitised cells, in TNF-α and UV desensitised cells treatment with sAn displays a partial and selective desensitisation, with the induction of the genes c-*fos,* c-*jun* and *junB* partially inhibited (Hazzalin et al. 1998). This shows that sAn shares the same down-regulated elements as stress stimuli.

The activation of IE genes by sAn is comparable to the activation observed after growth factor activation (Thomson et al. 1999). As the phenomenon of superinduction is characterised by increased stability of IE genes mRNA and a delay in shutting-off transcription (Edwards and Mahadevan 1992), the comparison of the RNA profiles obtained after sAn and anisomycin stimulation can inform on the effect of RNA degradation on the sAn-induced profiles. We have used

anisomycin in this chapter to investigate how the disruption of RNA degradation would affect the RNA profiles obtained after sAn activation.

4.1.3 Summary

In this chapter, we focus on the specific expression profiles of the IE genes c-*fos* and c-*jun*. We have obtained a high temporal resolution of these profiles by using a more sensitive method, to investigate their regulation. After revealing the presence of a turnover of phosphorylation in quiescent mouse C3H 10T½ cells (see Chapter 3), we studied the effect of the disruption of the turnover of phosphorylation by using OA, a phosphatase inhibitor, and kinase inhibitors at the level of gene expression. While some results suggest that the dynamics of the turnover rather than the activation of the kinase regulates c-*fos* and c-*jun* expression, co-treatment with sAn and OA reveals a more complex regulation. Moreover, we have explored the role of degradation of mRNA transcripts on quantitative regulation. We used a transcriptional inhibitor to reveal that the degradation of c-*fos* and c-*jun* transcripts is a constant process. The comparison of sAn and anisomycin profiles reveals similarity in their regulation. Transcriptional and translational inhibition results suggest that the degradation of mRNA has a limited role in the quantitative regulation of IE genes.

4.2 Results

4.2.1 Quantitative profiles of c-*fos* and c-*jun* after sAn activation

c-*fos* and c-*jun* expression data have already been described after various stimuli (Thomson et al. 1999). However, these were obtained for only a few time points.

Here we analysed and quantified gene induction after sAn activation for these two IE genes with a higher temporal resolution (from 5-minutes to 15-minutes intervals) and greater sensitivity.

4.2.1.1 c-fos *and c*-jun *have characteristic expression profiles*

We first used qRT-PCR to quantitatively monitor c-*fos* and c-*jun* expression. As previously described, activation with sAn produces distinct induction profiles for these two IE genes (Figure 4.1; Hazzalin et al. 1998). While the IE gene c-*fos* is rapidly and transiently induced (Figure 4.1 Bi), the c-*jun* induction lasts longer (Figure 4.1 Bii and Biii). Indeed, the expression of c-*fos* is observed after 10 minutes of sAn stimulation, peaks around 50 minutes and is back to basal levels after 90 minutes (Figure 4.1 Bi). Similarly to c-*fos*, c-*jun* expression is observed after 10 minutes of stimulation and is maximal around 50 minutes, but mRNA levels remain high after 90 minutes (Figure 4.1 Bii and Biii). For both c-*fos* and c-*jun* profiles, variations in experiments and the difficulties of obtaining reproducible quantitative data for mRNA levels (see Section 4.1.1) are illustrated by the big errors obtained by combining three experimental repeats (Figure 4.1).

A second set of primers, amplifying different parts of the transcript, was used for c-*jun,* to further evaluate reproducibility. Even though the overall shape of the c-*jun* profiles obtained by using different primer pairs is kept and reproducible (Figure 4.1 Bii and Biii), the higher temporal resolution of the profiles revealed variations in the experiments. Indeed, while the profiles are very similar for the first 45 minutes, corresponding to the increasing phase (Figure 4.1 Bii and Biii), the levels of mRNA for the profile obtained with the primer pair +1119 stay

Figure 4.1: Activation profiles of c-*fos* and c-*jun* after sAn stimulation obtained by qRT-PCR

A. Schematic representation of c-*jun*, c-*fos* and *gapdh* genes showing positions analysed by real-time PCR. Primer positions indicate the 5' position of the forward primer relative to the transcription start site. The primer sequences are shown in Table 2.3. Exons are represented by boxes, unfilled for untranslated regions and filled for translated regions. Termination sites are shown as filled circles.
B. cDNAs were derived (see Section 2.8.2) form mRNA extracted following the acid guanidinium thiocyanate-phenol-chloroform extraction (see Section 2.6), from quiescent C3H 10T½ cells stimulated with sAn (25 ng/ml) for various times and quantified by qRT-PCR. Data (mean of three biological repeats ± SEM) are presented as maximal activation and normalised against *gapdh*.

A.

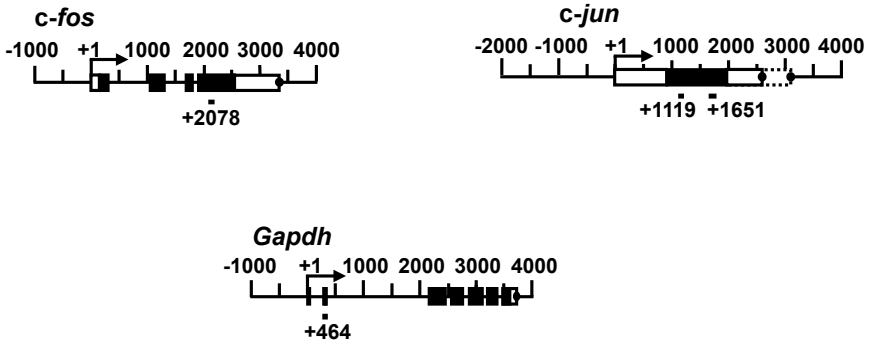

B.

i. c-*fos* induction profile after sAn stimulation

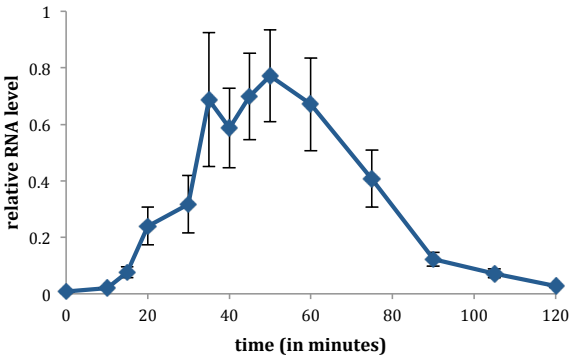

ii. c-*jun* induction profile after sAn stimulation (+1119)

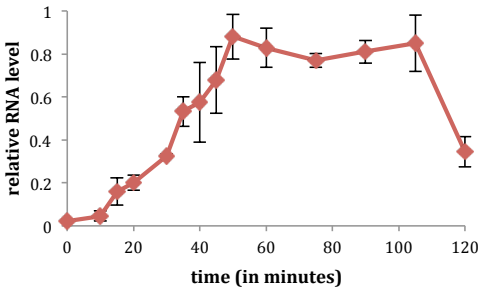

iii. c-*jun* induction profile after sAn stimulation (+1651)

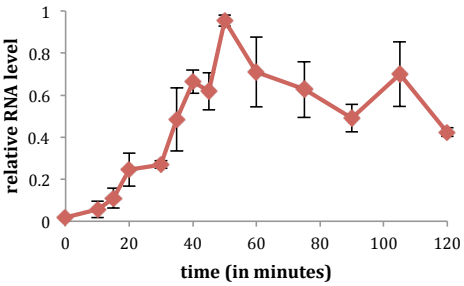

relatively constant until 100 minutes of stimulation (Figure 4.1 Bii), but not for the profile obtained with the primer pair +1651 (Figure 4.1 Biii).

The results obtained seem to indicate the presence of a drop in RNA levels around 40 minutes for c-*fos* (Figure 4.1 Bi) and around 50 and 80 minutes for c-*jun* (Figure 4.1 Bii and Biii), which was not previously observed. However, due to the lack of reproducibility of quantitative data related to the system (see Section 4.1), no conclusion can be drawn on this characteristic and it is outside of the consideration and discussion of this chapter.

The quantitative profiles of these genes were also analysed by Northern blotting to confirm the characteristics observed by qRT-PCR (Figure 4.2). The c-*fos* and c-*jun* blots (Figure 4.2 C) were visualised by Phosphorimager and quantified using ImageJ (see Chapter 2) to obtain the profiles (Figure 4.2 A and B). Similar observations can be made from these profiles as from the qRT-PCR profiles: c-*fos* is transiently activated (Figure 4.2 A), while c-*jun* is still expressed after 120 minutes of stimulation (Figure 4.2 B).

Thus, for both c-*fos* and c-*jun* the overall shapes of the profiles obtained by Northern blotting are similar to the one obtained by qRT-PCR. The main characteristics, that are, the fact that c-*fos* induction is transient while c-*jun* induction lasts longer, are observed (Figure 4.2). However, by presenting the three experimental repeats used to generate the average profiles (Figure 4.2 Aii and Bii), variations in experiments can be observed. Indeed, c-*fos* mRNA levels for the first two repeats peak around 60 minutes and around 40 minutes for the last one

Figure 4.2: Activation profiles of c-*fos* and c-*jun* after sAn stimulation obtained by Northern blotting

Quiescent C3H 10T½ mouse cells were stimulated with sAn (25 ng/ml) for times between 5 and 120 minutes or untreated. Total RNA was extracted following the acid thiocyanate-phenol-chloroform extraction (see Section 2.6) and probed by Northern blotting for expression of c-*fos*, c-*jun* and *gapdh*. The blots obtained for one experiment representative of three repeats are shown in C. C-*fos* induction profile obtained by quantification of c-*fos* blots is represented in A and c-*jun* induction profile in B.

A. Northern blot probed with c-*fos* probe (C, top) was visualised by phophorimaging and quantified using ImageJ. The average profile in (i; ± SEM) is obtained from three biological repeats (ii). Data are normalised against *gapdh* (C, bottom) and the maximal response for each set of data.
B. Northern blot probed with c-*jun* probe (C, middle) was visualised by phophorimaging and quantified using ImageJ. The average profile in (i; ± SEM) is obtained from three biological repeats (ii). Data are normalised against *gapdh* (C, bottom) and the maximal response for each set of data. Both bands are quantified together.

A. **i.**

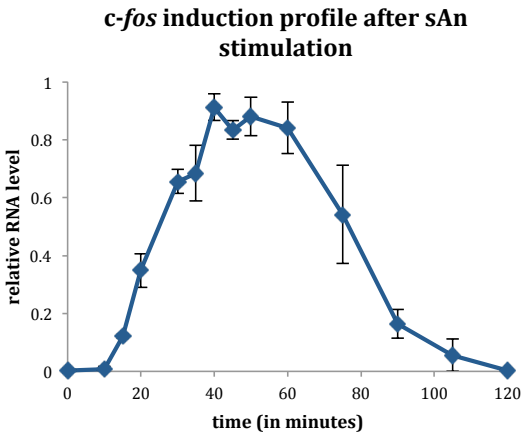
c-fos induction profile after sAn stimulation
relative RNA level
time (in minutes)

ii.

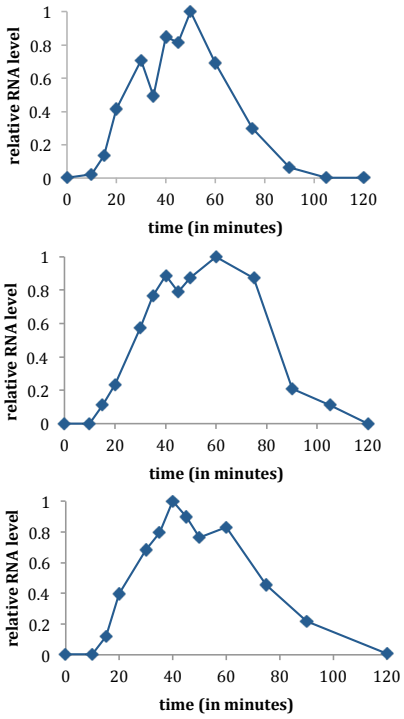
relative RNA level
time (in minutes)

B. **i.**

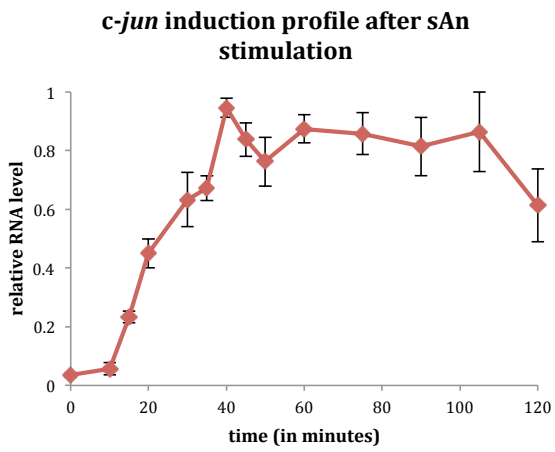
c-jun induction profile after sAn stimulation
relative RNA level
time (in minutes)

ii.

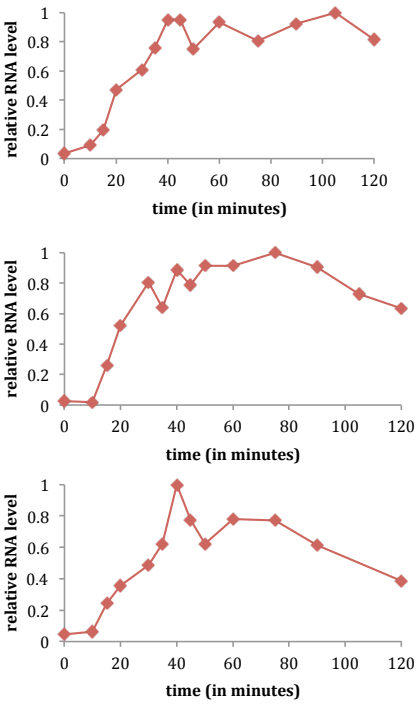
relative RNA level
time (in minutes)

Figure 4.2: Activation profiles of c-*fos* and c-*jun* after sAn stimulation obtained by Northern blotting

C. Quiescent C3H 10T1/2 cells were untreated (lane 1) or stimulated with sAn (25 ng/ml; lanes 2-14) for the indicated times. Total RNA was prepared and probed sequentially with c-*fos* (top), c-*jun* (middle) and *gapdh* (bottom) probes. This is one experiment representative of three repeats.

C.

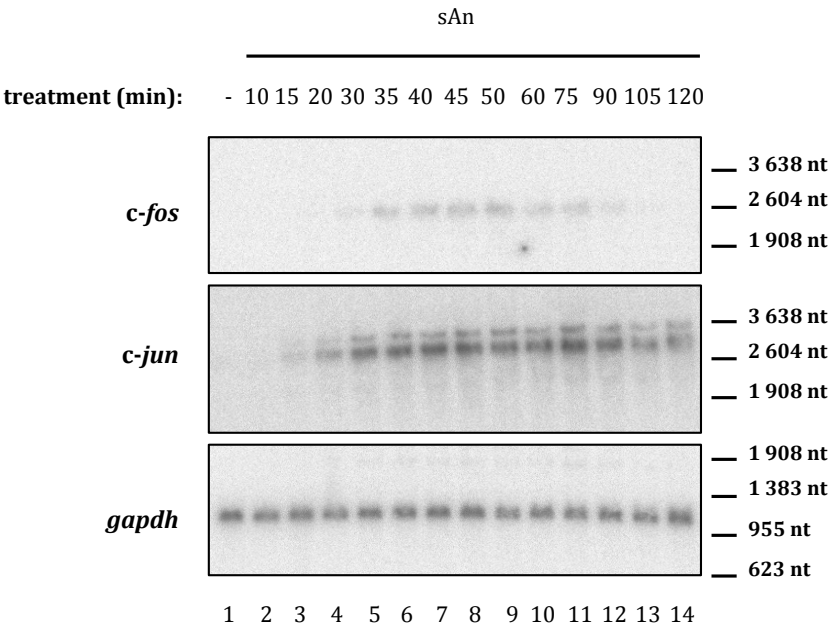
sAn
treatment (min): - 10 15 20 30 35 40 45 50 60 75 90 105 120
c-fos
3 638 nt
2 604 nt
1 908 nt
c-jun
3 638 nt
2 604 nt
1 908 nt
gapdh
1 908 nt
1 383 nt
955 nt
623 nt
1 2 3 4 5 6 7 8 9 10 11 12 13 14

(Figure 4.2 Aii). In a similar way, c-*jun* mRNA levels start to decrease after 100 minutes for the first repeat, 70 minutes for the second and 40 minutes for the last repeat (Figure 4.2 Bii). This indicates that even though the general characteristics of the gene profiles obtained after sAn are reproducible and gene specific, the reproducibility of quantitative data in this system is difficult.

As the average of the high temporal resolution of the expression profiles from Northern blotting (Figure 4.2) is similar to the profiles obtained by qRT-PCR (Figure 4.1), we used Northern blotting to further characterise IE gene regulation.

4.2.1.2 Alternative polyadenylated forms of c-jun

The use of Northern blotting allows for distinguishing between the two c-*jun* transcripts resulting from alternative polyadenylation (Ryseck et al. 1988). We investigated separately the alternative polyadenylation of c-*jun*. Thus, we quantified the two bands visible on the blots (Figure 4.2 C) separately (Figure 4.3 A). We can see that after sAn stimulation, the transcript corresponding to the lower band is strongly induced (Figure 4.3, black line), while the transcript corresponding to the upper band on c-*jun* blot is not and its induction stays relatively constant (Figure 4.3 grey line). Besides, the profile obtained for the upper band is similar to the total quantification (Figure 4.3, red and black lines). We therefore only considered the total quantification for the results presented in this Chapter.

Figure 4.3: Induction of the alternative polyadenylated forms on c-*jun* expression profile

Quiescent C3H 10T½ mouse cells were stimulated with sAn (25 ng/ml) for times between 5 and 120 minutes or untreated. Total RNA was extracted following the acid thiocyanate-phenol-chloroform extraction (see Section 2.6) and probed by Northern blotting for expression of c-*fos*, c-*jun* and *gapdh*. The blots obtained for one experiment representative of three repeats are shown in Figure 4.2 C. Northern blot probed with c-*jun* probe (Figure 4.2 C, middle) was visualised by phophorimaging and the two bands were quantified separately using ImageJ. Data (mean of three biological repeats ± SEM) are normalised against *gapdh* (Figure 4.2 C, bottom) and the maximal response for each set of data.

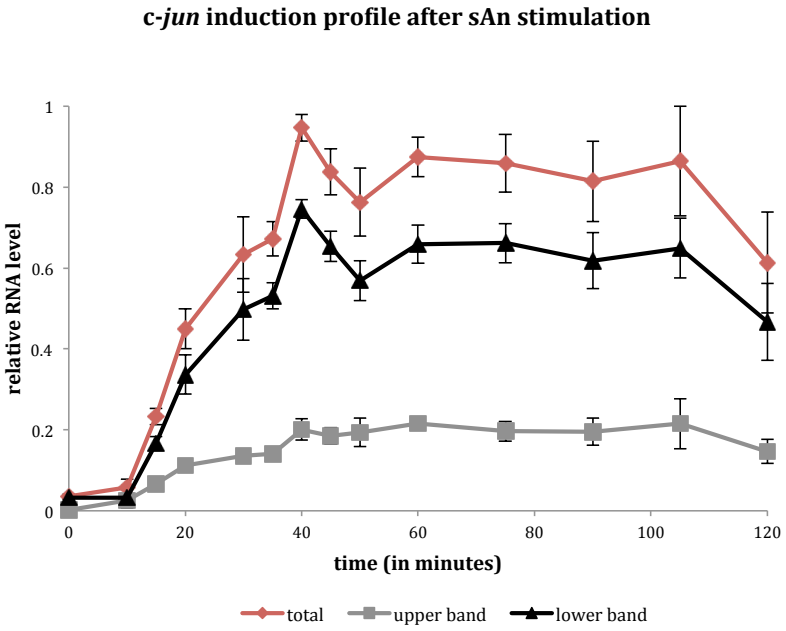
c-jun induction profile after sAn stimulation
relative RNA level
1
0.8
0.6
0.4
0.2
0
0
20
40
60
80
100
120
time (in minutes)
total
upper band
lower band

4.2.2 Effect of mRNA degradation on c-*fos* and c-*jun* profiles

The shapes of the curves observed for c-*fos* and c-*jun* profiles after sAn stimulation could result from regulation at various stages of the transcription process, such as initiation, elongation or degradation. We investigated the role of degradation in the regulation of these mRNA profiles by looking at the rate of degradation of their transcripts, by inhibition of transcription, and by blocking degradation using a translational inhibitor.

4.2.2.1 Inhibition of transcription reveals a constant rate of degradation

The degradation of c-*fos* and c-*jun* mRNA was analysed by inhibition of transcription with actinomycin D. We compared the rate of degradation of these gene transcripts for two time points from different phases of the profiles, to ask whether it changed between these phases (Figure 4.4). We choose one time point within the activation phase (30 minutes of sAn stimulation) and one where mRNA levels are maximum for both genes (60 minutes of sAn simulation; Figure 4.4). After sAn stimulation for 30 or 60 minutes, actinomycin D was added to the cells, and RNA harvested at different times after this to observe the change in transcript levels. The results observed are comparable to those obtained previously using DRB: c-*fos* transcripts are less stable than c-*jun* transcripts (Edwards and Mahadevan 1992). Looking more closely at the degradation profiles, a 20 minute treatment with actinomycin D results in a slight increase in c-*fos* mRNA levels after pre-treatment with sAn for 30 minutes, which is not the case after a 60 minute pre-treatment (Figure 4.4 Ai). However, the large error for this time point makes it difficult to conclude on this small increase. The other time points reveal a similar

degradation of c-*fos* transcripts after both 30 and 60 minutes' stimulation with sAn, as can be seen by parallel curves, suggesting a constant degradation rate throughout gene induction (Figure 4.4 Ai).

Even more strikingly than for c-*fos*, c-*jun* transcripts have very similar degradation rates after both 30 and 60 minutes' stimulation with sAn (Figure 4.4 Aii). The two curves representing the levels of c-*jun* mRNA post-treatment with actinomycin D are almost identical. Relatively stable levels are observed after the first 30 minutes of treatment with actinomycin D, after which the levels decrease in a similar way (Figure 4.4 Aii).

Thus, the degradation of c-*fos* and c-*jun* genes seems to be a constant process, and the shapes of the sAn-induced expression profiles observed on sAn-induced profiles of these genes are unlikely to be a result of variation of the degradation rates.

4.2.2.2 mRNA degradation does not affect the shape of the first phase of sAn-induced profiles

Previous experiments carried out in the lab have shown that IE genes are superinduced by inhibition of translation (Edwards and Mahadevan 1992). Here, we obtained a higher temporal resolution of c-*fos* and c-*jun* profiles after anisomycin treatment (inhibitory concentration), and compared anisomycin- and sAn-induced profiles (Figure 4.5). The use of sAn and anisomycin means that the same stimulation occurs in each case, and thus any differences in the expression

Figure 4.4: Constant rate of degradation for c-*fos* and c-*jun*

Quiescent C3H 10T½ were treated with sAn (25 ng/ml) for 30 minutes (light blue and red curves) or 60 minutes (dark blue and red curves) and further transcription was arrested by addition of actinomycin D (5 μg/ml). Total RNA was extracted following the acid thiocyanate-phenol-chloroform extraction (see Section 2.6) and probed by Northern blotting for expression of c-*fos*, c-*jun* and *gapdh*. The blots obtained for one experiment representative of two repeats are shown in B, c-*fos* blots quantification in Ai and c-*jun* blots quantification in Aii.

A. i. Northern blot probed with c-*fos* probe (B, top) was visualised by phophorimaging and quantified using ImageJ. Data (mean of two biological repeats ± SEM) are normalised against *gapdh* (B, bottom) and the sample without post-treatment with actinomycin D for each set of data. Time 0 refers to the time of addition of DRB. ii. Same as (i) for Northern blot probed with c-*jun* probe (B, middle).
B. Quiescent C3H 10T½ were treated with sAn (25 ng/ml) for 30 minutes (lanes 2-6) or 60 minutes (lanes 7-11) and further transcription was arrested by addition of actinomycin D (5 μg/ml; lanes 3, 4, 5, 6, 8, 9, 10, 11) for the indicated times. Time 0 refers to the time of addition of DRB and a total sAn treatment time, corresponding to the addition of sAn pre-treatment and DRB treatment (lanes 2-11), is indicated. Lanes 2 and 7 are controls without DRB indicated by '-', lane 1 is the negative control (untreated '-') and lane 12 is the DRB positive control. Total RNA was prepared and probed sequentially with c-*fos* (top), c-*jun* (middle) and *gapdh* (bottom) probes. This is one experiment representative of two repeats.

A.

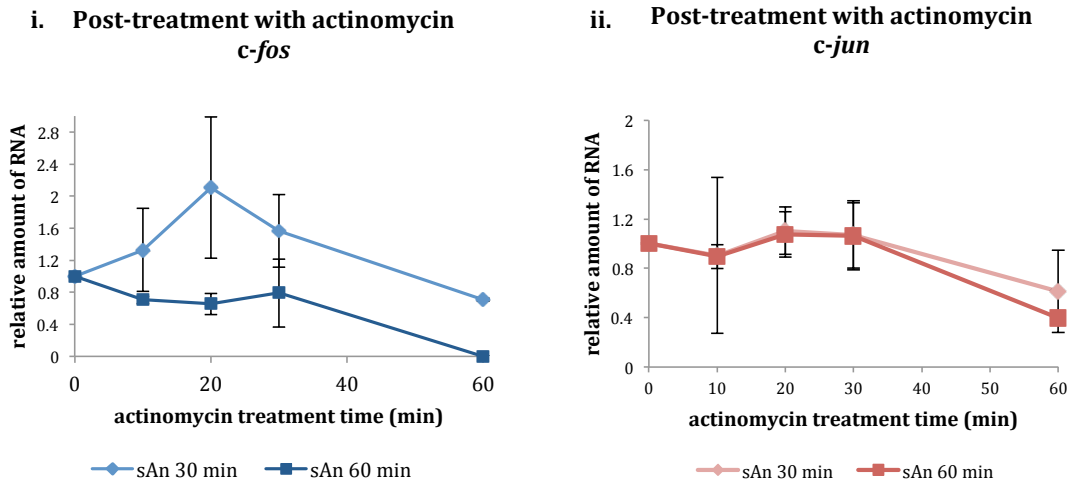
i. Post-treatment with actinomycin
c-fos
relative amount of RNA
2.8
2.4
2
1.6
1.2
0.8
0.4
0
0
20
40
60
actinomycin treatment time (min)
sAn 30 min
sAn 60 min
ii. Post-treatment with actinomycin
c-jun
relative amount of RNA
2
1.6
1.2
0.8
0.4
0
0
10
20
30
40
50
60
actinomycin treatment time (min)
sAn 30 min
sAn 60 min

B.

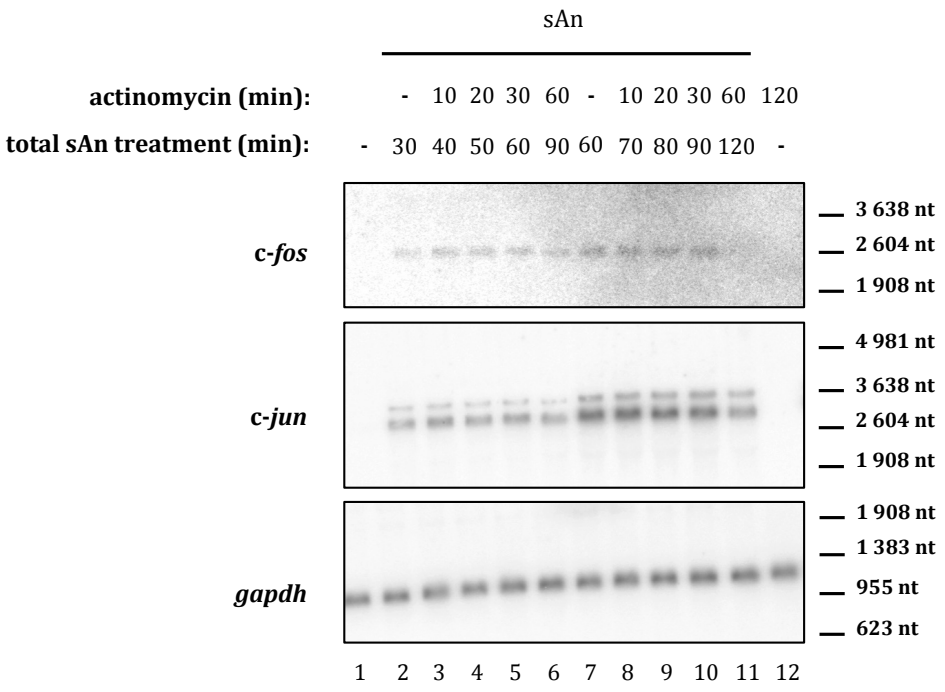
sAn
actinomycin (min): - 10 20 30 60 - 10 20 30 60 120
total sAn treatment (min): - 30 40 50 60 90 60 70 80 90 120 -
c-fos
3 638 nt
2 604 nt
1 908 nt
c-jun
4 981 nt
3 638 nt
2 604 nt
1 908 nt
gapdh
1 908 nt
1 383 nt
955 nt
623 nt
1 2 3 4 5 6 7 8 9 10 11 12

profiles can be identified as an effect of the absence of degradation (mRNA stabilisation) and delay in transcriptional shutdown (see Section 4.1.2.2). To allow a direct comparison of these two profiles, we were restricted to twenty samples to carry out Northern blotting on the same membrane. Due to this limitation, the sAn-induced profiles are not obtained with the same temporal resolution as in Figures 4.1 and 4.2, meaning that the curves appear slightly different (Figure 4.5).

As expected, stimulating mouse fibroblast cells with anisomycin at inhibitory concentration increases and prolongs c-*fos* and c-*jun* induction, compared to sAn (Figure 4.5). For the first 50 minutes of stimulation, sAn and anisomycin induce c-*fos* and c-*jun* in a similar way. But, after 50 minutes of treatment, while c-*fos* levels drop and c-*jun* levels stabilise for sAn activation, the levels of these two genes continue to increase for anisomycin activation (Figure 4.5). This increase results from the stabilisation of these transcripts and the inhibition of transcriptional shutdown due to translational inhibition (see Section 4.1.2.2).

For both c-*fos* and c-*jun* induction profiles, the increasing phases, that is, until 40 minutes of stimulation, observed after anisomycin or sAn stimulation are similar (Figure 4.5 A). This indicates that mRNA degradation does not seem to influence this part of the profile, as its absence (anisomycin stimulation) does not have an effect. The actinomycin D data, which suggested a constant degradation rates, are thus reinforced. However, this is under the assumption that the effect of the transcriptional shutdown is limited over the increasing phase of the profile. Any effect observed could also be due to this rather than loss of degradation.

Figure 4.5: Effect of superinduction on c-*jun* and c-*fos* characteristic profiles

Quiescent C3H 10T½ were treated with sAn (25 ng/ml; light blue and red curves) or anisomycin (10 µg/ml; dark blue and red curves) for the time indicated. Total RNA was extracted following the acid thiocyanate-phenol-chloroform extraction (see Section 2.6) and probed by Northern blotting for expression of c-*fos*, c-*jun* and *gapdh*. The blots obtained for one experiment representative of three repeats are shown in B, c-*fos* blots quantification in Ai and c-*jun* blots quantification in Aii.

A. i. Northern blot probed with c-*fos* probe (B, top) was visualised by phophorimaging and quantified using ImageJ. Data (mean of three biological repeats ± SEM) are normalised against *gapdh* (B, bottom) and the maximal activation for each set of data. ii. Same as (i) for Northern blot probed with c-*jun* probe (B, middle).
B. Quiescent C3H 10T½ were treated with sAn (25 ng/ml; lanes 2-7) or anisomycin (10 µg/ml; lanes 8-20) for the time indicated. Lane 1 is the negative control (untreated '-'). Total RNA was prepared and probed sequentially with c-*fos* (top), c-*jun* (middle) and *gapdh* (bottom) probes. This is one experiment representative of three repeats.

A.

i. c-*fos* induction profile after Anisomycin or sAn stimulation

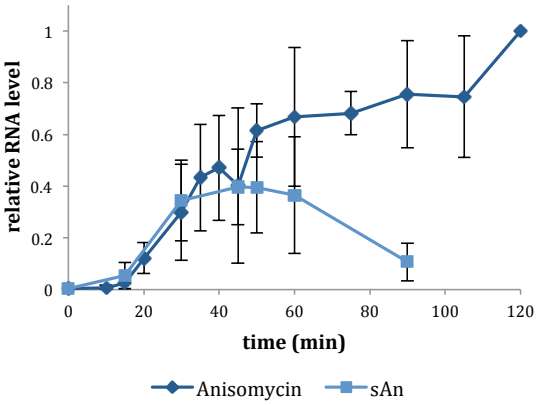

ii. c-*jun* induction profile after Anisomycin and sAn stimulation

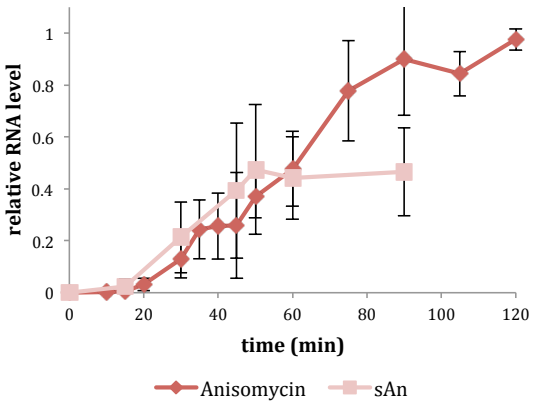

B.

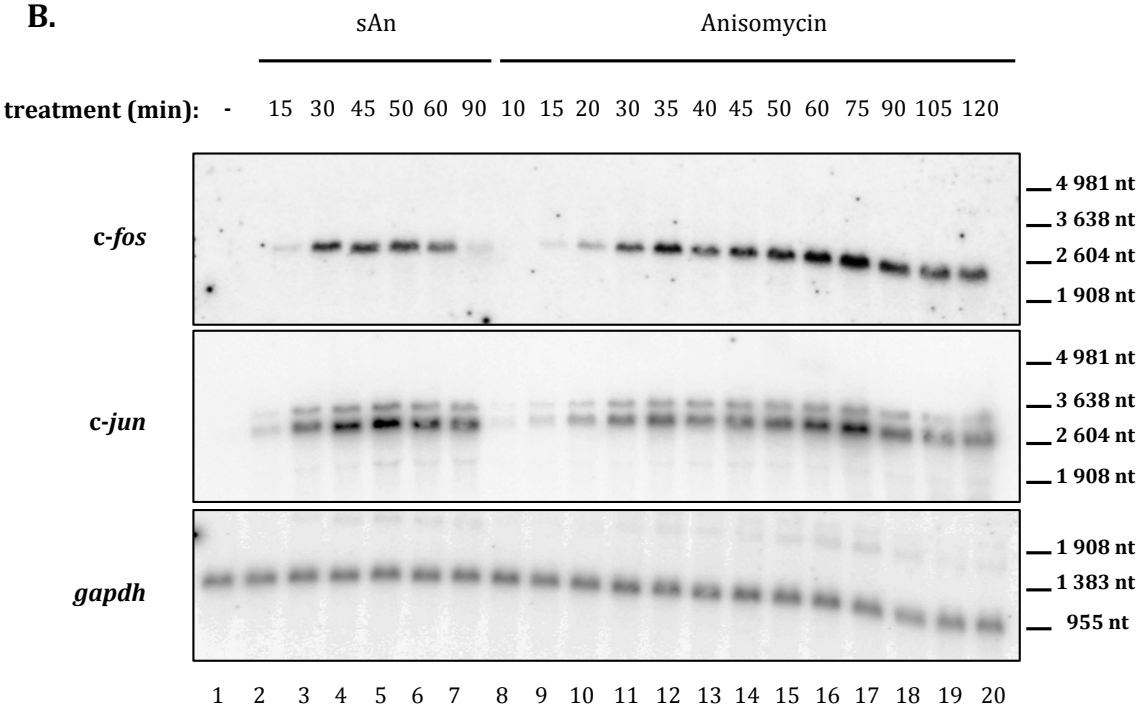

4.2.3 Disruption of the turnover of phosphorylation

IE gene expression is in part controlled by phosphorylation of transcription factors, which constitutes the link between the MAPK pathways and the IE gene induction (see Section 1.2.3). OA has been used to reveal the turnover of phosphorylation at these TFs (see Chapter 3). By using phosphatase and kinase inhibitors to disturb the phosphorylation turnover, we wanted to investigate its role and importance in c-*fos* and c-*jun* regulation.

4.2.3.1 Effect of phosphatase inhibitor

As previously shown, OA induces IE gene expression (see Figure 3.2). The blots shown in this Figure were quantified to further analyse this induction, and it revealed that c-*fos* and c-*jun* expression profiles are very similar after OA treatment (Figure 4.6 A), which was not the case after sAn activation (Figure 4.1 and Figure 4.2). Indeed, their mRNA levels start to increase after 20 minutes of OA treatment; they are at their maxima around 70 minutes and decrease from 70 minutes to 100 minutes (Figure 4.6 A).

In order to compare the levels of OA-induction of c-*fos* and c-*jun* with sAn-induction, we quantified blots from cells stimulated with sAn, OA or a combined stimulation of sAn and OA (Figure 4.6 C). While c-*fos* expression after OA treatment is at similar levels as after sAn stimulation (Figure 4.6 Bi), c-*jun* expression is greater after sAn stimulation (Figure 4.6 Bii). sAn has previously been described as an extremely strong inducer of c-*jun* and only a moderate inducer of c-*fos* (Hazzalin et al. 1997). This suggests that OA is a moderate inducer of c-*fos* and

Figure 4.6: Activation profiles of c-*fos* and c-*jun* after OA stimulation

A. Quiescent C3H 10T½ mouse cells were treated with OA (1 μM) for the indicated times. Total RNA was extracted following the acid thiocyanate-phenol-chloroform extraction (see Section 2.6) and probed by Northern blotting for expression of c-*fos*, c-*jun* and *gapdh*. The blots are presented Figure 3.2. Northern blots were visualised by phophorimaging and quantified using ImageJ. i. c-*fos* data and ii. c-*jun* data. Data (mean of three biological repeats ± SEM) are normalised against *gapdh* and the maximal response for each set of data.
B. Quiescent C3H 10T1/2 cells were stimulated with sAn (25 ng/ml) or with OA (1 μM) or with both sAn and OA for the indicated times. Total RNA was prepared following the acid thiocyanate-phenol-chloroform extraction (see Section 2.6) and probed sequentially with c-*fos*, c-*jun* and *gapdh* probes. The blots are presented in C. Northern blots were visualised by phophorimaging and quantified using ImageJ (i. c-*fos* data and ii. c-*jun* data). The dashed curves are a mathematical addition of the green and blue curves. Data are normalised against *gapdh* and the maximal response for each set of data.

A.

i. c-*fos* induction profile after OA treatment

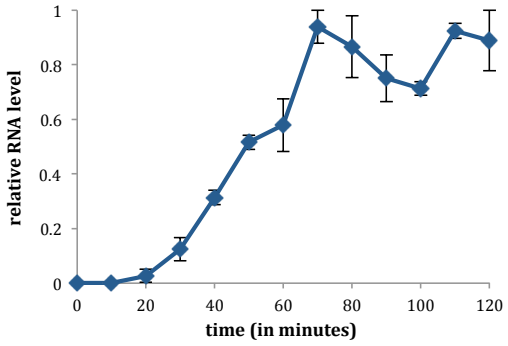

ii. c-*jun* induction profile after OA treatment

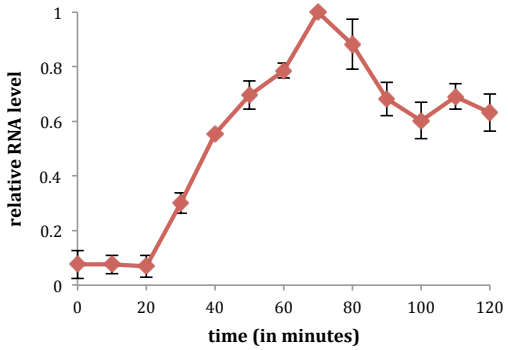

B.

i. c-*fos* induction after treatment with sAn and OA alone or in combination

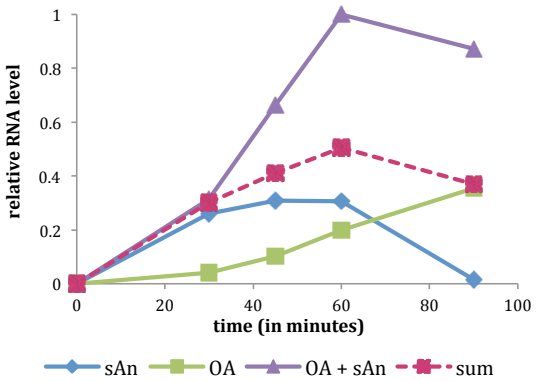

ii. c-*jun* induction after treatment with sAn and OA alone or in combination

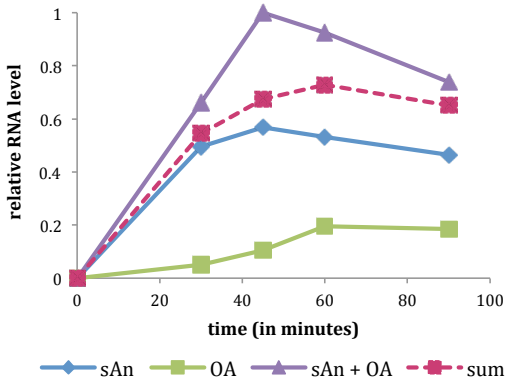

Figure 4.6: Activation profiles of c-*fos* and c-*jun* after OA stimulation

C. Quiescent C3H 10T1/2 cells were stimulated with sAn (25 ng/ml; lanes 2-5) or with OA (1 μM; lanes 6-10) or with both sAn and OA (lanes 11-14) for the indicated times. Lane 1 is the negative control (untreated '-'). Total RNA was prepared and probed sequentially with c-*fos* (top), c-*jun* (middle) and *gapdh* (bottom) probes. This experiment was carried out once.

C.

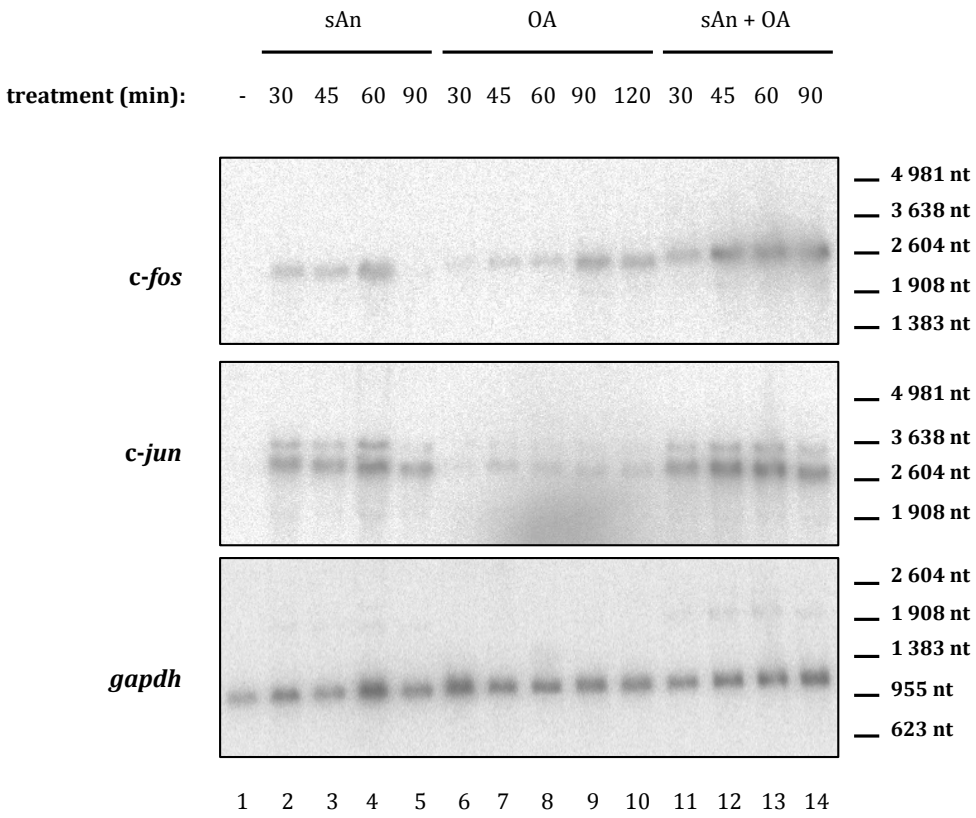
sAn
OA
sAn + OA
treatment (min):
- 30 45 60 90 30 45 60 90 120 30 45 60 90
c-fos
c-jun
gapdh
4 981 nt
3 638 nt
2 604 nt
1 908 nt
1 383 nt
955 nt
623 nt
1 2 3 4 5 6 7 8 9 10 11 12 13 14

c-*jun*. Besides, for both IE genes, OA-induction is late in comparison to sAn-induction, which can be related to the delay in MAPK pathways activation observed after OA treatment (see Chapter 3).

OA and sAn activate similar TFs (see Chapter 3), so we looked at the effect of a simultaneous treatment with these two compounds to investigate whether their induction is independent or if they interact. Co-treatment with OA and sAn further increases sAn-induction (Figure 4.6 B). This is made particularly clear by comparing the co-treatment curve with a curve generated by mathematical addition of the signals obtained after OA- and sAn-induction on their own. We can observe that co-treatment with OA and sAn has a synergistic effect, the shapes of the curves are similar (Figure 4.6 B), but the levels of expression are different. This indicates that OA and sAn do not act independently, but that they have interacting effects, which enhances expression levels.

4.2.3.2 Effect of kinase inhibitors

To better understand the role and importance of turnover of phosphorylation on IE gene induction, we also investigated the effect of its disruption by inhibiting kinase signalling with the SB 203580, SP 600125 and H89 inhibitors on their own or in combination (Figure 4.7).

As sAn activates both p38 and JNK pathways, it was expected that all three inhibitors used would modulate the induction of c-*fos* after sAn stimulation. We observed a partial inhibition of sAn-induction of c-*fos* after pre-treatment with the inhibitors on their own and a complete inhibition by pre-treatment with both

Figure 4.7: Pre-treatments with kinase inhibitors reveal difference in c-*fos* and c-*jun* induction

Quiescent C3H 10T1/2 cells were pre-treated with SB 203580 ('SB'; 10 μM) or H89 (10 μM) SP 600125 ('SP', 10 μM), followed by treatment with sAn (25 ng/ml) or OA (1 μM). Total RNA was extracted following the acid thiocyanate-phenol-chloroform extraction (see Section 2.6) and probed by Northern blotting for expression of c-*fos*, c-*jun* and *gapdh*. . The blots obtained for one experiment representative of three repeats are shown in B, c-*fos* blots quantification in Ai and c-*jun* blots quantification in Aii.

A. Northern blots in (B) were visualised by phophorimaging and quantified using ImageJ (i. c-*fos* data and ii. c-*jun* data). Data (mean of three biological repeats ± SEM) are normalised against *gapdh* and the maximal response for each set of data.
B. Quiescent C3H 10T1/2 cells were pre-treated for 30 minutes (indicated by '+') with SB 203580 ('SB', 10 μM; lanes 3, 6, 8, 11, 12 and 15) or H89 (10 μM; lanes 4, 9, 13) SP 600125 ('SP', 10 μM; lanes 5, 6, 10, 11, 14 and 15), followed by treatment with sAn (25 ng/ml; lanes 2-6) or OA (1 μM; lanes 7-11) or untreated ('-'; lanes 12-15). Lane 1 is the negative control (untreated '-'). Total RNA was prepared and probed sequentially with c-*fos* (top), c-*jun* (middle) and *gapdh* (bottom) probes. This is one experiment representative of three repeats.

A.

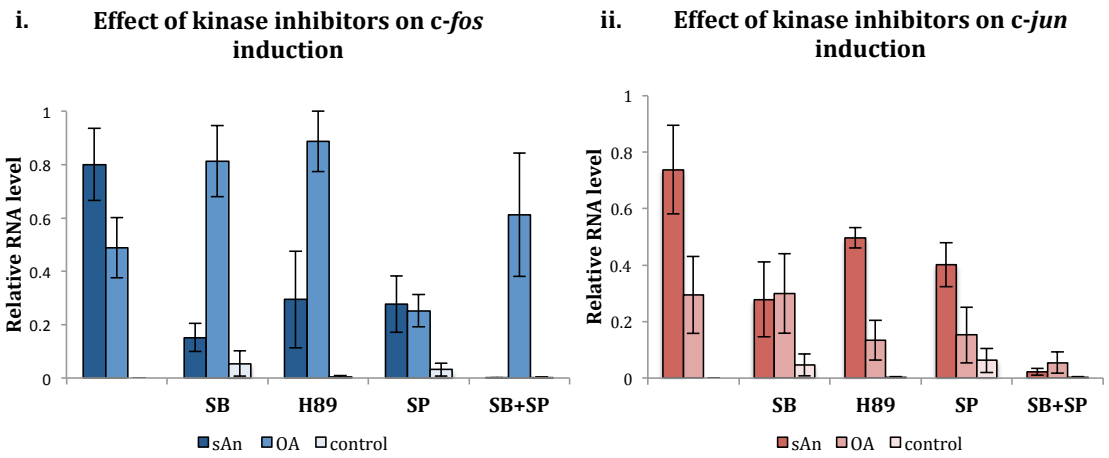
i.
Effect of kinase inhibitors on c-fos induction
Relative RNA level
1
0.8
0.6
0.4
0.2
0
SB
H89
SP
SB+SP
sAn
OA
control
ii.
Effect of kinase inhibitors on c-jun induction
Relative RNA level
1
0.8
0.6
0.4
0.2
0
SB
H89
SP
SB+SP
sAn
OA
control

B.

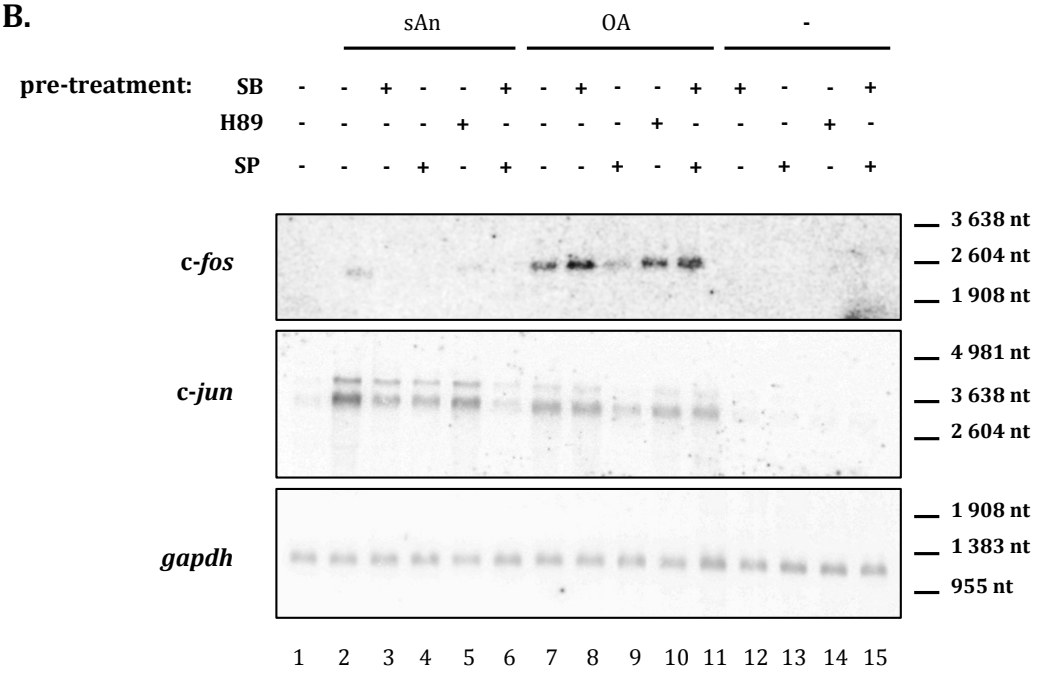
sAn
OA
-
pre-treatment:
SB - - + - - + - + - - + + - - +
H89 - - - - + - - - - + - - - + -
SP - - - + - + - - + - + - + - +
c-fos
3 638 nt
2 604 nt
1 908 nt
c-jun
4 981 nt
3 638 nt
2 604 nt
gapdh
1 908 nt
1 383 nt
955 nt
1 2 3 4 5 6 7 8 9 10 11 12 13 14 15

SB 203580 and SP 600125 (Figure 4.7 Ai). However, surprisingly OA induction of c-*fos* is enhanced by pre-treatment with SB 203580 and H89 (Figure 4.7 Ai), suggesting that negative feedback from downstream signalling targets of p38 has been inhibited. The partial inhibition of OA-induced c-*fos* expression by pre-treatment with SP 600125 is expected as OA activates TFs downstream of JNK. But c-*fos* expression is unchanged by pre-treatment with both SB 203580 and SP 600125 followed by OA treatment (Figure 4.7 Ai). This suggests the presence of some co-effect between these two inhibitors.

As for c-*fos*, the induction of c-*jun* after sAn stimulation is also partially inhibited by the three inhibitors and completely inhibited by pre-treatment with both SB 203580 and SP 600125 (Figure 4.7 Aii). However, pre-treatment with kinase inhibitors has different effect on OA-induction of c-*jun* than c-*fos*. Indeed, OA-induced c-*jun* expression is partially inhibited by pre-treatment with H89 and SP 600125, but not by SB 203580 (Figure 4.7 Aii). Thus, the inhibition of p38 does not affect c-*jun* expression after OA treatment but inhibition of either JNK or MSK1/2 does. Finally, a combined pre-treatment with SB 203580 and SP 600125 completely inhibits OA-induced c-*jun* expression, suggesting that the p38 and JNK pathways are both essential to convey OA induction but not sufficient on their own (Figure 4.7 Aii).

4.3 Discussion

4.3.1 Protein phosphatases play an important role in IE gene regulation

*4.3.1.1 OA induces c-*fos *and c-*jun *similarly*

OA and sAn induce c-*fos* and c-*jun* expression, and although both activate the TFs downstream of the p38 and JNK pathways (see Chapter 3), these compounds appear to induce completely different expression profiles, both compound and gene specific, for these two genes. Indeed, for a same gene, each compound (OA or sAn) induces a different and reproducible profile characteristic of the compound (Figure 4.2 and Figure 4.6 A), while c-*fos* and c-*jun* present different and reproducible profiles after sAn stimulation (Figure 4.1 and Figure 4.2). This illustrates the quantitative regulation of IE genes and their direct link to signalling pathways. The quantitative difference in signalling pathway activation by two compounds may be reflected in IE gene induction. For example, the fact that c-*fos* and c-*jun* induction can only be observed after 20 minutes for OA treatment (Figure 4.6 A), while it is observed after 10 minutes of sAn stimulation (Figure 4.1 and Figure 4.2), can be explained by the delay observed in OA activation of the signalling pathways (see Chapter 3).

After OA treatment and within the time frame of the experiment, c-*fos* and c-*jun* have similar expression profiles (Figure 4.6 A). However, these two genes usually have distinct profiles with a variety of different compounds, as can be seen after sAn activation (Figure 4.1 and Figure 4.2; reviewed in Hazzalin and Mahadevan 2002). This feature of OA suggests that OA-sensitive protein phosphatases, and

more precisely the turnover of phosphorylation, are important in the determination of the shape of the profile.

4.3.1.2 Link between turnover of phosphorylation and IE gene induction?

While OA induction of c-*fos* has a similar intensity to sAn induction, its induction of c-*jun* is lower (Figure 4.6 B). These low levels of induction are surprising, in view of the strong activation of TFs after OA treatment (see Chapter 3). The difference between the strength of OA-activation of signalling pathways and OA-induction of IE genes could be due to the disruption of the turnover of phosphorylation. It suggests that, in order for the gene to be induced, the fact that the kinases and TFs are activated (in a stable 'on' conformation) is not sufficient to induce IE gene expression. The induction of these genes may be more dynamic and require the presence of a turnover of phosphorylation (involving OA-sensitive phosphatases). Alternatively, the difference in intensity could also be the result of another action of OA. It could activate other pathway(s), which could have a negative effect on IE gene induction. It could also be explained by the inability of OA to activate TFs and/or downstream targets that are activated after sAn stimulation and essential to maximise sAn-induction, as only the activation of a few TFs were investigated in Chapter 3.

Not all evidence supports the turnover and dynamic regulation model. Stimulating the cells with OA and sAn in combination increases the sAn-induction of both c-*fos* and c-*jun,* which could suggest that the inhibition of dephosphorylation (maintaining the 'on' conformation) enhances the sAn effect. However, the synergistic effect observed after co-treatment with sAn and OA (Figure 4.6 B),

suggests a more complex regulation. Another example of synergistic effect is superinduction, the activation of the signalling pathway combined with inhibition of translation results in an increase induction linked to multiple causes (Edwards and Mahadevan 1992). The enhanced induction of c-*fos* and c-*jun* after co-treatment with sAn and OA could result from various effects. A different combination of TFs activated by both compounds than the one activated by these compounds on their own, which could produce the enhanced induction observed.

The fact that the enhancement of sAn induction observed after co-treatment with sAn and OA resembles the enhancement observed in superinduction conditions (Figure 4.5), suggesting that OA may act by a similar mechanism. But, due to the low levels observed after treatment with OA on its own (Figure 4.6 B) and the fact that OA-induction has been shown to stop after a few hours (Herschman et al. 1989), it is unlikely that this increase is due to stabilisation of the mRNA transcripts. However, to fully discount this possibility it would be necessary to evaluate the degradation rate of c-*fos* and c-*jun* transcripts after sAn and OA co-treatment by transcriptional inhibition.

The characteristics observed in superinduction conditions are also due to a delay in transcriptional shut-off, for example the translation of the dual protein phosphatase MKP-1, induced after stimulation and responsible for the MAPKs dephosphorylation (Sun et al. 1993; Slack et al. 2001; Owens and Keyse 2007), is inhibited. OA could also delay the transcriptional shut-off by inhibiting the protein phosphatases involved. However, there is no evidence of OA inhibiting DUSPs. Further investigations, such as nuclear run-on assay, should be carried out to

evaluate the effect of OA on transcriptional shut-off, as it has been done in the context of superinduction (Edwards and Mahadevan 1992).

4.3.2 Pre-treatment with kinase inhibitors reveals the complexity of IE gene regulation

4.3.2.1 c-fos *and c*-jun *induction cannot be attributed to a single pathway*

OA and sAn activate both the p38 and the JNK pathways. Investigating the effect of the p38 inhibitor, SB 203580, the MSK1 inhibitor, H89, and the JNK inhibitor, SP 600125, on c-*fos* and c-*jun* induction showed that their induction could not be attributed to any one of these pathways. Indeed, pre-treatment with any of the three inhibitors resulted in a partial inhibition of sAn induction (Figure 4.7). Similarly, for OA activation, H89 or SP 600125 pre-treatment partially inhibited OA-induced c-*jun* expression, suggesting that both the p38 and the JNK pathways account for c-*jun* induction after OA treatment. Moreover, as suggested by the study on signalling pathways (see Chapter 3), OA most likely acts on the negative regulation of downstream targets of p38, which could explain the absence of inhibition observed for SB 203580 pre-treatment for this compound (Figure 4.7 B). The complete inhibition of OA-induced c-*jun* expression by co-pre-treatment with SB 203580 and SP 600125 indicates that only the p38 and the JNK pathways are involved in c-*jun* induction. But, due to the non-specificity of SP 203580 (discussed in Chapter 3; Bain et al. 2003; Bain et al. 2007) we cannot exclude the possibility that OA could activate another pathway, which could also explain the partial inhibition observed after the kinase inhibitors are used.

4.3.2.2 The need for interactions between pathways

The enhancement observed for OA-induced c-*fos* expression by pre-treatment with SB 203560 and H89 (Figure 4.7 A) reveals the presence of interactions between the different pathways. These two inhibitors could inhibit negative feedback, downstream of p38. We have shown that pre-treatment with SB 203580 increases the activation of the JNK pathway by OA (see Section 3.2.3.2). This could explain the enhancement observed for the pre-treatment with this inhibitor. But, as it is not observed for sAn induction, and as pre-treatment with both SB 203580 and SP 600125 does not inhibit c-*fos* expression (Figure 4.7 A), other interactions need to be present. Pre-treatment with SB 203580 has been shown to increase the activity of MEK6, the kinase upstream of p38, and thus enhance c-*fos* and c-*jun* induction by TPA and EGF (Hazzalin et al. 1997). This kinase could induce c-*fos* by using downstream pathways other than p38 and be responsible for the enhanced induction observed. As the enhancement is only observed after OA treatment, this compound could prevent the deactivation of a downstream target of MEK6 other than p38 responsible for c-*fos* induction.

*4.3.2.3 Different expression of c-*fos *and c-*jun *reflects different TF binding sites in their promoters*

The fact that only c-*fos,* and not c-*jun,* is subjected to this increase in expression reveals a difference in their regulation. Even though these genes present a similar induction by OA (Figure 4.6 A), it seems that their induction is differently regulated, as c-*jun* induction is inhibited by pre-treatment with both SB 203580 and SP 600125, while c-*fos* is partially inhibited by SP 600125 but not by SB 203580 (Figure 4.7). This difference in regulation could result from the action

of a single TF or more likely from the combination of distinct TFs. Indeed, the promoter regions of c-*fos* and c-*jun* have multiple and different regulatory elements (see Section 1.2.3). p38 and JNK pathways activate multiple TFs, which can regulate either both IE genes, such as c-Jun and ATF-2, or only one of them, such as Elk-1, CREB, Elk-4 or MEF2C.

c-Jun and ATF-2, which are downstream targets of JNK, seem to have an enhanced phosphorylation after pre-treatment with SB 203580 and are inhibited by SP 600125 (see Figure 3.12). While ATF-2 has been identified as a p38 downstream target (Raingeaud et al. 1995), its sAn-induced activity is not inhibited by SB 203580 in C3H 10T½ cells (see Figure 3.13), suggesting that it is not downstream of p38 in these cells. These TFs can form complexes, which bind to AP-1 and AP-1-like regulatory element. As both c-*fos* and c-*jun* have AP-1 or AP-1-like regulatory element (see Section 1.2.3), it is unlikely that these two TFs on their own could explain the difference in the gene expression observed (Figure 4.7). Besides, both c-*fos* and c-*jun* inductions are partially inhibited by pre-treatment with SP 600125. However, the different AP-1 sites have been shown to have various affinities depending on the protein constituting the AP-1 complexes; while the jun1 site of c-*jun* binds Jun:Jun, Jun:Fos and Jun:ATF2 complexes, the jun2 site predominantly binds the Jun:ATF2 complex (see Section 1.2.3.3; Herdegen and Leah 1998). This could explain the difference in gene regulation.

CREB, downstream target of the p38 pathway, can regulate c-*fos* induction through its CRE regulatory element (see Section 1.2.3). The fact that OA-induced activation of CREB is not inhibited by pre-treatment with SB 203580 or SP 600125 (see

Figure 3.8) could explain the induction of c-*fos* observed after pre-treatment with SB 203580 on its own or in combination with SP 600125 (Figure 4.7). The partial inhibition of c-*fos* induction after pre-treatment with SP 600125 could be explained by the inhibition of the activity of other TFs, such as c-Jun and ATF-2 (see Figure 3.12). This demonstrates that c-*fos* and c-*jun* induction results in the activation of a combination of TFs.

The transcription factors Elk1, downstream of both JNK and p38, or Elk4, downstream of p38, can also regulate c-*fos* induction through its SRE regulatory element (see Section 1.2.3). These TFs could also be activated by OA and participate in explaining c-*fos* and c-*jun* induction profiles after pre-treatment with kinase inhibitors.

4.3.3 The specific IE gene profiles could be regulated at the initiation of transcription

Gene expression is a process regulated at multiple stages, including initiation, elongation and termination of transcription, and mRNA degradation (discussed further in Chapter 6). However, the degradation rates of c-*fos* and c-*jun* transcripts at different stages of sAn stimulation are similar (Figure 4.4), which suggests that it is a constant process. Moreover, inhibition of protein synthesis, which blocks degradation, did not affect the first part of sAn-induced profiles, again suggesting that degradation does not regulate them (Figure 4.5).

Quantitative differences in OA and sAn activation of the various TFs are reflected in quantitative differences in gene induction profiles, such as the delay observed in TF phosphorylation after OA activation and the effect of H89, SB 203580 and

SP 600125 (discussed in Section 4.3.2). The specific characteristics regarding the variation in mRNA levels (Figure 4.1 and Figure 4.2) observed on c-*fos* and c-*jun* profiles after sAn stimulation might result from a change in the rate of transcription. As transcription initiation is directly linked to the signalling pathways, this would provide an obvious way to link gene expression to the external stimuli. However, these results, discussed in this chapter, are a first approximation to investigate IE gene regulation and would need to be correlated using other methods to conclude.

Chapter 5: Investigation of a simplified computational model of the interface between MAPK pathways and IE genes

5.1 Introduction

In order to understand how cells regulate gene transcription to produce quantitative responses calibrated to the strength of the stimulus, we investigated signal transduction, by focusing on MAPK pathways (Chapter 3), and gene transcription (Chapter 4). The key factor of the quantitative regulation seems to lie at the interface between these two processes, and we used a simplified model of the interface to obtain new insight on the potential mechanisms regulating inducible gene expression.

5.1.1 Using computational models to gain insights into biological system

5.1.1.1 Computational modelling and model checking

Computational models of biological systems are increasingly used to obtain a better understanding of the mechanisms controlling the system. The information that one can obtain about the system depends on the modelling approach used (reviewed in Fisher and Henzinger 2007). A computational model which provides a sequence of steps that describes the system for an execution engine to execute and mimic the phenomenon would allow an easier analysis of the mechanisms of a biological system than a mathematical model, which describes the interactions between the different elements of the system over time by equations (Fisher and Henzinger 2007).

Computational models can be used to test different hypotheses by evaluating the effect of an alteration within the model and comparing it with the experimental data. If the behaviour of the model does not conform to the experimental data, two conclusions can be drawn. First, the model could be an incorrect representation of the system, in which case it needs to be modified and improved. Secondly, it could reveal behaviour of the biological system that is not detected by the experimental data and thus help identify further experimental investigations. Indeed, in the study of the Fibroblast Growth Factor (FGF) signalling pathway, the inhibition of a specific element of the pathway led to unexpected results, which were experimentally verified (Kwiatkowska and Heath 2009). This can be done automatically and is known as 'model checking'. Software tools have been developed, such as the probabilistic model checker, PRISM, used in this study (Kwiatkowska et al. 2011), that can evaluate all the possible executions by exploring the different states and state changes of the model.

Time constitutes one of the main factors while studying a biological system since experimental data is typically provided as a time course and require biological repeats. In order to understand the regulation of a biological system and interactions between the different elements of the system, the effect of inhibition or removal of each element over time needs to be verified. The use of model checking, on a computational model of this system, could predict the effect of these inhibitions and help prioritise experiments. This was the technique used in the study of the FGF signalling pathway in the probabilistic model checker PRISM (Heath et al. 2007).

The lack of quantitative data for the biological systems is one of the main limitations for computational models. Indeed, the concentrations and rates of equations are often derived from non-quantitative experiments, such as Western blotting, which only give relative values, or from non-physiological conditions as they are evaluated *in vitro*. Although these limitations prevent the model from providing the exact values of predicted quantities, it can still be informative on the behaviour of a system and on the most important steps and interactions of a system. Moreover, the process of building a model could allow thinking differently about a system and thus reveal unknown characteristics within the system (Kwiatkowska and Heath 2009).

5.1.1.2 Different modelling approaches

Different computational models, such as Boolean networks, Petri nets, interacting state machines, process calculi and hybrid models networks, are available and their applicability depends on the biological system considered (reviewed in Fisher and Henzinger 2007).

For this study we focused on state transition systems with transitions labelled with reaction rates, which have already been used to model signalling pathways. The probabilistic model checker PRISM (Kwiatkowska et al. 2011) was used to build a model based on the reactions of the MAPK pathways using the kinetic rates obtained from a study of the ERK pathway in *Xenopus* oocytes maturation (Huang and Ferrell 1996; Kwiatkowska et al. 2008). A population-based model was devised, where the number of each type of species is modelled together with the possible biochemical reactions. In the PRISM language, a number of modules

describing the evolution of each species of the system are developed, with state changes represented by guarded commands (Kwiatkowska et al. 2008). The reactions between different species are modelled by synchronising the guarded commands from the modules, representing the species involved in the reaction. The values for stochastic reaction rates are obtained from the kinetic rates. Such models allow analysing quantitative properties and provide insights on the dynamics of the system studied.

5.1.2 PRISM, a tool for analysing stochastic systems

5.1.2.1 The need of a stochastic model

For this study, we have investigated the interface between the MAPK signalling pathways and IE genes, for which no prior model is known. Both mathematical and computational models can be used to represent signalling pathways. The MAPK pathways have previously been described deterministically as a set of ordinary differential equations (ODEs; Huang and Ferrell 1996), or have been represented as stochastic computational systems using a process calculus model analysed using probabilistic model checking (Heath et al. 2007; Kwiatkowska and Heath 2009). Due to the small number of elements that need to be considered to study gene expression (only two copies of the gene are present in eukaryotic cells), stochastic methods are needed to investigate transcriptional regulation, as deterministic ODE models are valid only for high molecule counts.

Moreover, a study comparing deterministic models, which consider the average behaviour, and stochastic signals for gene expression observed that, even though

they can lead to similar conclusions under certain conditions (large system size and fast promoter kinetics) for the usual abstraction of gene expression (Figure 5.1), a deterministic signal hides the effect of noise (Kaern et al. 2005).

5.1.2.2 Modelling the interface

This study has focused on developing an abstract model of the interface between signalling pathways and IE genes. The simplified model usually used to investigate gene expression considers a single gene, the activation and deactivation of the promoter of this gene, rates of transcription and translation and rates of degradation for both mRNA and protein (Figure 5.1; Kaern et al. 2005). In this abstraction, all the rates are considered constant. Besides, once the promoter is turned 'on', the rate of transcription initiation is constant; the effect of an external stimulus is not taken into consideration.

While similar simplifications, such as a single gene and constant mRNA production and degradation rates, are made in our abstraction (see Section 5.2), the main focus is on the interface between signalling pathways and gene expression. Thus, we not only consider a constant rate of transcription but also investigate the effect of dynamic regulation of gene expression, by considering the rate of transcription initiation directly linked to the signalling pathway and varying with the intensity of the signal perceived. Thus, both a binary and a continuously variable switch for this interface are considered in this study (described in Section 1.5).

Figure 5.1: Abstraction of gene expression

Schematic representation of the typical simplified model used to investigate gene expression. k_{on} and k_{off} are the rate constants associated with the activation and deactivation of the promoter. s_A and d_M represent the synthesis and degradation rates of mRNA. s_P and d_P represent the synthesis and degradation rate of protein. Adapted from (Kaern et al. 2005).

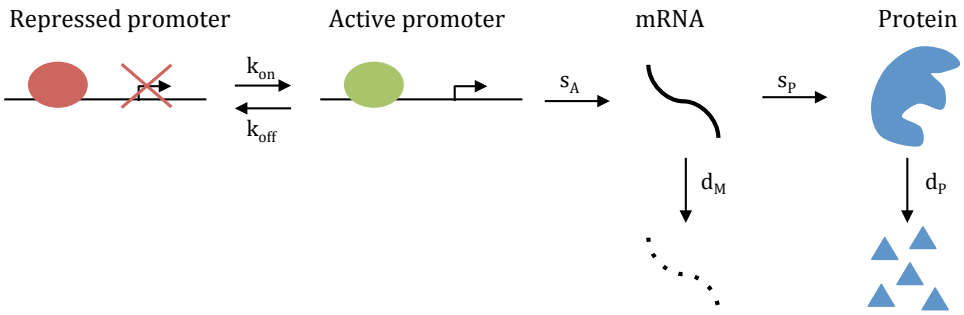
Repressed promoter
Active promoter
mRNA
Protein
k_{on}
k_{off}
s_A
s_P
d_M
d_P

5.1.2.3 The probabilistic model checker PRISM

Our study of IE gene regulation necessitates a stochastic and quantitative analysis of the interface between signalling pathways and gene expression. We choose to use probabilistic model checking, which is a variant of model checking allowing for quantitative analysis of a stochastic model as it considers the likelihood that transitions occur as well as the time they do so (Heath et al. 2007). We used the probabilistic model checker PRISM, inspired by prior success in signalling pathway modelling (Heath et al. 2007; Kwiatkowska et al. 2008) and due to recent improvements of PRISM based on fast adaptive uniformization (Dannenberg et al. 2014), which allows faster computation of probability and expectation evolution over time. PRISM performs an exhaustive analysis of the model, which is described as a state-transition system, where states are vectors of molecule counts and transitions are labelled with reaction rates. This discrete stochastic model (continuous-time Markov chain (CTMC)) is obtained from the reaction system represented as a collection of PRISM modules in the standard way (Kwiatkowska et al. 2010).

5.1.3 Summary

In this chapter, we developed a simplified model of the interface between MAPK pathways and an IE gene to better understand the quantitative regulation of these genes. We focused on comparing two hypotheses: an 'on/off' switch, which considers the gene as being in either a stable 'on' conformation, where initiation of transcription is possible, or an 'off' conformation, and a continuously variable switch, which considers the frequency of initiation as directly linked to the

intensity of the signal conveyed by the signalling pathways. Our abstraction considers a single TF constitutively bound to the regulatory element of a single gene. We performed a comparison of the two hypotheses, which suggested that the continuously variable switch hypothesis is better suited to producing mRNA profiles that matches signalling intensity. Although no direct comparison with the experimental mRNA profiles can be done due to the simplification made in our model, the process of building this abstraction led to new insight into quantitative regulation of inducible genes. This work was carried out in collaboration with Marta Kwiatkowska and Milan Ceska, Alessandro Ablate and David Safranek had valuable inputs in the discussion. Using insights derived from laboratory measurements of signaling and mRNA induction in live cells, I provided the modellers with the characteristics that such a system might have. This involved extensive discussion of how gene induction is mediated and key parameters that might be used in the model and how they might relate back to biological events in cells. Following this, Milan Ceska wrote the code and did the detailed modelling work to obtain the different curves presented in this thesis. All of the analysis of the results and interpretations developed here are mine. The results are presented and discussed in (Ceska et al., in preparation).

5.2 Description of the model

In order to gain more insight into the quantitative regulation of IE genes, and compare the characteristics of the two hypotheses, the 'on/off' switch and the continuously variable switch hypotheses (see Section 1.5), we developed a simplified computational model of the interface between these genes and the MAPK pathways. The 'on/off' switch hypothesis considers the gene in a stable 'off'

or 'on' conformation, the rate of initiation of transcription being constant while in the 'on' conformation. In the continuously variable switch hypothesis the rate of initiation of transcription is directly linked to the strength of signal perceived and coupled to the turnover of phosphorylation of the TF. The model is composed of three modules (signalling, initiation and mRNA modules) and an interface between the signalling and initiation modules (Figure 5.2). For all our analysis we have considered a time frame of 120 minutes to match the experimental data (Figure 5.3; see Figures 4.1 and 4.2). Table 5.1 lists the reactions on which the computational model was based. More details about the construction of the model can be found in (Ceska et al., in preparation).

5.2.1 The signalling module

The first module of the model, the signalling module, represents the signalling pathways leading to phosphorylation of TFs. The p38 and JNK pathways are activated by OA treatment on its own, suggesting the presence of turnover of phosphorylation and potentially a dynamic regulation of these pathways (see Chapter 3). Moreover, pre-treatment with SB 203580, a p38 inhibitor, and SP 600125, a JNK inhibitor, in combination inhibits the induction of c-*jun* and affects c-*fos* induction by OA (see Figure 4.7). Thus, we focused on these two pathways for the input signal of the model. As sAn also activates these pathways (see Chapter 3; Mahadevan and Edwards 1991) and its induction of c-*fos* and c-*jun* is inhibited by co-pre-treatment with SB 203560 and SP 600125 (see Figure 4.7), we choose this compound to obtain the activation profiles used in the model. Moreover, as our focus is on the interface between the signalling pathways and gene expression, we simplified the signalling pathways by considering only the

Figure 5.2: Schematic representation of the simplified model of the interface between the MAPK pathways and IE gene

The model is divided into three modules and an interface.

- Signalling module: represents the signalling pathways, two input signals (activation profile) are considered: JNK and p38.
- Interface: the link between signalling pathway and IE gene transcription is modelled by a regulation function (F_{reg}), which represents the transcription factor (TF) phosphorylation. The output is referred to as regulation profile.
- Initiation module: represents the initiation of transcription, a single gene with a single TF permanently bound is considered either in the inactive (E0) state, where transcription is not permitted and TF is not phosphorylated, or in the active state (E1), where transcription happens and TF is phosphorylated. The TF phosphorylation is regulated by F_{reg} (see Figure 5.5), while the TF dephosphorylation is regulated by phosphatases (Ptase), considered constant. The output of this module is referred to as initiation profile.
- mRNA module: represents the production and degradation of mRNA, one initiation resulting in one mRNA. Both rates are considered constant (see Section 5.2.3 for details). The output of this module is referred to as induction profile.

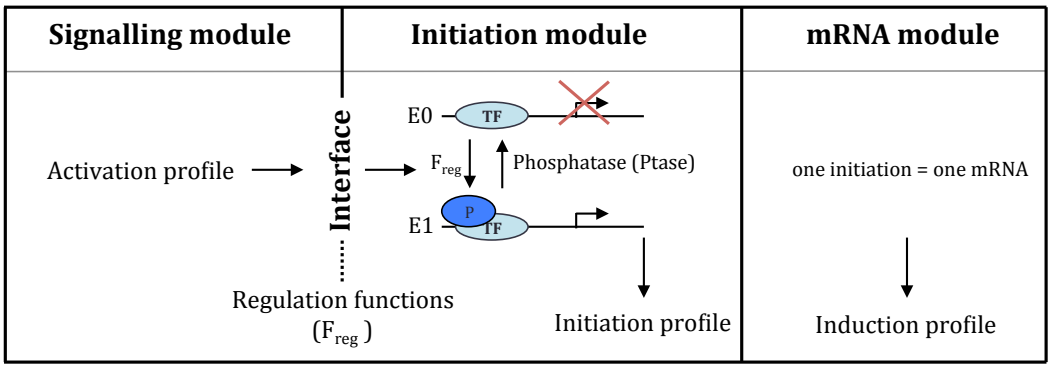
Signalling module
Initiation module
mRNA module
Activation profile
Interface
E0
TF
P
F_{reg}
Phosphatase (Ptase)
E1
P
TF
one initiation = one mRNA
Regulation functions
(F_{reg})
Initiation profile
Induction profile

Table 5.1: Reaction networks used for computational model

Representation of the reaction networks used to compute the model presented Figure 5.2.

- Signalling module: A and B are virtual substances and K-PP represents the phosphorylated MAPK. The production and degradation of phosphorylated kinase occur at the rate kProd and kDegr respectively, their values are detailed in Table 5.2. TF and TF_P represent the unphosphorylated and phosphorylated transcription factor respectively and Ptase the protein phosphatases. TF is phosphorylated at the rate r_1 and dephosphorylated at the rate r_2. Michaelis-Menten kinetics is used to determine these rates (see Figure 5.5).
- Initiation module: TF phosphorylation (transition from the state E0 to the state E1, see Figure 5.2) is regulated by the regulation function (F_{reg}) described in Figure 5.5, while TF dephosphorylation (transition from E1 to E0, see Figure 5.2) happens with the constant rate Ptase.
- mRNA module: The production of mRNA happens with the constant rate prod and the degradation of mRNA happens with the rate degr obtained from c-*fos* and c-*jun* half-lives ($t_{1/2} = \frac{ln\,(2)}{k_{degr}}$, see Section 5.2.3).

signalling module	kinase activation – bell-shape generator	
	$A + K_PP \xrightarrow{kProd} 2\ K_PP$	$kProd$ (see Table 5.2)
	$B + K_PP \xrightarrow{kDegr} 2B$	$kDegr$ (see Table 5.2)
	TF phosphorylation and dephosphorylation (Michaelis-Menten kinetics)	
	$TF + K_PP \xrightarrow{r_1} TF_P + K_PP$	$r_1 = p.[K_PP].\frac{[TF]^{expP}}{[TF]^{expP} + M_P^{expP}}$
	$TF_P + Ptase \xrightarrow{r_2} TF + Ptase$	$r_2 = d.[Ptase].\frac{[TF_P]^{expD}}{[TF_P]^{expD} + M_D^{expD}}$
initiation module	TF phosphorylation	
	$E0 \xrightarrow{F_{reg}} E1$	F_{reg} (see Figure 5.5)
	TF dephosphorylation	
	$E1 \xrightarrow{Ptase} E0$	$Ptase$ considered constant
mRNA module	mRNA production	
	$nascent\ RNA \xrightarrow{prod} mRNA$	$prod$ constant (zero order reaction)
	mRNA degradation	
	$mRNA \xrightarrow{degr} \emptyset$	$degr = 0.0231\ min^{-1}\ or\ 0.0462\ min^{-1}$ (see section 5.2.3 for details)

final kinase of the MAPK pathway tiered organisation ie. the MAPK (see Section 1.3.1).

5.2.1.1 Experimental activation profiles

The activation profiles after sAn stimulation of p38 and JNK, and of two TFs downstream of these kinases, CREB and c-Jun respectively, were obtained by quantification of Western blots (Figure 5.3). Anti-phospho antibodies, which recognised the phosphorylated form of the proteins, were used for p38, JNK and CREB (Figure 5.3 A, C and D), while an anti-c-Jun antibody was used for c-Jun (Figure 5.3 B). c-Jun activation was quantified by considering the relative intensity of the highest upper band over the intensity of the lower bands, which were considered together as the separation obtained by electrophoresis on SDS gels was not large enough to separate them (Figure 5.3 B).

For each protein, the linear range of the antibody, which indicates that the intensity of the signal is proportional to the concentration of protein, was evaluated by means of a standard curve (Figure 5.3 Ai, Bi, Ci and Di). The signal intensities of known amounts of activated protein were quantified using ImageJ. In order to avoid transfer differences between the samples for the titration curve, the same amounts of protein were loaded by mixing activated protein with non-activated protein from unstimulated cell samples. The maximal activation of the protein studied was considered to be obtained after 30 minutes of sAn stimulation, which produces the most intense signal. The intensities were normalised against the total amount of protein (using Ponceau staining or protein-specific antibody of the protein), for loading control, and against the intensity corresponding to the

Figure 5.3: Experimental activation profiles for the JNK and p38 pathways

A. i. Quiescent C3H 10T½ cells were stimulated with sAn (25 ng/ml) for 30 minutes or untreated. Cells were lysed with high-salt lysis buffer (see Section 2.3.1). Different percentages of activated protein (sAn 25 ng/ml for 30 minutes) were loaded on ERK gels (see Section 2.4.2) to obtain the standard curve. The same amounts of protein were loaded by mixing with untreated cells. The membranes were probed using phospho-specific JNK antibody (top) or protein-specific antibody JNK for loading control (bottom). The blots are quantified by measuring the signal intensities using imageJ and the percentage of maximum intensity is plotted against the percentage of maximum activation. ii. Quiescent C3H 10T½ cells were stimulated with sAn (25 ng/ml; lanes 11-20) for the indicated times. Lane 10 is the negative control (untreated cells). Cells were lysed with high-salt lysis buffer (see Section 2.3.1) and cell extracts were separated on ERK gels (see Section 2.4.2) and probed using phospho-specific JNK antibody (top) or protein-specific antibody JNK for loading control (bottom). The blots are quantified by measuring the signal intensities using imageJ and the percentage of maximum activation, obtained using the standard curve, is plotted against time. This is one experiment representative of three repeats.
B. Similar to A, but cell extracts were loaded on SDS-PAGE (see Section 2.4.1) and probed using protein-specific c-Jun antibody (top). Ponceau staining is used as loading control (bottom). This is one experiment representative of three repeats.

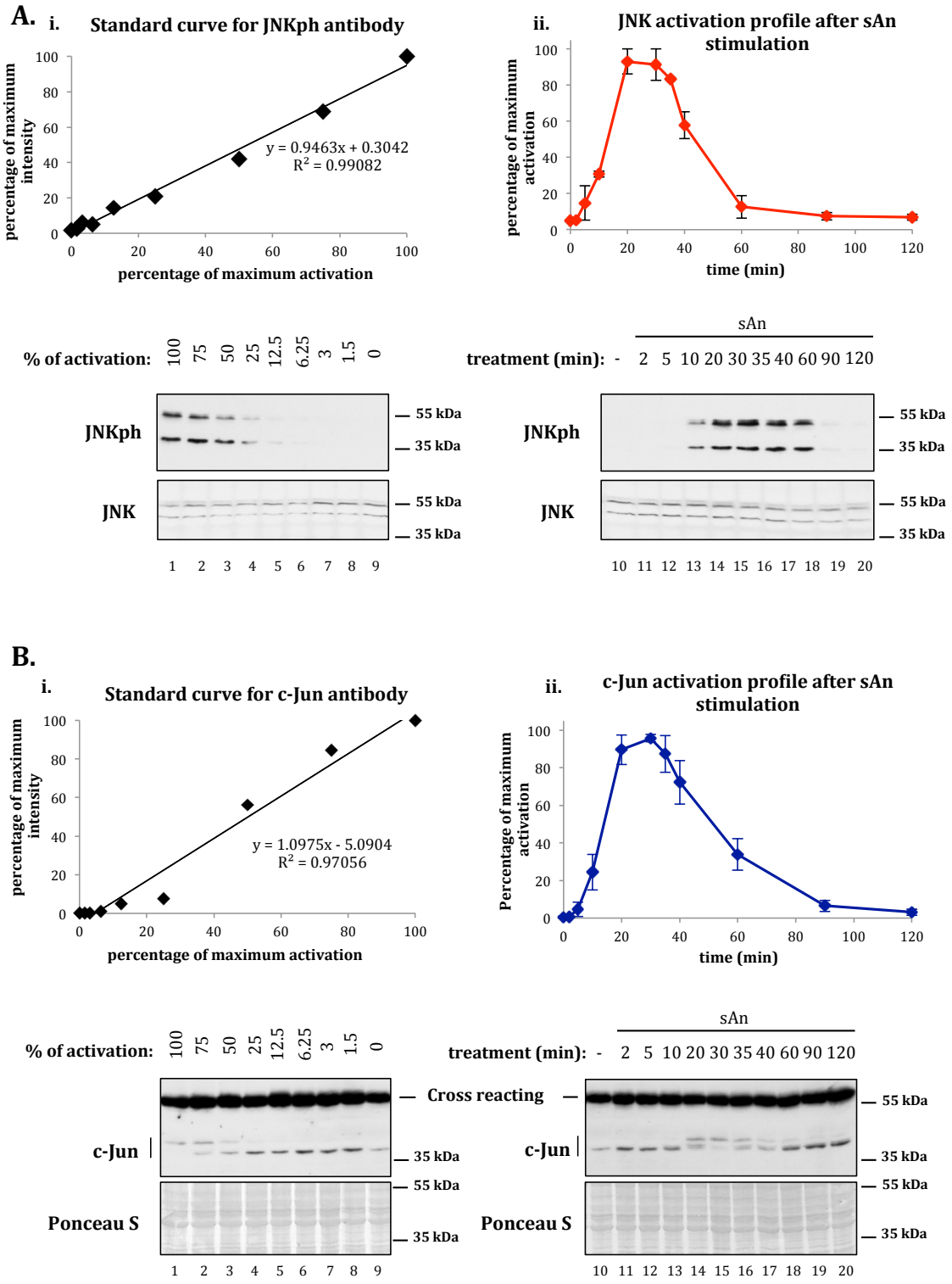
A.
i.
Standard curve for JNKph antibody
percentage of maximum intensity
y = 0.9463x + 0.3042
R² = 0.99082
percentage of maximum activation
ii.
JNK activation profile after sAn stimulation
percentage of maximum activation
time (min)
% of activation: 100 75 50 25 12.5 6.25 3 1.5 0
treatment (min): - 2 5 10 20 30 35 40 60 90 120
sAn
JNKph
JNK
55 kDa
35 kDa
1 2 3 4 5 6 7 8 9
10 11 12 13 14 15 16 17 18 19 20
B.
i.
Standard curve for c-Jun antibody
percentage of maximum intensity
y = 1.0975x - 5.0904
R² = 0.97056
percentage of maximum activation
ii.
c-Jun activation profile after sAn stimulation
Percentage of maximum activation
time (min)
% of activation: 100 75 50 25 12.5 6.25 3 1.5 0
treatment (min): - 2 5 10 20 30 35 40 60 90 120
sAn
Cross reacting
c-Jun
Ponceau S
55 kDa
35 kDa
1 2 3 4 5 6 7 8 9
10 11 12 13 14 15 16 17 18 19 20

Figure 5.3: Experimental activation profiles for the JNK and p38 pathways

C. Similar to A, but cell extracts were loaded on ERK gels (see Section 2.4.2) and probed using phospho-specific p38 antibody (top) or protein-specific p38 antibody (bottom) for loading control. This is one experiment representative of three repeats.
D. Similar to A, but cell extracts were loaded on big SDS-PAGE gels (see Section 2.4.1) and probed using phospho-specific CREB antibody (top). Ponceau staining is used as loading control (bottom). This is one experiment representative of three repeats.

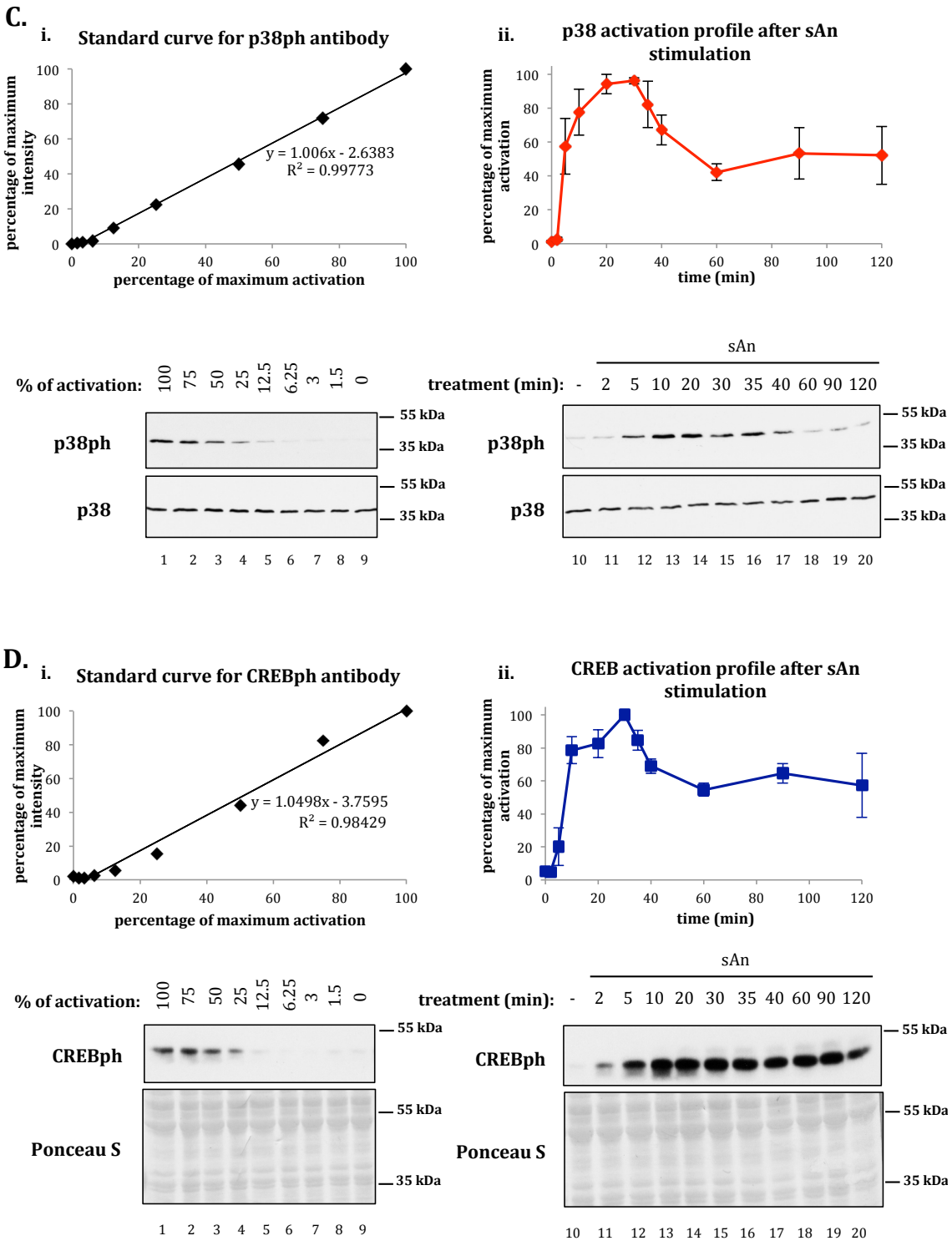
C.
i.
Standard curve for p38ph antibody
percentage of maximum intensity
y = 1.006x - 2.6383
R² = 0.99773
percentage of maximum activation
ii.
p38 activation profile after sAn stimulation
percentage of maximum activation
time (min)
% of activation: 100 75 50 25 12.5 6.25 3 1.5 0
treatment (min): - 2 5 10 20 30 35 40 60 90 120
sAn
p38ph
p38
55 kDa
35 kDa
1 2 3 4 5 6 7 8 9
10 11 12 13 14 15 16 17 18 19 20
D.
i.
Standard curve for CREBph antibody
percentage of maximum intensity
y = 1.0498x - 3.7595
R² = 0.98429
percentage of maximum activation
ii.
CREB activation profile after sAn stimulation
percentage of maximum activation
time (min)
% of activation: 100 75 50 25 12.5 6.25 3 1.5 0
treatment (min): - 2 5 10 20 30 35 40 60 90 120
sAn
CREBph
Ponceau S
55 kDa
35 kDa
1 2 3 4 5 6 7 8 9
10 11 12 13 14 15 16 17 18 19 20

maximal activation and plotted according to their corresponding percentage of activation. The standard curve was then used to obtain the activation profiles of these four proteins after sAn stimulation by associating a percentage of activation to the signal intensity obtained after sAn time-course (Figure 5.3 Aii, Bii, Cii and Dii). These data are the average of three repeats of the quantification.

A linear standard curve was obtained for both the anti-phospho-JNK and phospho-p38 antibodies (Figure 5.3 Ai and Ci), indicating that they were used in their linear range of action; the intensity of these antibodies is thus proportional to the concentration of activated protein. However, sigmoidal curves were obtained for the anti-phospho-CREB and anti-c-Jun antibodies (Figure 5.3 Bi and Di), suggesting that at low and high concentrations the signal is not proportional to the concentration of activated protein. For these values the intensity may not be representative of the actual concentrations. As only the kinase profiles are considered in our model, an approximation of c-Jun and CREB activation profiles can be derived from the standard curves obtained.

p38 and its downstream substrate CREB, and JNK and its substrate c-Jun, have similar profiles after sAn activation (Figure 5.4 A) with the caveat concerning c-Jun quantification, suggesting that the main regulation of the pathway happens upstream or at the level of MAPK. As CREB is not directly downstream of p38 but is phosphorylated by its downstream kinase MSK1/2 (Deak et al. 1998; Arthur and Cohen 2000), this suggests that the whole pathway downstream of the MAPK behaves in a similar way. While JNK and c-Jun have transient activation, p38 and CREB stay activated for longer. Indeed, JNK and c-Jun reach their maxima after 30

minutes of stimulation and are back to basal levels of phosphorylation within 90 minutes (Figure 5.3 Aii and Bii). In contrast, p38 and CREB, after being rapidly activated and reaching their maxima after 30 minutes of stimulation, drop to half of their maximal activation within 60 minutes and stay at a relatively constant level of phosphorylation until at least 120 minutes (Figure 5.3 Cii and Dii).

5.2.1.2 Modelled activation profiles

Having obtained experimental profiles, these were used to compute the input signal of the model (work done by our collaborator Milan Ceska; Figure 5.3). They are obtained by ODEs, which are derived from the bell-shape generator equations (Cardelli 2009) using two virtual substances (A and B) controlling respectively the production and degradation of the effector (K-PP; Table 5.2). A semi-automatic estimation of the parameters (Table 5.2) was used to fit the experimental data using COPASI software (Hoops et al. 2006). As the model is simplified to a single copy of a hypothetical gene permanently bound by a single TF (Figure 5.2), we also used a stochastic variant of the equations (Table 5.2) in PRISM (Kwiatkowska et al. 2011), because this tool's features allow an investigation of the effect of stochastic noise.

5.2.2 The initiation module and regulation functions

The initiation module represents regulation of the rate of initiation of transcription, as our hypothesis stipulates that the quantitative control of IE gene transcription occurs by modulating the rate of initiation. In an attempt to understand a theoretical mechanism specific to each hypothesis tested, we

Figure 5.4: Approximation of p38 and JNK activation profiles

A. i. c-Jun and JNK experimental activation profiles obtained as explained in Figure 5.3 A and B. ii. CREB and p38 activation profiles obtained as explained in Figure 5.3 C and D.
B. Representation of the ODE approximation of JNK (i) and p38 (ii) activation profiles using COPASI. The parameters used are described in Table 5.2.

A.

i. **JNK and c-Jun activation profile after sAn stimulation**

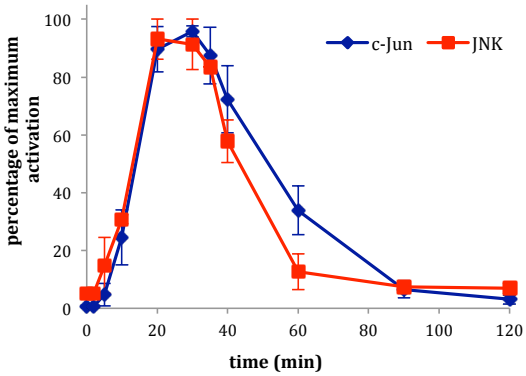

ii. **p38 and CREB activation profiles after sAn stimulation**

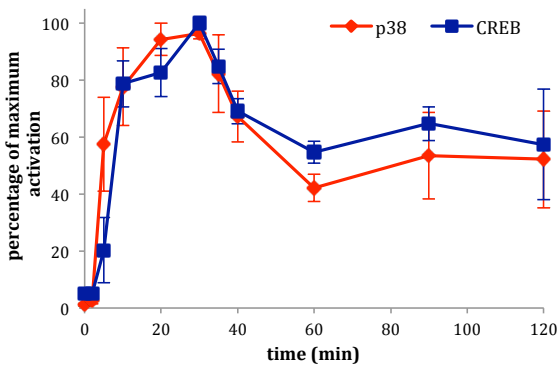

B.

i. **Approximation of the JNK activation profile**

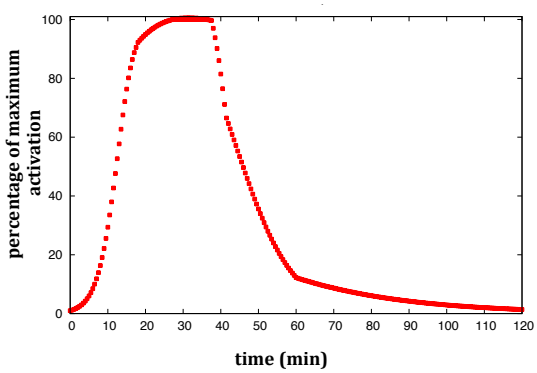

ii. **Approximation of the p38 activation profile**

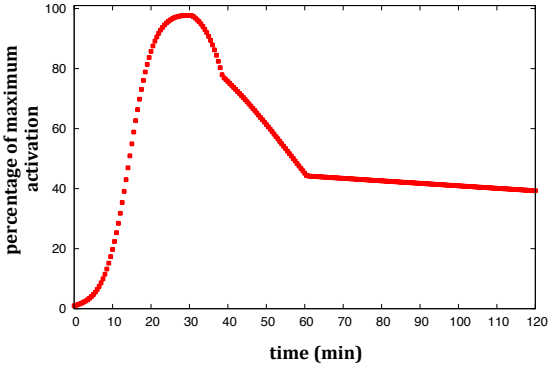

Table 5.2: Parameters used to obtain approximation of p38 and JNK activation profiles estimated with COPASI

ODEs, derived from the bell-shape generator equations (Cardelli 2009), are used to obtain JNK and p38 activation profile. A and B are virtual substances and K-PP represents the phosphorylated MAPK. The production and degradation of phosphorylated kinase occur at the rate kProd and kDegr respectively. A semi-automatic estimation of the parameters using COPASI software (Hoops et al. 2006) was carried out to fit experimental data. The initial values of A, B and K-PP as well as the rates used for p38 are regrouped in the left column and for JNK in the right column.

$$A + \text{K-PP} \xrightarrow{kProd} 2\ \text{K-PP}$$

$$B + \text{K-PP} \xrightarrow{kDegr} 2\ B$$

kinase	p38	JNK
initial conditions	A = 100 B = 1 K-PP = 1	A = 115 B = 1 K-PP = 1
parameters	$kProd = 0.0032$ $kDegr = \begin{cases} 0.00082, & 0 \le B < 4 \text{ or } 25 \le B < 58 \\ 0.0026, & 4 \le B < 25 \\ 0.000033, & 57 \le B < 100 \end{cases}$	$kProd = \begin{cases} 0.00115, & 0 \le A \le 17 \\ 0.00319, & A > 17 \end{cases}$ $kDegr = \begin{cases} 0.000359, & 0 \le B < 8 \\ 0.00032, & 8 \le B < 15 \\ 0.00348, & 15 \le B < 49 \\ 0.00114, & 49 \le B < 104 \\ 0.00033, & 104 \le B < 110 \end{cases}$

simplified the representation by only considering a single hypothetical gene permanently bound by a single TF, which is regulated by phosphorylation.

Genomic footprinting experiments showed that binding sites of c-*fos* promoter region, such as the serum response element (SRE; Herrera et al. 1989; Treisman 1992), and c-*jun* promoter region, such as the AP-1 sites (Herr et al. 1994), SP-1, CCAAT box, NF-jun sequence and RSRF binding sites (Rozek and Pfeifer 1995), are constitutively occupied, their occupancy being unchanged before and during induction. Moreover, analyses of the c-*fos* and c-*jun* promoter region using expression vector showed that, for some binding sites, their presence alone was sufficient to induce gene expression. For example, the c-*jun* RSRF as well as the c-*jun* AP-1 sites were found sufficient for TPA, EGF or serum induction (Han et al. 1992).

The hypothetical IE gene of our abstraction can either be in the state E0, where the TF is not phosphorylated and initiation of transcription is not permitted, or in the state E1, where the TF is phosphorylated and initiation of transcription is allowed (Figure 5.2). Each initiation of transcription is associated with a single TF phosphorylation/dephosphorylation event.

Phosphorylation of the TF is controlled by a regulation function F_{reg}, which provides a rate of initiation of transcription based on the kinase activation profile, while the dephosphorylation is controlled by a constant rate, 'Ptase', representing the activity of phosphatase, considered constant in our model (Figure 5.2). Although DUSPs, which dephosphorylate MAPKs, such as MKP-1 encoded by an IE

gene and induced by growth factor (Sun et al. 1993; Zheng and Guan 1993), stress and heat shock (Keyse and Emslie 1992), and produce a negative feedback, we do not consider their effect in the model and focus on the regulation of initiation of transcription by kinase activation profiles. These profiles include their own deactivation, so part of the negative feedback present in the signalling pathway is incorporated in the model. The similarity of the kinase and TF activation profiles suggests that no additional feedback is present at the TFs level; the phosphatase activity at this level could thus be considered constant. Moreover, the effect of increased phosphatase activity does not influence the initial stage of transcription, for example, MKP-1 mRNA levels are low in unstimulated cells and increase over 30 minutes (Keyse and Emslie 1992; Charles et al. 1993).

The form of the regulation function, controlling TF phosphorylation in the model, varies depending on the hypothesis considered (Figure 5.4). The 'on/off' switch hypothesis is represented by a step function. This function assumes that there is a specific concentration ('threshold') of the effector X, activated kinase, above which initiation happens at a constant rate ('max_{rate}'; Figure 5.5). The continuously variable switch hypothesis is represented by a sigmoidal curve. In this function, 'max_{rate}' corresponds to the maximum rate of initiation of transcription, 'threshold' represents the value for which the rate is half of its maximum and 'exp' determines the steepness of the continuous switch, that is to say the gradient of the tangent around the 'threshold' (Figure 5.5). From the regulation profiles, an initiation profile is obtained, representing the number of initiations of transcription events over time.

Figure 5.5: Schematic explanation of the parameters threshold and exponent

Schematic representation of the two regulation functions (F_{reg}), controlling TF phosphorylation rate (see Figure 5.2), studied.

A. binary switch: the threshold corresponds to a specific concentration of the substance X for which F_{reg} switches from 0 to its maximum value (max_{rate}).
B. continuously variable switch: the threshold corresponds to the concentration of the substance X for which F_{reg} is equal to half its maximum value ($max_{rate}/2$) and the exponent (exp) is the gradient to the curve at the threshold.

A. Binary switch

$$F_{reg}(X) = \begin{cases} max_{rate}, & X \geq threshold \\ 0, & otherwise \end{cases}$$

B. Continuously variable switch

$$F_{reg}(X) = max_{rate} . \frac{[X]^{exp}}{threshold^{exp} + [X]^{exp}}$$

Abstract representation of the binary switch regulation function

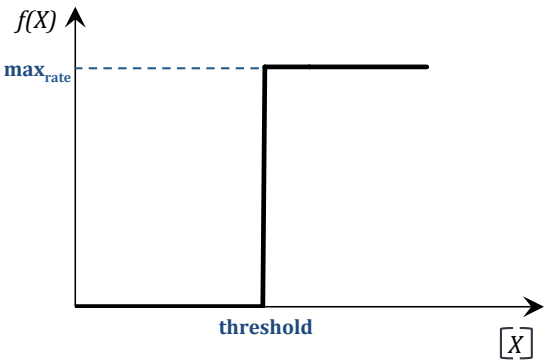

Abstract representation of the continuously variable switch regulation function

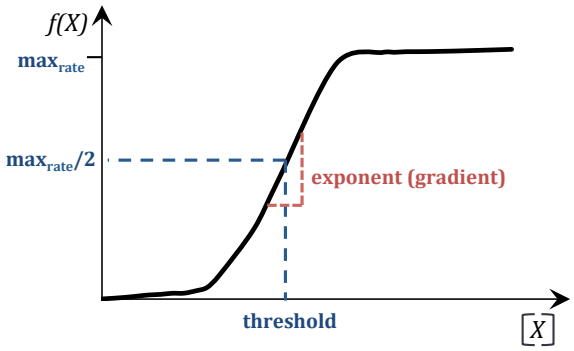

5.2.3 The mRNA module

To relate results obtained with our abstraction of the interface (calculating initiation frequency) to IE gene expression profiles obtained experimentally (see Figure 4.1 and Figure 4.2), we consider an additional module representing the production and degradation of mRNA. The output of this module returns the expected number of mature mRNA transcripts over time, using the transcription initiation rate as the input. As this is a simplified, first attempt to model the interface between signalling pathways and a hypothetical IE gene, we have considered the production and degradation of mRNA as constant processes and assumed that every initiation of transcription results in a mature mRNA.

The mRNA production rate includes elongation, termination of transcription, polyadenylation, 5' end capping, splicing and stabilisation of mRNA. As IE genes are quantitatively regulated and this regulation depends on the signal conveyed by MAPK pathways, we focused here on the impact of initiation of transcription in this regulation and decided to make the production rate constant in the first instance. Different values were tested for the production rate and only the range of values giving profiles similar to the ones obtained experimentally for c-*fos* and c-*jun* after sAn stimulation (Figure 4.1 and Figure 4.2) were further studied (see Section 5.2.3.1 and Section 5.2.4.1). The maximum number of transcripts per minute (11 transcripts/min) was taken from the modelling study of transcriptional regulation based on experiments on sea urchin (Bolouri and Davidson 2003).

The mRNA degradation rates considered in our model were taken from previous experimental results of c-*jun* and c-*fos* half-lives obtained by using DRB to inhibit

transcription after sAn stimulation (Edwards and Mahadevan 1992). We considered a first order reaction, for which the half-life is linked to the degradation rate by the equation: $t_{1/2} = \frac{\ln(2)}{k_{degr}}$. Thus, the c-*fos* and c-*jun* half-lives, 15 and 30 minutes respectively, resulted in the degradation rates of 0.0462 and 0.0231 min^{-1}. Furthermore, degradation of mRNA appears to be a constant process for c-*fos* and c-*jun*, because treatment with the transcriptional inhibitor, actinomycin D, after 30 minutes and 60 minutes of sAn activation produced similar degradation curves (see Figure 4.4).

5.2.4 Obtaining the initiation and induction curves

The equations representing the system were described both by ODEs and as modules in PRISM for stochastic considerations. The description of signalling pathways as ODEs allowed the estimation of the parameters to obtain JNK and p38 activation profiles using COPASI. These parameters were converted for stochastic models and used in the PRISM model, with which we obtained the expected number of initiation events (initiation profile) and the expected number of mRNA (induction profile).

5.3 Results

5.3.1 Comparison of the two regulation functions

5.3.1.1 Difference in the information conveyed through regulation function

The influence of the different parameters of the regulation functions (threshold and exponent, Figure 5.5) on the output were investigated by varying their values

(Figure 5.6 Ai and Figure 5.6 Bi). For both input signals, corresponding to the p38 or JNK activation profiles (Figure 5.4 B), two values, a high and a low value, of each parameter were studied. As expected, the information retained from the activation profile in the rate of initiation of transcription profiles depends on the hypothesis considered. While the continuously variable switch hypothesis representation conserves the shape of the input signal (Figure 5.6 Bi and Figure 5.4 B), the representation of the binary switch only conveys the information through the length of the plateau of the curve (Figure 5.6 Ai and Figure 5.4 B).

The binary switch presents a transient response to the JNK activation profile for both thresholds, the response being 'on' from 10 to 55 minutes at low threshold (Figure 5.6 Ai; JNK threshold = 30, cyan line) and from 15 to 40 minutes at high threshold (Figure 5.6 Ai; JNK threshold = 70, yellow line). In contrast, while the response to p38 activation profile is transient at high threshold and 'on' from 20 to 45 minutes (Figure 5.6 Ai; p38 threshold = 70, green line), its response at low threshold is stably 'on' from 10 minutes to at least 120 minutes (Figure 5.6 Ai; p38 threshold = 30, red line), as the input signal does not drop back down to below the threshold in this time.

Similar behaviour can be observed in the responses for the continuously variable switch, but the rate of initiation of transcription varies with the intensity of the signal (Figure 5.4 B and Figure 5.6 Bi). In response to the JNK activation profile, transcription is transient for all the conditions tested (Figure 5.6 Bi; cyan, yellow, black and grey lines), and stays 'on' for longer at low thresholds for both exponents (Figure 5.6 Bi; cyan and black lines). While it is 'on' from 5 to 90 minutes or from

Figure 5.6: Threshold and exponent effects on the regulation and induction profiles

A. Two values of the parameter thresholds for the binary switch hypothesis (see Figure 5.5) were studied for both JNK (threshold = 30, cyan curve and threshold = 70, yellow curve) and p38 (threshold = 30, red curve and threshold = 70, green curve) input signals. The different regulation profiles obtained are presented in (i) and the initiation profiles in (ii).
B. Two values of the parameter thresholds and exponent for the continuously variable switch hypothesis (see Figure 5.5) were studied for both JNK (threshold = 30, exponent = 2 (cyan curve), 10 (black curve); threshold = 70, exponent = 2 (yellow curve), 10 (grey curve)) and p38 (threshold = 30, exponent = 2 (red curve), 10 (blue curve); threshold = 70, exponent = 2 (green curve), 10 (purple curve)) input signals. The different regulation profiles obtained are presented in (i) and the initiation profiles in (ii).

A. Binary switch

i. **regulation profile**

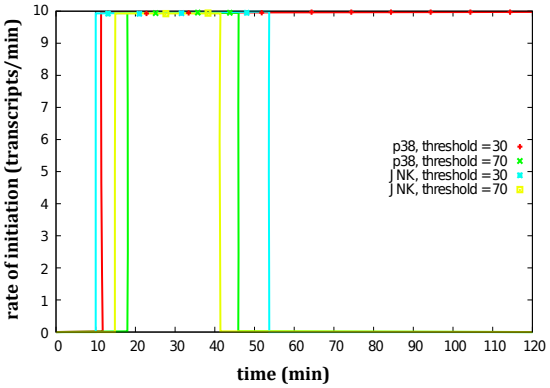

ii. **initiation profile**

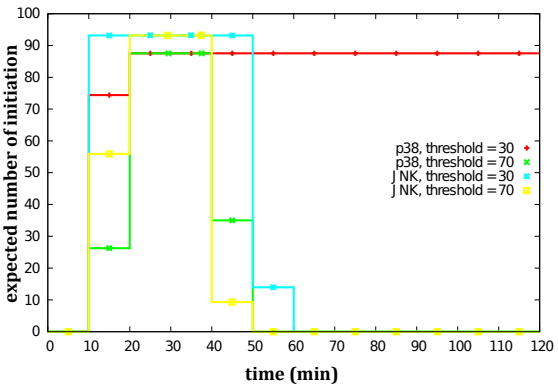

B. Continuously variable switch

i. **regulation profile**

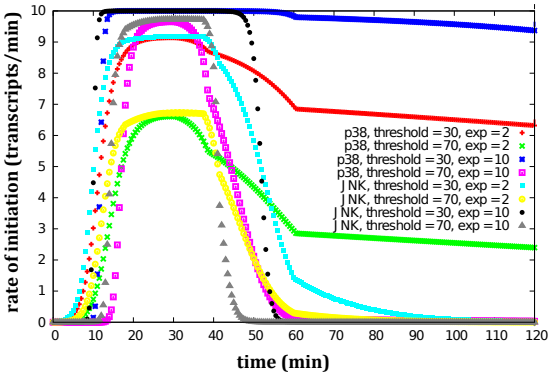

ii. **initiation profile**

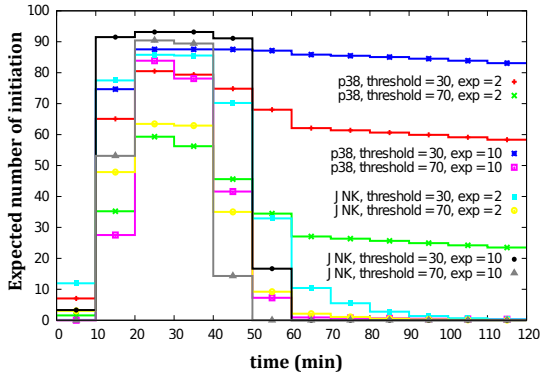

10 to 55 minutes for low and high exponent, respectively, at low threshold (Figure 5.6 Bi; JNK threshold = 30, exponent = 2 (cyan line) and 10 (black line)), it is 'on' from 5 to 60 minutes or from 10 to 45 minutes at high threshold (Figure 5.6 Bi; JNK threshold = 70, exponent = 2 (yellow line) and 10 (grey line)). Besides, the rate of initiation of transcription reaches a higher maximum at high exponent (Figure 5.6 Bi; JNK threshold = 30 (black line) and 70, exponent = 10 (grey line)). In response to the p38 activation profile (Figure 5.6 Bi; red, green, blue and pink lines), only a high threshold and a high exponent condition result in a transient response (Figure 5.6 Bi; p38 threshold = 70, exponent = 10 (pink line)). Once again, the rate of initiation of transcription reaches higher values for a high exponent (Figure 5.6; p38 threshold = 30 (blue line) and 70 (pink line), exponent = 10). Thus, for both inputs, it seems that a low threshold induces longer responses, which can be explained by the bell-shape of the JNK activation profile compared to the fact that around 40 % of p38 stays activated until at least 120 minutes (Figure 5.4 Bii). Further, for both inputs, a high exponent generates higher rates of initiation of transcription.

5.3.1.2 The initiation profiles are similar to the rate of initiation of transcription

The initiation profiles closely resemble the regulation profiles (compare Figure 5.6 Aii with Figure 5.6 Ai and Figure 5.6 Bii with Figure 5.6 Bi), which represent the regulation functions. Indeed, only the length of the plateau varies in the initiation profiles for the binary switch hypothesis (Figure 5.6 A), but due to the fact that the initiation profile reflects the expected number of initiation of transcription events over 10-minute time frames, the bipartite nature of the curve is lost in the representation for the binary switch (Figure 5.6 Aii). The initiation profiles of the

continuously variable switch hypothesis present more complex dynamics and similarity to the activation profile (Figure 5.6 Bii).

The influence of the parameters, that is, threshold for the binary switch, and threshold and exponent for the continuously variable switch, was investigated. They have the same effect on the rate of initiation of transcription as they have on the number of initiation events, which indicates that these two parameters are key elements for the control of gene expression in our model.

5.3.2 The two types of switch induce different mRNA profiles

5.3.2.1 The capacity of the binary switch to convey dynamically varying quantitative information is limited

We showed that the regulation function for the binary switch hypothesis carries information from the input signal through to initiation of transcription by varying the length of the time spent in the stable 'on' conformation. We wondered if conveying the information received from the signalling pathways this way could produce stimulus-specific responses, as can be observed experimentally (see Section 4.2.1.1). Using the p38 and JNK activation profiles as input signals, we analysed the effects of the various initiation profiles, obtained with different values of the threshold, on the mRNA profiles for the binary switch hypothesis (Figure 5.7). In comparison to the initiation profile, the mRNA profiles do not present step-like shape curves but bell-shape curves, suggesting that the production and degradation rates can induce some variation in the signal conveyed.

By fixing the value of all the other parameters and varying the threshold as indicated (Figure 5.7), we have recorded the effect of this parameter on the mRNA profiles. In response to the JNK activation profile, a difference between the mRNA profiles can only be observed at low thresholds (Figure 5.7 Ai; thresholds = 20, 10 or 5; blue, green and red lines). Indeed, for these thresholds the return of mRNA levels to background levels is delayed compared to the other values of thresholds studied, for which the mRNA profiles are almost identical (Figure 5.7 Ai and Aii; thresholds = 30 to 80). This indicates that the binary switch does not convey small variations of the JNK activation. Indeed, by analysing the different thresholds against the JNK activation profile (Figure 5.7 Aiii), a small difference, such as that observed between the threshold values 80 and 60, does not generate differences at the mRNA profile stage, but a larger difference, such as that observed between the threshold 80 and 20, results in a delay in the decrease of mRNA levels (Figure 5.7 Ai and Aii).

In response to the p38 activation profile, as for the initiation profiles, two types of mRNA profiles can be observed depending on the value of the threshold. At high thresholds, mRNA levels are only transiently detected (Figure 5.7 Bi and Bii; threshold = 45 to 80), while at low thresholds mRNA levels, after activation, remain high (Figure 5.7 Bi; threshold = 20 to 40). The value of the threshold at which the change occurs is between 40 and 45. This can be related to the value at which the phosphorylated p38 stabilises at later time points (Figure 5.7 Biii). At high thresholds, although mRNA levels reach their maxima at different times, the overall time frame of the signal is unchanged (Figure 5.7 Bii).

Figure 5.7: Threshold effect on mRNA profile for the binary switch

A. The JNK activation profile (see Figure 5.3 A) is considered as input signal for the model. mRNA profiles obtained at low thresholds are represented in (i) and high thresholds in (ii). The differences between the thresholds on the JNK activation profile are represented in (iii).

A. Input signal = JNK activation profile

i. **mRNA profile (low thresholds)**

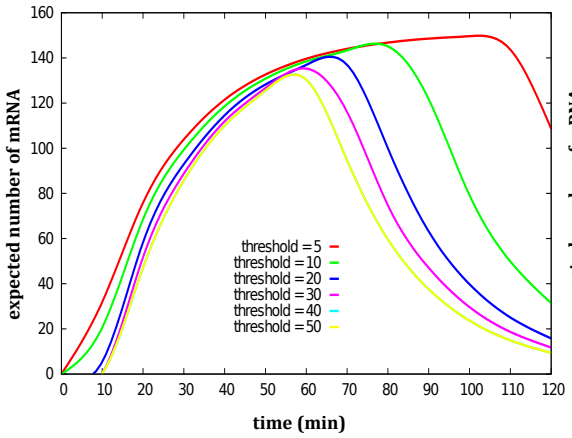

ii. **mRNA profile (high thresholds)**

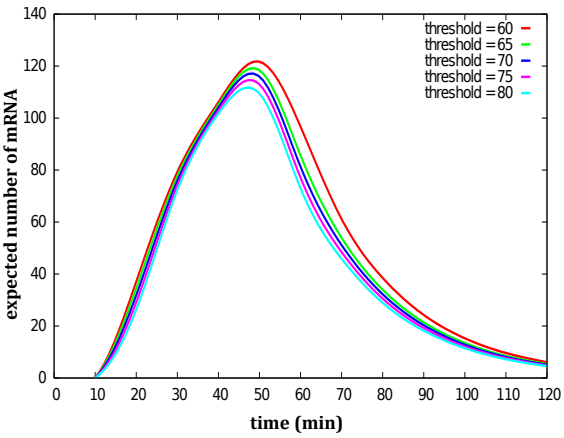

iii. **Approximation of the JNK activation profile**

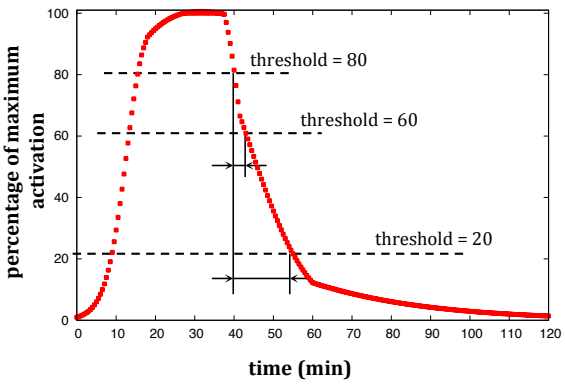

Figure 5.7: Threshold effect on mRNA profile for the binary switch

B. The p38 activation profile (see Figure 5.3 C) is considered as input signal for the model. mRNA profiles obtained at low thresholds are presented in (i) and high thresholds in (ii). The differences between the thresholds on the p38 activation profile are represented in (iii).

B. Input signal = p38 activation profile

i. **mRNA profile (low thresholds)**

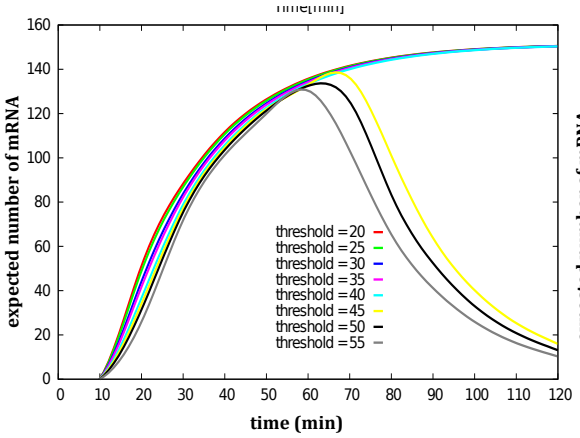

ii. **mRNA profile (high thresholds)**

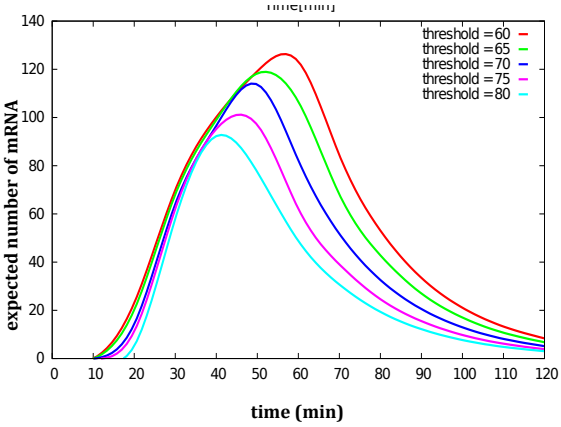

iii. **Approximation of the p38 activation profile**

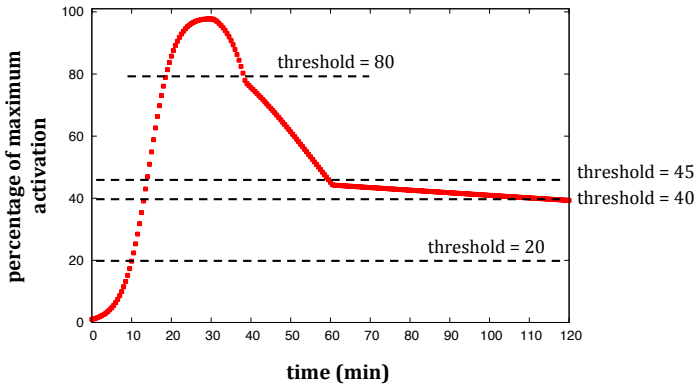

At high thresholds (values from 45 to 80), the responses to p38 and JNK activation profiles are very similar (Figure 5.7 Aii and Bii), with the binary switch failing to distinguish between these two input signals. Altogether these results suggest that the binary switch, by only varying the length of the 'on' state carries limited dynamic information from the signalling pathway to gene expression.

5.3.2.2 The continuously variable switch hypothesis induces quantitative mRNA profiles

In parallel to the study carried out for the binary switch, we analysed the characteristics of a continuously variable switch in our abstraction. Surprisingly, in response to the JNK activation profile, variation of the threshold value affected the mRNA profiles in a similar way for the binary switch (Figure 5.7 A) and the continuously variable switch (Figure 5.8 A) hypotheses. The only difference is observed at high thresholds, where the maximum value of the mRNA levels decreases slightly more with increasing the threshold, for the continuously variable switch hypothesis (Figure 5.8 Aii). This suggests that, for a bell-shape of input signal, such as the JNK activation profile, both hypotheses convey similar dynamic information to produce these profiles.

In contrast, unlike the JNK activation profile, the p38 activation profile induces different mRNA profiles for each hypothesis (Figure 5.8 B). Considering the continuously variable switch, at high and medium thresholds (from 45 to 80), the mRNA profiles follow the input signal, as the rate of mRNA decrease changes at about 70 minutes (Figure 5.8 B), with a slower decline matching the stabilisation of p38 phosphorylation levels after 60 minutes (Figure 5.7 Biii). At lower

Figure 5.8: Threshold effect on mRNA profile for the continuously variable switch

A. The JNK activation profile (see Figure 5.3 A) is considered as input signal for the model. mRNA profiles obtained at low thresholds are presented in (i) and high thresholds in (ii).
B. The p38 activation profile (see Figure 5.3 C) is considered as input signal for the model. mRNA profiles obtained at low thresholds are presented in (i) and high thresholds in (ii).

A. Input signal = JNK activation profile

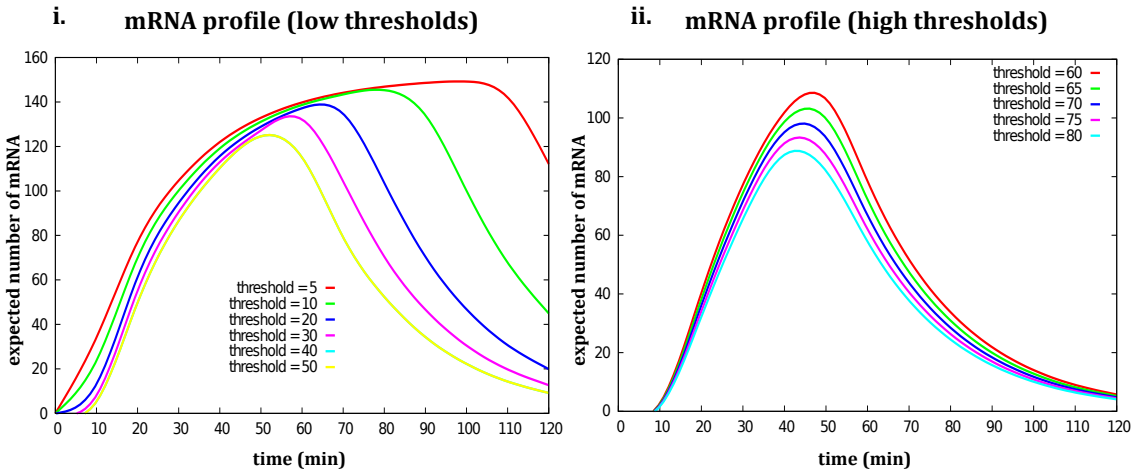

B. Input signal = p38 activation profile

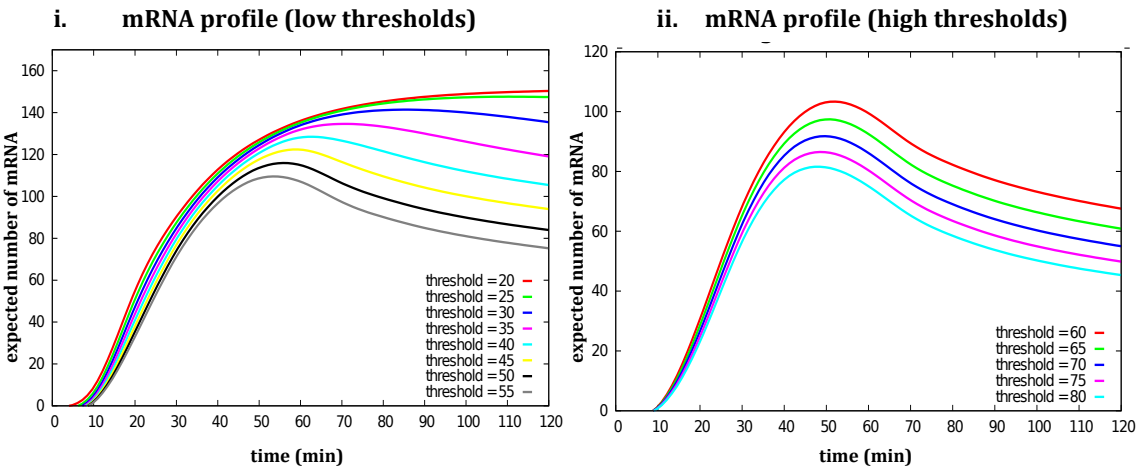

thresholds than 45, after which p38 phosphorylation stabilises (Figure 5.7 Biii), this change in the rate of decrease is not observed within the time frame studied (Figure 5.8 Bi; threshold = 40 (cyan line), 35 (pink line), 30 (blue line), 25 (green line) and 20 (red line)). This indicates that, under specific parameters, a variation in intensity within the input signal, such as the variations observed for the p38 activation profile after sAn stimulation (Figure 5.7 Biii), can be conveyed by the regulation function of the continuously variable switch and influence gene expression.

For the continuously variable switch, the JNK and p38 input signals result in different mRNA profiles (Figure 5.8), suggesting that this hypothesis can produce transcription that matches the input signal. The information seems to be transmitted all the way from the input of the model to the output by this hypothesis.

5.3.3 The production and degradation rates control different phases of the mRNA profile

In our simplified model, the continuously variable switch hypothesis, in contrast to the binary switch hypothesis, seems to induce signal-dependent responses at the mRNA profile stage. However, incorporation of mRNA production and degradation rates were shown to add some variation in the profiles obtained with the binary switch (Figure 5.7), suggesting that they add some regulatory controls. We further investigated the influence of these rates on the mRNA profiles, in order to evaluate whether variation of these rates could recover some information lost in the binary switch hypothesis.

Different values of production and degradation rates were studied. While more production rates were investigated, only three are represented here to illustrate the trend observed (Figure 5.9 and Figure 5.10). The two degradation rates obtained from experimental data for c-*fos* and c-*jun* (Edwards and Mahadevan 1992; see Section 5.2.1.3) were used.

In our abstraction of IE gene regulation with a binary switch, varying the production rate had the same effect on the responses to both p38 and JNK activation profiles, although the shapes of the curves were different (Figure 5.9). Increasing the production rate resulted in an increase of the maximum of mRNA levels, and this maximum was reached faster (Figure 5.9, compare solid green, blue and pink lines together, and dotted green, blue and pink lines together). This trend can be observed in Table 5.3, which regroups the maximum value and the time at which it is reached for the different conditions. Considering the JNK input signal at threshold 30 and degradation rate 0.0231 transcript/minute, increasing the production rate from 5 to 11 transcript/minute increases the maximum value from 175 transcripts to 240 transcripts and reduces the time of the maximum from 80 minutes to 50 minutes (Figure 5.9 and Table 5.3, line 1 and 3). A similar effect can be observed for different thresholds and degradation rates and for the p38 input signal (Figure 5.9 and Table 5.3). This indicates that, as expected, the production rate controls the initial phase of the mRNA profiles.

For the continuously variable switch hypothesis, variation of the production rate had limited effects on the responses to p38 or JNK activation profiles (Figure 5.10).

Figure 5.9: Production and degradation rate effects on mRNA profiles for the binary switch

mRNA profiles were obtained for two different degradation rates (0.0462 transcripts/minutes dashed lines; 0.0231 transcripts/minutes, solid lines) and for three different production rates (5 transcripts/minutes, green lines; 7 transcripts/minutes, blue lines; 11 transcripts/minutes, purple lines). The red dashed lines represent the initiation profiles.

A. mRNA profiles obtained form the JNK activation profile (see Figure 5.3 A)
B. mRNA profiles obtained from the p38 activation profile (see Figure 5.3 C)

A. Input signal = JNK activation profile

i. mRNA profile (low threshold)

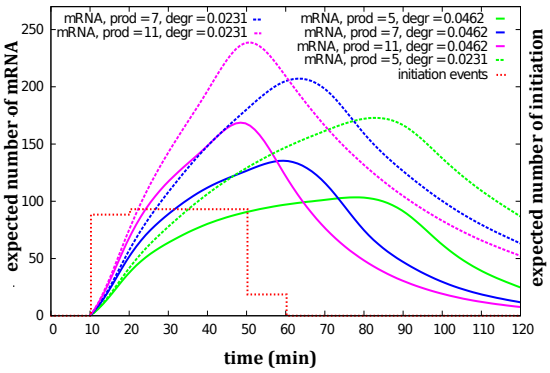

ii. mRNA profile (high threshold)

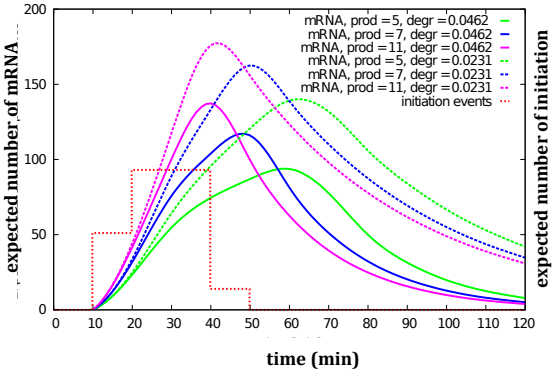

B. Input signal = p38 activation profile

i. mRNA profile (low threshold)

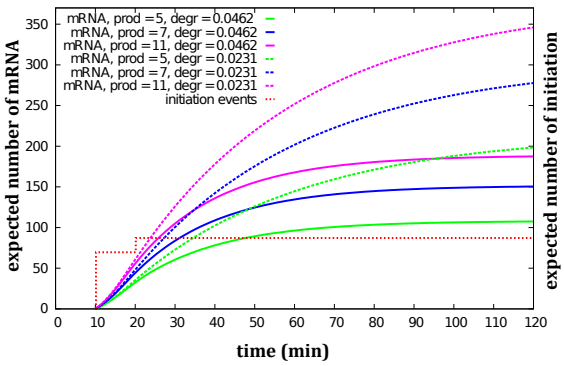

ii. mRNA profile (high threshold)

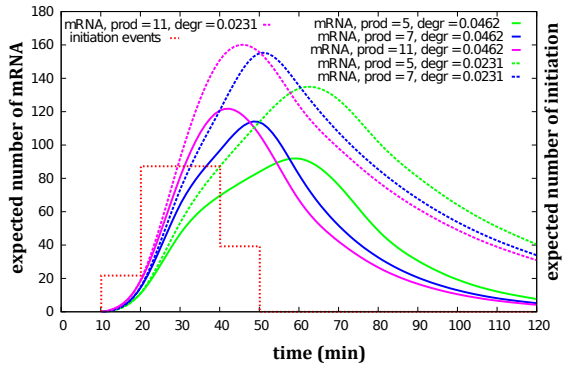

Table 5.3: Maximal and the time of the maximum

The table regroups the values and the times at which the maximum of mRNA level is reached for the different mRNA profiles shown in Figure 5.9.
For p38 at low threshold (30), the maximum not reached is represented by '-'.

input signal	threshold	degradation rate (transcript/min)	production rate (transcript/min)	maximum value (transcript)	maximum time (min)
JNK	30	0.0231	5	175	80
			7	210	60
			11	240	50
		0.0462	5	100	80
			7	140	60
			11	160	50
	70	0.0231	5	140	60
			7	160	50
			11	180	40
		0.0462	5	100	60
			7	120	50
			11	140	40
p38	30	0.0231	5	-	-
			7	-	-
			11	-	-
		0.0462	5	-	-
			7	-	-
			11	-	-
	70	0.0231	5	135	60
			7	155	50
			11	160	45
		0.0462	5	95	60
			7	115	50
			11	120	45

As before, the higher the production rate, the faster and higher the maximum for the response to the JNK activation profile, but the effect is more pronounced for the binary switch. Besides, at high threshold, the maximum did not change for the production rates 7 and 11 transcript/minute (Figure 5.10 Aii, compare solid and dotted blue lines with solid and dotted and pink lines respectively; Table 5.4). In a similar way, the magnitude of the maximum in response to the p38 activation profile did not change for both low and high thresholds for all three production rates (Figure 5.10, compare solid and dotted lines separately), but the time at which it is reached did, which is reduced from 60 minutes for a production rate of 5 transcript/minute to 50 minutes for a production rate of 7 or 11 transcript/minute (Table 5.4). Thus, as with the binary switch hypothesis, the major effect of a variation of the production rate is observed over the first part of the mRNA profiles, suggesting that the production rate controls mRNA profile during the increasing phase of the profile.

The effects observed for a variation of the production rate can be seen for both values of the degradation rate of mRNA, with only the value of the maximum affected by the degradation (Figure 5.9 and Figure 5.10, compare solid and dashed lines). Besides, the mRNA profiles can be clustered with respect to the value of the degradation rate, as a variation of the degradation rate affects the curves corresponding to the three different production rates in a similar way (Figure 5.9 and Figure 5.10). This suggests that the degradation rate affects the magnitude of the whole curve and, as it is considered as constant in our abstraction, this effect is similar throughout the curve. Thus, the production rate, which is linked to the shape of the initiation profile, influences the shape of the curve, and more precisely

Figure 5.10: Production and degradation rate effects on mRNA profiles for the continuously variable switch

mRNA profiles were obtained for two different degradation rates (0.0462 transcripts/minutes dashed lines; 0.0231 transcripts/minutes, solid lines) and for three different production rates (5 transcripts/minutes, green lines; 7 transcripts/minutes, blue lines; 11 transcripts/minutes, purple lines). The red dashed lines represent the initiation profiles.

A. mRNA profiles obtained form the JNK activation profile (see Figure 5.3 A)
B. mRNA profiles obtained from the p38 activation profile (see Figure 5.3 C)

A. Input signal = JNK activation profile

i. mRNA profile (low threshold)

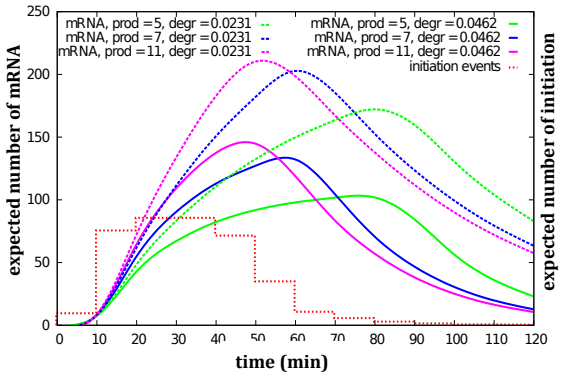

ii. mRNA profile (high threshold)

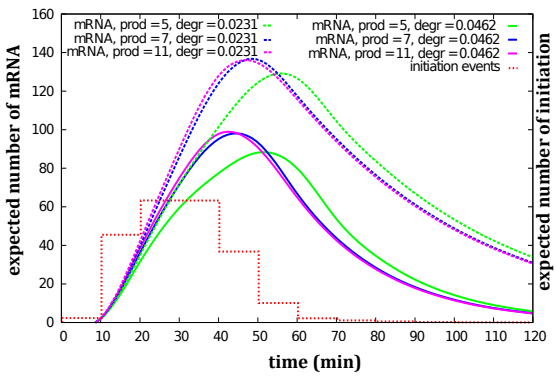

B. Input signal = p38 activation profile

i. mRNA profile (low threshold)

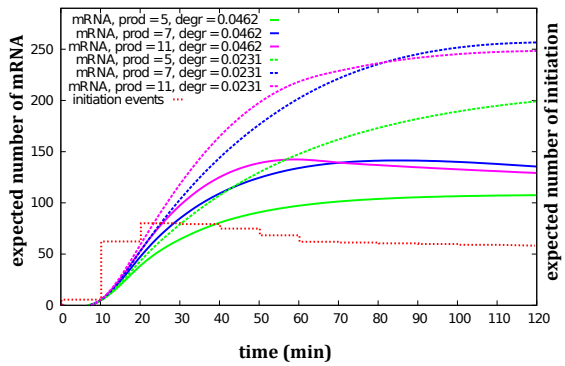

ii. mRNA profile (high threshold)

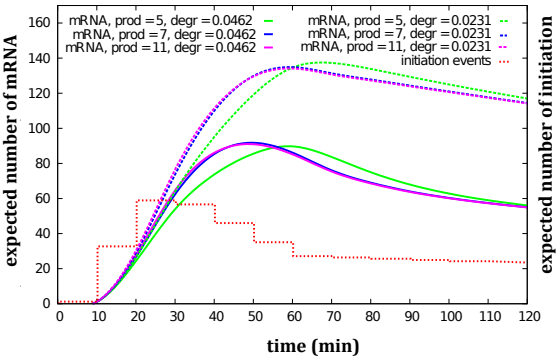

Table 5.4: Maximal and the time of the maximum

The table regroups the values and the times at which the maximum of mRNA level is reached for the different mRNA profiles shown in Figure 5.10.
For p38 at low threshold (30), the maximum not reached is represented by '-'.

input signal	threshold	degradation rate (transcript/min)	production rate (transcript/min)	maximum value (transcript)	maximum time (min)
JNK	30	0.0231	5	175	80
			7	200	60
			11	210	50
		0.0462	5	100	80
			7	140	60
			11	145	50
	70	0.0231	5	130	55
			7	140	45
			11	140	45
		0.0462	5	90	55
			7	100	45
			11	100	45
p38	30	0.0231	5	-	-
			7	-	-
			11	-	-
		0.0462	5	-	-
			7	-	-
			11	-	-
	70	0.0231	5	140	60
			7	140	50
			11	140	50
		0.0462	5	90	60
			7	90	50
			11	90	50

the increasing phase of the mRNA profiles, while the degradation rate, which is constant and independent of any profile, affects the magnitude of the whole profile.

5.4 Discussion

5.4.1 Characteristics of continuously variable switch and binary switch

5.4.1.1 The continuously variable switch better conveys quantitative signal information

In the profiles obtained with our interface abstraction, the main difference observed between the two switch hypotheses is the capacity to distinguish the two input signals (p38 and JNK) in the mRNA profile with the continuously variable switch but not the binary switch (Figure 5.7 and Figure 5.8). This suggests that the continuously variable switch hypothesis is a better fit to induce quantitative responses.

For the binary switch, as seen more clearly for the p38 input signal, the intensity information of the signal is lost at both the initiation profile (Figure 5.6 A, red and green lines) and the mRNA profile stages (Figure 5.7 B). Indeed, even though the percentage of activated p38 drops and then stabilises after 60 minutes (Figure 5.3 Cii), these variations of the input signal are not conserved at low or high thresholds, with either continuous transcription or complete shutdown, respectively (Figure 5.7 B). Thus, the loss of the magnitude of the signal for these conditions results in non-quantitative gene expression. The reason that the production and degradation rates do not overcome this lack of information could be due to the fact that they are considered as constant in our abstraction, and are

not directly dependent on the kinase activation profile. Although experimental results evaluating the stability of the c-*fos* and c-*jun* transcripts (see Chapter 4) suggest that the degradation of mRNA is a constant process for these genes, considering the production rate, which takes into account elongation rates, termination of transcription and transcript stabilisation as constant may be an oversimplification. The loss of the quantitative information at the level of transcription initiation could be recovered by a non-constant production rate, but it is unlikely to reflect the signal perceived.

The continuously variable switch considers that the rate of transcription initiation varies with the strength of the signal. As the mRNA profiles have a similar shape to the input signal (Figure 5.4 and Figure 5.8), it seems that by being able to vary the rate of initiation of transcription, and so the frequency of transcription initiation, the continuously variable switch allows for quantitative regulation. The information from the input signal is retained in the output of the model using the continuously variable switch.

Thus, the binary switch can control the time period for which initiation of transcription is allowed, but, unlike the continuously variable switch, does not control the rate of initiation of transcription, and thus does not convey the intensity of the signal. The regulation functions used are a good representation of our hypotheses for the quantitative regulation of IE gene expression (detailed in Section 1.5).

5.4.1.2 The continuously variable switch behaves like a binary switch under specific conditions

At high threshold and high exponent, the regulation function of the continuously variable switch loses the shape of the p38 activation profile (Figure 5.6 Bi, pink line). However, this is not the case at high threshold and low exponent (Figure 5.6, green line) or at low threshold and high exponent (Figure 5.6, blue line). This indicates that if a high concentration of activated kinase is required for the rate of initiation of transcription to be significant and if a small perturbation around this specific concentration provokes a large variation of the rate of transcription initiation, then the continuously variable switch conveys all-or-none response. As these conditions are similar to those of a step-shaped curve, this explains why the continuously variable switch behaves in a similar way to the binary switch under these conditions. Moreover, this behaviour is not observed at low threshold or at low exponent due to the shape of p38 activation profile (Figure 5.7 Biii). Indeed, p38 stays phosphorylated at a relatively constant level after 60 minutes. A threshold lower than this constant level would prevent initiation of transcription from shutting down, since a low exponent integrates perturbations in a less drastic way than high exponent. The fact that the amount of phosphorylated p38 stays relatively constant prevents transcriptional shut-off in our model.

5.4.1.3 Frequency of transcription initiation is controlled by spatial constraint or dynamic turnover of phosphorylation

The binary switch hypothesis considers that there exists an intrinsic rate of initiation of transcription within the system, and the signalling pathways, by TF phosphorylation, control the length of the gene induction time period. The frequency of initiation of transcription is constant. In this hypothesis, one

mechanism to achieve this may be that the rate of initiation of transcription is linked to the occupancy of the start site by the preinitiation complex. Spatial constraints could enforce this rate, as a certain distance between two transcriptional complexes might be required. The spatial constraint could thus enforce a rate of transcription initiation while TF is phosphorylated.

However, if TF dephosphorylation occurs as soon as the preinitiation complex departs, then the frequency of transcription initiation could be controlled by TF phosphorylation and thus be dynamic and directly linked to the signalling pathways. This could be considered for the continuously variable switch hypothesis, which necessitates a dynamic turnover of phosphorylation at the TF level. If we consider that one phosphorylation/dephosphorylation event leads to a single initiation of transcription, TF dephosphorylation would be required for re-initiation. TF dephosphorylation could be carried out by one of the proteins of the preinitiation complex, or this complex or TFs could recruit a protein phosphatase to achieve TF dephosphorylation and thus allow the rate of transcription initiation to be dictated by the TF turnover of phosphorylation.

5.4.2 Biological interpretation of the parameters

The analyses of the different profiles obtained with our abstraction of the interface between signalling pathways and a hypothetical IE gene have allowed the identification of important parameters for the model, including the threshold and exponent of the regulation functions. Although this model simplifies all the biological processes involved in this regulation, it can provide an initial indication of the key features involved in each of the switch hypothesis. These parameters

can then be transposed to find biological equivalents, and thus offer new insight on quantitative regulation of gene expression.

5.4.2.1 The threshold as a specific activated kinase concentration

The threshold parameter (Figure 5.5) was shown to influence the shape of the initiation and mRNA profiles for both switch hypotheses (Figure 5.6, Figure 5.7 and Figure 5.8). For the regulation functions, the threshold represents the concentration of activated kinase at which the rate of initiation of transcription starts to be detectable. Could the MAPK act in a similar way in the cell? One way to think of the threshold could be as a specific concentration of phosphorylated MAPK required to overcome phosphatase activity and diffusional limitations for productive phosphorylation of TF and thus induce gene expression. This view considers that the stable 'on' phosphorylated state of TF is needed for initiation of transcription. For a more dynamic regulation of gene expression, the threshold could be the minimal concentration of activated MAPK needed to compete with phosphatase activity to increase the turnover of phosphorylation to sufficiently increase the frequency of initiation of transcription producing detectable expression levels.

However, considering the threshold as a specific concentration of MAPK restricts it to a single biological component. Due to the fact that external stimuli can activate different pathways in parallel, the threshold could be the result of a combination of events and/or effectors in the system, such as the phosphorylation of multiple TFs allowing the transcriptional machinery to bind the promoter region. For example, c-*fos* and c-*jun* promoter regions are controlled by multiple TFs (see Section 1.2.3),

which are downstream of multiple MAPK pathways, such as Elk-1 and ATF-2 downstream of both p38 and JNK (Gille et al. 1995; Gupta et al. 1995; Raingeaud et al. 1995; Whitmarsh et al. 1995; Raingeaud et al. 1996), although our investigation of the signalling pathways using kinase inhibitors suggests that ATF-2 is not downstream of p38 in mouse C3H 10T½ cells, as pre-treatment with SB 203580, a p38 inhibitor, does not affect sAn stimulation of ATF-2 (see Figure 3.12). It could also be viewed as an intrinsic parameter of the MAPK pathways resulting from their three-tiered organisation. However, the fact that p38 and CREB, and JNK and c-Jun activation profiles, are respectively similar suggests that the effect of the threshold could be incorporated in one step. Further development of the signalling module of our abstraction would be needed to investigate this parameter.

5.4.2.2 The exponent as kinase activity

The other parameter influencing the regulation of initiation of transcription by the continuously variable switch is the exponent (Figure 5.6). As previously mentioned, this parameter represents the magnitude of the effect registered within the system caused by a small perturbation around the threshold, with a large effect corresponding to a high exponent value (Figure 5.5). Thus, the threshold and exponent are linked.

Considering the threshold as a specific concentration of activated MAPK means that the exponent, in our model, reflects the magnitude of the effect of a small perturbation of the activated MAPK concentration on the rate of initiation of transcription. As our model relates the rate of initiation of transcription to the phosphorylation of TF, the exponent could reflect the enzymatic activity of the

protein kinase and more precisely the kinetic constant of TF phosphorylation. If this value is high, then a small perturbation of the concentration of activated kinase would greatly affect the equilibrium between phosphorylated and dephosphorylated TF, while a low kinase activity would only slightly impact the equilibrium. The fact that the exponent is an influential parameter in our model (Figure 5.6) suggests, if this interpretation is correct, that equilibrium between phosphorylated and dephosphorylated TF, and thus the turnover of phosphorylation, may be essential in gene expression regulation for the continuously variable switch hypothesis.

However, the exponent could also represent the efficiency of the phosphorylated TF to induce transcription. For this interpretation, the efficiency could refer to the length of time the TF needs to be phosphorylated in order to induce transcription. If the TF is really efficient, then a small perturbation in TF phosphorylation would result in a significant increase in transcription. On the other hand, if the TF is inefficient, a small perturbation would only have a small impact on transcription.

5.4.2.3 The role of mRNA production and degradation rates

While the production and degradation rates each seem to exercise control on one phase or on the magnitude of the mRNA profiles, the overall shape of the response seems to be controlled by the parameter threshold (Figure 5.5). The threshold value determines how transient the response to JNK and p38 profiles is. Surprisingly, for the continuously variable switch, the mRNA profiles in response to both JNK and p38 activation profiles seem robust towards variation in the production rate at high thresholds. Indeed, the curves obtained for the three values

tested are similar (Figure 5.9 Aii and Bii; see Section 5.2.3.2). This suggests that, at high threshold, the continuously variable switch responses can only be controlled by the value of the parameter threshold, so the mRNA profiles are controlled at the initiation of transcription by the input signal.

5.4.2.4 Additional regulatory steps

Although JNK and p38 input curves produce distinct mRNA profiles for the continuously variable switch hypothesis (Figure 5.10), these profiles are not the same as the characteristic profiles measured for c-*fos* and c-*jun* by Northern blotting or qRT-PCR (see Section 4.2.1.1). These differences can be explained by the additional complexity present in the cells in comparison to our abstraction.

As previously mentioned, some IE genes encode for protein phosphatases; this is the case for MKP-1, which exercises a negative feedback on MAPK pathways (Keyse and Emslie 1992; Charles et al. 1993; Sun et al. 1993; Zheng and Guan 1993). Other IE genes encode for TFs, such as c-Jun and c-Fos, which can thus exercise positive feedback, such as c-Jun binding to the AP-1 site of c-*jun* (Angel et al. 1988), or negative feedback, as it is thought for c-Fos (Sassone-Corsi et al. 1988), on their own induction or on the induction of other genes (reviewed in Herschman 1991; McMahon and Monroe 1992). These feedbacks are not considered in our abstraction. Another simplification in the model is to consider the elongation rate as constant.

IE gene promoter regions, such as c-*fos* and c-*jun* promoter regions (see Section 1.2.2), exhibit multiple regulatory elements. Thus, multiple TFs could co-regulate

the same gene. For example ATF-2, c-Jun and MEF2 are implicated in c-*jun* regulation (Derijard et al. 1994; Kyriakis et al. 1994; Gupta et al. 1995; Han and Prywes 1995; Livingstone et al. 1995; Raingeaud et al. 1995; van Dam et al. 1995; Han et al. 1997), while SRF, Elk-1 and CREB are implicated in c-*fos* regulation (Rivera et al. 1993; Gille et al. 1995; Whitmarsh et al. 1995; Raingeaud et al. 1996; Deak et al. 1998; Arthur and Cohen 2000). Besides, these TFs are downstream of multiple and different MAPK pathways, which are activated in parallel by various stimuli, and produce means for convergence of signals (Treisman 1996; Kyriakis and Avruch 2001). Thus, the quantitative regulation of IE gene induction could result from a combination of signals and TFs. By considering a single TF and the activation of a single MAPK pathway, our model abstracts from the complexity linked to the convergence of the signals at the promoter region of IE genes.

Moreover, our abstraction does not reflect the effect observed after treatment with phosphatase inhibitor, such as OA. Indeed, OA have been shown to induce IE gene expression, revealing that a basal level of turnover of phosphorylation occurs within the signalling pathways (see Chapter 3). In our abstraction initiation is linked to deactivation, and thus by inhibiting the effect of the phosphatase initiation is also inhibited. Our model needs to be modified in order to adequately represent the experimental data. One way to achieve this would be to consider a 'self-loop', which would allow multiple transcription events to happen once TF is phosphorylated. However, by allowing multiple transcription events to happen the direct link between turnover of phosphorylation and the magnitude of the signal is lost, which suggests that the continuously variable switch hypothesis would need to be rethought. OA inhibits PP1 and PP2A, and so other protein phosphatases

could thus be involved in regulating transcription (further developed in Chapter 6).

Chapter 6: Discussion

6.1 Dynamic regulation of MAPK pathways?

6.1.1 Bistability of the MAPK pathways

Work in this thesis suggests that the MAPK pathways are dynamically regulated and behave as continuously variable switches, as is revealed by the presence of a turnover of phosphorylation of the TFs in quiescent cells for the p38 and JNK pathways (discussed in Chapter 3). However, the ERK pathway is not activated by treatment with OA (Figure 3.4), which could indicate an absence of turnover of phosphorylation in this pathway. This pathway seems to have a bistable response to stimulus. Previous studies on MAPK pathways in the context of *Xenopus laevis* oocyte maturation (Ferrell 1999; Bagowski and Ferrell 2001) have identified these pathways as bistable switches being able to transform a graded stimulus into an all-or-none response.

The oocytes are arrested in G2 state with inactive cyclin-dependent kinase Cdc2 and an intact germinal vesicle. Exposure to progesterone induces oocytes to undergo maturation (Schorderet-Slatkine 1972), and ERK signalling is an essential pathway in this process (Muslin et al. 1993; Kosako et al. 1994; Huang and Ferrell 1996; reviewed in Ferrell 1999). In this context, the MAPK pathways were shown both experimentally and by modelling to present all-or-none and ultransensitive responses (Huang and Ferrell 1996; Bagowski and Ferrell 2001). Thus, these studies reveal that the MAPK pathway can behave as a bistable switch and transform a graded signal, the concentration of progesterone, into an all-or-none

cell fate decision, maturation of the oocyte. Various mechanisms, such as ultrasensitivity and feedback loops, seem to allow the MAPK pathway to behave as a bistable system (see Section 1.5).

The ERK pathway (Mos/MEK1/ERK) indirectly activates Cdc2 by inhibiting Myt1 (reviewed in Ferrell 1999). Cdc2 is itself inhibited by phosphorylation of Thr14 and Tyr15 (reviewed in Morgan 1995), carried out by Myt1 in immature oocytes (Murakami and Vande Woude 1998). A mathematical model of the MAPK pathways, in the context of *Xenopus laevis* oocyte maturation, showed that the stimulus-response curves, which represent the activation of the kinase against the concentration of stimulus, increase in ultrasensitivity when going further down the kinase cascade, each step of the cascade increasing the ultrasensitivity (Huang and Ferrell 1996). This indicates that the three-tired organisation of the MAPK pathways could contribute to the conversion of a graded response to an all-or-none response. These predictions were verified experimentally and while Mos, a MAPKKK, observed a standard Michaelis-Menten kinetics stimulus-response curve to progesterone, MEK-1 and ERK2 have ultrasensitive stimulus-response curves at the single cell level in *Xenopus laevis* oocytes (Huang and Ferrell 1996). Moreover, the dual phosphorylation of the MAPK, if occurring in two collision steps, has been suggested to increase the ultrasensitivity of the stimulus response curves (Ferrell 1996; Huang and Ferrell 1996; Ferrell and Bhatt 1997).

The presence of a mechanism allowing an autocatalysis step within the pathway, such as a positive feedback loop, is an essential element to produce a binary switch (Ferrell 2002). It has been shown that, during *Xenopus laevis* oocyte maturation,

ERK2 activation induces Mos synthesis as well as enhancing Mos activation (Matten et al. 1996). Thus, the Mos-MEK-1-ERK2 pathway has a positive feedback loop, which could explain its ability to generate an all-or-none cell fate decision from the graded concentration of progesterone.

As for the ERK pathway, the responses of the JNK pathway to a physiological stimulus (progesterone) and to pathological stress (sorbitol) were observed to be bistable responses in *Xenopus laevis* oocytes (Bagowski and Ferrell 2001). Indeed, JNK presented ultrasensitive stimulus-response curves to both stimuli, with JNK activation being all-or-none and temporally abrupt in individual cells. The system also displays autocatalytic activity, as the cytoplasm of sorbitol-activated oocytes injected in unstimulated oocytes produced a full activation of the JNK pathway in these oocytes (Bagowski and Ferrell 2001). JNK responses to graded stimuli have also been described as bistable in mammalian cells. In HeLa, HEK 293 and Jurkat T cells, JNK pathway responses to sorbitol or anisomycin were ultrasensitive while studied in populations of cells, suggesting an all-or-none response at the single cell level (Bagowski et al. 2003).

The absence of a turnover of phosphorylation in quiescent cells for the ERK pathway also suggests bistable switch behaviour in the context of IE gene induction. Although the phosphorylation of c-Jun and ATF-2, which are downstream of the JNK pathway, has been shown to be a dynamic process even in quiescent cells (Figure 3.12), the JNK activation profile obtained after sAn stimulation (Figure 5.3 Aii) suggests an all-or-none response to stimulus, which could result from the bistable character of the pathway as described above.

While the ERK and JNK pathways have been shown to have bistable switch behaviour in specific contexts, this is not the case for the p38 pathway. The p38 activation profile shows intermediate levels of activation after 40 minutes (Figure 5.3 Cii), which indicates a graded response. The regulation of this pathway may differ from the other two pathways, or the MAPK pathways could have the ability to behave as either a bistable or continuously variable switch, for example with the stimulation perceived generating a specific regulation of the different pathways.

6.1.2 The signalling pathways can behave as binary or continuously variable switch depending on the conditions

The predominant view of MAPK pathway signalling is that they behave as binary switches to induce cell fate responses, as described for *Xenopus* oocyte maturation above. However, the work described in this thesis suggests that this may not be true under all circumstances. The immediate early genes, which are controlled by the MAPK pathways, present a specific, quantitative and stimulus-dependent expression (Figure 3.2, Figure 4.1 and Figure 4.2). Thus, it seems that, in this context, the MAPK pathways convey graded responses, which are dependent on the stimulus. In addition, one of the main results in this study is the identification of a turnover of phosphorylation in quiescent C3H 10T½ cells, which suggests a more dynamic and continuously variable regulation of the responses by the MAPK pathways. Thus MAPK pathways may display different behaviour depending on the conditions.

Investigations of the effect of an activator (Gal4) and a repressor (Mig1) on the expression of *Gal1* in *Saccharomyces cerevisiae* showed that signalling pathways

could generate both binary and graded gene expression (Biggar and Crabtree 2001). *Gal1* expression is induced in the presence of galactose, although it is repressed in glucose-rich media (Lohr et al. 1995). The effects of these regulators were studied either individually or in the context of intact signalling pathways. The expression of the reporter *Gal1-GFP* was measured by fluorescence-activated cell sorting (FACS). A binary response would produce two peaks of specific intensities (expressed or not) and only the magnitude of the peaks would change with the stimulus, representing the amount of cells responding to the stimulus. However, a graded response would produce a single peak for each set of cells, and the intensity of the peak would vary with the stimulus, thus indicating the presence of intermediate responses.

To study the direct recruitment of Gal4 to the *Gal1* promoter, two separate fusion proteins were used: the Gal4 binding domain was fused to FKBP12 (Gal4BD-FKBP), while the Gal4 activation domain was fused to calcineurin A (Gal4AD-CN). After treatment with the compound FK506, the complex FKBP-FK506 binds to CN. Thus, the biding and activating domains of Gal4 are brought together and it induces *Gal1-GFP* expression. Variations of FK506 concentration induced graded and dose-dependent changes in gene expression. In the presence of glucose, *Gal1* expression was reduced in a glucose-dependent manner (Biggar and Crabtree 2001). Similar graded responses were observed using wild-type *Gal4* and varying galactose concentration. However, in the presence of glucose, physiological regulation of *Gal1* promoter generated binary changes. This is due to the repression exercised by Gal80 on Gal4, as cells lacking *Gal80* presented graded responses to glucose (Biggar and Crabtree 2001). Thus, depending on growth

conditions, the same transcription factors conveyed binary or graded changes in gene expression in this system. The experimental results did not allow distinguishing between a continuous variation of the initiation rates, or a pulsatile transcription, for which graded responses could be obtained by a variation of the pulse length, to explain the capacity of the promoter to induce both graded and binary changes.

A similar situation could allow the MAPK pathways to produce cell fate decisions, such as oocyte maturation or apoptosis, and to quantitatively control gene expression, as is observed for IE gene expression (see Chapter 4). A difference in the regulatory mechanisms could explain this duality in the information conveyed by MAPK pathways. These pathways could behave as a binary switch or continuously variable switch depending on the presence or absence of feedback, and could induce all-or-none or graded changes in gene expression due to a variation in the activation and regulation of transcriptional repressors and activators dependent on the external stimulus, as observed for *Gal1* expression.

6.1.3 Implications in diseases

The MAPK pathways are involved in many pathologies, such as cancer, inflammatory responses and neurological diseases (reviewed in Kim and Choi 2010). Thus understanding their mechanisms of control may help to identify specific and new drug targets to treat these diseases.

6.1.3.1 The p38 and JNK pathways in disease

The p38 MAPK pathway is activated by stress and inflammatory cytokines. This pathway was first recognised for its role in inflammation, as it regulates the synthesis of pro-inflammatory cytokines, such as IL-1, TNFα and IL6, which play key roles in chronic inflammatory and rheumatoid arthritis (reviewed in Feldmann et al. 1996; Ishihara and Hirano 2002; Cohen and Fleischmann 2010). In support of this, p38 was first identified as the target of potent anti-inflammatory pyridinyl imidazoles (Lee et al. 1994) and different p38 inhibitors have been shown to have anti-inflammatory effects and progressed to clinical trials (Kumar et al. 2003; Cohen and Fleischmann 2010), such as the compound SCIO-469 developed by Scios as a rheumatoid arthritis treatment. Moreover, in Alzheimer's disease and other neurodegenerative disorders, an overexpression of inflammatory cytokines is observed as well as an accumulation of neurofilaments made by the protein Tau (Wang et al. 2001; Wang and Liu 2008). This accumulation is probably due to the hyper-phosphorylation of the protein Tau. As aberrantly activated JNK and p38 have also been reported in these cells, these proteins could contribute to the hyper-phosphorylation of Tau (Atzori et al. 2001). p38 has also been associated with cardiovascular dysfunction, apoptosis, cell cycle, cell development and cell differentiation. A defect in the p38 pathway may result in cell cycle defects and tumorigenesis (Aouadi et al. 2006; Thornton and Rincon 2009).

The JNK pathway has been shown to be involved in many physiological processes, and in particular in apoptosis (reviewed in Dhanasekaran and Reddy 2008). Thus, an aberrant activation of the JNK pathway can cause pathological cell death and various pathologies. As p38, JNK, is thought to be involved in Tau hyper-

phosphorylation in Alzheimer's disease and other tauopathies, as well as other neurodegenerative diseases, such as Parkinson's disease and amyotrophic lateral sclerosis (reviewed in Cui et al. 2007). The JNK pathway was suggested to be implicated in modulating insulin action by phosphorylating the insulin receptor substrate 1 (IRS-1), and thus to be involved in obesity and type 2 diabetes (Aguirre et al. 2000; Hirosumi et al. 2002).

6.1.3.2 Phosphatases as potential drug targets

Protein kinases constitute one of the main classes of drug targets (Cohen 2002). For example, rapamycin inhibits the serine/threonine kinase mTOR (mammalian target of rapamycin) within mTOR Complex 1 and is used as an immunosuppressant to prevent rejection after kidney transplantation. By inhibiting mTOR, rapamycin blocks interleukin-2 (IL-2)-dependent T cell proliferation (Law 2005). Moreover, due to the key role of mTOR in cell cycle, rapamycin has efficacy as an anti-tumour agent (Law 2005). Another example is the cytokine-synthesis anti-inflammatory drugs (CSAIDs), which are ATP-competitive inhibitors for p38 and show efficacy in chronic inflammatory diseases (Cohen 2002).

However, most of the kinase inhibitors developed fail to be specific, as they are mainly ATP-competitive (Cohen 2002), such as SB 203580, SP 600125 and H89. The ATP binding site of the protein kinases was found to be highly conserved by structural study of protein kinase A (PKA; Knighton et al. 1991). Therefore protein kinase inhibitors that are not ATP-competitive must be developed, such as the MKK1 inhibitor PD 98059, by targeting less well-conserved regions of the protein.

Another alternative could be to target protein phosphatases instead of protein kinases, to modulate phosphorylation-regulated processes. Our study reveals the presence of a turnover of phosphorylation in quiescent cells (Chapter 3), suggesting a dynamic regulation of the MAPK pathways, and thus protein phosphatases could be an interesting drug target. Indeed, for the serine/threonine phosphatases, both the catalytic subunit directly and complex formation can be targeted (see Section 1.4.2.1). Naturally occurring compounds, such as cyclosporine A and FK506, have been identified and found to have immunosuppressive or anticancer properties by inhibiting the serine/threonine phosphatase PP2B catalytic subunit (McConnell and Wadzinski 2009). Fostriecin, which was discovered for its antitumor properties, inhibits the PP2A catalytic subunit, and triggers premature entry into mitosis, resulting in apoptosis. However, some phosphatase inhibitors are toxic, OA was first discovered as a marine toxin responsible for diarrheic shellfish poisoning (Cohen et al. 1990). Besides, the large number of substrates for these phosphatases means that it is difficult to target individual pathways using catalytic subunit inhibitors. Disrupting the complex between regulatory and catalytic subunits could prevent association with its substrate, and could allow a more specific inhibition than targeting the catalytic subunit (McConnell and Wadzinski 2009), because the regulatory subunits target the phosphatase to a smaller number of substrates.

Therefore, targeting phosphatases may be a way to disrupt MAPK signalling. OA on its own was shown to strongly activate the p38 (Figure 3.3, Figure 3.7, Figure 3.7 and Figure 3.9) and JNK (Figure 3.11) downstream targets, but to only weakly induce c-*fos* and c-*jun* transcription (Figure 3.2 and Figure 4.6) and in combination

with sAn to enhance induction of these genes (Figure 4.6). Thus, understanding how this compound regulates the MAPK pathways and produces a different gene induction profile to sAn, which also strongly activates p38 and JNK, could reveal other ways and drug targets to alter the action of MAPK pathways. OA or other PP2A or PP1 inhibitors, less toxic for the cells, could be used to control or enhance the induction of a specific set of IE genes and thus regulate the action of MAPK pathways. Fostriecin, a PP2A inhibitor, has been shown to have similar effect to OA (Buck et al. 2003), while being less toxic (Walsh et al. 1997). However, as this compound is susceptible to oxidation, the phase I of the clinical trial was suspended due to drug instability (McConnell and Wadzinski 2009). Moreover, once the regulatory subunits required in the MAPK pathways are identified, specific inhibitors for these subunits could be developed to directly target a particular step and pathway

6.2 A role for turnover of phosphorylation of TFs in quantitative IE gene regulation?

6.2.1 Gene expression

Gene transcription is a complex process with multiple steps, with one model dividing it into eight steps (Fuda et al. 2009; Figure 6.1). It begins with gaining access to the promoter region, involving chromatin modification and TF binding (step 1), then a pre-initiation complex is formed at the promoter and recruits RNA polymerase II (Pol II; step 2), which initiates transcription (step 3) and proceeds to the promoter-proximal pause region (step 4). Transcription restarts after hyperphosphorylation of Pol II C-terminal domain (CTD) on Serine 2 (step 5) and elongation proceeds (step 6) followed by termination (step 7). Finally, Pol II is

reinitiated by CTD dephosphorylation to start a new round of transcription (step 8). All these steps are controlled and can be rate-limiting. The distribution of Pol II across a gene allows identification of the rate-limiting step and three types have been identified (Fuda et al. 2009). While genes exhibiting no Pol II or evenly spread Pol II complexes across the locus are limited by step 1 or step 2, genes presenting an accumulation of Pol II complexes at the 5' end are limited by step downstream of Pol II recruitment to the promoter (steps 3 to 5). ChIP-seq in mouse ES cells suggests that a large proportion of genes have Pol II, in its initiation form, bound at their promoter (Guenther et al. 2007). For these genes, transcription elongation (steps 5 and 6) seems to play an important role in their regulation.

The recruitment of Pol II to the promoter region is highly regulated by TFs. There are two types of TFs: the gene-specific TFs, which bind to regulatory element located in the promoter or enhancer regions of the gene, and the general transcription factors (GTFs), which together with Pol II form the pre-initiation complex. The gene-specific TFs regulate transcription through different mechanisms. They recruit co-repressors or co-activators, which may recruit the pre-initiation complex, or catalyse chromatin remodelling. For example, the co-activator CBP (CREB-binding protein) binds to the TF CREB (Chrivia et al. 1993; Kwok et al. 1994) and p300 complements its activity (Lundblad et al. 1995). p300/CBP mediates dynamic H3K4me3 acetylation, which is essential for RNA Pol II association and gene induction (Crump et al. 2011).

Figure 6.1: Gene transcription in 8 steps

Schematic representation of gene transcription in 8 steps. Step 1: Access to the promoter region, binding of transcription factor (TF) and chromatin posttranslational modification (PTM). Step 2: Pre-initiation complex formation, binding of the general transcription factor (GTF) and recruitment of RNA polymerase II (Pol II). Step 3: initiation of transcription, the green line represents RNA. Step 4: Promoter clearance and pausing of Pol II, Pol II escape the promoter and is phosphorylated on Serine 5 ('P') of the C-terminal domain (CTD). Step 5: Transcription restarts, Pol II is phosphorylated ('P') on Serine 2 of the CTD. Step 6: Elongation. Step 7: Termination. Step 8: Pol II is dephosphorylated and free to start a new round of transcription. Adapted from (Fuda et al. 2009).

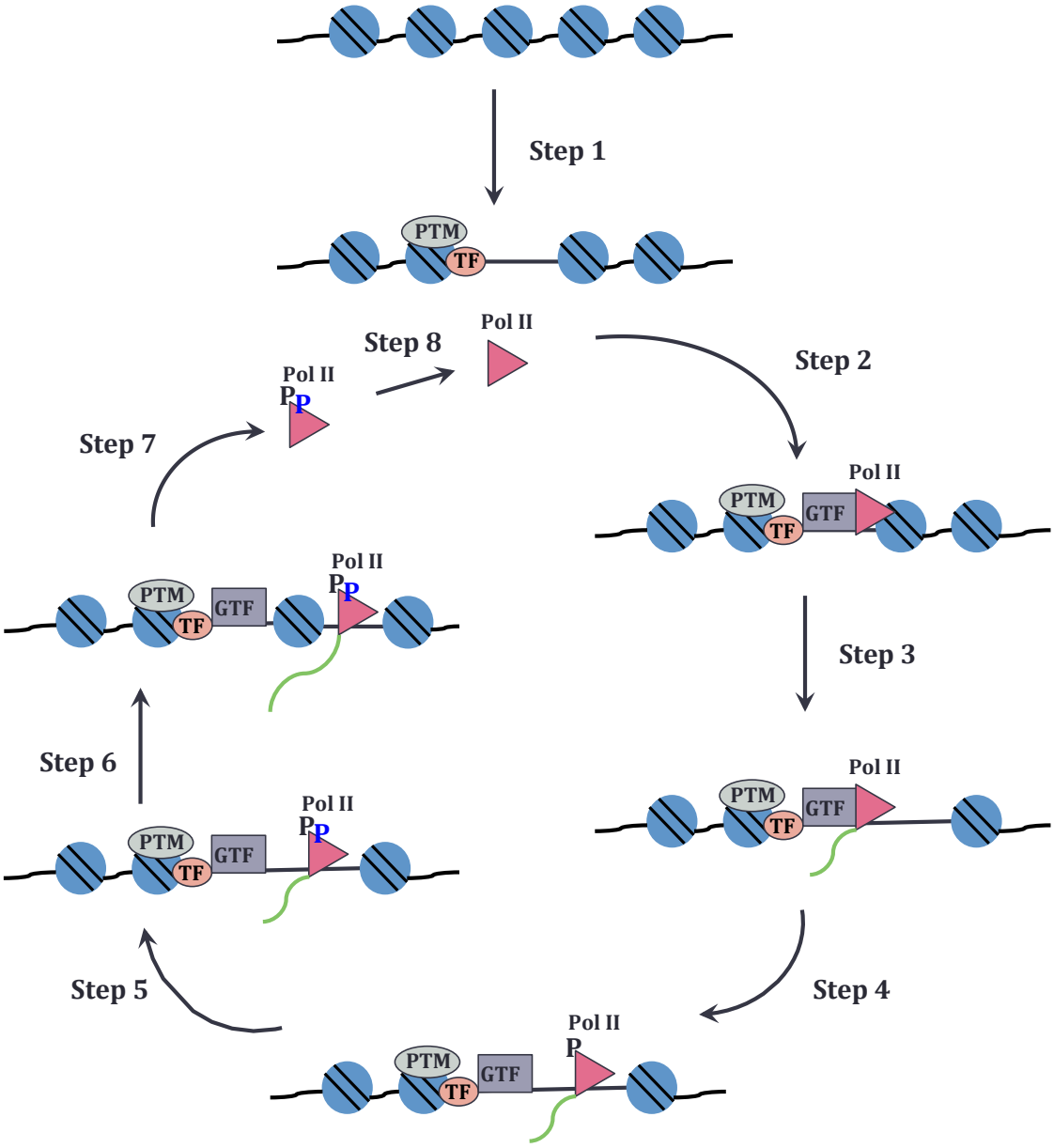
Step 1
PTM
TF
Step 2
Pol II
PTM
GTF
TF
Step 3
Pol II
PTM
GTF
TF
Step 4
Pol II
P
PTM
GTF
TF
Step 5
Pol II
P
PTM
GTF
TF
Step 6
Pol II
P
PTM
GTF
TF
Step 7
Pol II
P
P
Step 8
Pol II

The IE gene c-*fos* and c-*jun* promoter regions include multiple regulatory elements, which are recognised by various TFs and control their transcription (see Section 1.2.3). For c-*fos*, Pol II has been reported to be blocked at a site close to the boundary between exon 1 and intron 1 (see map in Figure 4.1 A; Fort et al. 1987; Lamb et al. 1990; Collart et al. 1991; Mechti et al. 1991). Thus, the release of Pol II is required for transcription elongation. The promoter-proximal pausing of Pol II does not constitute a repression mechanism but allows a rapid expression of c-*fos* under stimulation (Fivaz et al. 2000). ChIP experiments looking at the distribution of Pol II at c-*fos* and c-*jun* genes showed that high levels of Pol II are present at the transcription start sites of these genes (Crump et al. 2011), even in the absence of stimulation. However, induction with EGF highly increased the levels of Pol II at all sites studied (Crump et al. 2011), which suggests that there is a recruitment of Pol II at the promoter region of c-*fos*, under induction. Thus, the main control of c-*fos* seems to be both at the initiation of transcription and promoter-proximal pausing. These experiments were carried out in the same cells as the one used in this analysis, mouse C3H 10T½ cells, which makes it directly applicable to this work. However, in this thesis, as a first attempt to understand the IE gene quantitative regulation, we focused on the regulation at the initiation of transcription, which constitutes the direct link between gene induction and signalling pathways. Further investigations on whether OA has an effect on the promoter-proximal pausing, and further development of our simplified abstraction, which currently does not consider Pol II proximal pausing, would be required to fully understand IE gene regulation.

6.2.2 Phosphorylation/dephosphorylation cycles allow resetting of transcription components

The presence of turnover of phosphorylation at the TF level in the p38 and JNK MAPK pathways suggests dynamic regulation of gene expression by phosphorylation. Hypothetically, a cycle of phosphorylation and dephosphorylation events of TF could induce one event of initiation of transcription. The dephosphorylation of the TF could be viewed as a way to recycle the TF and thus allow another cycle of initiation of transcription. Disruption of the basal turnover of TF phosphorylation induces gene expression, as is seen after sAn (Figure 4.1 and Figure 4.3) or OA treatment (Figure 4.6).

In the context of gene transcription, dynamic phosphorylation has already been shown to have a regulatory role and incorporates a process to reset the transcription machinery (step 8). Indeed, the phosphorylation patterns of the Pol II CTD, which comprises 52 repeats of the sequence Tyr-Ser-Pro-Thr-Ser-Pro-Ser, control the different stages of transcription (reviewed in Phatnani and Greenleaf 2006; Heidemann et al. 2013). A non-phosphorylated Pol II is recruited at the promoter and its CTD undergoes Serine 2 and 5 phosphorylation by pTEFb and TFIIH respectively, to proceed to elongation. The phosphorylation patterns allow recruitment of factors needed for elongation of transcription, or dissociation of negative regulatory factors. While serine 5 phosphorylation has been linked to the dissociation of Pol II from the start site, for example the general transcription factor TFIID, which binds the TATA box, only binds to Pol II in its unphosphorylated state, serine 2 is associated with elongation. Among others, the protein phosphatase FCP1 has been shown to dephosphorylate the CTD of Pol II. This dephosphorylation results in the recycling of Pol II, which can, once

dephosphorylated, bind to the pre-initiation complex and another transcription cycle can begin. Thus, in this process, a phosphorylation and dephosphorylation cycle is used to reset a protein in order to re-initiate the transcription cycle.

6.2.3 Example of dynamic regulation of IE gene expression: dynamic acetylation

We saw that, in the context of gene expression, dynamic phosphorylation can be used as a regulatory process. Another dynamic process has already been described in IE gene transcription. Dynamic acetylation of histone H3 has been observed and is associated with IE gene expression (Hazzalin and Mahadevan 2005).

In a similar way as OA revealed the presence of a turnover of phosphorylation in MAPK pathways in quiescent cells (Chapter 3), the use of histone deacetylase inhibitors, such as TSA, results in the hyperacetylation of lysine 4-methylated histone H3, which revealed the presence of a dynamic acetylation (Hazzalin and Mahadevan 2005). ChIP experiments indicated that the TSA hypersensitivity observed is targeted to the promoter and transcription start site of c-*fos* and c-*jun* genes. TSA treatment results in partial inhibition of c-*fos* and c-*jun* induction, demonstrating the importance of deacetylation activity. Thus, it is not only acetylation that correlates with IE gene induction, but the dynamic acetylation of histone H3 that is relevant.

In the same way that TSA causes histone acetylation (Hazzalin and Mahadevan 2005), OA treatment caused increased histone phosphorylation (Figure 3.3), as well as that of TFs (Figure 3.8 and Figure 3.11). TF phosphorylation could behave similarly to histone acetylation, and the turnover of phosphorylation rather than

enhanced phosphorylation could be the relevant factor in IE gene expression regulation. However, unlike TSA, OA induces transcription on its own (Figure 4.6) and does not inhibit c-*fos* and c-*jun* expression while in co-treatment with sAn (Figure 4.6). This suggests that the dynamic acetylation and phosphorylation may have different roles in regulation of transcription. But, as phosphorylation is involved in many processes, OA inhibits dephosphorylation of multiple proteins, which makes the results of turnover of phosphorylation harder to interpret. Moreover, the strong activation of MAPK pathways by OA does not compare well with the weak induction of c-*fos* and c-*jun* induction. Indeed, by comparing OA treatment with sAn, while they similarly activate some TFs (Figure 3.8 and Figure 3.11), they induce gene expression differently (Figure 4.6). This suggests that TF phosphorylation is not enough to explain gene induction. One explanation may be that sAn activates additional events by stimulating complete MAPK pathways, or OA may inhibit a specific dephosphorylation event that is required for gene induction.

6.3 Future work

While the work in this thesis presents new insights on the potential role of turnover of TF phosphorylation regulated by the MAPK pathways in IE gene expression, further investigations are needed to fully characterise its role and understand the mechanism behind the quantitative regulation of IE genes.

6.3.1 Gene knockdown and knockout of proteins involved in the MAPK pathways

The use of phosphatase and kinase inhibitors allowed a first investigation of the turnover of phosphorylation in MAPK pathways. However, the limited specificity of some of these inhibitors makes it difficult to conclusively and precisely identify the step(s) involved in activation by OA. Knockdown and knockout experiments targeting individual genes could validate the results obtained by Western blotting.

PP1 and PP2A are composed of several subunits (see Section 1.4.2) and are involved in many different processes, therefore, rather than a direct knockdown or knockout of these phosphatases, which would not be helpful, siRNA experiments for the different scaffold and regulatory subunits of PP2A could be done. Such experiments have previously been carried out to study PRC1 phosphorylation (Cundell et al. 2013). Similar experiments could be done in our system for both PP2A and PP1 to validate the effects on MAPK pathway and IE gene induction observed by OA treatment, and identify the specific phosphatase complex involved. Moreover, it would allow distinguishing between the effects due to PP1 or PP2A inhibition.

The combination of OA and kinase inhibitor treatment has revealed a complex activation of the MAPK pathways by OA (discussed in Chapter 3, Figure 3.13 and Figure 3.14). Therefore, knockdown or knockout of specific kinases and TFs would allow identification of where OA acts in these pathways as well as validating the results obtained using inhibitors. It is to note, however, that the existence of multiple isoforms of JNK and p38 in mouse would be an issue to perform knockdown experiments. Pre-treatment with the p38 inhibitor, SB 203580,

followed by treatment with OA did not have a strong effect on MSK1 and downstream targets (Figure 3.7), while pre-treatment with the JNK inhibitor, SP 600125, inhibited MSK1 (Figure 3.7), histone H3 (Figure 3.6) and HMGN1 (Figure 3.9) activation, suggesting the presence of a kinase other than p38 phosphorylating MSK1 after OA treatment. A knockdown of p38 would validate SB 203580 pre-treatment results, and a JNK knockdown would indicate whether JNK is the potential kinase responsible for activation of MSK1 after OA stimulation. In addition, pre-treatment with SP 600125 inhibited ATF-2 and c-Jun activation (Figure 3.12). Thus, a JNK knockdown could also validate these results and identify PP1 and/or PP2A as the opposing phosphatase to JNK for dynamic phosphorylation of ATF-2 and c-Jun.

Kinase knockdown could also be informative on c-*fos* and c-*jun* induction. c-*jun* but not c-*fos* induction was inhibited by pre-treatment with both SB 203580 and SP 600125 in combination (Figure 4.7). A double knockdown of p38 and JNK could validate these results, while a single knockdown could indicate whether these pathways are essential or sufficient for OA induction.

Finally, in a similar way as p38 and JNK knockdown, respectively, would validate SB 203580 and SP 600125 pre-treatment results, MSK1 knockdown could validate H89 pre-treatment results and provide information on OA action downstream of p38.

6.3.2 Single cell experiments

Whilst Northern blotting and qRT-PCR allowed investigating the c-*fos* and c-*jun* induction profiles in the same system as the one used for signalling pathway investigation, the behaviour observed at the population level can sometimes vary from that observed at single cell levels (Ferrell 1999; Bagowski and Ferrell 2001). Thus, the results obtained here should be corroborated with single cell experiments. These experiments would allow a more specific investigation of the initiation of individual transcription events, because the initiation of transcription can be directly observed.

MS2 tagging experiments have already been used to investigate transcription in living cells at the promoter region (Golding et al. 2005; Chubb et al. 2006). This method is based on the capacity of the bacteriophage capsid protein MS2 to recognise a specific RNA sequence. By tagging the RNA sequence of interest with the MS2 RNA sequence, an MS2-GFP fusion protein can be used to detect the tagged RNA and quantified by fluorescence. Thus, the kinetics of initiation of transcription, rather than the mRNA production, would be directly detected by the use of this method. However, this technique presents some drawbacks, such as the ignorance of the number of RNA molecules required to visualise a focus, which prevent the exact quantification of RNA transcripts.

6.3.3 A simplified biological model

The simplifications considered for the development of the computational model described here prevent any direct comparison with the mRNA profiles obtained

experimentally for c-*fos* and c-*jun*. In order to gain further insights into quantitative IE gene regulation, a simplified biological model, which would present more similarity with our computational model, could be generated by cloning.

For example, a reporter gene could be created which is controlled by a single regulatory element from the c-*fos* or c-*jun* gene promoter. Transcription could be measured under various stimuli, which would correspond more closely to our simplified computational model. Moreover, by varying the regulatory element of the gene, the activation profile used can also be changed to correspond to either p38 or JNK input signal for the computational model.

As the computational abstraction considers the degradation rate of c-*fos* and c-*jun*, obtained experimentally, the 3' untranslated regions of these genes need to be added to the reporter gene, in order for the simplified biological and computational models to represent similar conditions. This construct, by allowing a direct comparison with the computational abstraction of the interface, can help to further develop this abstraction and thus allow an in depth investigation of the regulation at the interface between MAPK signalling pathways and IE gene induction.

6.3.4 Further development for the computational model

As well as developing a simplified biological model to compare it to our abstraction, the computational model needs to be further developed by providing additional modules to take into account additional biological complexity.

As previously mentioned, the simplified computational model, as is, fails to replicate the effects of the phosphatase inhibitor observed experimentally (see Figure 4.6). Indeed, our model stipulates that each dephosphorylation of the TF is associated with a single initiation event, in order to represent the potential regulation of initiation of transcription by the turnover of phosphorylation. Integrating the effects of OA observed on IE gene induction would require developing another method to record the initiation events. However, as the action of OA and the step at which it acts are not fully identified, simply varying the parameter representing the action of the protein phosphatases may be sufficient to account for the effect observed by OA, which would not require changing our method of tracking the initiation events.

Another component which could be incorporated into our abstraction of the interface is the effect of translation inhibitors on IE gene induction that was observed experimentally (Mahadevan and Edwards 1991; Edwards and Mahadevan 1992). This consists of the stabilisation of the transcripts and an enhanced transcription, and could be predicted with the computational model in order to validate this abstraction of the interface.

Further development of the model could allow investigating another type of TF by considering the effect of the binding step of the TF. A three states initiation module has already been developed in order to take this additional step into considerations, but the conditions (values of the different parameters) studied (data not shown) showed similar behaviour as the two states initiation module described in chapter 5.

6.4 Conclusion

The work described in this thesis provides new insights into the quantitative regulation of IE gene induction. It discusses a functional role for dynamic phosphorylation of TFs in this regulation. The identification of a turnover of phosphorylation in quiescent cells for the p38 and JNK pathways but not for the ERK pathway using the phosphatase inhibitor OA suggests the possibility of two modes of regulation of the MAPK pathways: 'on/off' or continuously variable switch. Moreover, the development of a simplified computational model of the interface between the MAPK pathways and IE genes will allow further differentiation of these two modes and the characteristics of the responses they can convey.

References

Abraham, S. E., S. Lobo, et al. (1993). "p300, and p300-associated proteins, are components of TATA-binding protein (TBP) complexes." Oncogene **8**(6): 1639-1647.

Adams, M. D., A. R. Kerlavage, et al. (1995). "Initial assessment of human gene diversity and expression patterns based upon 83 million nucleotides of cDNA sequence." Nature **377**(6547 Suppl): 3-174.

Agalioti, T., G. Chen, et al. (2002). "Deciphering the transcriptional histone acetylation code for a human gene." Cell **111**(3): 381-392.

Aguirre, V., T. Uchida, et al. (2000). "The c-Jun NH(2)-terminal kinase promotes insulin resistance during association with insulin receptor substrate-1 and phosphorylation of Ser(307)." Journal of Biological Chemistry **275**(12): 9047-9054.

Alepuz, P. M., E. de Nadal, et al. (2003). "Osmostress-induced transcription by Hot1 depends on a Hog1-mediated recruitment of the RNA Pol II." EMBO J **22**(10): 2433-2442.

Alessi, D. R., Y. Saito, et al. (1994). "Identification of the sites in MAP kinase kinase-1 phosphorylated by p74raf-1." EMBO J **13**(7): 1610-1619.

Alexander, M. C., M. Lomanto, et al. (1988). "Insulin stimulates glyceraldehyde-3-phosphate dehydrogenase gene expression through cis-acting DNA sequences." Proceedings of the National Academy of Sciences of the United States of America **85**(14): 5092-5096.

Allegra, P., R. Sterner, et al. (1987). "Affinity chromatographic purification of nucleosomes containing transcriptionally active DNA sequences." Journal of Molecular Biology **196**(2): 379-388.

Allfrey, V. G., R. Faulkner, et al. (1964). "Acetylation and Methylation of Histones and Their Possible Role in the Regulation of Rna Synthesis." Proceedings of the National Academy of Sciences of the United States of America **51**: 786-794.

Almendral, J. M., D. Sommer, et al. (1988). "Complexity of the early genetic response to growth factors in mouse fibroblasts." Molecular and Cellular Biology **8**(5): 2140-2148.

Anderson, N. G., J. L. Maller, et al. (1990). "Requirement for integration of signals from two distinct phosphorylation pathways for activation of MAP kinase." Nature **343**(6259): 651-653.

Angel, P., K. Hattori, et al. (1988). "The jun proto-oncogene is positively autoregulated by its product, Jun/AP-1." Cell **55**(5): 875-885.

Angel, P., M. Imagawa, et al. (1987). "Phorbol ester-inducible genes contain a common cis element recognized by a TPA-modulated trans-acting factor." Cell **49**(6): 729-739.

Angel, P. and M. Karin (1991). "The role of Jun, Fos and the AP-1 complex in cell-proliferation and transformation." Biochimica et Biophysica Acta **1072**(2-3): 129-157.

Aouadi, M., B. Binetruy, et al. (2006). "Role of MAPKs in development and differentiation: lessons from knockout mice." Biochimie **88**(9): 1091-1098.

Arias, J., A. S. Alberts, et al. (1994). "Activation of cAMP and mitogen responsive genes relies on a common nuclear factor." Nature **370**(6486): 226-229.

Arino, J., C. W. Woon, et al. (1988). "Human liver phosphatase 2A: cDNA and amino acid sequence of two catalytic subunit isotypes." Proceedings of the National Academy of Sciences of the United States of America **85**(12): 4252-4256.

Armstrong, C. G., G. J. Browne, et al. (1997). "PPP1R6, a novel member of the family of glycogen-targetting subunits of protein phosphatase 1." FEBS Letters **418**(1-2): 210-214.

Armstrong, C. G., M. J. Doherty, et al. (1998). "Identification of the separate domains in the hepatic glycogen-targeting subunit of protein phosphatase 1 that interact with phosphorylase a, glycogen and protein phosphatase 1." Biochemical Journal **336 (Pt 3)**: 699-704.

Arthur, J. S. and P. Cohen (2000). "MSK1 is required for CREB phosphorylation in response to mitogens in mouse embryonic stem cells." FEBS Letters **482**(1-2): 44-48.

Atzori, C., B. Ghetti, et al. (2001). "Activation of the JNK/p38 pathway occurs in diseases characterized by tau protein pathology and is related to tau phosphorylation but not to apoptosis." Journal of Neuropathology & Experimental Neurology **60**(12): 1190-1197.

Austin, D. W., M. S. Allen, et al. (2006). "Gene network shaping of inherent noise spectra." Nature **439**(7076): 608-611.

Avruch, J., X. F. Zhang, et al. (1994). "Raf meets Ras: completing the framework of a signal transduction pathway." Trends in Biochemical Sciences **19**(7): 279-283.

Bagowski, C. P., J. Besser, et al. (2003). "The JNK cascade as a biochemical switch in mammalian cells: ultrasensitive and all-or-none responses." Current Biology **13**(4): 315-320.

Bagowski, C. P. and J. E. Ferrell, Jr. (2001). "Bistability in the JNK cascade." Current Biology **11**(15): 1176-1182.

Bain, J., H. McLauchlan, et al. (2003). "The specificities of protein kinase inhibitors: an update." Biochemical Journal **371**(Pt 1): 199-204.

Bain, J., L. Plater, et al. (2007). "The selectivity of protein kinase inhibitors: a further update." Biochemical Journal **408**(3): 297-315.

Bannister, A. J. and T. Kouzarides (1996). "The CBP co-activator is a histone acetyltransferase." Nature **384**(6610): 641-643.

Barbacid, M. and D. Vazquez (1975). "Ribosome changes during translation." Journal of Molecular Biology **93**(4): 449-463.

Barber, R. D., D. W. Harmer, et al. (2005). "GAPDH as a housekeeping gene: analysis of GAPDH mRNA expression in a panel of 72 human tissues." Physiological Genomics **21**(3): 389-395.

Barford, D. (1996). "Molecular mechanisms of the protein serine/threonine phosphatases." Trends in Biochemical Sciences **21**(11): 407-412.

Barford, D., A. K. Das, et al. (1998). "The structure and mechanism of protein phosphatases: insights into catalysis and regulation." Annual Review of Biophysics and Biomolecular Structure **27**: 133-164.

Barratt, M. J., C. A. Hazzalin, et al. (1994). "Mitogen-stimulated phosphorylation of histone H3 is targeted to a small hyperacetylation-sensitive fraction." Proceedings of the National Academy of Sciences of the United States of America **91**(11): 4781-4785.

Barratt, M. J., C. A. Hazzalin, et al. (1994). "A mitogen- and anisomycin-stimulated kinase phosphorylates HMG-14 in its basic amino-terminal domain in vivo and on isolated mononucleosomes." EMBO J **13**(19): 4524-4535.

Bartel, D. P., M. Sheng, et al. (1989). "Growth factors and membrane depolarization activate distinct programs of early response gene expression: dissociation of fos and jun induction." Genes & Development **3**(3): 304-313.

Becskei, A., B. B. Kaufmann, et al. (2005). "Contributions of low molecule number and chromosomal positioning to stochastic gene expression." Nature Genetics **37**(9): 937-944.

Becskei, A. and L. Serrano (2000). "Engineering stability in gene networks by autoregulation." Nature **405**(6786): 590-593.

Bengtsson, M., A. Stahlberg, et al. (2005). "Gene expression profiling in single cells from the pancreatic islets of Langerhans reveals lognormal distribution of mRNA levels." Genome Research **15**(10): 1388-1392.

Bertrand, E., P. Chartrand, et al. (1998). "Localization of ASH1 mRNA particles in living yeast." Molecular Cell **2**(4): 437-445.

Bhoumik, A., P. Lopez-Bergami, et al. (2007). "ATF2 on the double - activating transcription factor and DNA damage response protein." Pigment Cell Res **20**(6): 498-506.

Bialojan, C. and A. Takai (1988). "Inhibitory effect of a marine-sponge toxin, okadaic acid, on protein phosphatases. Specificity and kinetics." Biochemical Journal **256**(1): 283-290.

Biggar, S. R. and G. R. Crabtree (2001). "Cell signaling can direct either binary or graded transcriptional responses." EMBO J **20**(12): 3167-3176.

Blake, W. J., K. A. M, et al. (2003). "Noise in eukaryotic gene expression." Nature **422**(6932): 633-637.

Blank, J. L., P. Gerwins, et al. (1996). "Molecular cloning of mitogen-activated protein/ERK kinase kinases (MEKK) 2 and 3. Regulation of sequential phosphorylation pathways involving mitogen-activated protein kinase and c-Jun kinase." Journal of Biological Chemistry **271**(10): 5361-5368.

Boffa, L. C., J. Walker, et al. (1990). "Factors affecting nucleosome structure in transcriptionally active chromatin. Histone acetylation, nascent RNA and inhibitors of RNA synthesis." European Journal of Biochemistry **194**(3): 811-823.

Bohmann, D., T. J. Bos, et al. (1987). "Human proto-oncogene c-jun encodes a DNA binding protein with structural and functional properties of transcription factor AP-1." Science **238**(4832): 1386-1392.

Bollen, M. (2001). "Combinatorial control of protein phosphatase-1." Trends in Biochemical Sciences **26**(7): 426-431.

Bolouri, H. and E. H. Davidson (2003). "Transcriptional regulatory cascades in development: initial rates, not steady state, determine network kinetics." Proceedings of the National Academy of Sciences of the United States of America **100**(16): 9371-9376.

Boulton, T. G. and M. H. Cobb (1991). "Identification of multiple extracellular signal-regulated kinases (ERKs) with antipeptide antibodies." Cell Regul **2**(5): 357-371.

Bravo, R. (1990). "Growth factor-responsive genes in fibroblasts." Cell Growth & Differentiation **1**(6): 305-309.

Brightman, F. A. and D. A. Fell (2000). "Differential feedback regulation of the MAPK cascade underlies the quantitative differences in EGF and NGF signalling in PC12 cells." FEBS Letters **482**(3): 169-174.

Brownell, J. E., J. Zhou, et al. (1996). "Tetrahymena histone acetyltransferase A: a homolog to yeast Gcn5p linking histone acetylation to gene activation." Cell **84**(6): 843-851.

Bruna, A., M. Nicolas, et al. (2003). "Glucocorticoid receptor-JNK interaction mediates inhibition of the JNK pathway by glucocorticoids." EMBO J **22**(22): 6035-6044.

Buck, S. B., C. Hardouin, et al. (2003). "Fundamental role of the fostriecin unsaturated lactone and implications for selective protein phosphatase inhibition." Journal of the American Chemical Society **125**(51): 15694-15695.

Bustin, S. A., V. Benes, et al. (2005). "Quantitative real-time RT-PCR--a perspective." Journal of Molecular Endocrinology **34**(3): 597-601.

Butte, A. J., V. J. Dzau, et al. (2001). "Further defining housekeeping, or "maintenance," genes Focus on "A compendium of gene expression in normal human tissues"." Physiological Genomics **7**(2): 95-96.

Campos, E. I. and D. Reinberg (2009). "Histones: annotating chromatin." Annual Review of Genetics **43**: 559-599.

Camps, M., A. Nichols, et al. (2000). "Dual specificity phosphatases: a gene family for control of MAP kinase function." FASEB Journal **14**(1): 6-16.

Cano, E., C. A. Hazzalin, et al. (1995). "Neither ERK nor JNK/SAPK MAP kinase subtypes are essential for histone H3/HMG-14 phosphorylation or c-fos and c-jun induction." Journal of Cell Science **108 (Pt 11)**: 3599-3609.

Cano, E., C. A. Hazzalin, et al. (1994). "Anisomycin-activated protein kinases p45 and p55 but not mitogen-activated protein kinases ERK-1 and -2 are implicated in the induction of c-fos and c-jun." Molecular and Cellular Biology **14**(11): 7352-7362.

Cano, E. and L. C. Mahadevan (1995). "Parallel signal processing among mammalian MAPKs." Trends in Biochemical Sciences **20**(3): 117-122.

Cardelli, L. (2009). Artificial Biochemistry. Algorithmic Bioprocesses. A. Condon, D. Harel, J. N. Kok, A. Salomaa and E. Winfree, Springer Berlin Heidelberg**:** 429-462.

Caunt, C. J. and S. M. Keyse (2013). "Dual-specificity MAP kinase phosphatases (MKPs): shaping the outcome of MAP kinase signalling." FEBS J **280**(2): 489-504.

Ceska, M., C. Schneider, et al. "Stochastic Modelling of the Interface between Regulatory Enzymes and Transcriptional Initiation at Inducible Genes."

Chang, C. I., B. E. Xu, et al. (2002). "Crystal structures of MAP kinase p38 complexed to the docking sites on its nuclear substrate MEF2A and activator MKK3b." Molecular Cell **9**(6): 1241-1249.

Chang, L. and M. Karin (2001). "Mammalian MAP kinase signalling cascades." Nature **410**(6824): 37-40.

Chao, T. H., M. Hayashi, et al. (1999). "MEKK3 directly regulates MEK5 activity as part of the big mitogen-activated protein kinase 1 (BMK1) signaling pathway." Journal of Biological Chemistry **274**(51): 36035-36038.

Chapman, S. and A. R. Asthagiri (2004). "Resistance to signal activation governs design features of the MAP kinase signaling module." Biotechnology and Bioengineering **85**(3): 311-322.

Charles, C. H., H. Sun, et al. (1993). "The growth factor-inducible immediate-early gene 3CH134 encodes a protein-tyrosine-phosphatase." Proceedings of the National Academy of Sciences of the United States of America **90**(11): 5292-5296.

Chen, J., B. L. Martin, et al. (1992). "Regulation of protein serine-threonine phosphatase type-2A by tyrosine phosphorylation." Science **257**(5074): 1261-1264.

Chen, T. A. and V. G. Allfrey (1987). "Rapid and reversible changes in nucleosome structure accompany the activation, repression, and superinduction of murine fibroblast protooncogenes c-fos and c-myc." Proceedings of the National Academy of Sciences of the United States of America **84**(15): 5252-5256.

Cheung, P., K. G. Tanner, et al. (2000). "Synergistic coupling of histone H3 phosphorylation and acetylation in response to epidermal growth factor stimulation." Molecular Cell **5**(6): 905-915.

Chiu, R., M. Imagawa, et al. (1987). "Multiple cis- and trans-acting elements mediate the transcriptional response to phorbol esters." Nature **329**(6140): 648-651.

Chomczynski, P. and N. Sacchi (1987). "Single-step method of RNA isolation by acid guanidinium thiocyanate-phenol-chloroform extraction." Analytical Biochemistry **162**(1): 156-159.

Chrivia, J. C., R. P. Kwok, et al. (1993). "Phosphorylated CREB binds specifically to the nuclear protein CBP." Nature **365**(6449): 855-859.

Chubb, J. R., T. Trcek, et al. (2006). "Transcriptional pulsing of a developmental gene." Current Biology **16**(10): 1018-1025.

Churchman, L. S. and J. S. Weissman (2012). "Native elongating transcript sequencing (NET-seq)." Curr Protoc Mol Biol **Chapter 4**: Unit 4 14 11-17.

Clayton, A. L., C. A. Hazzalin, et al. (2006). "Enhanced histone acetylation and transcription: a dynamic perspective." Molecular Cell **23**(3): 289-296.

Clayton, A. L. and L. C. Mahadevan (2003). "MAP kinase-mediated phosphoacetylation of histone H3 and inducible gene regulation." FEBS Letters **546**(1): 51-58.

Clayton, A. L., S. Rose, et al. (2000). "Phosphoacetylation of histone H3 on c-fos- and c-jun-associated nucleosomes upon gene activation." EMBO J **19**(14): 3714-3726.

Cochran, B. H., A. C. Reffel, et al. (1983). "Molecular cloning of gene sequences regulated by platelet-derived growth factor." Cell **33**(3): 939-947.

Cohen, P. (1989). "The structure and regulation of protein phosphatases." Annual Review of Biochemistry **58**: 453-508.

Cohen, P. (1997). "The search for physiological substrates of MAP and SAP kinases in mammalian cells." Trends in Cell Biology **7**(9): 353-361.

Cohen, P. (2002). "Protein kinases--the major drug targets of the twenty-first century?" Nat Rev Drug Discov **1**(4): 309-315.

Cohen, P., C. F. Holmes, et al. (1990). "Okadaic acid: a new probe for the study of cellular regulation." Trends in Biochemical Sciences **15**(3): 98-102.

Cohen, P., S. Klumpp, et al. (1989). "An improved procedure for identifying and quantitating protein phosphatases in mammalian tissues." FEBS Letters **250**(2): 596-600.

Cohen, P. T. (1988). "Two isoforms of protein phosphatase 1 may be produced from the same gene." FEBS Letters **232**(1): 17-23.

Cohen, P. T. (2002). "Protein phosphatase 1--targeted in many directions." Journal of Cell Science **115**(Pt 2): 241-256.

Cohen, S. and R. Fleischmann (2010). "Kinase inhibitors: a new approach to rheumatoid arthritis treatment." Current Opinion in Rheumatology **22**(3): 330-335.

Collart, M. A., N. Tourkine, et al. (1991). "c-fos gene transcription in murine macrophages is modulated by a calcium-dependent block to elongation in intron 1." Molecular and Cellular Biology **11**(5): 2826-2831.

Collins, M. K. and E. Rozengurt (1984). "Homologous and heterologous mitogenic desensitization of Swiss 3T3 cells to phorbol esters and vasopressin: role of receptor and postreceptor steps." Journal of Cellular Physiology **118**(2): 133-142.

Cook, S. J., N. Aziz, et al. (1999). "The repertoire of fos and jun proteins expressed during the G1 phase of the cell cycle is determined by the duration of mitogen-activated protein kinase activation." Molecular and Cellular Biology **19**(1): 330-341.

Cool, D. E., P. R. Andreassen, et al. (1992). "Cytokinetic failure and asynchronous nuclear division in BHK cells overexpressing a truncated protein-tyrosine-phosphatase." Proceedings of the National Academy of Sciences of the United States of America **89**(12): 5422-5426.

Cool, D. E., N. K. Tonks, et al. (1990). "Expression of a human T-cell protein-tyrosine-phosphatase in baby hamster kidney cells." Proceedings of the National Academy of Sciences of the United States of America **87**(18): 7280-7284.

Cool, D. E., N. K. Tonks, et al. (1989). "cDNA isolated from a human T-cell library encodes a member of the protein-tyrosine-phosphatase family." Proceedings of the National Academy of Sciences of the United States of America **86**(14): 5257-5261.

Cooper, J. A. (1994). "MAP kinase pathways. Straight and narrow or tortuous and intersecting?" Current Biology **4**(12): 1118-1121.

Crump, N. T., C. A. Hazzalin, et al. (2011). "Dynamic acetylation of all lysine-4 trimethylated histone H3 is evolutionarily conserved and mediated by p300/CBP." Proceedings of the National Academy of Sciences of the United States of America **108**(19): 7814-7819.

Csortos, C., S. Zolnierowicz, et al. (1996). "High complexity in the expression of the B' subunit of protein phosphatase 2A0. Evidence for the existence of at least seven novel isoforms." Journal of Biological Chemistry **271**(5): 2578-2588.

Cuenda, A., G. Alonso, et al. (1996). "Purification and cDNA cloning of SAPKK3, the major activator of RK/p38 in stress- and cytokine-stimulated monocytes and epithelial cells." EMBO J **15**(16): 4156-4164.

Cuenda, A., P. Cohen, et al. (1997). "Activation of stress-activated protein kinase-3 (SAPK3) by cytokines and cellular stresses is mediated via SAPKK3 (MKK6); comparison of the specificities of SAPK3 and SAPK2 (RK/p38)." EMBO J **16**(2): 295-305.

Cui, J., M. Zhang, et al. (2007). "JNK pathway: diseases and therapeutic potential." Acta Pharmacologica Sinica **28**(5): 601-608.

Cundell, M. J., R. N. Bastos, et al. (2013). "The BEG (PP2A-B55/ENSA/Greatwall) pathway ensures cytokinesis follows chromosome separation." Molecular Cell **52**(3): 393-405.

Curran, T., W. P. MacConnell, et al. (1983). "Structure of the FBJ murine osteosarcoma virus genome: molecular cloning of its associated helper virus and the cellular homolog of the v-fos gene from mouse and human cells." Molecular and Cellular Biology **3**(5): 914-921.

Curran, T., A. D. Miller, et al. (1984). "Viral and cellular fos proteins: a comparative analysis." Cell **36**(2): 259-268.

Curran, T. and N. M. Teich (1982). "Identification of a 39,000-dalton protein in cells transformed by the FBJ murine osteosarcoma virus." Virology **116**(1): 221-235.

Dallas, P. B., P. Yaciuk, et al. (1997). "Characterization of monoclonal antibodies raised against p300: both p300 and CBP are present in intracellular TBP complexes." Journal of Virology **71**(2): 1726-1731.

Dannenberg, F., E. M. Hahn, et al. (2014). "Computing Cumulative Rewards using Fast Adaptive Uniformisation." ACM Transactions on Modeling and Computer Simulation, Special Issue on Comutational Methods in Systems Biology.

Davies, S. P., H. Reddy, et al. (2000). "Specificity and mechanism of action of some commonly used protein kinase inhibitors." Biochemical Journal **351**(Pt 1): 95-105.

De Nadal, E., M. Zapater, et al. (2004). "The MAPK Hog1 recruits Rpd3 histone deacetylase to activate osmoresponsive genes." Nature **427**(6972): 370-374.

Deak, M., A. D. Clifton, et al. (1998). "Mitogen- and stress-activated protein kinase-1 (MSK1) is directly activated by MAPK and SAPK2/p38, and may mediate activation of CREB." EMBO J **17**(15): 4426-4441.

Derijard, B., M. Hibi, et al. (1994). "JNK1: a protein kinase stimulated by UV light and Ha-Ras that binds and phosphorylates the c-Jun activation domain." Cell **76**(6): 1025-1037.

Derijard, B., J. Raingeaud, et al. (1995). "Independent human MAP-kinase signal transduction pathways defined by MEK and MKK isoforms." Science **267**(5198): 682-685.

Dhalluin, C., J. E. Carlson, et al. (1999). "Structure and ligand of a histone acetyltransferase bromodomain." Nature **399**(6735): 491-496.

Dhanasekaran, D. N. and E. P. Reddy (2008). "JNK signaling in apoptosis." Oncogene **27**(48): 6245-6251.

Dickinson, R. J. and S. M. Keyse (2006). "Diverse physiological functions for dual-specificity MAP kinase phosphatases." Journal of Cell Science **119**(Pt 22): 4607-4615.

Diercks, A., H. Kostner, et al. (2009). "Resolving cell population heterogeneity: real-time PCR for simultaneous multiplexed gene detection in multiple single-cell samples." PLoS One **4**(7): e6326.

Dikic, I., G. Tokiwa, et al. (1996). "A role for Pyk2 and Src in linking G-protein-coupled receptors with MAP kinase activation." Nature **383**(6600): 547-550.

Doherty, M. J., P. R. Young, et al. (1996). "Amino acid sequence of a novel protein phosphatase 1 binding protein (R5) which is related to the liver- and muscle-specific glycogen binding subunits of protein phosphatase 1." FEBS Letters **399**(3): 339-343.

Dombradi, V., J. M. Axton, et al. (1990). "Drosophila contains three genes that encode distinct isoforms of protein phosphatase 1." European Journal of Biochemistry **194**(3): 739-745.

Dorow, D. S., L. Devereux, et al. (1993). "Identification of a new family of human epithelial protein kinases containing two leucine/isoleucine-zipper domains." European Journal of Biochemistry **213**(2): 701-710.

Dublanche, Y., K. Michalodimitrakis, et al. (2006). "Noise in transcription negative feedback loops: simulation and experimental analysis." Mol Syst Biol **2**: 41.

Dyson, M. H., S. Thomson, et al. (2005). "MAP kinase-mediated phosphorylation of distinct pools of histone H3 at S10 or S28 via mitogen- and stress-activated kinase 1/2." Journal of Cell Science **118**(Pt 10): 2247-2259.

Eberharter, A. and P. B. Becker (2002). "Histone acetylation: a switch between repressive and permissive chromatin. Second in review series on chromatin dynamics." EMBO Reports **3**(3): 224-229.

Edmunds, J. W. and L. C. Mahadevan (2004). "MAP kinases as structural adaptors and enzymatic activators in transcription complexes." Journal of Cell Science **117**(Pt 17): 3715-3723.

Edmunds, J. W., L. C. Mahadevan, et al. (2008). "Dynamic histone H3 methylation during gene induction: HYPB/Setd2 mediates all H3K36 trimethylation." EMBO J **27**(2): 406-420.

Edwards, D. R. and L. C. Mahadevan (1992). "Protein synthesis inhibitors differentially superinduce c-fos and c-jun by three distinct mechanisms: lack of evidence for labile repressors." EMBO J **11**(7): 2415-2424.

Egloff, M. P., P. T. Cohen, et al. (1995). "Crystal structure of the catalytic subunit of human protein phosphatase 1 and its complex with tungstate." Journal of Molecular Biology **254**(5): 942-959.

Egloff, M. P., D. F. Johnson, et al. (1997). "Structural basis for the recognition of regulatory subunits by the catalytic subunit of protein phosphatase 1." EMBO J **16**(8): 1876-1887.

Eisenberg, E. and E. Y. Levanon (2003). "Human housekeeping genes are compact." Trends in Genetics **19**(7): 362-365.

Eisenberg, E. and E. Y. Levanon (2013). "Human housekeeping genes, revisited." Trends in Genetics **29**(10): 569-574.

Ellinger-Ziegelbauer, H., K. Brown, et al. (1997). "Direct activation of the stress-activated protein kinase (SAPK) and extracellular signal-regulated protein kinase (ERK) pathways by an inducible mitogen-activated protein Kinase/ERK kinase kinase 3 (MEKK) derivative." Journal of Biological Chemistry **272**(5): 2668-2674.

Elowitz, M. B., A. J. Levine, et al. (2002). "Stochastic gene expression in a single cell." Science **297**(5584): 1183-1186.

English, J. M., C. A. Vanderbilt, et al. (1995). "Isolation of MEK5 and differential expression of alternatively spliced forms." Journal of Biological Chemistry **270**(48): 28897-28902.

Faux, M. C. and J. D. Scott (1996). "More on target with protein phosphorylation: conferring specificity by location." Trends in Biochemical Sciences **21**(8): 312-315.

Feldmann, M., F. M. Brennan, et al. (1996). "Role of cytokines in rheumatoid arthritis." Annual Review of Immunology **14**: 397-440.

Femino, A. M., F. S. Fay, et al. (1998). "Visualization of single RNA transcripts in situ." Science **280**(5363): 585-590.

Ferrell, J. E., Jr. (1996). "Tripping the switch fantastic: how a protein kinase cascade can convert graded inputs into switch-like outputs." Trends in Biochemical Sciences **21**(12): 460-466.

Ferrell, J. E., Jr. (1998). "How regulated protein translocation can produce switch-like responses." Trends in Biochemical Sciences **23**(12): 461-465.

Ferrell, J. E., Jr. (1999). "Building a cellular switch: more lessons from a good egg." BioEssays **21**(10): 866-870.

Ferrell, J. E., Jr. (1999). "Xenopus oocyte maturation: new lessons from a good egg." BioEssays **21**(10): 833-842.

Ferrell, J. E., Jr. (2002). "Self-perpetuating states in signal transduction: positive feedback, double-negative feedback and bistability." Current Opinion in Cell Biology **14**(2): 140-148.

Ferrell, J. E., Jr. and R. R. Bhatt (1997). "Mechanistic studies of the dual phosphorylation of mitogen-activated protein kinase." Journal of Biological Chemistry **272**(30): 19008-19016.

Ferrell, J. E., Jr. and E. M. Machleder (1998). "The biochemical basis of an all-or-none cell fate switch in Xenopus oocytes." Science **280**(5365): 895-898.

Fisch, T. M., R. Prywes, et al. (1987). "c-fos sequence necessary for basal expression and induction by epidermal growth factor, 12-O-tetradecanoyl phorbol-13-acetate and the calcium ionophore." Molecular and Cellular Biology **7**(10): 3490-3502.

Fisch, T. M., R. Prywes, et al. (1989). "An AP1-binding site in the c-fos gene can mediate induction by epidermal growth factor and 12-O-tetradecanoyl phorbol-13-acetate." Molecular and Cellular Biology **9**(3): 1327-1331.

Fisher, J. and T. A. Henzinger (2007). "Executable cell biology." Nature Biotechnology **25**(11): 1239-1249.

Fivaz, J., M. C. Bassi, et al. (2000). "RNA polymerase II promoter-proximal pausing upregulates c-fos gene expression." Gene **255**(2): 185-194.

Forsberg, E. C., K. M. Downs, et al. (2000). "Developmentally dynamic histone acetylation pattern of a tissue-specific chromatin domain." Proceedings of the National Academy of Sciences of the United States of America **97**(26): 14494-14499.

Forsdyke, D. R. (1985). "cDNA cloning of mRNAS which increase rapidly in human lymphocytes cultured with concanavalin-A and cycloheximide." Biochemical and Biophysical Research Communications **129**(3): 619-625.

Fort, P., J. Rech, et al. (1987). "Regulation of c-fos gene expression in hamster fibroblasts: initiation and elongation of transcription and mRNA degradation." Nucleic Acids Research **15**(14): 5657-5667.

Foster, D. N., L. J. Schmidt, et al. (1982). "Polyadenylylated RNA complementary to a mouse retrovirus-like multigene family is rapidly and specifically induced by epidermal growth factor stimulation of quiescent cells." Proceedings of the National Academy of Sciences of the United States of America **79**(23): 7317-7321.

Frangioni, J. V., P. H. Beahm, et al. (1992). "The nontransmembrane tyrosine phosphatase PTP-1B localizes to the endoplasmic reticulum via its 35 amino acid C-terminal sequence." Cell **68**(3): 545-560.

Freshney, N. W., L. Rawlinson, et al. (1994). "Interleukin-1 activates a novel protein kinase cascade that results in the phosphorylation of Hsp27." Cell **78**(6): 1039-1049.

Fuda, N. J., M. B. Ardehali, et al. (2009). "Defining mechanisms that regulate RNA polymerase II transcription in vivo." Nature **461**(7261): 186-192.

Gallo, K. A., M. R. Mark, et al. (1994). "Identification and characterization of SPRK, a novel src-homology 3 domain-containing proline-rich kinase with serine/threonine kinase activity." Journal of Biological Chemistry **269**(21): 15092-15100.

Gerwins, P., J. L. Blank, et al. (1997). "Cloning of a novel mitogen-activated protein kinase kinase kinase, MEKK4, that selectively regulates the c-Jun amino terminal kinase pathway." Journal of Biological Chemistry **272**(13): 8288-8295.

Gille, H., M. Kortenjann, et al. (1995). "ERK phosphorylation potentiates Elk-1-mediated ternary complex formation and transactivation." EMBO J **14**(5): 951-962.

Gille, H., T. Strahl, et al. (1995). "Activation of ternary complex factor Elk-1 by stress-activated protein kinases." Current Biology **5**(10): 1191-1200.

Gilman, M. Z., R. N. Wilson, et al. (1986). "Multiple protein-binding sites in the 5'-flanking region regulate c-fos expression." Molecular and Cellular Biology **6**(12): 4305-4316.

Glenney, J. R. (1991). "Isolation of tyrosine-phosphorylated proteins and generation of monoclonal antibodies." Methods in Enzymology **201**: 92-100.

Golding, I., J. Paulsson, et al. (2005). "Real-time kinetics of gene activity in individual bacteria." Cell **123**(6): 1025-1036.

Gomez, N. and P. Cohen (1991). "Dissection of the protein kinase cascade by which nerve growth factor activates MAP kinases." Nature **353**(6340): 170-173.

Gong, Y. and X. Zhao (2003). "Shc-dependent pathway is redundant but dominant in MAPK cascade activation by EGF receptors: a modeling inference." FEBS Letters **554**(3): 467-472.

Goto, H., Y. Tomono, et al. (1999). "Identification of a novel phosphorylation site on histone H3 coupled with mitotic chromosome condensation." Journal of Biological Chemistry **274**(36): 25543-25549.

Goto, H., Y. Yasui, et al. (2002). "Aurora-B phosphorylates Histone H3 at serine28 with regard to the mitotic chromosome condensation." Genes to Cells **7**(1): 11-17.

Green, D. D., S. I. Yang, et al. (1987). "Molecular cloning and sequence analysis of the catalytic subunit of bovine type 2A protein phosphatase." Proceedings of the National Academy of Sciences of the United States of America **84**(14): 4880-4884.

Green, J. B., H. V. New, et al. (1992). "Responses of embryonic Xenopus cells to activin and FGF are separated by multiple dose thresholds and correspond to distinct axes of the mesoderm." Cell **71**(5): 731-739.

Green, J. B. and J. C. Smith (1990). "Graded changes in dose of a Xenopus activin A homologue elicit stepwise transitions in embryonic cell fate." Nature **347**(6291): 391-394.

Greenberg, M. E., A. L. Hermanowski, et al. (1986). "Effect of protein synthesis inhibitors on growth factor activation of c-fos, c-myc, and actin gene transcription." Molecular and Cellular Biology **6**(4): 1050-1057.

Greenberg, M. E., Z. Siegfried, et al. (1987). "Mutation of the c-fos gene dyad symmetry element inhibits serum inducibility of transcription in vivo and

the nuclear regulatory factor binding in vitro." Molecular and Cellular Biology **7**(3): 1217-1225.

Greenberg, M. E. and E. B. Ziff (1984). "Stimulation of 3T3 cells induces transcription of the c-fos proto-oncogene." Nature **311**(5985): 433-438.

Gruda, M. C., K. Kovary, et al. (1994). "Regulation of Fra-1 and Fra-2 phosphorylation differs during the cell cycle of fibroblasts and phosphorylation in vitro by MAP kinase affects DNA binding activity." Oncogene **9**(9): 2537-2547.

Guan, K. L., S. S. Broyles, et al. (1991). "A Tyr/Ser protein phosphatase encoded by vaccinia virus." Nature **350**(6316): 359-362.

Guan, K. L. and J. E. Dixon (1991). "Evidence for protein-tyrosine-phosphatase catalysis proceeding via a cysteine-phosphate intermediate." Journal of Biological Chemistry **266**(26): 17026-17030.

Guenther, M. G., S. S. Levine, et al. (2007). "A chromatin landmark and transcription initiation at most promoters in human cells." Cell **130**(1): 77-88.

Gupta, S., T. Barrett, et al. (1996). "Selective interaction of JNK protein kinase isoforms with transcription factors." EMBO J **15**(11): 2760-2770.

Gupta, S., D. Campbell, et al. (1995). "Transcription factor ATF2 regulation by the JNK signal transduction pathway." Science **267**(5196): 389-393.

Gurdon, J. B. and P. Y. Bourillot (2001). "Morphogen gradient interpretation." Nature **413**(6858): 797-803.

Gurdon, J. B., P. Harger, et al. (1994). "Activin signalling and response to a morphogen gradient." Nature **371**(6497): 487-492.

Hai, T. and T. Curran (1991). "Cross-family dimerization of transcription factors Fos/Jun and ATF/CREB alters DNA binding specificity." Proceedings of the National Academy of Sciences of the United States of America **88**(9): 3720-3724.

Halazonetis, T. D., K. Georgopoulos, et al. (1988). "c-Jun dimerizes with itself and with c-Fos, forming complexes of different DNA binding affinities." Cell **55**(5): 917-924.

Han, J., Y. Jiang, et al. (1997). "Activation of the transcription factor MEF2C by the MAP kinase p38 in inflammation." Nature **386**(6622): 296-299.

Han, J., J. D. Lee, et al. (1994). "A MAP kinase targeted by endotoxin and hyperosmolarity in mammalian cells." Science **265**(5173): 808-811.

Han, T. H., W. W. Lamph, et al. (1992). "Mapping of epidermal growth factor-, serum-, and phorbol ester-responsive sequence elements in the c-jun promoter." Molecular and Cellular Biology **12**(10): 4472-4477.

Han, T. H. and R. Prywes (1995). "Regulatory role of MEF2D in serum induction of the c-jun promoter." Molecular and Cellular Biology **15**(6): 2907-2915.

Hanks, S. K., A. M. Quinn, et al. (1988). "The protein kinase family: conserved features and deduced phylogeny of the catalytic domains." Science **241**(4861): 42-52.

Hattori, K., P. Angel, et al. (1988). "Structure and chromosomal localization of the functional intronless human JUN protooncogene." Proceedings of the National Academy of Sciences of the United States of America **85**(23): 9148-9152.

Hayashi, K., S. M. Lopes, et al. (2008). "Dynamic equilibrium and heterogeneity of mouse pluripotent stem cells with distinct functional and epigenetic states." Cell Stem Cell **3**(4): 391-401.

Hayes, T. E., A. M. Kitchen, et al. (1987). "Inducible binding of a factor to the c-fos regulatory region." Proceedings of the National Academy of Sciences of the United States of America **84**(5): 1272-1276.

Hazzalin, C. A., E. Cano, et al. (1996). "p38/RK is essential for stress-induced nuclear responses: JNK/SAPKs and c-Jun/ATF-2 phosphorylation are insufficient." Current Biology **6**(8): 1028-1031.

Hazzalin, C. A., A. Cuenda, et al. (1997). "Effects of the inhibition of p38/RK MAP kinase on induction of five fos and jun genes by diverse stimuli." Oncogene **15**(19): 2321-2331.

Hazzalin, C. A., R. Le Panse, et al. (1998). "Anisomycin selectively desensitizes signalling components involved in stress kinase activation and fos and jun induction." Molecular and Cellular Biology **18**(4): 1844-1854.

Hazzalin, C. A. and L. C. Mahadevan (2002). "MAPK-regulated transcription: a continuously variable gene switch?" Nature Reviews Molecular Cell Biology **3**(1): 30-40.

Hazzalin, C. A. and L. C. Mahadevan (2005). "Dynamic acetylation of all lysine 4-methylated histone H3 in the mouse nucleus: analysis at c-fos and c-jun." PLoS Biol **3**(12): e393.

Healy, A. M., S. Zolnierowicz, et al. (1991). "CDC55, a Saccharomyces cerevisiae gene involved in cellular morphogenesis: identification, characterization, and homology to the B subunit of mammalian type 2A protein phosphatase." Molecular and Cellular Biology **11**(11): 5767-5780.

Heath, J., M. Kwiatkowska, et al. (2007). "Probabilistic Model Checking of Complex Biological Pathways."

Hebbes, T. R., A. L. Clayton, et al. (1994). "Core histone hyperacetylation co-maps with generalized DNase I sensitivity in the chicken beta-globin chromosomal domain." EMBO J **13**(8): 1823-1830.

Heidemann, M., C. Hintermair, et al. (2013). "Dynamic phosphorylation patterns of RNA polymerase II CTD during transcription." Biochimica et Biophysica Acta **1829**(1): 55-62.

Hemmings, B. A., C. Adams-Pearson, et al. (1990). "alpha- and beta-forms of the 65-kDa subunit of protein phosphatase 2A have a similar 39 amino acid repeating structure." Biochemistry **29**(13): 3166-3173.

Hendzel, M. J., Y. Wei, et al. (1997). "Mitosis-specific phosphorylation of histone H3 initiates primarily within pericentromeric heterochromatin during G2 and spreads in an ordered fashion coincident with mitotic chromosome condensation." Chromosoma **106**(6): 348-360.

Herdegen, T. and J. D. Leah (1998). "Inducible and constitutive transcription factors in the mammalian nervous system: control of gene expression by Jun, Fos and Krox, and CREB/ATF proteins." Brain Res Brain Res Rev **28**(3): 370-490.

Herr, I., H. van Dam, et al. (1994). "Binding of promoter-associated AP-1 is not altered during induction and subsequent repression of the c-jun promoter by TPA and UV irradiation." Carcinogenesis **15**(6): 1105-1113.

Herrera, R. E., P. E. Shaw, et al. (1989). "Occupation of the c-fos serum response element in vivo by a multi-protein complex is unaltered by growth factor induction." Nature **340**(6228): 68-70.

Herschman, H. R. (1991). "Primary response genes induced by growth factors and tumor promoters." Annual Review of Biochemistry **60**: 281-319.

Herschman, H. R., R. W. Lim, et al. (1989). "The tumor promoters 12-O-tetradecanoylphorbol-13-acetate and okadaic acid differ in toxicity, mitogenic activity and induction of gene expression." Carcinogenesis **10**(8): 1495-1498.

Hibi, M., A. Lin, et al. (1993). "Identification of an oncoprotein- and UV-responsive protein kinase that binds and potentiates the c-Jun activation domain." Genes & Development **7**(11): 2135-2148.

Hill, C. S. and R. Treisman (1995). "Transcriptional regulation by extracellular signals: mechanisms and specificity." Cell **80**(2): 199-211.

Hirai, S. I., R. P. Ryseck, et al. (1989). "Characterization of junD: a new member of the jun proto-oncogene family." EMBO J **8**(5): 1433-1439.

Hirosumi, J., G. Tuncman, et al. (2002). "A central role for JNK in obesity and insulin resistance." Nature **420**(6913): 333-336.

Hirschhorn, R. R., P. Aller, et al. (1984). "Cell-cycle-specific cDNAs from mammalian cells temperature sensitive for growth." Proceedings of the National Academy of Sciences of the United States of America **81**(19): 6004-6008.

Holzman, L. B., S. E. Merritt, et al. (1994). "Identification, molecular cloning, and characterization of dual leucine zipper bearing kinase. A novel serine/threonine protein kinase that defines a second subfamily of mixed lineage kinases." Journal of Biological Chemistry **269**(49): 30808-30817.

Hoops, S., S. Sahle, et al. (2006). "COPASI--a COmplex PAthway SImulator." Bioinformatics **22**(24): 3067-3074.

Hsiao, L. L., F. Dangond, et al. (2001). "A compendium of gene expression in normal human tissues." Physiological Genomics **7**(2): 97-104.

Huang, C. Y. and J. E. Ferrell, Jr. (1996). "Dependence of Mos-induced Cdc2 activation on MAP kinase function in a cell-free system." EMBO J **15**(9): 2169-2173.

Huang, C. Y. and J. E. Ferrell, Jr. (1996). "Ultrasensitivity in the mitogen-activated protein kinase cascade." Proceedings of the National Academy of Sciences of the United States of America **93**(19): 10078-10083.

Hubbard, M. J. and P. Cohen (1993). "On target with a new mechanism for the regulation of protein phosphorylation." Trends in Biochemical Sciences **18**(5): 172-177.

Ishihara, K. and T. Hirano (2002). "IL-6 in autoimmune disease and chronic inflammatory proliferative disease." Cytokine & Growth Factor Reviews **13**(4-5): 357-368.

Janssens, V. and J. Goris (2001). "Protein phosphatase 2A: a highly regulated family of serine/threonine phosphatases implicated in cell growth and signalling." Biochemical Journal **353**(Pt 3): 417-439.

Johnson, G. L. and R. Lapadat (2002). "Mitogen-activated protein kinase pathways mediated by ERK, JNK, and p38 protein kinases." Science **298**(5600): 1911-1912.

Kaern, M., T. C. Elston, et al. (2005). "Stochasticity in gene expression: from theories to phenotypes." Nature Reviews Genetics **6**(6): 451-464.

Kallunki, T., B. Su, et al. (1994). "JNK2 contains a specificity-determining region responsible for efficient c-Jun binding and phosphorylation." Genes & Development **8**(24): 2996-3007.

Karin, M. and T. Hunter (1995). "Transcriptional control by protein phosphorylation: signal transmission from the cell surface to the nucleus." Current Biology **5**(7): 747-757.

Karin, M., Z. Liu, et al. (1997). "AP-1 function and regulation." Current Opinion in Cell Biology **9**(2): 240-246.

Kee, B. L., J. Arias, et al. (1996). "Adaptor-mediated recruitment of RNA polymerase II to a signal-dependent activator." Journal of Biological Chemistry **271**(5): 2373-2375.

Kepler, T. B. and T. C. Elston (2001). "Stochasticity in transcriptional regulation: origins, consequences, and mathematical representations." Biophysical Journal **81**(6): 3116-3136.

Keyse, S. M. (2000). "Protein phosphatases and the regulation of mitogen-activated protein kinase signalling." Current Opinion in Cell Biology **12**(2): 186-192.

Keyse, S. M. and E. A. Emslie (1992). "Oxidative stress and heat shock induce a human gene encoding a protein-tyrosine phosphatase." Nature **359**(6396): 644-647.

Kim, E. K. and E. J. Choi (2010). "Pathological roles of MAPK signaling pathways in human diseases." Biochimica et Biophysica Acta **1802**(4): 396-405.

King, A. J., H. Sun, et al. (1998). "The protein kinase Pak3 positively regulates Raf-1 activity through phosphorylation of serine 338." Nature **396**(6707): 180-183.

Kinoshita, N., H. Yamano, et al. (1993). "Negative regulation of mitosis by the fission yeast protein phosphatase ppa2." Genes & Development **7**(6): 1059-1071.

Knighton, D. R., J. H. Zheng, et al. (1991). "Crystal structure of the catalytic subunit of cyclic adenosine monophosphate-dependent protein kinase." Science **253**(5018): 407-414.

Kofahl, B. and E. Klipp (2004). "Modelling the dynamics of the yeast pheromone pathway." Yeast **21**(10): 831-850.

Kolch, W., M. Calder, et al. (2005). "When kinases meet mathematics: the systems biology of MAPK signalling." FEBS Letters **579**(8): 1891-1895.

Kosako, H., Y. Gotoh, et al. (1994). "Requirement for the MAP kinase kinase/MAP kinase cascade in Xenopus oocyte maturation." EMBO J **13**(9): 2131-2138.

Kostenko, S., A. Shiryaev, et al. (2011). "Cross-talk between protein kinase A and the MAPK-activated protein kinases RSK1 and MK5." J Recept Signal Transduct Res **31**(1): 1-9.

Kovary, K. and R. Bravo (1991). "Expression of different Jun and Fos proteins during the G0-to-G1 transition in mouse fibroblasts: in vitro and in vivo associations." Molecular and Cellular Biology **11**(5): 2451-2459.

Kovary, K. and R. Bravo (1992). "Existence of different Fos/Jun complexes during the G0-to-G1 transition and during exponential growth in mouse fibroblasts: differential role of Fos proteins." Molecular and Cellular Biology **12**(11): 5015-5023.

Kremmer, E., K. Ohst, et al. (1997). "Separation of PP2A core enzyme and holoenzyme with monoclonal antibodies against the regulatory A subunit: abundant expression of both forms in cells." Molecular and Cellular Biology **17**(3): 1692-1701.

Kruijer, W., J. A. Cooper, et al. (1984). "Platelet-derived growth factor induces rapid but transient expression of the c-fos gene and protein." Nature **312**(5996): 711-716.

Kumar, S., J. Boehm, et al. (2003). "p38 MAP kinases: key signalling molecules as therapeutic targets for inflammatory diseases." Nat Rev Drug Discov **2**(9): 717-726.

Kuo, M. H. and C. D. Allis (1998). "Roles of histone acetyltransferases and deacetylases in gene regulation." BioEssays **20**(8): 615-626.

Kuo, M. H., J. E. Brownell, et al. (1996). "Transcription-linked acetylation by Gcn5p of histones H3 and H4 at specific lysines." Nature **383**(6597): 269-272.

Kutejova, E., J. Briscoe, et al. (2009). "Temporal dynamics of patterning by morphogen gradients." Current Opinion in Genetics & Development **19**(4): 315-322.

Kwiatkowska, M., G. Norman, et al. (2008). "Using probabilistic model checking in systems biology." ACM SIGMETRICS Performance Evaluation Review **35**(4): 14-21.

Kwiatkowska, M., G. Norman, et al. (2010). Probabilistic Model Checking for Systems Biology. Symbolic Systems Biology, Jones and Bartlett**:** 31-59.

Kwiatkowska, M., G. Norman, et al. (2011). PRISM 4.0: Verification of Probabilistic Real-time Systems. Computer Aided Verification, Springer Berlin Heidelberg**:** 585-591.

Kwiatkowska, M. Z. and J. K. Heath (2009). "Biological pathways as communicating computer systems." Journal of Cell Science **122**(Pt 16): 2793-2800.

Kwok, R. P., J. R. Lundblad, et al. (1994). "Nuclear protein CBP is a coactivator for the transcription factor CREB." Nature **370**(6486): 223-226.

Kyriakis, J. M. and J. Avruch (2001). "Mammalian mitogen-activated protein kinase signal transduction pathways activated by stress and inflammation." Physiological Reviews **81**(2): 807-869.

Kyriakis, J. M., P. Banerjee, et al. (1994). "The stress-activated protein kinase subfamily of c-Jun kinases." Nature **369**(6476): 156-160.

Laemmli, U. K. (1970). "Cleavage of structural proteins during the assembly of the head of bacteriophage T4." Nature **227**(5259): 680-685.

Lamb, N. J., A. Fernandez, et al. (1990). "Demonstration in living cells of an intragenic negative regulatory element within the rodent c-fos gene." Cell **61**(3): 485-496.

Lamph, W. W., P. Wamsley, et al. (1988). "Induction of proto-oncogene JUN/AP-1 by serum and TPA." Nature **334**(6183): 629-631.

Lange-Carter, C. A., C. M. Pleiman, et al. (1993). "A divergence in the MAP kinase regulatory network defined by MEK kinase and Raf." Science **260**(5106): 315-319.

Langer-Safer, P. R., M. Levine, et al. (1982). "Immunological method for mapping genes on Drosophila polytene chromosomes." Proceedings of the National Academy of Sciences of the United States of America **79**(14): 4381-4385.

Lau, L. F. and D. Nathans (1985). "Identification of a set of genes expressed during the G0/G1 transition of cultured mouse cells." EMBO J **4**(12): 3145-3151.

Lau, L. F. and D. Nathans (1987). "Expression of a set of growth-related immediate early genes in BALB/c 3T3 cells: coordinate regulation with c-fos or c-myc." Proceedings of the National Academy of Sciences of the United States of America **84**(5): 1182-1186.

Law, B. K. (2005). "Rapamycin: an anti-cancer immunosuppressant?" Crit Rev Oncol Hematol **56**(1): 47-60.

Lawler, S., Y. Fleming, et al. (1998). "Synergistic activation of SAPK1/JNK1 by two MAP kinase kinases in vitro." Current Biology **8**(25): 1387-1390.

Leaman, D. W., S. Pisharody, et al. (1996). "Roles of JAKs in activation of STATs and stimulation of c-fos gene expression by epidermal growth factor." Molecular and Cellular Biology **16**(1): 369-375.

Lecuit, T. and S. M. Cohen (1998). "Dpp receptor levels contribute to shaping the Dpp morphogen gradient in the Drosophila wing imaginal disc." Development **125**(24): 4901-4907.

Lee, B. M. and L. C. Mahadevan (2009). "Stability of histone modifications across mammalian genomes: implications for 'epigenetic' marking." Journal of Cellular Biochemistry **108**(1): 22-34.

Lee, J. C., J. T. Laydon, et al. (1994). "A protein kinase involved in the regulation of inflammatory cytokine biosynthesis." Nature **372**(6508): 739-746.

Lee, J. D., R. J. Ulevitch, et al. (1995). "Primary structure of BMK1: a new mammalian map kinase." Biochemical and Biophysical Research Communications **213**(2): 715-724.

Lee, P. D., R. Sladek, et al. (2002). "Control genes and variability: absence of ubiquitous reference transcripts in diverse mammalian expression studies." Genome Research **12**(2): 292-297.

Lee, T. H., C. Turck, et al. (1994). "Inhibition of cdc2 activation by INH/PP2A." Molecular Biology of the Cell **5**(3): 323-338.

Lee, W., A. Haslinger, et al. (1987). "Activation of transcription by two factors that bind promoter and enhancer sequences of the human metallothionein gene and SV40." Nature **325**(6102): 368-372.

Lee, W., P. Mitchell, et al. (1987). "Purified transcription factor AP-1 interacts with TPA-inducible enhancer elements." Cell **49**(6): 741-752.

Levsky, J. M., S. M. Shenoy, et al. (2002). "Single-cell gene expression profiling." Science **297**(5582): 836-840.

Li, J., M. Gorospe, et al. (2001). "Transcriptional induction of MKP-1 in response to stress is associated with histone H3 phosphorylation-acetylation." Molecular and Cellular Biology **21**(23): 8213-8224.

Li, L. and J. E. Dixon (2000). "Form, function, and regulation of protein tyrosine phosphatases and their involvement in human diseases." Semin Immunol **12**(1): 75-84.

Li, M. and Z. Damuni (1994). "Okadaic acid and microcystin-LR directly inhibit the methylation of protein phosphatase 2A by its specific methyltransferase." Biochemical and Biophysical Research Communications **202**(2): 1023-1030.

Lim, R. W., B. C. Varnum, et al. (1987). "Cloning of tetradecanoyl phorbol ester-induced 'primary response' sequences and their expression in density-arrested Swiss 3T3 cells and a TPA non-proliferative variant." Oncogene **1**(3): 263-270.

Linzer, D. I. and D. Nathans (1983). "Growth-related changes in specific mRNAs of cultured mouse cells." Proceedings of the National Academy of Sciences of the United States of America **80**(14): 4271-4275.

Livingstone, C., G. Patel, et al. (1995). "ATF-2 contains a phosphorylation-dependent transcriptional activation domain." EMBO J **14**(8): 1785-1797.

Lloyd, A. C. (2006). "Distinct functions for ERKs?" J Biol **5**(5): 13.

Lohr, D., P. Venkov, et al. (1995). "Transcriptional regulation in the yeast GAL gene family: a complex genetic network." FASEB Journal **9**(9): 777-787.

Ludlow, J. W., C. L. Glendening, et al. (1993). "Specific enzymatic dephosphorylation of the retinoblastoma protein." Molecular and Cellular Biology **13**(1): 367-372.

Ludlow, J. W., J. Shon, et al. (1990). "The retinoblastoma susceptibility gene product undergoes cell cycle-dependent dephosphorylation and binding to and release from SV40 large T." Cell **60**(3): 387-396.

Luger, K., A. W. Mader, et al. (1997). "Crystal structure of the nucleosome core particle at 2.8 A resolution." Nature **389**(6648): 251-260.

Lundblad, J. R., R. P. Kwok, et al. (1995). "Adenoviral E1A-associated protein p300 as a functional homologue of the transcriptional co-activator CBP." Nature **374**(6517): 85-88.

Macdonald, N., J. P. Welburn, et al. (2005). "Molecular basis for the recognition of phosphorylated and phosphoacetylated histone h3 by 14-3-3." Molecular Cell **20**(2): 199-211.

Mahadevan, L. C. and D. R. Edwards (1991). "Signalling and superinduction." Nature **349**(6312): 747-748.

Mahadevan, L. C., A. C. Willis, et al. (1991). "Rapid histone H3 phosphorylation in response to growth factors, phorbol esters, okadaic acid, and protein synthesis inhibitors." Cell **65**(5): 775-783.

Maki, Y., T. J. Bos, et al. (1987). "Avian sarcoma virus 17 carries the jun oncogene." Proceedings of the National Academy of Sciences of the United States of America **84**(9): 2848-2852.

Marais, R., J. Wynne, et al. (1993). "The SRF accessory protein Elk-1 contains a growth factor-regulated transcriptional activation domain." Cell **73**(2): 381-393.

Marshall, C. J. (1994). "MAP kinase kinase kinase, MAP kinase kinase and MAP kinase." Current Opinion in Genetics & Development **4**(1): 82-89.

Marshall, C. J. (1995). "Specificity of receptor tyrosine kinase signaling: transient versus sustained extracellular signal-regulated kinase activation." Cell **80**(2): 179-185.

Masui, Y. and H. J. Clarke (1979). "Oocyte maturation." International Review of Cytology **57**: 185-282.

Matten, W. T., T. D. Copeland, et al. (1996). "Positive feedback between MAP kinase and Mos during Xenopus oocyte maturation." Developmental Biology **179**(2): 485-492.

Mayer, R. E., P. Hendrix, et al. (1991). "Structure of the 55-kDa regulatory subunit of protein phosphatase 2A: evidence for a neuronal-specific isoform." Biochemistry **30**(15): 3589-3597.

Mayer-Jaekel, R. E. and B. A. Hemmings (1994). "Protein phosphatase 2A--a 'menage a trois'." Trends in Cell Biology **4**(8): 287-291.

Mayr, B. and M. Montminy (2001). "Transcriptional regulation by the phosphorylation-dependent factor CREB." Nature Reviews Molecular Cell Biology **2**(8): 599-609.

McAdams, H. H. and A. Arkin (1999). "It's a noisy business! Genetic regulation at the nanomolar scale." Trends in Genetics **15**(2): 65-69.

McConnell, J. L. and B. E. Wadzinski (2009). "Targeting protein serine/threonine phosphatases for drug development." Molecular Pharmacology **75**(6): 1249-1261.

McCright, B., A. M. Rivers, et al. (1996). "The B56 family of protein phosphatase 2A (PP2A) regulatory subunits encodes differentiation-induced phosphoproteins that target PP2A to both nucleus and cytoplasm." Journal of Biological Chemistry **271**(36): 22081-22089.

McCright, B. and D. M. Virshup (1995). "Identification of a new family of protein phosphatase 2A regulatory subunits." Journal of Biological Chemistry **270**(44): 26123-26128.

McGhee, J. D. and G. Felsenfeld (1980). "Nucleosome structure." Annual Review of Biochemistry **49**: 1115-1156.

McMahon, S. B. and J. G. Monroe (1992). "Role of primary response genes in generating cellular responses to growth factors." FASEB Journal **6**(9): 2707-2715.

Mechti, N., M. Piechaczyk, et al. (1991). "Sequence requirements for premature transcription arrest within the first intron of the mouse c-fos gene." Molecular and Cellular Biology **11**(5): 2832-2841.

Meier, R., J. Rouse, et al. (1996). "Cellular stresses and cytokines activate multiple mitogen-activated-protein kinase kinase homologues in PC12 and KB cells." European Journal of Biochemistry **236**(3): 796-805.

Montminy, M. R. and L. M. Bilezikjian (1987). "Binding of a nuclear protein to the cyclic-AMP response element of the somatostatin gene." Nature **328**(6126): 175-178.

Morgan, D. O. (1995). "Principles of CDK regulation." Nature **374**(6518): 131-134.

Morrison, D. K. and R. J. Davis (2003). "Regulation of MAP kinase signaling modules by scaffold proteins in mammals." Annual Review of Cell and Developmental Biology **19**: 91-118.

Morrison, D. K., M. S. Murakami, et al. (2000). "Protein kinases and phosphatases in the Drosophila genome." Journal of Cell Biology **150**(2): F57-62.

Muller, R., R. Bravo, et al. (1984). "Induction of c-fos gene and protein by growth factors precedes activation of c-myc." Nature **312**(5996): 716-720.

Mumby, M. C. and G. Walter (1993). "Protein serine/threonine phosphatases: structure, regulation, and functions in cell growth." Physiological Reviews **73**(4): 673-699.

Murakami, M. S. and G. F. Vande Woude (1998). "Analysis of the early embryonic cell cycles of Xenopus; regulation of cell cycle length by Xe-wee1 and Mos." Development **125**(2): 237-248.

Murphy, D. (1993). "Nuclear run-on analysis of transcription." Methods in Molecular Biology **18**: 355-361.

Muslin, A. J., A. M. MacNicol, et al. (1993). "Raf-1 protein kinase is important for progesterone-induced Xenopus oocyte maturation and acts downstream of mos." Molecular and Cellular Biology **13**(7): 4197-4202.

Mustelin, T., T. Vang, et al. (2005). "Protein tyrosine phosphatases and the immune response." Nat Rev Immunol **5**(1): 43-57.

Nakabeppu, Y., K. Ryder, et al. (1988). "DNA binding activities of three murine Jun proteins: stimulation by Fos." Cell **55**(5): 907-915.

Nakajima, T., C. Uchida, et al. (1997a). "RNA helicase A mediates association of CBP with RNA polymerase II." Cell **90**(6): 1107-1112.

Nakajima, T., C. Uchida, et al. (1997b). "Analysis of a cAMP-responsive activator reveals a two-component mechanism for transcriptional induction via signal-dependent factors." Genes & Development **11**(6): 738-747.

Neish, A. S., S. F. Anderson, et al. (1998). "Factors associated with the mammalian RNA polymerase II holoenzyme." Nucleic Acids Research **26**(3): 847-853.

Nichols, A., M. Camps, et al. (2000). "Substrate recognition domains within extracellular signal-regulated kinase mediate binding and catalytic

activation of mitogen-activated protein kinase phosphatase-3." Journal of Biological Chemistry **275**(32): 24613-24621.

Nishida, E. and Y. Gotoh (1993). "The MAP kinase cascade is essential for diverse signal transduction pathways." Trends in Biochemical Sciences **18**(4): 128-131.

Nishimoto, S. and E. Nishida (2006). "MAPK signalling: ERK5 versus ERK1/2." EMBO Reports **7**(8): 782-786.

Nishizawa, M., N. Furuno, et al. (1993). "Degradation of Mos by the N-terminal proline (Pro2)-dependent ubiquitin pathway on fertilization of Xenopus eggs: possible significance of natural selection for Pro2 in Mos." EMBO J **12**(10): 4021-4027.

Noguchi, T., R. Metz, et al. (1993). "Structure, mapping, and expression of erp, a growth factor-inducible gene encoding a nontransmembrane protein tyrosine phosphatase, and effect of ERP on cell growth." Molecular and Cellular Biology **13**(9): 5195-5205.

Nomura, N., M. Ide, et al. (1990). "Isolation of human cDNA clones of jun-related genes, jun-B and jun-D." Nucleic Acids Research **18**(10): 3047-3048.

Nowak, S. J., C. Y. Pai, et al. (2003). "Protein phosphatase 2A activity affects histone H3 phosphorylation and transcription in Drosophila melanogaster." Molecular and Cellular Biology **23**(17): 6129-6138.

Ogryzko, V. V., R. L. Schiltz, et al. (1996). "The transcriptional coactivators p300 and CBP are histone acetyltransferases." Cell **87**(5): 953-959.

Owens, D. M. and S. M. Keyse (2007). "Differential regulation of MAP kinase signalling by dual-specificity protein phosphatases." Oncogene **26**(22): 3203-3213.

Ozbudak, E. M., M. Thattai, et al. (2002). "Regulation of noise in the expression of a single gene." Nature Genetics **31**(1): 69-73.

Pannifer, A. D., A. J. Flint, et al. (1998). "Visualization of the cysteinyl-phosphate intermediate of a protein-tyrosine phosphatase by x-ray crystallography." Journal of Biological Chemistry **273**(17): 10454-10462.

Payne, D. M., A. J. Rossomando, et al. (1991). "Identification of the regulatory phosphorylation sites in pp42/mitogen-activated protein kinase (MAP kinase)." EMBO J **10**(4): 885-892.

Phatnani, H. P. and A. L. Greenleaf (2006). "Phosphorylation and functions of the RNA polymerase II CTD." Genes & Development **20**(21): 2922-2936.

Pontecorvi, A., J. R. Tata, et al. (1988). "Selective degradation of mRNA: the role of short-lived proteins in differential destabilization of insulin-induced creatine phosphokinase and myosin heavy chain mRNAs during rat skeletal muscle L6 cell differentiation." EMBO J **7**(5): 1489-1495.

Pot, D. A. and J. E. Dixon (1992). "Active site labeling of a receptor-like protein tyrosine phosphatase." Journal of Biological Chemistry **267**(1): 140-143.

Price, M. A., F. H. Cruzalegui, et al. (1996). "The p38 and ERK MAP kinase pathways cooperate to activate Ternary Complex Factors and c-fos transcription in response to UV light." EMBO J **15**(23): 6552-6563.

Pulverer, B. J., J. M. Kyriakis, et al. (1991). "Phosphorylation of c-jun mediated by MAP kinases." Nature **353**(6345): 670-674.

Quantin, B. and R. Breathnach (1988). "Epidermal growth factor stimulates transcription of the c-jun proto-oncogene in rat fibroblasts." Nature **334**(6182): 538-539.

Rahmsdorf, H. J., A. Schonthal, et al. (1987). "Posttranscriptional regulation of c-fos mRNA expression." Nucleic Acids Research **15**(4): 1643-1659.

Raingeaud, J., S. Gupta, et al. (1995). "Pro-inflammatory cytokines and environmental stress cause p38 mitogen-activated protein kinase activation by dual phosphorylation on tyrosine and threonine." Journal of Biological Chemistry **270**(13): 7420-7426.

Raingeaud, J., A. J. Whitmarsh, et al. (1996). "MKK3- and MKK6-regulated gene expression is mediated by the p38 mitogen-activated protein kinase signal transduction pathway." Molecular and Cellular Biology **16**(3): 1247-1255.

Raj, A., C. S. Peskin, et al. (2006). "Stochastic mRNA synthesis in mammalian cells." PLoS Biol **4**(10): e309.

Raj, A. and A. van Oudenaarden (2008). "Nature, nurture, or chance: stochastic gene expression and its consequences." Cell **135**(2): 216-226.

Raj, A. and A. van Oudenaarden (2009). "Single-molecule approaches to stochastic gene expression." Annu Rev Biophys **38**: 255-270.

Raser, J. M. and E. K. O'Shea (2004). "Control of stochasticity in eukaryotic gene expression." Science **304**(5678): 1811-1814.

Raser, J. M. and E. K. O'Shea (2005). "Noise in gene expression: origins, consequences, and control." Science **309**(5743): 2010-2013.

Reue, K. (1998). "mRNA quantitation techniques: considerations for experimental design and application." Journal of Nutrition **128**(11): 2038-2044.

Richmond, T. J., J. T. Finch, et al. (1984). "Structure of the nucleosome core particle at 7 A resolution." Nature **311**(5986): 532-537.

Rivera, V. M., C. K. Miranti, et al. (1993). "A growth factor-induced kinase phosphorylates the serum response factor at a site that regulates its DNA-binding activity." Molecular and Cellular Biology **13**(10): 6260-6273.

Robinson, P. J. and D. Rhodes (2006). "Structure of the '30 nm' chromatin fibre: a key role for the linker histone." Current Opinion in Structural Biology **16**(3): 336-343.

Rouse, J., P. Cohen, et al. (1994). "A novel kinase cascade triggered by stress and heat shock that stimulates MAPKAP kinase-2 and phosphorylation of the small heat shock proteins." Cell **78**(6): 1027-1037.

Rozek, D. and G. P. Pfeifer (1995). "In vivo protein-DNA interactions at the c-jun promoter in quiescent and serum-stimulated fibroblasts." Journal of Cellular Biochemistry **57**(3): 479-487.

Ryseck, R. P. and R. Bravo (1991). "c-JUN, JUN B, and JUN D differ in their binding affinities to AP-1 and CRE consensus sequences: effect of FOS proteins." Oncogene **6**(4): 533-542.

Ryseck, R. P., S. I. Hirai, et al. (1988). "Transcriptional activation of c-jun during the G0/G1 transition in mouse fibroblasts." Nature **334**(6182): 535-537.

Sagata, N. (1996). "Meiotic metaphase arrest in animal oocytes: its mechanisms and biological significance." Trends in Cell Biology **6**(1): 22-28.

Sagata, N. (1997). "What does Mos do in oocytes and somatic cells?" BioEssays **19**(1): 13-21.

Sagata, N., M. Oskarsson, et al. (1988). "Function of c-mos proto-oncogene product in meiotic maturation in Xenopus oocytes." Nature **335**(6190): 519-525.

Sasaki, K., H. Shima, et al. (1990). "Identification of members of the protein phosphatase 1 gene family in the rat and enhanced expression of protein phosphatase 1 alpha gene in rat hepatocellular carcinomas." Japanese Journal of Cancer Research **81**(12): 1272-1280.

Sassone-Corsi, P., J. C. Sisson, et al. (1988). "Transcriptional autoregulation of the proto-oncogene fos." Nature **334**(6180): 314-319.

Saxena, M. and T. Mustelin (2000). "Extracellular signals and scores of phosphatases: all roads lead to MAP kinase." Semin Immunol **12**(4): 387-396.

Schaeffer, H. J., A. D. Catling, et al. (1998). "MP1: a MEK binding partner that enhances enzymatic activation of the MAP kinase cascade." Science **281**(5383): 1668-1671.

Schillace, R. V. and J. D. Scott (1999). "Association of the type 1 protein phosphatase PP1 with the A-kinase anchoring protein AKAP220." Current Biology **9**(6): 321-324.

Schoeberl, B., C. Eichler-Jonsson, et al. (2002). "Computational modeling of the dynamics of the MAP kinase cascade activated by surface and internalized EGF receptors." Nature Biotechnology **20**(4): 370-375.

Schorderet-Slatkine, S. (1972). "Action of progesterone and related steroids on oocyte maturation in Xenopus laevis. An in vitro study." Cell Differ **1**(3): 179-189.

Schreiber, S. L. and B. E. Bernstein (2002). "Signaling network model of chromatin." Cell **111**(6): 771-778.

Seger, R. and E. G. Krebs (1995). "The MAPK signaling cascade." FASEB Journal **9**(9): 726-735.

Seo, M., Y. I. Lee, et al. (2002). "Bi-directional regulation of UV-induced activation of p38 kinase and c-Jun N-terminal kinase by G protein beta gamma-subunits." Journal of Biological Chemistry **277**(27): 24197-24203.

Shalek, A. K., R. Satija, et al. (2013). "Single-cell transcriptomics reveals bimodality in expression and splicing in immune cells." Nature **498**(7453): 236-240.

Shaw, P. E., H. Schroter, et al. (1989). "The ability of a ternary complex to form over the serum response element correlates with serum inducibility of the human c-fos promoter." Cell **56**(4): 563-572.

Sheng, M., S. T. Dougan, et al. (1988). "Calcium and growth factor pathways of c-fos transcriptional activation require distinct upstream regulatory sequences." Molecular and Cellular Biology **8**(7): 2787-2796.

Sigal, A., R. Milo, et al. (2006). "Variability and memory of protein levels in human cells." Nature **444**(7119): 643-646.

Slack, D. N., O. M. Seternes, et al. (2001). "Distinct binding determinants for ERK2/p38alpha and JNK map kinases mediate catalytic activation and substrate selectivity of map kinase phosphatase-1." Journal of Biological Chemistry **276**(19): 16491-16500.

Slack, J. M. (1991). "The nature of the mesoderm-inducing signal in Xenopus: a transfilter induction study." Development **113**(2): 661-669.

Smale, S. T. (2009). "Nuclear run-on assay." Cold Spring Harb Protoc **2009**(11): pdb prot5329.

Smeal, T., B. Binetruy, et al. (1991). "Oncogenic and transcriptional cooperation with Ha-Ras requires phosphorylation of c-Jun on serines 63 and 73." Nature **354**(6353): 494-496.

Sng, J. C., H. Taniura, et al. (2004). "A tale of early response genes." Biological & Pharmaceutical Bulletin **27**(5): 606-612.

Sobell, H. M. (1985). "Actinomycin and DNA transcription." Proceedings of the National Academy of Sciences of the United States of America **82**(16): 5328-5331.

Soloaga, A., S. Thomson, et al. (2003). "MSK2 and MSK1 mediate the mitogen- and stress-induced phosphorylation of histone H3 and HMG-14." EMBO J **22**(11): 2788-2797.

Somsen, O. J., M. Siderius, et al. (2002). "Selectivity in overlapping MAP kinase cascades." Journal of Theoretical Biology **218**(3): 343-354.

Sontag, E., S. Fedorov, et al. (1993). "The interaction of SV40 small tumor antigen with protein phosphatase 2A stimulates the map kinase pathway and induces cell proliferation." Cell **75**(5): 887-897.

Stahlberg, A. and M. Bengtsson (2010). "Single-cell gene expression profiling using reverse transcription quantitative real-time PCR." Methods **50**(4): 282-288.

Sterner, D. E. and S. L. Berger (2000). "Acetylation of histones and transcription-related factors." Microbiology and Molecular Biology Reviews **64**(2): 435-459.

Sterner, R., L. C. Boffa, et al. (1987). "Cell cycle-dependent changes in conformation and composition of nucleosomes containing human histone gene sequences." Nucleic Acids Research **15**(11): 4375-4391.

Stone, S. R., J. Hofsteenge, et al. (1987). "Molecular cloning of cDNAs encoding two isoforms of the catalytic subunit of protein phosphatase 2A." Biochemistry **26**(23): 7215-7220.

Strack, S., D. Chang, et al. (1999). "Cloning and characterization of B delta, a novel regulatory subunit of protein phosphatase 2A." FEBS Letters **460**(3): 462-466.

Strahl, B. D. and C. D. Allis (2000). "The language of covalent histone modifications." Nature **403**(6765): 41-45.

Sun, H., C. H. Charles, et al. (1993). "MKP-1 (3CH134), an immediate early gene product, is a dual specificity phosphatase that dephosphorylates MAP kinase in vivo." Cell **75**(3): 487-493.

Swain, P. S., M. B. Elowitz, et al. (2002). "Intrinsic and extrinsic contributions to stochasticity in gene expression." Proceedings of the National Academy of Sciences of the United States of America **99**(20): 12795-12800.

Takasuka, N., M. R. White, et al. (1998). "Dynamic changes in prolactin promoter activation in individual living lactotrophic cells." Endocrinology **139**(3): 1361-1368.

Tan, Y., J. Rouse, et al. (1996). "FGF and stress regulate CREB and ATF-1 via a pathway involving p38 MAP kinase and MAPKAP kinase-2." EMBO J **15**(17): 4629-4642.

Tanabe, O., T. Nagase, et al. (1996). "Molecular cloning of a 74-kDa regulatory subunit (B" or delta) of human protein phosphatase 2A." FEBS Letters **379**(1): 107-111.

Tanoue, T., M. Adachi, et al. (2000). "A conserved docking motif in MAP kinases common to substrates, activators and regulators." Nature Cell Biology **2**(2): 110-116.

Tanoue, T., R. Maeda, et al. (2001). "Identification of a docking groove on ERK and p38 MAP kinases that regulates the specificity of docking interactions." EMBO J **20**(3): 466-479.

Tanoue, T., T. Yamamoto, et al. (2002). "Modular structure of a docking surface on MAPK phosphatases." Journal of Biological Chemistry **277**(25): 22942-22949.

Taverna, S. D., H. Li, et al. (2007). "How chromatin-binding modules interpret histone modifications: lessons from professional pocket pickers." Nat Struct Mol Biol **14**(11): 1025-1040.

Tehrani, M. A., M. C. Mumby, et al. (1996). "Identification of a novel protein phosphatase 2A regulatory subunit highly expressed in muscle." Journal of Biological Chemistry **271**(9): 5164-5170.

Thellin, O., W. Zorzi, et al. (1999). "Housekeeping genes as internal standards: use and limits." Journal of Biotechnology **75**(2-3): 291-295.

Theodosiou, A. and A. Ashworth (2002). "MAP kinase phosphatases." Genome Biol **3**(7): REVIEWS3009.

Thomson, S., A. L. Clayton, et al. (1999). "The nucleosomal response associated with immediate-early gene induction is mediated via alternative MAP kinase cascades: MSK1 as a potential histone H3/HMG-14 kinase." EMBO J **18**(17): 4779-4793.

Thomson, S., A. L. Clayton, et al. (2001). "Independent dynamic regulation of histone phosphorylation and acetylation during immediate-early gene induction." Molecular Cell **8**(6): 1231-1241.

Thornton, T. M. and M. Rincon (2009). "Non-classical p38 map kinase functions: cell cycle checkpoints and survival." Int J Biol Sci **5**(1): 44-51.

Treisman, R. (1985). "Transient accumulation of c-fos RNA following serum stimulation requires a conserved 5' element and c-fos 3' sequences." Cell **42**(3): 889-902.

Treisman, R. (1986). "Identification of a protein-binding site that mediates transcriptional response of the c-fos gene to serum factors." Cell **46**(4): 567-574.

Treisman, R. (1987). "Identification and purification of a polypeptide that binds to the c-fos serum response element." EMBO J **6**(9): 2711-2717.

Treisman, R. (1992). "The serum response element." Trends in Biochemical Sciences **17**(10): 423-426.

Treisman, R. (1996). "Regulation of transcription by MAP kinase cascades." Current Opinion in Cell Biology **8**(2): 205-215.

Turner, B. M. (2000). "Histone acetylation and an epigenetic code." BioEssays **22**(9): 836-845.

Turowski, P., A. Fernandez, et al. (1995). "Differential methylation and altered conformation of cytoplasmic and nuclear forms of protein phosphatase 2A during cell cycle progression." Journal of Cell Biology **129**(2): 397-410.

van Dam, H., D. Wilhelm, et al. (1995). "ATF-2 is preferentially activated by stress-activated protein kinases to mediate c-jun induction in response to genotoxic agents." EMBO J **14**(8): 1798-1811.

Vayttaden, S. J., S. M. Ajay, et al. (2004). "A spectrum of models of signaling pathways." ChemBioChem **5**(10): 1365-1374.

Wagner, B. J., T. E. Hayes, et al. (1990). "The SIF binding element confers sis/PDGF inducibility onto the c-fos promoter." EMBO J **9**(13): 4477-4484.

Walsh, A. H., A. Cheng, et al. (1997). "Fostriecin, an antitumor antibiotic with inhibitory activity against serine/threonine protein phosphatases types 1 (PP1) and 2A (PP2A), is highly selective for PP2A." FEBS Letters **416**(3): 230-234.

Walter, W., D. Clynes, et al. (2008). "14-3-3 interaction with histone H3 involves a dual modification pattern of phosphoacetylation." Molecular and Cellular Biology **28**(8): 2840-2849.

Walton, K. M. and J. E. Dixon (1993). "Protein tyrosine phosphatases." Annual Review of Biochemistry **62**: 101-120.

Wang, J., Y. C. Tung, et al. (2001). "Hyperphosphorylation and accumulation of neurofilament proteins in Alzheimer disease brain and in okadaic acid-treated SY5Y cells." FEBS Letters **507**(1): 81-87.

Wang, J. Z. and F. Liu (2008). "Microtubule-associated protein tau in development, degeneration and protection of neurons." Prog Neurobiol **85**(2): 148-175.

Warren, L., D. Bryder, et al. (2006). "Transcription factor profiling in individual hematopoietic progenitors by digital RT-PCR." Proceedings of the National Academy of Sciences of the United States of America **103**(47): 17807-17812.

Warrington, J. A., A. Nair, et al. (2000). "Comparison of human adult and fetal expression and identification of 535 housekeeping/maintenance genes." Physiological Genomics **2**(3): 143-147.

Wartlick, O., A. Kicheva, et al. (2009). "Morphogen gradient formation." Cold Spring Harb Perspect Biol **1**(3): a001255.

Watanabe, N., G. F. Vande Woude, et al. (1989). "Specific proteolysis of the c-mos proto-oncogene product by calpain on fertilization of Xenopus eggs." Nature **342**(6249): 505-511.

Watson, Hopkins, et al. (1965). The functioning of higher eucaryotic genes. Molecular Biology of the gene. B. Cummings. **1:** 704.

Wei, Y., L. Yu, et al. (1999). "Phosphorylation of histone H3 is required for proper chromosome condensation and segregation." Cell **97**(1): 99-109.

Wera, S. and B. A. Hemmings (1995). "Serine/threonine protein phosphatases." Biochemical Journal **311 (Pt 1)**: 17-29.

Wheat, W. H., W. J. Roesler, et al. (1994). "Simian virus 40 small tumor antigen inhibits dephosphorylation of protein kinase A-phosphorylated CREB and regulates CREB transcriptional stimulation." Molecular and Cellular Biology **14**(9): 5881-5890.

Whitmarsh, A. J., J. Cavanagh, et al. (1998). "A mammalian scaffold complex that selectively mediates MAP kinase activation." Science **281**(5383): 1671-1674.

Whitmarsh, A. J., P. Shore, et al. (1995). "Integration of MAP kinase signal transduction pathways at the serum response element." Science **269**(5222): 403-407.

Whitmarsh, A. J., S. H. Yang, et al. (1997). "Role of p38 and JNK mitogen-activated protein kinases in the activation of ternary complex factors." Molecular and Cellular Biology **17**(5): 2360-2371.

Widmann, C., S. Gibson, et al. (1999). "Mitogen-activated protein kinase: conservation of a three-kinase module from yeast to human." Physiological Reviews **79**(1): 143-180.

Wiley, H. S., S. Y. Shvartsman, et al. (2003). "Computational modeling of the EGF-receptor system: a paradigm for systems biology." Trends in Cell Biology **13**(1): 43-50.

Winter, S., E. Simboeck, et al. (2008). "14-3-3 proteins recognize a histone code at histone H3 and are required for transcriptional activation." EMBO J **27**(1): 88-99.

Wolpert, L. (1969). "Positional information and the spatial pattern of cellular differentiation." Journal of Theoretical Biology **25**(1): 1-47.

Wu, J., U. Kleiner, et al. (1996). "Protein phosphatase type-1 and glycogen bind to a domain in the skeletal muscle regulatory subunit containing conserved hydrophobic sequence motif." Biochemistry **35**(43): 13858-13864.

Wu, J., J. Liu, et al. (1998). "A conserved domain for glycogen binding in protein phosphatase-1 targeting subunits." FEBS Letters **439**(1-2): 185-191.

Wu, J. Q., J. Y. Guo, et al. (2009). "PP1-mediated dephosphorylation of phosphoproteins at mitotic exit is controlled by inhibitor-1 and PP1 phosphorylation." Nature Cell Biology **11**(5): 644-651.

Yang, E., L. Lerner, et al. (2003). "Independent and cooperative activation of chromosomal c-fos promoter by STAT3." Journal of Biological Chemistry **278**(18): 15794-15799.

Yang, S. H., A. D. Sharrocks, et al. (2003). "Transcriptional regulation by the MAP kinase signaling cascades." Gene **320**: 3-21.

Yang, S. H., A. J. Whitmarsh, et al. (1998). "Differential targeting of MAP kinases to the ETS-domain transcription factor Elk-1." EMBO J **17**(6): 1740-1749.

Yasuda, J., A. J. Whitmarsh, et al. (1999). "The JIP group of mitogen-activated protein kinase scaffold proteins." Molecular and Cellular Biology **19**(10): 7245-7254.

Zander, N. F., J. A. Lorenzen, et al. (1991). "Purification and characterization of a human recombinant T-cell protein-tyrosine-phosphatase from a baculovirus expression system." Biochemistry **30**(28): 6964-6970.

Zandomeni, R., B. Mittleman, et al. (1982). "Mechanism of action of dichloro-beta-D-ribofuranosylbenzimidazole: effect on in vitro transcription." Proceedings of the National Academy of Sciences of the United States of America **79**(10): 3167-3170.

Zecca, M., K. Basler, et al. (1995). "Sequential organizing activities of engrailed, hedgehog and decapentaplegic in the Drosophila wing." Development **121**(8): 2265-2278.

Zeng, L. and M. M. Zhou (2002). "Bromodomain: an acetyl-lysine binding domain." FEBS Letters **513**(1): 124-128.

Zhang, Z. Y. (1998). "Protein-tyrosine phosphatases: biological function, structural characteristics, and mechanism of catalysis." Critical Reviews in Biochemistry and Molecular Biology **33**(1): 1-52.

Zhang, Z. Y., Y. Wang, et al. (1994a). "Dissecting the catalytic mechanism of protein-tyrosine phosphatases." Proceedings of the National Academy of Sciences of the United States of America **91**(5): 1624-1627.

Zhang, Z. Y., Y. Wang, et al. (1994b). "The Cys(X)5Arg catalytic motif in phosphoester hydrolysis." Biochemistry **33**(51): 15266-15270.

Zhao, S. and E. Y. Lee (1997). "A protein phosphatase-1-binding motif identified by the panning of a random peptide display library." Journal of Biological Chemistry **272**(45): 28368-28372.

Zheng, C. F. and K. L. Guan (1993). "Dephosphorylation and inactivation of the mitogen-activated protein kinase by a mitogen-induced Thr/Tyr protein phosphatase." Journal of Biological Chemistry **268**(22): 16116-16119.

Zhou, G., Z. Q. Bao, et al. (1995). "Components of a new human protein kinase signal transduction pathway." Journal of Biological Chemistry **270**(21): 12665-12669.

Zhou, G., J. M. Denu, et al. (1994). "The catalytic role of Cys124 in the dual specificity phosphatase VHR." Journal of Biological Chemistry **269**(45): 28084-28090.

Zhu, J., F. He, et al. (2008). "How many human genes can be defined as housekeeping with current expression data?" BMC Genomics **9**: 172.

Zhu, Y., T. Pe'ery, et al. (1997). "Transcription elongation factor P-TEFb is required for HIV-1 tat transactivation in vitro." Genes & Development **11**(20): 2622-2632.

Zinck, R., R. A. Hipskind, et al. (1993). "c-fos transcriptional activation and repression correlate temporally with the phosphorylation status of TCF." EMBO J **12**(6): 2377-2387.

Zolnierowicz, S., C. Csortos, et al. (1994). "Diversity in the regulatory B-subunits of protein phosphatase 2A: identification of a novel isoform highly expressed in brain." Biochemistry **33**(39): 11858-11867.

Zolnierowicz, S., C. Van Hoof, et al. (1996). "The variable subunit associated with protein phosphatase 2A0 defines a novel multimember family of regulatory subunits." Biochemical Journal **317 (Pt 1)**: 187-194.